FACULTY OF PHARMACY AND MEDICINE

Ph.D. Thesis in Pharmaceutical Sciences

XXXI cycle

Synthesis and biological evaluation of new saccharin-based inhibitors of cancer-related carbonic anhydrase IX and XII isoforms

&

Benzo[*b*]tiophen-3-ol derivatives as effective inhibitors of hMAOs: design, synthesis and biological activity

Ph.D. student

Dr. Paolo Guglielmi

Supervisor

Prof. Daniela Secci

To those who pointed me the direction,

giving me the freedom and opportunity

to choose the road

Table of contents

Chapter 1

Carbonic anhydrases: functions and dark side

Chapter 2

Open saccharin-based secondary sulfonamides as potent and selective inhibitors of cancer-related carbonic anhydrase IX and XII isoforms

Chapter 3

Design, synthesis and biological activity of saccharin/isoxazole and saccharin/isoxazoline derivatives as selective inhibitors of carbonic anhydrase IX and XII isoforms

Chapter 4

Human monoamine oxidases (hMAOs)

Chapter 5

Benzo[b]tiophen-3-ol derivatives as effective inhibitors of hMAOs: design, synthesis and biological activity

During my PhD studies, I have worked with two enzymatic targets having diverse functions and so, different physiological/pathological features.

The first part focused on the design and synthesis of human carbonic anhydrase inhibitors, which were tested against four hCA isoforms, the ubiquitous CA I and CA II and the tumor-associated ones CA IX and CA XII, thanks to the precious collaboration of Prof. Claudiu T. Supuran and colleagues.

I have spent the last part of my PhD for the discovery of human monoamine oxidases inhibitors, which were tested against hMAOs and cortex synaptosomes thank to the valuable collaboration of Prof. Jacobus P. Petzer and Prof. Claudio Ferrante.

Chapter 1

Carbonic anhydrases: functions and dark side

1.1 Introduction

Carbonic anhydrases (CAs, EC 4.2.1.1) are ubiquitous enzymes found in numerous organisms across the tree of life, encoded by seven genetically distinct CA families: α-, β-, γ-, δ-, η-, ζ- and the last discovered family θ-CAs [1–9]. Carbonic anhydrases are metalloenzymes and they are catalytically effective only with one metal ion bound within the active site cavity, the apoenzymes being devoid of any catalytic action [10–16]. The active centre contains three amino acid residues which act as ligands, coordinating in a tetrahedral geometry the central divalent ion M(II). All the seven genetic families of CA may contain Zn(II) as metal ion, although it is substitutable with Cd(II) in the ζ-CAs [10]. γ-CAs seem to be endowed with Fe(II) ion, at least in anaerobic conditions [4,17], whereas Co(II) may substitute the zinc ion in many α-CAs without significant loss of the catalytic activity [1,18–20].

Carbonic anhydrases catalyse reversible hydration of CO_2 (eq.1) transforming two neutral molecules, CO_2 and water, into a weak base (bicarbonate) and a strong acid (H^+ ions). This very simple reaction is particularly slow at the physiological pH, while it becomes very effective at higher pH values, being instantaneous at pH > 12 [12,19,21–23].

$$CO_2 + H_2O \rightleftharpoons HCO_3^- + H^+ \qquad \text{eq.1}$$

Carbonic anhydrases make faster this reaction in physiological condition that is important for pH regulation, as well as for other crucial physiological processes like respiration, photosynthesis, pH homeostasis, CO_2 transport and electrolyte secretion, virtually in all tissues in organisms [5,6,9–11,13,24–34].

To date, fifteen isoforms of human carbonic anhydrase (hCAs) have been discovered (hCAI-XIV). They belong to the α-class and share a common organization of the active site, located in a deep cleft and containing a central zinc ion (Zn^{2+}), coordinated by

three histidine residues (His94, His96 and His119) and a water molecule/hydroxide ion (**Figure 1.1**) [5,19,32,35].
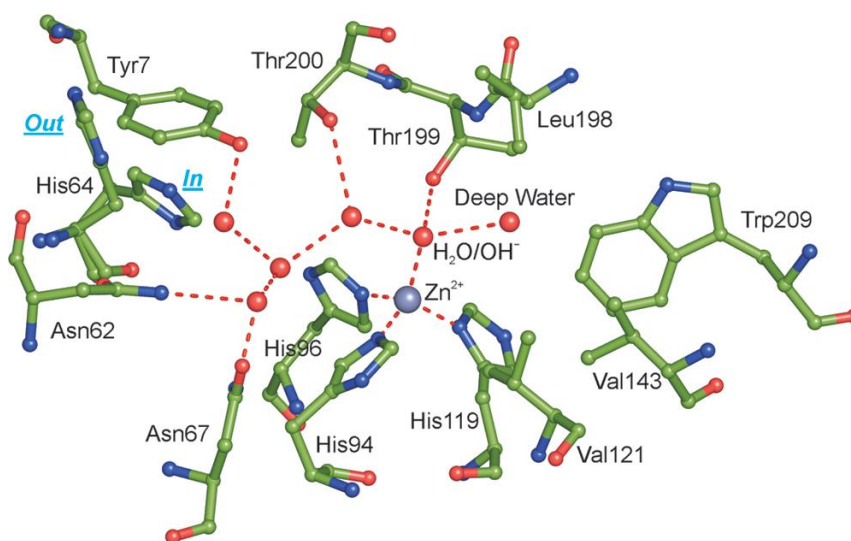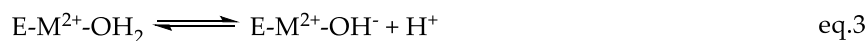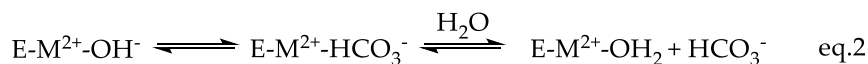

Figure 1.1 Active site of hCA II, showing the network of interactions in the active site. Water molecules are indicated as red circles. The side chain of His64 is shown in both the "*in*" and "*out*" conformations [19].

The zinc-bound water molecule/hydroxide ion establishes hydrogen bond network with the hydroxyl group of Thr residue (Thr 199), and with two water molecules positioned on two opposite side: the first called "deep water" is located in a hydrophobic cavity, while the second is in a hydrophilic environment toward the entrance of the active site (**Figure 1.1**) [19,36]. All these interactions are able to increase zinc bound water molecule nucleophilicity. As a consequence, the proton transfer occurs leading to the production of the catalytically active form of the enzyme containing zinc-bound hydroxide ion. The hydration of carbon dioxide proceeds through a two-step catalytic mechanism (eq.2 and 3).

The first step (eq.2) is the nucleophilic zinc-bound hydroxide ion attack on the CO_2 molecule located in a hydrophobic binding pocket, to obtain metal coordinated bicarbonate. The interaction between bicarbonate and central zinc ion is fairly weak; so, it is displaced by a water molecule and released in solution forming water

coordinated Zn^{2+}, which is the acidic and inactive form of the enzyme (catalytically inactive enzyme, eq.2).

$$E\text{-}M^{2+}\text{-}OH^- \rightleftharpoons E\text{-}M^{2+}\text{-}HCO_3^- \xrightleftharpoons{H_2O} E\text{-}M^{2+}\text{-}OH_2 + HCO_3^- \qquad eq.2$$

$$E\text{-}M^{2+}\text{-}OH_2 \rightleftharpoons E\text{-}M^{2+}\text{-}OH^- + H^+ \qquad eq.3$$

The second step is the rate limiting one in which enzyme's active form (eq.3) is regenerated by the proton transfer directly to the buffer or assisted by His 64, which serves as a proton shuttle between the metal center and buffer molecules of the medium [37]. The presence of His 64 that works as a "proton-shuttle" affects positively the catalytic activity. Indeed the absence of this system in enzymes as CAIII, impaires activity about 500-fold [29,38–40].

This working machinery based on a "ping-pong" mechanism, makes some of the members of the CA superfamily among the most effective enzymes known in nature, with k_{cat}/K_M values close to the limit of the diffusion-controlled processes [25]. How anticipated, human carbonic anhydrases exist in fifteen isoforms which differ by molecular features, oligomeric arrangement, cellular localization, distribution in organs and tissues, expression levels, kinetic properties and response to different classes of inhibitors [5,34,35,41].

Five of these enzymes are cytosolic (hCA I-III, hCA VII and hCA XIII), two are mitochondrial (CA VA and VB), four are membrane bound (hCA IV, hCA IX, hCA XII and hCA XIV), one is secreted (hCA VI) and three are acatalytic hCA-related proteins (CARPs, hCA VIII, X and XI) (**Figure 1.2**). Even if CARPs are acatalytic isozymes because of the absence of metal ion (these proteins not possess histidine residues required for the coordination of the zinc atom) [42], they still possess significant functions in physiologic and pathologic processes as well as the other hCA isoforms (**Table 1.1**) [43].
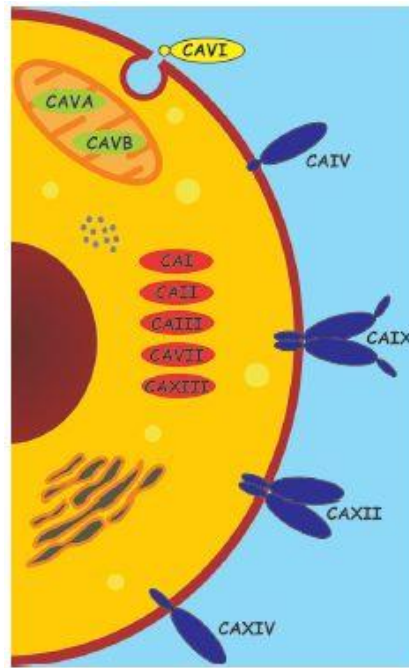
Figure 1.2. Domain composition and subcellular localization of catalytically active human α-Cas [19].

CA I is the major isozyme found in human erythrocytes with a concentration of about 6-fold higher than CA II, also found in erythrocytes. However, the specific activity of CA I in erythrocytes is $2 \times 10^5\,s^{-1}$, whereas the specific activity of CA II in erythrocytes is $10^6\,s^{-1}$. Although CA I has been found to be expressed in a variety of tissues, its physiological role is not completely clear [19]. Feeener's group demonstrated that this enzyme is involved in retinal and cerebral edema, and its inhibition may be a valuable tool for fighting these conditions [44]. CA II is the high activity or "rapid" isozyme in order to distinguish it from the low activity or "slow" one, hCA I. It is expressed in the cytoplasm of many cell types and it is involved in processes spanning from bone resorption to respiration and pH regulation. Other functions include urine formation and bicarbonate reabsorption in the kidney tubules, biosynthetic reactions such as gluconeogenesis, lipogenesis and ureagenesis, bone resorption and calcification, and probably many other less well understood physiologic/pathologic processes [19,45,46]. Deficiency of hCA II is characterized by renal tubular acidosis, osteopetrosis, cerebral calcification, and growth retardation [47]. hCA III is known as muscle isoform because

it is found in high levels in red skeletal muscle, even if this isoform is present also in adipocytes. The activity of hCA III is only 3% that of hCA II and is thought that its physiological importance is beyond its catalytical activity. In fact, this enzyme possesses two reactive sulfhydryl groups able to reversibly bind glutathione, protecting cells from irreversible protein oxidation [48–50]. hCA IV is found in heart [51], brain [52], capillary bed of the eye [53], and erythrocytes [54] and is a possible drug target for several pathologies, including glaucoma (together with CA II and XII), retinitis pigmentosa and stroke [55,56]. The two mitochondrial isoforms hCA VA and hCA VB are implicated in metabolism. hCA VA is found in the mitochondria of the kidney, heart, lung, spleen and intestines; it provides bicarbonate for gluconeogenesis and fatty acids for pyrimidine base synthesis [57]. On the other hand, hCA VB is found in pancreas, kidney and salivary glands mitochondria, showing intermediate role in metabolism [58]. These two isoforms could be useful targets for antiobesity agents [59]. CA VI, the secreted isoform, is implicated in cariogenesis [60,61]. hCA VII has been implicated in neuronal excitation, contributing to epileptiform activity together with CA II and XIV [60–62]. Although hCAVIII not possess catalytic activity, its role has been documented in various pathologies. Indeed, has been associated with neurodegenerative diseases with studies conducted in mice and then in human, showing how mutations in *CA8* gene cause mental retardation and ataxia. CARP VIII is known to be also involved in tumors, being upregulated in colorectal, lung and several other cancers [63]. The precise physiological/pathological roles of the remaining two acatalytic isoforms CA X and XI are poorly known, albeit ongoing studies are trying to shed light on these proteins.

Table 1.1. hCA isoforms, their organ/tissue distribution, subcellular localization, relative CO_2 hydratase activity and diseases in which they are involved.

Isoform	Organ/tissue distribution	Subcellular localization	Catalitic Activity	Involved diseases
CA I	erythrocytes, eye, gastrointestinal tract	cytosol	low	retinal/cerebral edema
CA II	bone osteoclasts, brain, erythrocytes, eye, gastrointestinal tract, kidney, lung, testis	cytosol	high	glaucoma, edema, epilepsy, altitude sickness
CA III	adipocytes, skeletal muscle	cytosol	very low	oxidative stress
CA IV	brain capillaries, colon, eye, kidney, lung, heart muscle pancreas	membrane-bound	medium	glaucoma, retinitis pigmentosa, stroke
CA VA	liver	mitochondria	low	obesity
CA VB	Gastrointestinal tract, kidney, heart and skeletal muscle, pancreas, spinal cord	mitochondria	high	obesity
CA VI	salivary and mammary glands	secreted into saliva and milk	low	cariogenesis
CA VII	central nervous system	cytosol	high	epilepsy
CA VIII	central nervous system	cytosol	acatalytic	neurodegeneration, cancer
CA IX	tumours, gastrointestinal mucosa	transmembrane	high	cancer
CA X	central nervous system	cytosol	acatalytic	NA
CA XI	central nervous system	cytosol	acatalytic	NA
CA XII	Eye, intestine, kidney, reproductive epithelia, tumors	transmembrane	low	cancer, glaucoma
CA XIII	brain, gut, kidney, lung, reproductive tract	cytosol	low	sterility
CA XIV	eye, brain, kidney, liver,	transmembrane	low	epilepsy, retinopathy

hCA XIII was localized in several tissues as the thymus, kidney, submandibular gland, small intestine, and notably in reproductive organs, accounting for its involvement in the sperm motility processes (probably together with CA XIV) [64]. hCA XIV is involved in epileptogenesis and has been localized to the apical and basal membranes of the retinal pigment epithelium. This implies that CA XIV have specific and unique functions in the context of acid-based balance in the retina.

1.2 Involvement of carbonic anhydrase IX and XII isoforms in tumors: the dark side of the enzyme

The two remaining isoforms are the established tumor-related enzymes IX and XII [58,65,66]. These membrane-bound isoforms show a limited expression in normal tissues, unlike hCA I and hCA II [67]. hCA IX is a dimeric transmembrane glycoprotein possessing the catalytic domain oriented toward the extracellular milieu, working at the outer side of the cells [65,68–70]. It is overexpressed mainly in hypoxic tumours, being regulated by hypoxia and facilitate also the metastatic spread of solid tumors [69]. The extracellular acidosis is known to negatively affect drug uptake and radiation damage, so the overexpression of hCA IX is associated to radio- and chemotherapy resistance [71]. hCA XII shares common features with hCA IX, as the secondary structure, orientation and hypoxia induced expression; however, it is a monomer and lacks the proteoglycan-like domain [72]. It has a wider tissue distribution compared with isoform IX, including kidney, lung, prostate, ovaries, uterine endometrium, breast. Unlike isoform hCA IX, hCA XII is regulated by estrogens and in breast cancer patients, hCA XII expression correlates with positive prognosis [73,74]. hCA XII possesses catalytic activity lower than hCA IX [75], and is generally associated with less-aggressive, well-differentiated tumor phenotypes, compared to the hCA IX-expressing tumors [67,76,77]. hCA IX mainly, but probably also hCA XII, regulates intra- and extracellular pH variations which take place in cellular metabolism stimulated by hypoxia. In fact, hypoxia is able to affect genes regulation through hypoxia-inducible factor 1, (HIF-1) favouring cellular adaptation to an anaerobic metabolism [78,79]. HIF-1 is a transcriptional factor protein constituted by two subunits: HIF-1α and HIF-1β. HIF-1β subunit is constitutively expressed and is located inside the nucleus. HIF-1α is an oxygen-regulated subunit working as "O$_2$ sensor" system. During normoxia condition its concentration is influenced by degradation mechanism controlled by oxygen availability. Prolyl-4-hydroxylase (PHD), is able to hydroxylates the P564 on HIF-1α. This modification works as a signal for the von

Hippel-Lindau protein that binds HIF-1α and targets it for degradation by the ubiquitin–proteasome system (**Figure 1.3, a**) [80–88].
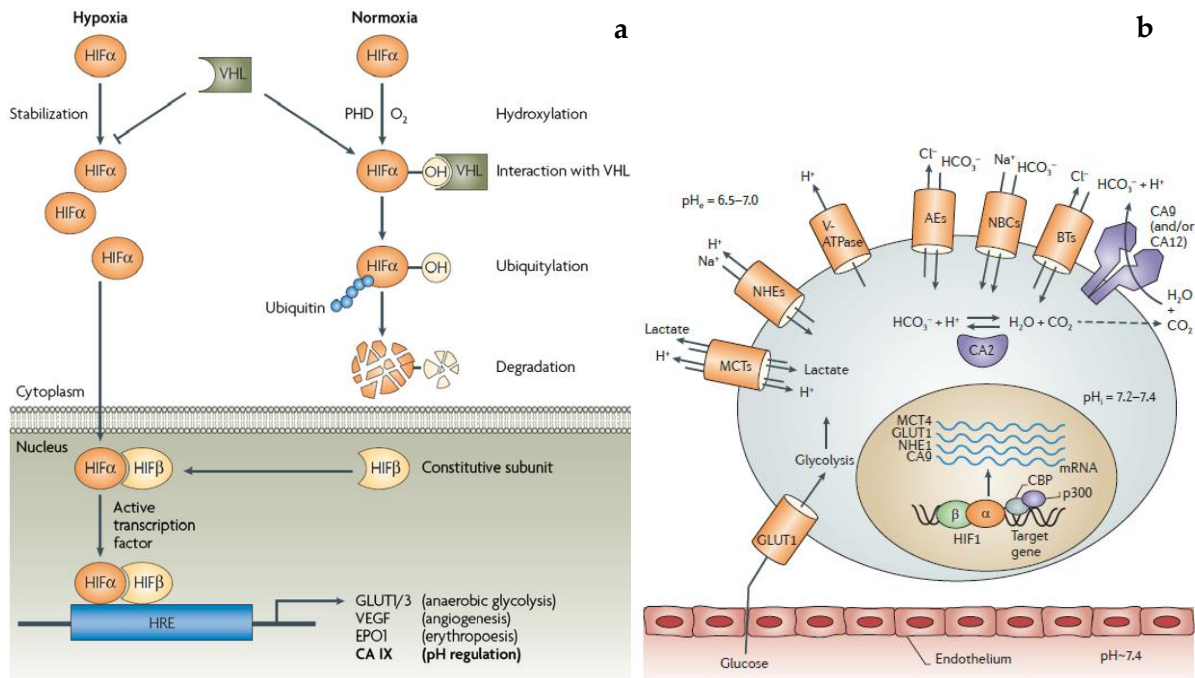

Figure 1.3 (**a**) Mechanism of hypoxia-induced gene expression mediated by the HIF transcription factor [88]; (**b**) Proteins involved in pH regulation within a tumour cell [23].

On the other hand, the lack of oxygen under hypoxia inhibits the PHD activity leading to the absence of HIF-1α hydroxylation which cannot be recognized by the VHL protein. So, HIF-1α translocates to the nucleus where dimerizes with the HIF-1β, constituting the active form of the transcription factor that binds the hypoxia response element (HRE) in target genes and activate their transcription. Target genes include glucose transporters (GLUT1 and GLUT3) that increase glucose caption and take part in glucose metabolism, vascular endothelial growth factor (VEGF) that triggers neoangiogenesis, erythropoietin (EPO1) involved in erythropoiesis, carbonic anhydrase (CA) IX involved in pH regulation and tumorigenesis, and additional genes with functions in cell survival, proliferation, metabolism and other processes. The final effect of this transformation is a cell ready to face hypoxic condition switching the metabolism to anaerobic route. In normal tissues glucose follows the normal aerobic

processes (glycolysis, Krebs-cycle and oxidative phosphorylation) until its complete oxidation to carbon dioxide and water. Cancer cells in hypoxic conditions produce energy from glycolysis and lactic acid fermentation in the cytosol, completely changing its metabolism (the so-called Warburg effect). In this condition cells organize a complex machinery system constituted by transporters, pumps and carbonic anhydrases, able to cope the new state (**Figure 1.3 b**). The new system encourages the extracellular acidification and the maintaining of a weakly alkaline pH, which is optimal for cell proliferation and tumour survival as well as metastatic behaviour [66,89,90].

1.3 Carbonic anhydrase inhibition

Since the discovery of Mann and Keilinin in 1940 about the capability of sulfanilamide to inhibit carbonic anhydrase, the researchers have discovered a huge number of molecules which effectively inhibit hCAs isoforms.

Up to day, five inhibition mechanism have been discovered [91]:

1. CAIs anchoring to the central zinc ion: this kind of inhibition mechanism belong to most of the inhibitors discovered up to day. Compounds exercising this mechanism have a scaffold endowed with an anchoring group (AG) which works as zinc binder group (ZBG) [92–95]. The most used ZBG is the primary sulfonamide moiety, although other groups are able to coordinate central zinc ion (e.g. sulfamates, and sulfamides, which are in fact sulfonamide isosters) [96].

    Although these inhibitors are very effective, inhibiting hCAs in the low nanomolar range, they lack of selectivity due to the common active site organization of the fifteen isoforms. With the aim to increase selectivity, these inhibitors are designed using the "tail approach" [97], which takes advantage from the insertion of functional groups able to interact fairly away from the Zn^{2+} ion, where more differences among the isoforms occur (**Figure 1.4)**.
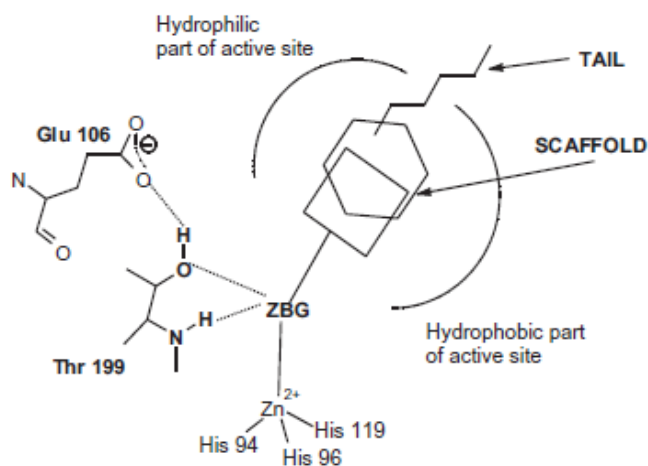
Figure 1.4. CAIs anchoring to the central zinc ion.

2. CAIs anchoring to the zinc-coordinated water/hydroxide ion: belong to this class compounds able to anchor the zinc-coordinated water molecule/hydroxide ion. This mechanism was observed for the first time with phenol, but other compounds showing this kind of inhibition contain primary amine, carboxylic acids or esters, and sulfonic acids [98–100]. The scaffold of these compounds can be aromatic, aliphatic, heterocyclic, or sugar-based type and could be designed keeping in mind the "tail approach" (**Figure 1.5**).
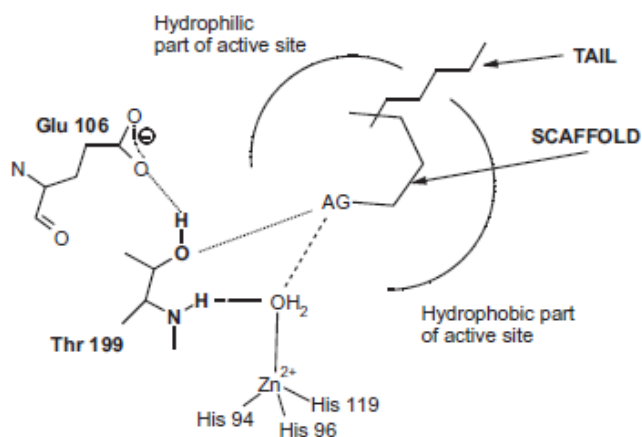

Figure 1.5. CAIs anchoring to the zinc-coordinated water/hydroxide ion.

3. CA inhibition by occlusion of the active site entrance: the first compound with this interesting CA inhibition mechanism was a natural compound with coumarin structure [101]. The *de facto* inhibitor is in this case the hydrolysed form of coumarin, produced because of the esterase activity of hCAs. Other compounds endowed with "sticky group" showed similar activity [102]. The most notable aspect of this inhibition mechanism is that the inhibitors bind the active site region, which is the most variable between the various isoforms, i.e. the entrance to the cavity (**Figure 1.6**).
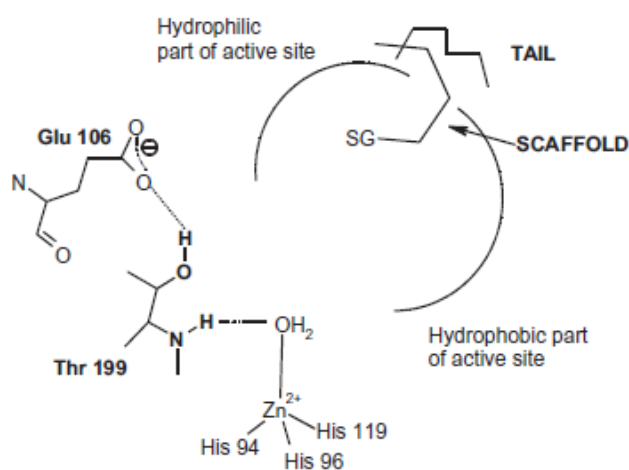

Figure 1.6. CA inhibition by occlusion of the active site entrance

4. Out of the active site binding as a CA inhibition mechanism: this is the last mechanism discovered with crystal structure obtained between hCA II and 2-(benzylsulfonyl)-benzoic acid [103]. The electronic density of the inhibitor was not observed within the active site but in a binding pocket next to to the active site. The compound inhibits hCA blocking the proton-shuttling residue His64 in the "out" conformation, interfering with the transfer of a proton from the zinc-coordinated water molecule to the environment. In this way it prevents the formation of zinc-coordinated hydroxide ion, the active form of the enzyme (**Figure 1.7**).
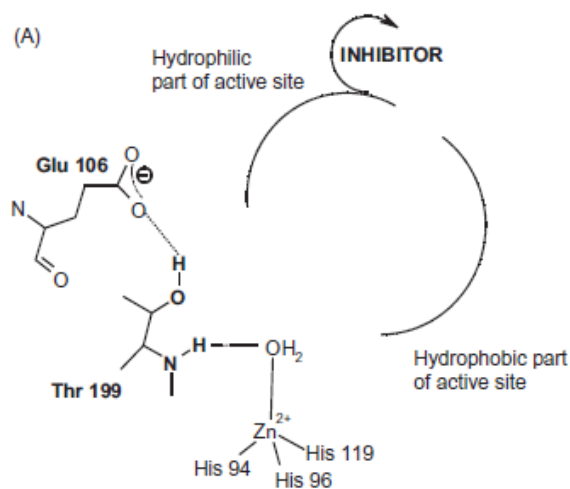
Figure 1.7. Out of the active site binding CA inhibition mechanism.

5. Compounds acting as CAIs with an unknown mechanism of action: finally, there are a series of compounds whose inhibition mechanism has not been discovered, due to the absence of their co-crystal with hCA enzymes. Compounds based on saccharin scaffold, belong to this class.

1.4 Development of new saccharin inhibitors

Saccharin derivatives have been documented as good inhibitors of hCA by various research groups, that in the last years focused their attention towards the development of new molecules based on this scaffold [104–109]. By analysing the structure and substitution pattern of published compounds possessing saccharin scaffold, it is possible to find that for the design of new molecules two general approach have been exploited (**Figure 1.5**). The first is relative to compounds obtained through the substitution of benzene ring of saccharin, with various substituents, maintaining the secondary sulfonamide functional group free (**Figure 1.5**, **I** and **II**). Compounds containing secondary sulfonamides, have been extensively studied for their ability to inhibit hCAs [110–112]. In fact, this approach produced molecules endowed with activity in the nanomolar range against isoforms IX and XII, although residual activity against the off-targets hCA I and hCA II was unfortunately observed [107,113].
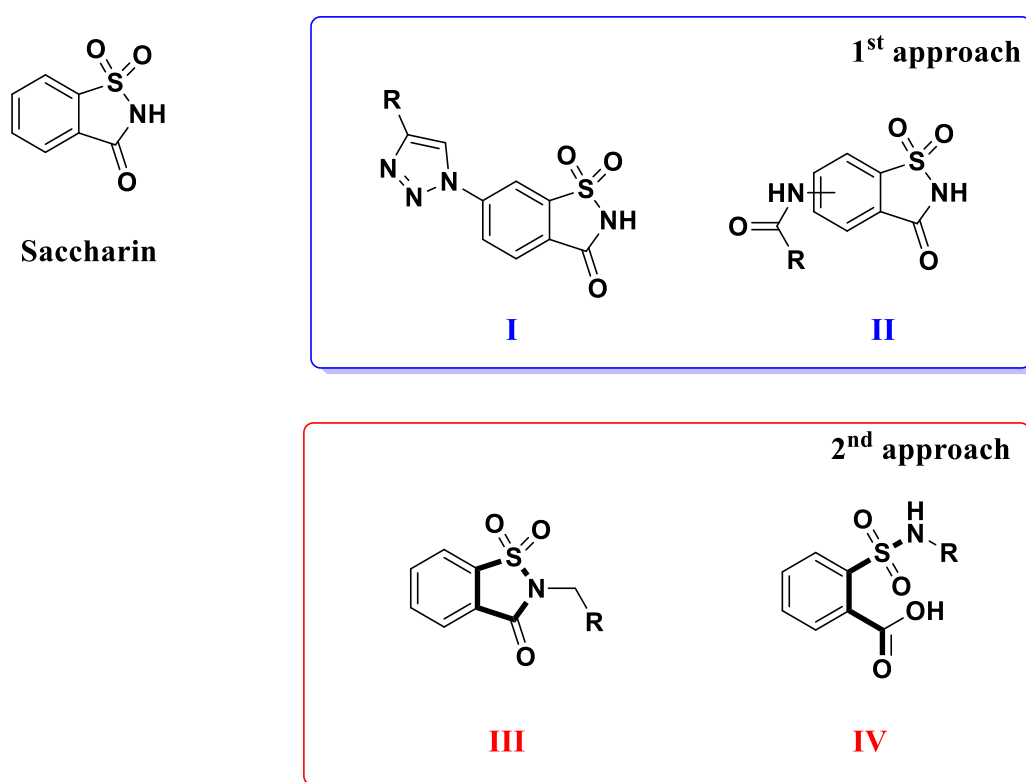

Figure 1.5 The two different approaches for the synthesis of hCAs inhibitors based on saccharin scaffold.

The second approach was based on the substitution of saccharin nitrogen with different groups, in order to obtain *N*-substituted saccharins (**Figure 1.5**, **III**). Tertiary sulfonamides have been investigated for the atypical mechanism that these substances must possess, because they are not able to coordinate zinc ion due to the absence of deprotonable nitrogen atom [114–117]. *N*-substituted saccharins were effective inhibitors of hCA IX and XII, even if some of them retained activity against off-targets [106,109].

Here I report two approaches used to increase activity and selectivity of saccharin-based inhibitors of the two tumor-related isoforms hCA IX and XII. The outcomes of these strategies were the open saccharin-based secondary sulfonamides and the saccharin/isoxazole - saccharin/isoxazoline derivatives.
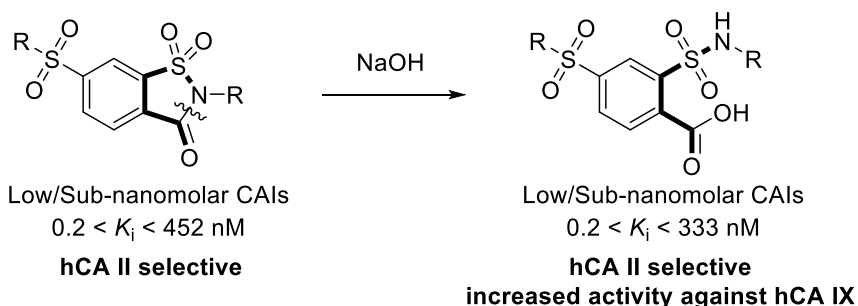
Open saccharin-based secondary sulfonamides as potent and selective

inhibitors of cancer-related carbonic anhydrase IX and XII isoforms

2.1 Open saccharin-based secondary sulfonamides: aim of the work

In a recent publication, Ivanova *et al.* reported on the spontaneous ring opening of cyclic tertiary sulfonamides under basic (pH= 9) crystallization conditions [118]. Since hCAs do not possess any peptidase activity, they concluded that the base-catalysed hydrolysis of the saccharin isothiazolone ring happened before the inhibitor entered the active site, and proved their hypothesis by testing both open and closed analogues against a panel of hCAs (hCA I, hCA II, hCA IX and hCA XII) [119]. In particular, these open saccharin derivatives determined an increased inhibition of hCA IX, while retaining high activity against hCA II. I used a reductive ring opening approach to induce the 5-membered isothiazolone ring of saccharin to collapse into its corresponding secondary sulfonamide and benzyl alcohol (**Figure 2.1**) [120].

Previous work from Ivanova *et al.*:

Low/Sub-nanomolar CAIs
$0.2 < K_i < 452$ nM
hCA II selective

Low/Sub-nanomolar CAIs
$0.2 < K_i < 333$ nM
hCA II selective
increased activity against hCA IX

This paper:

Nanomolar CAIs
$4.3 < K_i < 1570$ nM

hCA II, IX and XII

Nanomolar CAIs
$4.3 < K_i < 382$ nM

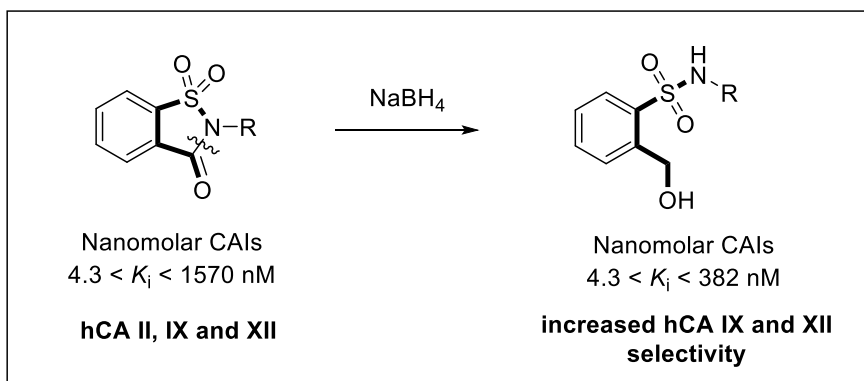**increased hCA IX and XII selectivity**

Figure 2.1. Design of new open-saccharin based inhibitors.

The rationale behind this choice could be found in the opportunity of generating two new potential anchoring points for the zinc ion, while introducing several degrees of freedom to the bonds connecting the two hydrophobic phenyl substituents to the polar core of the molecule. In general, the newly synthesized compounds (**1-21**) proved to be as potent as or slightly less potent than parent inhibitors (**I-XXI**), while the selectivity for the cancer-related isoforms (hCA IX and XII) over the off-target hCA I and II improved dramatically. In fact, none of the reported compounds inhibited hCA I and II isoforms at concentrations lower than 10 nM, while K_i values spanned from 20 to 298 nM against hCA IX and from 4.3 to 382 nM against hCA XII.

2.2 Chemistry

Saccharin (1.0 eq.) was activated using freshly ground anhydrous potassium carbonate and the corresponding salt was then directly reacted with a proper electrophile (2 eq. of substituted benzyl halide or α-haloacetophenone) by stirring the reaction mixture in N,N-dimethylformamide at 80 °C overnight (Scheme 1). Following these optimized conditions (polar aprotic solvent), we strictly obtained only the more stable regioisomers (N-substituted saccharin derivatives) limiting the Chapman-Mumm thermal rearrangement to the less stable O-substituted counterparts [121]. N-substituted saccharin (the parent drugs) derivatives were then subjected to reductive ring opening with an excess of NaBH$_4$ in dry methanol at room temperature for 2-8 hrs to give the corresponding secondary sulfonamide compounds **1-21** in discrete yields following a previously reported procedure with slight modifications [120].
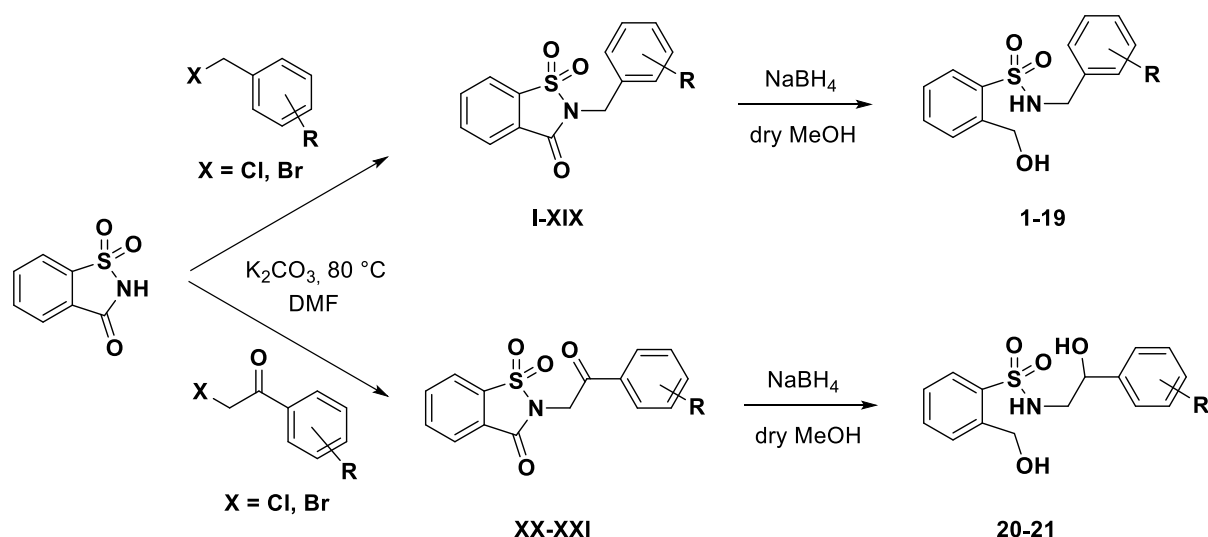
Scheme 2.1. Synthesis and structure of compounds **I-XXI** and **1-21**. For R substituents see **Table 2.1** and **2.2**.

The choice of NaBH$_4$ as a reducing agent was influenced by preliminary experiments which suggested that (*i*) the sulfone group was not affected by these mild reducing conditions leading to the carbonyl group reduction to the alcohol level only with saccharin ring cleavage and that (*ii*) similar results were obtained for the preparation of *o*-hydroxymethyl-*N*-alkyl-benzamides starting from *N*-alkyl-phthalimides [120]. In their IR spectra, I usually registered for the open saccharin derivatives new but expected signals for the OH and NH stretching at 3240 and 3470 cm^{-1}, respectively, and the disappearance of the C=O stretching at 1735 cm^{-1}.

2.3 Biological evaluation

All the synthesized compounds were tested to evaluate their inhibitory activity towards the ubiquitous off-target isoforms, hCA I and II, and the cancer-related ones, hCA IX and XII, by a stopped-flow, CO$_2$ hydrase assay method and their CA inhibition data (K_i) are summarized in **Table 2.1** and **Table 2.2**.

2.4 Results and discussion
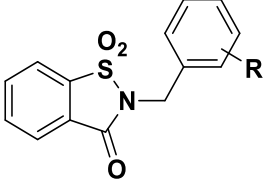
2.4.1 Inhibition of hCA I, II, IX, and XII.

The analysis of the biological data was accomplished comparing the open saccharin-based derivatives (**Table 1**) with their corresponding parent compounds (activities reported in **Table 2**) in order to evaluate if the ring opening enhanced or reduced their biological activity. All the tested compounds had no affinity for the common off-target hCA I and II isoforms (K_is> 10000 nM) compared to their corresponding parent drugs. Moreover, our molecules with a benzyl alcohol group, instead of a carboxylic acid one [118], abolished completely this inhibitory activity improving the biological profile of this scaffold. The inhibition profile of the open saccharin-based derivatives against the two tumor-related hCA IX and XII isoforms also displayed some important changes compared to parent drugs. Among the new open saccharin derivatives reported here, the best activity was obtained toward hCA XII isoform by compounds **1**, **5**, **6**, **10** and **11**, all provided of CH_3 or CF_3 groups. These molecules exhibited a slightly preference for hCA XII respect to hCA IX isoform, although the inhibition of the latter was also in the nanomolar range. Compound **5**, containing a phenyl ring substituted with methyl group in *meta* position, had the highest inhibitory activity against hCA XII (K_i = 4.3 nM), but also compound **6,** containing a *meta* trifluoromethyl substituent on phenyl ring, exhibited similar inhibitory activity (K_i = 4.4 nM). Comparable profile against hCA XII was observed for compounds **10** (K_i = 5.7 nM) and **11** (K_i = 7.2 nM), which are *para* substituted regioisomers of **5** and **6**, respectively. Compound **1**, which had a methyl group at *ortho* position of phenyl ring, showed similar inhibitory activity (K_i hCA XII = 4.7 nM) with respect to **5** and **6**. Other compounds with strong selectivity between hCA IX and XII were **9** (K_i hCA IX = 267 nM, K_i hCA XII = 64 nM) with bromine in *meta* position of phenyl ring, **12** (K_i hCA IX = 126 nM, K_i hCA XII = 57 nM) containing a cyano group in *para* position, **15** (K_i hCA IX = 154 nM, K_i hCA XII = 48 nM) which had a *para* chloro-substituted phenyl ring, **17** and **18** with, respectively, 2,6-difluoro and 3,4-dichloro-substituted phenyl rings.
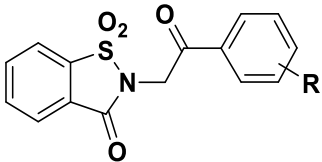
Conversely, some compounds displayed a good selectivity towards hCA IX isoform. Compounds with nitro substituents in *ortho* (**3**), *meta* (**7**) or *para* (**13**) position of the ring had potent inhibitory activity preferentially against this overexpressed isoform in the hypoxic tumoral niche.

For compounds **20** (K_i hCA IX = 224 nM, K_i hCA XII = 64 nM) and **21** (K_i hCA IX = 31 nM, K_i hCA XII = 355 nM), the reaction with NaBH$_4$ led to the further reduction of exocyclic carbonyl moiety. The presence of this additional group maintained the biological profile with a loss of inhibitory activity against hCA I and II and a preferential selectivity against the cancer-related isoforms.

Collectively, these promising data showed that the reductive ring opening of the saccharin nucleus improved the hCA inhibitory activity with a better selectivity with respect to the off-target isoforms. From the above, we also observed that the inhibition profile was affected positively or negatively by the substitution pattern.
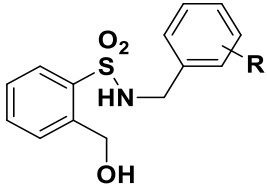
Table 2.1. Inhibitory activity of the saccharin parent drugs **I-XXI** and acetazolamide as a reference drug, against selected hCA isoforms by a stopped-flow CO_2 hydrase assay.

Compound	R	K_i (nM)*			
		hCA I	hCA II	hCA IX	hCA XII
I	2-CH$_3$	1368	> 10000	221	16
II	2-CF$_3$	3579	> 10000	616	15
III	2-NO$_2$	> 10000	40.9	91	28.1
IV	2-Br	> 10000	43.5	> 10000	25.1
V	3-CH$_3$	1503	> 10000	184	26
VI	3-CF$_3$	> 10000	> 10000	19	17
VII	3-NO$_2$	> 10000	39.1	11	24.6
VIII	3-F	> 10000	91	380	2690

IX	3-Br	> 10000	86.8	360	21.1
X	4-CH$_3$	> 10000	> 10000	234	5.1
XI	4-CF$_3$	1347	> 10000	51	4.7
XII	4-CN	> 10000	47.6	240	150
XIII	4-NO$_2$	324	> 10000	1169	29
XIV	4-F	2479	> 10000	539	41
XV	4-Cl	2361	> 10000	19	4.4
XVI	4-Br	> 10000	> 10000	22	4.3
XVII	2,6-diF	>10000	460	> 10000	1310
XVIII	3,4-diCl	> 10000	> 10000	390	2760
XIX	-CH=CH- CH=CH-	> 10000	> 10000	> 10000	2540

XX	H	> 10000	> 10000	> 10000	1780
XXI	3-OCH$_3$	1342	> 10000	1570	6.0
AAZ (acetazolamide)		250	12	25	6.0

*Mean from 3 different assays (errors were in the range of ±5–10% of the reported values).

Table 2.2. Inhibitory activity of the open saccharin-based derivatives **1-21** and acetazolamide as a reference drug, against selected hCA isoforms by a stopped-flow CO_2 hydrase assay.
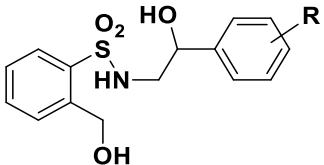

Compound	R	K_i (nM)*			
		hCA I	hCA II	hCA IX	hCA XII
1	2-CH$_3$	>10000	>10000	218	4.6
2	2-CF$_3$	>10000	>10000	200	54
3	2-NO$_2$	>10000	>10000	104	383

4	2-Br	>10000	>10000	113	323
5	3-CH$_3$	>10000	>10000	223	4.3
6	3-CF$_3$	>10000	>10000	238	4.4
7	3-NO$_2$	>10000	>10000	176	382
8	3-F	>10000	>10000	268	247
9	3-Br	>10000	>10000	267	64
10	4-CH$_3$	>10000	>10000	120	5.7
11	4-CF$_3$	>10000	>10000	253	7.2
12	4-CN	>10000	>10000	126	57
13	4-NO$_2$	>10000	>10000	20	54
14	4-F	>10000	>10000	26	63
15	4-Cl	>10000	>10000	154	48
16	4-Br	>10000	>10000	145	432
17	2,6-diF	>10000	>10000	296	45
18	3,4-diCl	>10000	>10000	298	40
19	-CH=CH- CH=CH-	>10000	>10000	294	345
20	H	>10000	>10000	224	64
21	3-OCH$_3$	>10000	>10000	31	355
AAZ (acetazolamide)		250	12	25	6.0

*Mean from 3 different assays (errors were in the range of ±5–10% of the reported values).

2.4.2 Docking studies into the active site of hCA XII

The open saccharin analogs (compounds **1–21**) were endowed with inhibition values in the nanomolar range against hCA XII isoform (K_i values: 4.3–432 nM, Table 1, approximately 100-fold difference between lowest and highest K_i values). The interaction of compound **6** with the active site of hCA XII was shown as an example

(**Figure 2.2**). Docking studies indicated that the hydroxymethyl group and one of the sulfonamide oxygen atoms could interact simultaneously with the Zn^{2+}-ion, whereas the other sulfonamide oxygen atom was water accessible. This oxygen might also form hydrogen bonds with the backbone of Thr199. The other polar substituents of the molecule were water accessible.
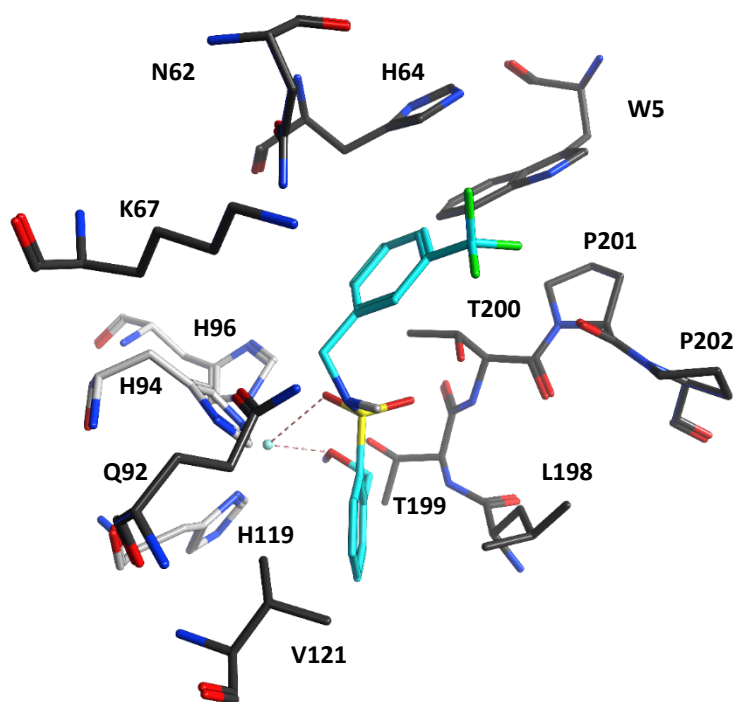

Figure 2.2 Docked pose of compound **6** in the active site of hCA XII. Hydrogen bonds and interactions to the Zn^{2+}-ion are depicted in red dashed lines. The Zn^{2+}-ion is depicted as a turquoise sphere. The three zinc-binding Histidines (H94, H96 and H119) are depicted in light grey for clarity.

2.5 Conclusions

The design, synthesis, characterization and *in vitro* pharmacological evaluation of several new secondary sulfonamides based on the open saccharin scaffold as selective inhibitors of human carbonic anhydrase, have been proposed. They were shown to be inactive against the two cytosolic off-target hCA I and II (K_is > 10 μM); conversely, all these compounds inhibited hCA IX and XII in the low nanomolar range with K_is ranging between 4.3 and 432 nM. The analysis of the K_i values showed as the

substituent on phenyl moiety that gives the best outcomes relative to inhibition of hCA XII isoform are methyl and trifluoromethyl groups. The results were also rationalized by means of docking studies into the active site of hCA XII. Since these two cancer-related hCA isoforms were recently validated as drug targets, these results provided the development of new anticancer candidates.

2.6 Experimental section

General

Solvents and reagents were used as supplied without further purification. Where mixtures of solvents are specified, the stated ratios are volume:volume. Acetazolamide was purchased by Sigma-Aldrich (Italy) and used in the biological assays without further purification. All synthesized compounds have been fully characterized by analytical and spectral data. Column chromatography was carried out using Sigma-Aldrich® silica gel (high purity grade, pore size 60 Å, 200-425 mesh particle size). Analytical thin-layer chromatography was carried out on Sigma-Aldrich® silica gel on TLA aluminum foils with fluorescent indicator. Visualization was carried out under UV irradiation (254 nm). ^{1}H-NMR spectra were recorded on a Bruker AV400 (^{1}H: 400 MHz, ^{13}C: 101 MHz). ^{19}F-NMR spectra were recorded on a Bruker AVANCE 600 spectrometer (^{19}F: 564.7 MHz). Chemical shifts are quoted in ppm, based on appearance rather than interpretation, and are referenced to the residual non deuterated solvent peak. In the case of ^{19}F, chemical shifts are referenced to an external standard (CF$_3$COOH, δ -76.55 ppm). Infra-red spectra were recorded on a Bruker Tensor 27 FTIR spectrometer equipped with an attenuated total reflectance attachment with internal calibration. Absorption maxima (ν_{max}) are reported in wavenumbers (cm^{-1}). All melting points were measured on a Stuart® melting point apparatus SMP1 and are uncorrected. Temperatures are reported in °C. Where given, systematic compound names are those generated by ChemBioDraw Ultra® 12.0 following IUPAC conventions.

**Synthesis and characterization data of compounds I-XXI and 1-21**
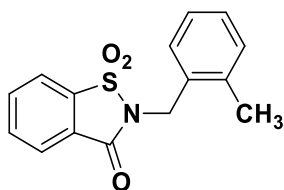
2-(2-Methylbenzyl)-1,2-benzothiazol-3(2*H*)-one 1,1-dioxide (**I**): anhydrous potassium carbonate (1.1 eq.) were added to a stirring solution of saccharin (1.0 eq.) in 10 mL of *N,N*-dimethylformamide. 2-Methylbenzyl bromide (1.1 eq.) was added and the reaction stirred at 80 °C for 48 h. The mixture was poured on ice and the resulting suspension was filtered. Purification *via* column chromatography on silica gel (ethyl acetate:*n*-hexane, 1:2) gave the title compound as a white solid (72% yield); mp 153-155 °C; IR ν_{max} 3073 (ν C$_{sp2}$-H), 1726 (ν C=O), 1335 (ν_{as} S=O), 1244 (ν C-N), 1181 (ν_s S=O), 754 (δ C$_{sp2}$-H), 676 (δ C$_{sp2}$-H) cm^{-1}; ^{1}H-NMR (400 MHz, CDCl$_3$) δ 2.50 (3H, s, CH$_3$), 4.98 (2H, s, CH$_2$), 7.21-7.25 (m, 3H, Ar), 7.44 (d, J = 7.2 Hz, 1H, Ar), 7.83-7.91 (m, 2H, Ar), 7.95 (d, J = 6.8 Hz, 1H, Ar), 8.10 (d, J = 8.0 Hz, 1H, Ar); ^{13}C-NMR (101 MHz, CDCl$_3$) δ 19.3 (CH$_3$), 40.6 (CH$_2$), 121.0 (Ar), 125.3 (Ar), 126.3 (Ar), 127.3 (Ar), 128.3 (Ar), 128.7 (Ar), 130.5 (Ar), 132.1 (Ar), 134.4 (Ar), 134.9 (Ar), 136.3 (Ar), 137.9 (Ar), 159.0 (C=O). Anal. Calcd for C$_{15}$H$_{13}$NO$_3$S: C, 62.70; H, 4.56; N, 4.87. Found: C, 62.52 ; H, 4.81; N, 5.06.
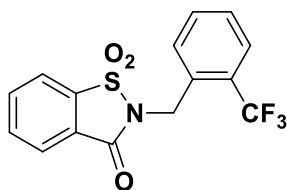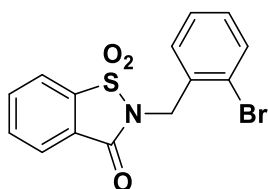

2-(2-Trifluoromethylbenzyl)-1,2-benzothiazol-3(2*H*)-one 1,1-dioxide (**II**): anhydrous potassium carbonate (1.1 eq.) were added to a stirring solution of saccharin (1.0 eq.) in 10 mL of *N,N*-dimethylformamide. 2-Trifluoromethylbenzyl bromide (1.1 eq.) was added and the reaction stirred at 80 °C for 48 h. The mixture was poured on ice and the resulting suspension was filtered. Purification *via* column chromatography on silica gel (ethyl acetate:*n*-hexane, 1:2) gave the title compound as a white solid (60%

yield); mp 142-143 °C; IR ν_{max} 3095 (ν C_{sp2}-H), 1733 (ν C=O), 1336 (ν_{as} S=O), 1241 (ν C-N), 1171 (ν_s S=O), 749 (δ C_{sp2}-H), 676 (δ C_{sp2}-H) cm^{-1}; ^{1}H-NMR (400 MHz, CDCl$_3$) δ 5.20 (2H, s, CH$_2$), 7.41-7.45 (t, 1H, Ar), 7.51-7.57 (m, 2H, Ar), 7.72 (d, J = 8.0 Hz, 1H, Ar), 7.87-7.95 (m, 3H, Ar), 8.13 (d, J = 7.6 Hz, 1H, Ar); ^{13}C-NMR (101 MHz, CDCl$_3$) δ 39.0 (CH$_2$), 121.2 (Ar), 122.9 (Ar), 125.5 (Ar), 126.2 (Ar), 127.0 (Ar), 128.0 (Ar), 128.3 (Ar), 132.3 (Ar), 133.0 (Ar), 134.6 (Ar), 135.1 (Ar), 137.9 (Ar), 159.1 (C=O). ^{19}F-NMR (564.7 MHz, CDCl$_3$) δ -57.34 (s, CF$_3$). Anal. Calcd for C$_{15}$H$_{10}$F$_3$NO$_3$S: C, 52.79; H, 2.95; N, 4.10. Found: C, 52.55 ; H, 3.17; N, 3.91.
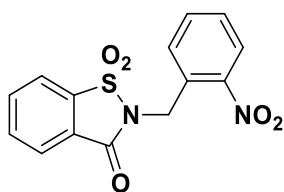
2-(2-nitrobenzyl)benzo[*d*]isothiazol-3(2*H*)-one **1,1-dioxide** **(III):** anhydrous potassium carbonate (1.1 eq.) was added to a stirring solution of saccharin (1.0 eq.) in 10 mL of *N*,*N*-dimethylformamide at room temperature. 2-Nitrobenzyl chloride (1.1 eq.) was added and the reaction mixture was stirred at 80 °C for 24 h. The mixture was poured on ice and the resulting suspension was filtered. Purification by column chromatography on silica gel (ethyl acetate:*n*-hexane 1:2) gave title compound as a white solid (78% yield); mp 173-178 °C; IR ν_{max} 3086 (ν C_{sp2}-H), 1721 (ν C=O), 1526 (ν_{as} N-O), 1333 (ν_{as} SO$_2$), 1302 (ν_s N-O), 1259 (ν C-N), 1178 (ν_s SO$_2$), 723 (δ C_{sp2}-H), 670 (δ C_{sp2}-H) cm^{-1}; ^{1}H-NMR (400 MHz, DMSO-*d$_6$*): δ 5.33 (s, 2H, CH$_2$), 7.63-7.65 (m, 2H, 2 x Ar), 7.75-7.76 (m, 1H, Ar), 8.04-8.18 (m, 4H, 4 x Ar), 8.37-8.38 (m, 1H, Ar); ^{13}C-NMR (101 MHz, DMSO-*d$_6$*): δ 122.18 (Ar), 125.63 (Ar), 125.82 (Ar), 126.72 (Ar), 129.77 (Ar), 129.97 (Ar), 130.36 (Ar), 134.72 (Ar), 135.83 (Ar), 136.45 (Ar), 137.34 (Ar), 148.16 (Ar), 159.28 (*C*=O), (CH$_2$ signal missing due to overlap with DMSO-*d$_6$*).
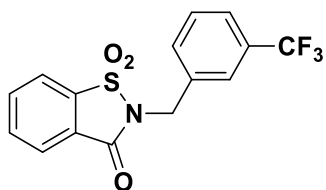
2-(2-bromobenzyl)benzo[*d*]isothiazol-3(2*H*)-one   1,1-dioxide   (IV):   anhydrous potassium carbonate (1.1 eq.) was added to a stirring solution of saccharin (1.0 eq.) in 10 mL of *N,N*-dimethylformamide at room temperature. 2-Bromobenzyl bromide (1.1 eq.) was added and the reaction mixture was stirred at 80 °C overnight. The mixture was poured on ice and the resulting suspension was filtered and washed with *n*-hexane and diethyl ether to give the title compound as a white solid (46% yield); mp 160-161 °C; IR ν_{max} 3095 (ν C$_{sp2}$-H), 1730 (ν C=O), 1334 (ν_{as} SO$_2$), 1259 (ν C-N), 1173 (ν_s SO$_2$), 746 (δ C$_{sp2}$-H), 673 (δ C$_{sp2}$-H) cm^{-1}; ^{1}H-NMR (400 MHz, DMSO-*d*$_6$): δ 4.98 (s, 2H, CH$_2$), 7.25-7.31 (m, 1H, Ar), 7.37-7.45 (m, 2H, Ar), 7.68 (d, J = 8.0 Hz, 1H, Ar), 8.01-8.11 (m, 2H, 2 x Ar), 8.16 (d, J = 7.6 Hz, 1H, Ar), 8.35 (d, J = 7.6 Hz, 1H, Ar); ^{13}C-NMR (101 MHz, DMSO-*d*$_6$): δ 42.48 (*C*H$_2$), 122.13 (Ar), 122.70 (Ar), 125.79 (Ar), 126.69 (Ar), 128.52 (Ar), 129.72 (Ar), 130.41 (Ar), 133.15 (Ar), 134.02 (Ar), 135.81 (Ar), 136.44 (Ar), 137.35 (Ar), 159.08 (*C*=O).
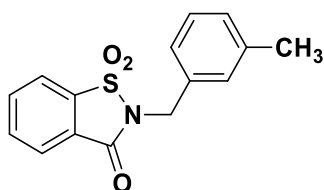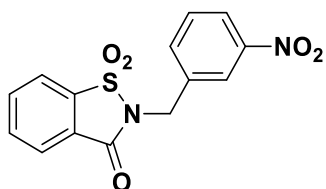

2-(3-Methylbenzyl)-1,2-benzothiazol-3(2*H*)-one   1,1-dioxide   (V):   anhydrous potassium carbonate (1.1 eq.) were added to a stirring solution of saccharin (1.0 eq.) in 10 mL of *N,N*-dimethylformamide. 3-Methylbenzyl bromide (1.1 eq.) was added and the reaction stirred at 80 °C for 48 h. The mixture was poured on ice and the resulting suspension was filtered. Purification *via* column chromatography on silica gel (ethyl acetate:*n*-hexane, 1:2) gave the title compound as a white solid (72% yield); mp 94-96 °C; IR ν_{max} 3065 (ν C$_{sp2}$-H), 1729 (ν C=O), 1329 (ν_{as} S=O), 1260 (ν C-N), 1178 (ν_s S=O), 748 (δ C$_{sp2}$-H), 676 (δ C$_{sp2}$-H) cm^{-1}; ^{1}H-NMR (400 MHz, CDCl$_3$) δ 2.37 (3H, s, CH$_3$), 4.90

(2H, s, CH$_2$), 7.14 (d, J = 7.6 Hz, 1H, Ar), 7.24-7.33 (m, 3H, Ar), 7.82-7.88 (m, 2H, Ar), 7.95 (d, J = 7.2 Hz, 1H, Ar), 8.08 (d, J = 8.0 Hz, 1H, Ar); ^{13}C-NMR (101 MHz, CDCl$_3$) δ 21.4 (CH$_3$), 42.7 (CH$_2$), 121.0 (Ar), 125.2 (Ar), 125.8 (Ar), 127.3 (Ar), 128.6 (Ar), 129.1 (Ar), 129.4 (Ar), 134.3 (Ar), 134.4 (Ar), 134.8 (Ar), 137.8 (Ar), 138.4 (Ar), 158.9 (C=O). Anal. Calcd for C$_{15}$H$_{13}$NO$_3$S: C, 62.70; H, 4.56; N, 4.87. Found: C, 62.99; H, 4.28; N, 4.69.

8.2.4. 2-(3-Trifluoromethylbenzyl)-1,2-benzothiazol-3(2H)-one 1,1-dioxide (VI): anhydrous potassium carbonate (1.1 eq.) were added to a stirring solution of saccharin (1.0 eq.) in 10 mL of *N,N*-dimethylformamide. 3-Trifluoromethylbenzyl bromide (1.1 eq.) was added and the reaction stirred at 80 °C for 48 h. The mixture was poured on ice and the resulting suspension was filtered.. Purification *via* column chromatography on silica gel (ethyl acetate:*n*-hexane, 1:2) gave the title compound as a white solid (79% yield); mp 128-130 °C; IR ν_{max} 3092 (ν C$_{sp2}$-H), 1720 (ν C=O), 1332 (ν_{as} S=O), 1263 (ν C-N), 1175 (ν_s S=O), 752 (δ C$_{sp2}$-H), 680 (δ C$_{sp2}$-H) cm^{-1}; ^{1}H-NMR (400 MHz, CDCl$_3$) δ 4.97 (2H, s, CH$_2$), 7.49-7.52 (m, 1H, Ar), 7.60 (d, J = 8.0 Hz, 1H, Ar), 7.72 (d, J = 7.6 Hz, 1H, Ar), 7.79 (s, 1H, Ar), 7.84-7.97 (m, 3H, Ar), 8.09 (d, J = 7.6 Hz, 1H, Ar); ^{13}C-NMR (101 MHz, CDCl$_3$) δ 42.1 (CH$_2$), 121.1 (Ar), 125.3 (Ar), 125.4 (Ar), 125.6 (Ar), 127.1 (Ar), 129.3 (Ar), 131.0 (Ar), 132.1 (Ar), 134.5 (Ar), 135.0 (Ar), 135.5 (Ar), 137.7 (Ar), 158.9 (C=O). ^{19}F-NMR (564.7 MHz, CDCl$_3$) δ -60.08 (s, CF$_3$). Anal. Calcd for C$_{15}$H$_{10}$F$_3$NO$_3$S: C, 52.79; H, 2.95; N, 4.10. Found: C, 52.98; H, 2.76; N, 4.32.
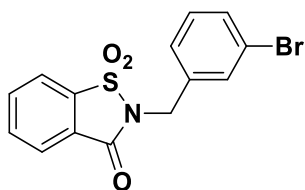
2-(3-nitrobenzyl)benzo[*d*]isothiazol-3(2*H*)-one 1,1-dioxide (VII): anhydrous potassium carbonate (1.1 eq.) was added to a stirring solution of saccharin (1.0 eq.) in 10 mL of *N,N*-dimethylformamide at room temperature. 3-Nitrobenzyl bromide (1.1 eq.) was added and the reaction mixture was stirred at 80 °C for 72 h. The mixture was poured on ice and extracted with dichloromethane. The organics were reunited, dried over sodium sulfate and concentrated *in vacuo*. Purification by column chromatography on silica gel (ethyl acetate:*n*-hexane 1:1) gave the title compound as a white solid (37 % yield); mp 179-181 °C; IR ν_{max} 3091 (ν C_{sp2}-H), 1734 (ν C=O), 1529 (ν_{as} N-O), 1324 (ν_{as} SO_2), 1294 (ν_s N-O), 1263 (ν C-N), 1180 (ν_s SO_2), 751 (δ C_{sp2}-H), 696 (δ C_{sp2}-H) cm^{-1}; ^{1}H-NMR (400 MHz, CD_2Cl_2): δ 4.83 (s, 2H, CH_2), 7.39-7.43 (m, 1H, Ar), 7.68-7.82 (m, 4H, 4 x Ar), 7.91 (d, J = 7.2 Hz, 1H, Ar), 8.01 (d, J = 7.2 Hz, 1H, Ar), 8.18 (s, 1H, Ar); ^{13}C-NMR (101 MHz, CD_2Cl_2): δ 41.58 (*CH*$_2$), 121.13 (Ar), 123.16 (Ar), 123.40 (Ar), 125.30 (Ar), 127.03 (Ar), 129.76 (Ar), 134.59 (Ar), 134.69 (Ar), 135.27 (Ar), 136.94 (Ar), 137.55 (Ar), 148.10 (Ar), 158.94 (*C*=O).
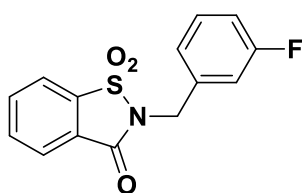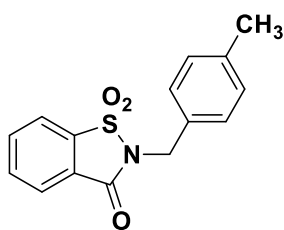

2-(3-fluorobenzyl)benzo[*d*]isothiazol-3(2*H*)-one 1,1-dioxide (VIII): anhydrous potassium carbonate (1.1 eq.) was added to a stirring solution of saccharin (1.0 eq.) in 10 mL of *N,N*-dimethylformamide at room temperature. 3-Fluorobenzyl chloride (1.1 eq.) was added and the reaction mixture was stirred at 80 °C for 48 h. The mixture was poured on ice and the resulting suspension was filtered and washed with petroleum ether to give compound **18a** as a white solid (34% yield); mp 105-107 °C; IR ν_{max} 3075 (ν C_{sp2}-H), 1735 (ν C=O), 1316 (ν_{as} SO_2), 1264 (ν C-N), 1179 (ν_s SO_2), 752 (δ C_{sp2}-H), 673

(δ C$_{sp2}$-H) cm^{-1}; ^{1}H-NMR (400 MHz, DMSO-d_6): δ 4.96 (s, 2H, CH$_2$), 7.12-7.17 (m, 1H, Ar), 7.26-7.28 (m, 2H, 2 x Ar), 7.39-7.44 (m, 1H, Ar), 7.94-8.18 (m, 3H, Ar), 8.35 (d, J = 7.2 Hz, 1H, Ar); ^{13}C-NMR (101 MHz, DMSO-d_6): δ 41.47 (CH$_2$), 114.98 (Ar), 115.19 (Ar), 122.12 (Ar), 124.28 (Ar), 125.71 (Ar), 126.72 (Ar), 131.04 (Ar), 135.77 (Ar), 136.37 (Ar), 137.26 (Ar), 138.54 (Ar), 159.12 (C=O), 162.57 (d, J = 244.42 Hz, Ar).

2-(3-bromobenzyl)benzo[*d*]isothiazol-3(2*H*)-one 1,1-dioxide (IX): anhydrous potassium carbonate (1.1 eq.) was added to a stirring solution of saccharin (1.0 eq.) in 10 mL of *N*,*N*-dimethylformamide at room temperature. 3-Bromobenzyl bromide (1.1 eq.) was added and the reaction mixture was stirred at 80 °C for 72 h. The mixture was poured on ice and extracted with dichloromethane. The organics were reunited, dried over sodium sulfate, and evaporated *in vacuo*. Purification by column chromatography on silica gel (ethyl acetate:petroleum ether 1:2) gave the title compounds as a white solid (86% yield); mp 92-95 °C; IR ν$_{max}$ 1720 (ν C=O), 1330 (ν$_{as}$ SO$_2$), 1265 (ν C-N), 1180 (ν$_s$ SO$_2$), 705 (δ C$_{sp2}$-H) cm^{-1}; ^{1}H-NMR (400 MHz, DMSO-d_6): δ 4.95 (s, 2H, CH$_2$), 7.31-7.35 (m, 1H, Ar), 7.43-7.45 (m, 1H, Ar), 7.49-7.51 (m, 1H, Ar), 7.65 (s, 1H, Ar), 7.98-8.12 (m, 3H, Ar), 8.34 (d, J = 7.2 Hz, 1H, Ar); ^{13}C-NMR (101 MHz, DMSO-d_6): δ 41.35 (CH$_2$), 122.13 (Ar), 125.73 (Ar), 126.70 (Ar), 127.38 (Ar), 131.03 (Ar), 131.16 (Ar), 135.79 (Ar), 136.38 (Ar), 137.25 (Ar), 138.42 (Ar), 159.13 (C=O) (two aromatic carbon missing due to signals overlapping).
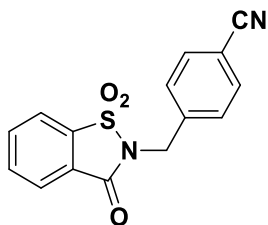
2-(4-Methylbenzyl)-1,2-benzothiazol-3(2*H*)-one   1,1-dioxide   (X):   anhydrous potassium carbonate (1.1 eq.) were added to a stirring solution of saccharin (1.0 eq.) in 10 mL of *N,N*-dimethylformamide. 4-Methylbenzyl bromide (1.1 eq.) was added and the reaction stirred at 80 °C for 48 h. The mixture was poured on ice and the resulting suspension was filtered. Purification *via* column chromatography on silica gel (ethyl acetate:*n*-hexane, 1:2) gave the title compound as a white solid (67% yield); mp 111-113 °C; IR ν_{max} 2920 (ν C_{sp3}-H), 1732 (ν C=O), 1329 (ν_{as} S=O), 1257 (ν C-N), 1174 (ν_s S=O), 747 (δ C_{sp2}-H), 674 (δ C_{sp2}-H) cm^{-1}; ^{1}H-NMR (400 MHz, CDCl$_3$) δ 2.35 (3H, s, CH$_3$), 4.89 (2H, s, CH$_2$), 7.18 (d, J = 8.0 Hz, 2H, Ar), 7.42 (d, J = 8.0 Hz, 2H, Ar), 7.81-7.88 (m, 3H, Ar), 8.06 (d, J = 8.0 Hz, 1H, Ar); ^{13}C-NMR (101 MHz, CDCl$_3$) δ 21.2 (CH$_3$), 42.5 (CH$_2$), 121.0 (Ar), 125.2 (Ar), 127.4 (Ar), 128.8 (Ar), 129.4 (Ar), 131.5 (Ar), 134.3 (Ar), 134.7 (Ar), 137.8 (Ar), 138.1 (Ar), 158.9 (C=O). Anal. Calcd for C$_{15}$H$_{13}$NO$_3$S: C, 62.70; H, 4.56; N, 4.87. Found: C, 62.57; H, 4.34; N, 4.58.
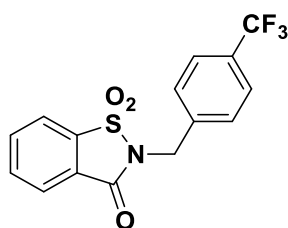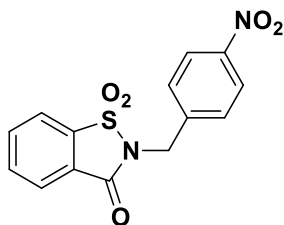

2-(4-Trifluoromethylbenzyl)-1,2-benzothiazol-3(2*H*)-one   1,1-dioxide   (XI): anhydrous potassium carbonate (1.1 eq.) were added to a stirring solution of saccharin (1.0 eq.) in 10 mL of *N,N*-dimethylformamide. 4-Trifluoromethylbenzyl bromide (1.1 eq.) was added and the reaction stirred at 80 °C for 48 h. The mixture was poured on ice and the resulting suspension was filtered. Purification *via* column chromatography on silica gel (ethyl acetate:*n*-hexane, 1:2) gave the title compound as a white solid (57% yield); mp 119-121 °C; IR ν_{max} 2963 (ν C_{sp3}-H), 1741 (ν C=O), 1319 (ν_{as} S=O), 1264 (ν C-N), 1167 (ν_s S=O), 750 (δ C_{sp2}-H), 679 (δ C_{sp2}-H) cm^{-1}; ^{1}H-NMR (400 MHz, CDCl$_3$) δ 4.97 (2H, s, CH$_2$), 7.64 (bs, 4H, Ar), 7.84-7.98 (m, 3H, Ar), 8.08 (d, J = 8.0 Hz, 1H, Ar); ^{13}C-NMR (101 MHz, CDCl$_3$) δ 42.0 (CH$_2$), 121.2 (Ar), 125.4 (Ar), 125.6 (Ar), 125.7 (Ar), 127.1 (Ar), 129.0 (Ar), 134.5 (Ar), 135.0 (Ar), 137.7 (Ar), 138.4 (Ar), 158.9 (C=O). ^{19}F-NMR

(564.7 MHz, CDCl₃) δ -60.12 (s, CF₃). Anal. Calcd for $C_{15}H_{10}F_3NO_3S$: C, 52.79; H, 2.95; N, 4.10. Found: C, 53.04; H, 2.78; N, 3.95.

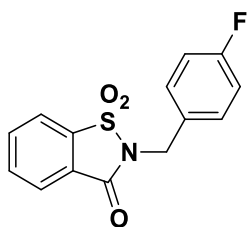**4-((1,1-dioxido-3-oxobenzo[*d*]isothiazol-2(3*H*)-yl)methyl)benzonitrile** **(XII):** anhydrous potassium carbonate (1.1 eq.) was added to a stirring solution of saccharin (1.0 eq.) in 10 mL of *N,N*-dimethylformamide at room temperature. 4-(Bromomethyl)benzonitrile (1.1 eq.) was added and the reaction mixture was stirred at 80 °C for 72 h. The mixture was poured on ice and the resulting suspension was filtered. Purification by column chromatography on silica gel (ethyl acetate:petroleum ether 1:1) gave compound **10a** as a white solid (71% yield); mp 178-180 °C; IR ν_{max} 3096 (ν C$_{sp2}$-H), 2227 (ν C≡N), 1723 (ν C=O), 1334 (ν_{as} SO₂), 1254 (ν C-N), 1181 (ν_s SO₂), 751 (δ C$_{sp2}$-H), 673 (δ C$_{sp2}$-H) cm⁻¹; ¹H-NMR (400 MHz, DMSO-*d₆*): δ 5.05 (s, 2H, CH₂), 7.62 (d, J = 7.2 Hz, 2H, 2 x Ar), 7.85 (d, J = 7.2 Hz, 2H, 2 x Ar), 8.01-8.16 (m, 3H, 3 x Ar), 8.37 (d, J = 7.6 Hz, 1H, Ar); ¹³C-NMR (101 MHz, DMSO-*d₆*): δ 41.57 (*C*H₂), 111.05 (*C*N), 119.08 (Ar), 122.18 (Ar), 125.77 (Ar), 126.69 (Ar), 129.03 (Ar), 132.94 (Ar), 135.85 (Ar), 136.45 (Ar), 137.26 (Ar), 141.37 (Ar), 159.15 (*C*=O).
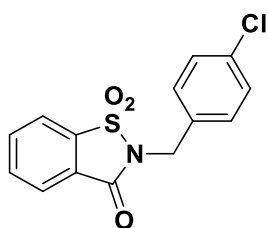

2-(4-Nitrobenzyl)-1,2-benzothiazol-3(2*H*)-one **1,1-dioxide** **(XIII)**: anhydrous potassium carbonate (1.1 eq.) was added to a stirring solution of saccharin (1.0 eq.) in 10 mL of *N,N*-dimethylformamide. Then 4-nitrobenzyl bromide (1.1 eq.) was added and the reaction mixture was stirred at 80 °C for 24 h. The mixture was poured on ice
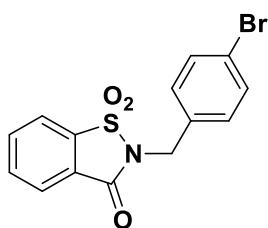
and the resulting suspension was filtered and washed with water and *n*-hexane. Purification by column chromatography on silica gel (ethyl acetate:petroleum ether, 1:3) gave the title compound as a yellow powder (91% yield); mp 178-180 °C; IR ν_{max} 3092 (ν C_{sp2}-H), 1727 (ν C=O), 1516 (ν_{as} N-O), 1338 (ν_{as} S=O), 1299 (ν_s N-O), 1248 (ν C-N), 1197 (ν_s S=O), 755 (δ C_{sp2}-H) cm^{-1}; ^{1}H-NMR (400 MHz, DMSO-d_6) δ 5.10 (s, 2H, CH$_2$), 7.69-7.71 (m, 2H, Ar), 8.03-8.36 (m, 6H, Ar); ^{13}C-NMR (101 MHz, DMSO-d_6) δ 41.3 (CH$_2$), 122.2 (Ar), 124.1 (Ar), 125.7 (Ar), 126.7 (Ar), 129.3 (Ar), 135.8 (Ar), 136.4 (Ar), 137.2 (Ar), 143.3 (Ar), 147.5 (Ar), 159.1 (*C*=O). Anal. Calcd for C$_{14}$H$_{10}$N$_2$O$_5$S: C, 52.83; H, 3.17; N, 8.80. Found: C, 52.56; H, 3.41; N, 9.04.

2-(4-Fluorobenzyl)-1,2-benzothiazol-3(2*H*)-one 1,1-dioxide (**XIV**): anhydrous potassium carbonate (1.1 eq.) was added to a stirring solution of saccharin (1.0 eq.) in 10 mL of *N,N*-dimethylformamide. Then 4-fluorobenzyl bromide (1.5 eq.) was added and the reaction mixture was stirred at 80 °C for 72 h. The mixture was poured on ice and the resulting suspension was filtered and washed with water and petroleum ether. Purification by column chromatography on silica gel (ethyl acetate:*n*-hexane, 1:3) gave the title compound as a white powder (89% yield); mp 125-126 °C; IR ν_{max} 1726 (ν C=O), 1335 (ν_{as} S=O), 1295 (ν C-N), 1180 (ν_s S=O), 1158 (ν C_{sp2}-F), 838 (δ C_{sp2}-H) cm^{-1}; ^{1}H-NMR (400 MHz, DMSO-d_6) δ 4.92 (s, 2H, CH$_2$), 7.18 (t, J = 8.8 Hz, 2H, Ar), 7.47-7.50 (m, 2H, Ar), 7.97-8.11 (m, 3H, Ar), 8.31 (d, J = 7.6 Hz, 1H, Ar); ^{13}C-NMR (101 MHz, DMSO-d_6) δ 41.4 (CH$_2$), 115.6 (Ar), 115.9 (Ar), 122.1 (Ar), 125.6 (Ar), 126.7 (Ar), 130.6 (Ar), 130.7 (Ar), 131.8 (Ar), 135.7 (Ar), 136.3 (Ar), 137.3 (Ar), 159.1 (*C*=O), 162.2 (d, J$_{C-F}$ = 244.9 Hz, Ar). ^{19}F-NMR (564.7 MHz, CDCl$_3$) δ -111.04 (tt, J$_{F-H}$ = 8.6 Hz (ortho), 5.2 Hz (meta), CF). Anal. Calcd for C$_{14}$H$_{10}$FNO$_3$S: C, 57.72; H, 3.46; N, 4.81. Found: C, 57.99; H, 3.67; N, 4.55.
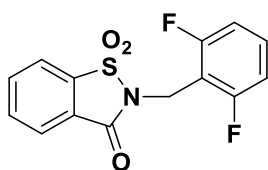
2-(4-Chlorobenzyl)-1,2-benzothiazol-3(2*H*)-one 1,1-dioxide (**XV**): anhydrous potassium carbonate (1.1 eq.) was added to a stirring solution of saccharin (1.0 eq.) in 10 mL of *N,N*-dimethylformamide. Then 4-chlorobenzyl bromide (1.1 eq.) was added and the reaction mixture was stirred at 80 °C for 48 h. The mixture was poured on ice and the resulting suspension was filtered and washed with water, petroleum ether and diethyl ether. Purification by column chromatography on silica gel (ethyl acetate:petroleum ether, 1:3) gave the title compound as a white powder (89% yield); mp 153-155 °C; IR ν_{max} 3092 (ν C_{sp2}-H), 1726 (ν C=O), 1331 (ν_{as} S=O), 1307 (ν C-N), 1197 (ν_s S=O), 749 (δ C_{sp2}-H) cm^{-1}; ^{1}H-NMR (400 MHz, DMSO-d_6) δ 4.93 (s, 2H, CH$_2$), 7.41-7.45 (m, 4H, Ar), 7.98-8.08 (m, 3H, Ar), 8.30-8.32 (m, 1H, Ar); ^{13}C-NMR (101 MHz, DMSO-d_6) δ 41.4 (*C*H$_2$), 122.1 (Ar), 125.6 (Ar), 126.7 (Ar), 128.9 (Ar), 130.3 (Ar), 133.0 (Ar), 134.6 (Ar), 135.6 (Ar), 136.3 (Ar), 137.2 (Ar), 159.1 (*C*=O). Anal. Calcd for C$_{14}$H$_{10}$ClNO$_3$S: C, 54.64; H, 3.28; N, 4.55. Found: C, 54.90; H, 3.47; N, 4.27.
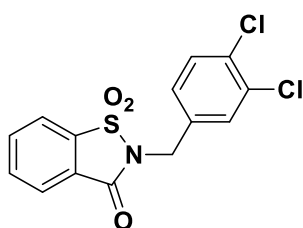

2-(4-Bromobenzyl)-1,2-benzothiazol-3(2*H*)-one 1,1-dioxide (**XVI**): anhydrous potassium carbonate (1.1 eq.) was added to a stirring solution of saccharin (1.0 eq.) in 10 mL of *N,N*-dimethylformamide. Then 4-bromobenzyl bromide (1.5 eq.) was added and the reaction mixture was stirred at 80 °C for 72 h. The mixture was poured on ice and the resulting suspension was filtered and washed with water and petroleum ether. Purification by column chromatography on silica gel (ethyl acetate:petroleum ether,

1:3) gave the title compound as a white powder (89% yield); mp 158-160 °C; IR ν_{max} 1725 (ν C=O), 1332 (ν_{as} S=O), 1303 (ν C-N), 1180 (ν_s S=O or ν C-Br), 861 (δ C_{sp2}-H) cm^{-1}; ^{1}H-NMR (400 MHz, CDCl$_3$) δ 4.87 (s, 2H, CH$_2$), 7.40 (d, J = 8.4 Hz, 2H, Ar), 7.49 (d, J = 8.4 Hz, 2H, Ar), 7.81-7.95 (m, 3H, Ar), 8.06 (d, J = 7.2 Hz, 1H, Ar); ^{13}C-NMR (101 MHz, CDCl$_3$) δ 42.0 (CH$_2$), 121.1 (Ar), 122.4 (Ar), 125.3 (Ar), 127.1 (Ar), 130.5 (Ar), 131.9 (Ar), 133.6 (Ar), 134.5 (Ar), 134.9 (Ar), 137.6 (Ar), 158.9 (C=O). Anal. Calcd for C$_{14}$H$_{10}$BrNO$_3$S: C, 47.74; H, 2.86; N, 3.98. Found: C, 47.92; H, 3.01; N, 4.15.

2-(2,6-difluorobenzyl)benzo[d]isothiazol-3(2H)-one 1,1-dioxide (XVII): anhydrous potassium carbonate (1.1 eq.) was added to a stirring solution of saccharin (1.0 eq.) in 10 ml of N,N-dimethylformamide at room temperature. 2,6-Difluorbenzyl bromide (1.1 eq.) was added and the reaction mixture was stirred at 80 °C overnight. The mixture was poured on ice and the resulting suspension was filtered and washed with petroleum ether to give compound **20a** as a white solid (81% yield); mp 173-175 °C; IR ν_{max} 1733 (ν C=O), 1338 (ν_{as} SO$_2$), 1295 (ν C_{sp2}-F), 1252 (ν C-N), 1181 (ν_s SO$_2$), 753 (δ C_{sp2}-H), 673 (δ C_{sp2}-H) cm^{-1}; ^{1}H-NMR (400 MHz, DMSO-d_6): δ 5.01 (s, 2H, CH$_2$), 7.13-7.17 (m, 2H, 2 x Ar), 7.46-7.50 (m, 1H, Ar), 8.01-8.06 (m, 2H, 2 x Ar), 8.15 (d, J = 7.2 Hz, 1H, Ar), 8.28 (d, J = 7.2 Hz, 1H, Ar); ^{13}C-NMR (101 MHz, DMSO-d_6): δ 30.27 (CH$_2$), 110.81 (Ar), 112.02 (Ar), 121.93 (Ar), 125.78 (Ar), 126.45 (Ar), 131.82 (Ar), 135.82 (Ar), 136.48 (Ar), 137.17 (Ar), 158.21 (C=O), 161.52 (d, J = 258.36 Hz, Ar).
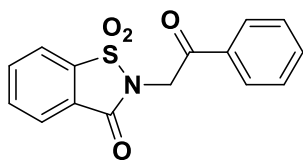
2-(3,4-dichlorobenzyl)benzo[*d*]isothiazol-3(2*H*)-one 1,1-dioxide (XVIII): anhydrous potassium carbonate (1.1 eq.) was added to a stirring solution of saccharin (1.0 eq.) in 10 mL of *N,N*-dimethylformamide at room temperature. 3,4-Dichlorobenzyl chloride (1.1 eq.) was added and the reaction mixture was stirred at 80 °C for 48 h. The mixture was poured on ice and the resulting suspension was filtered and washed with petroleum ether and diethyl ether to give the title compound as a white solid (46% yield); mp 135-137 °C; IR ν_{max} 3079 (ν C_{sp2}-H), 1726 (ν C=O), 1312 (ν_{as} SO_2), 1263 (ν C-N), 1182 (ν_s SO_2), 749 (δ C_{sp2}-H), 675 (δ C_{sp2}-H) cm^{-1}; ^{1}H-NMR (400 MHz, DMSO-d_6): δ 4.76 (s, 2H, CH_2), 7.22 (d, J = 7.6 Hz, 1H, Ar), 7.43 (d, J = 8.0 Hz, 1H, Ar), 7.51 (s, 1H, Ar), 7.81-7.93 (m, 3H, 3 x Ar), 8.15 (d, J = 7.2 Hz, 1H, Ar); ^{13}C-NMR (101 MHz, DMSO-d_6): δ 40.83 (CH_2), 122.14 (Ar), 125.74 (Ar), 126.74 (Ar), 128.66 (Ar), 130.39 (Ar), 130.98 (Ar), 131.17 (Ar), 131.54 (Ar), 135.79 (Ar), 136.38 (Ar), 136.89 (Ar), 137.22 (Ar), 159.12 (*C*=O).
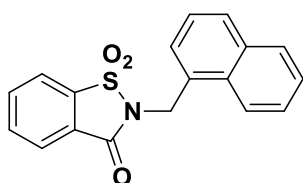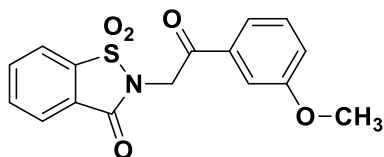

2-(naphthalen-1-ylmethyl)benzo[*d*]isothiazol-3(2*H*)-one   1,1-dioxide   (XIX): anhydrous potassium carbonate (1.1 eq.) was added to a stirring solution of saccharin (1.0 eq.) in 10 mL of *N,N*-dimethylformamide at room temperature. 1-(Chloromethyl)naphthalene (1.1 eq.) was added and the reaction mixture was stirred at 80 °C for 72 h. The mixture was poured on ice and extracted with dichloromethane. The organics were reunited, dried over sodium sulfate and evaporated *in vacuo*. Purification by column chromatography on silica gel (ethyl acetate:petroleum ether 1:2) gave the title compound as a white solid (19% yield); mp 142-145 °C; IR ν_{max} 3047 (ν C_{sp2}-H), 1726 (ν C=O), 1336 (ν_{as} SO_2), 1298 (ν C-N), 1171 (ν_s SO_2), 748 (δ C_{sp2}-H), 675 (δ C_{sp2}-H) cm^{-1}; ^{1}H-NMR (400 MHz, DMSO-d_6): δ 5.43 (s, 2H, CH_2), 7.49-7.63 (m, 4H, 4 x Ar), 7.92-8.09 (m, 4H, 4 x Ar), 8.18-8.24 (m, 2H, Ar), 8.33-8.35 (m, 1H, Ar); ^{13}C-NMR (101 MHz, DMSO-d_6): δ 122.05 (Ar), 123.53 (Ar), 125.81 (Ar), 125.85 (Ar), 126.54 (Ar),

126.65 (Ar), 127.12 (Ar), 129.07 (Ar), 129.16 (Ar), 130.48 (Ar), 130.94 (Ar), 133.71 (Ar), 135.80 (Ar), 136.45 (Ar), 137.46 (Ar), 159.27 (C=O), (CH_2 signal missing due to overlap with DMSO-d_6).
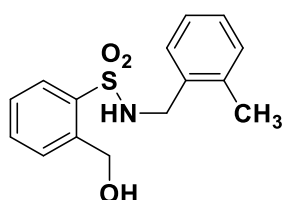

2-(2-oxo-2-phenylethyl)benzo[d]isothiazol-3(2H)-one 1,1-dioxide (XX): anhydrous potassium carbonate (1.1 eq.) was added to a stirring solution of saccharin (1.0 eq.) in 10 mL of N,N-dimethylformamide at room temperature. α-Bromoacetophenone (1.1 eq.) was added and the reaction mixture was stirred at 80 °C overnight. The mixture was poured on ice and the resulting suspension was filtered and washed with petroleum ether and diethyl ether to give the title compound as a yellow solid (89% yield); mp 192-194 °C; IR ν_{max} 3070 (ν C_{sp2}-H), 1735 (ν C=O), 1698 (ν C=O), 1332 (ν_{as} SO_2), 1296 (ν C-N), 1180 (ν_s SO_2), 744 (δ C_{sp2}-H), 673 (δ C_{sp2}-H) cm^{-1}; ^{1}H-NMR (400 MHz, DMSO-d_6): δ 5.49 (s, 2H, CH_2), 7.60 (t, J = 7.4 Hz, 2H, 2 x Ar), 7.74 (t, J = 7.2 Hz, 1H, Ar), 8.03-8.07 (m, 1H, Ar), 8.09-8.12 (m, 3H, 3 x Ar), 8.17 (d, J = 7.6 Hz, 1H, Ar), 8.37 (d, J = 7.6 Hz, 1H, Ar); ^{13}C-NMR (101 MHz, DMSO-d_6): δ 45.32 (CH_2), 122.22 (Ar), 125.64 (Ar), 126.67 (Ar), 128.86 (Ar), 129.43 (Ar), 134.28 (Ar), 134.77 (Ar), 135.86 (Ar), 136.50 (Ar), 137.72 (Ar), 159.35 (C=O), 190.61 (C=O).


2-[2-(3-Methoxyphenyl)-2-oxoethyl]-1,2-benzothiazol-3(2H)-one 1,1-dioxide (**XXI**): anhydrous potassium carbonate (1.1 eq.) was added to a stirring solution of saccharin (1.0 eq.) in 10 mL of N,N-dimethylformamide. 2-bromo-3′-methoxyacetophenone (1.1 eq.) was added and the reaction mixture was stirred at 80 °C for 72 h. The mixture was poured on ice and the resulting suspension was filtered and washed with water and

petroleum ether. Purification by column chromatography on silica gel (ethyl acetate:petroleum ether, 1:3) gave the title compound as a yellow powder (58% yield); mp 167-169 °C; mp 167-169 °C; IR ν_{max} 1736 (ν C=O), 1694 (ν C=O), 1328 (ν_{as} S=O), 1258 (ν C-N), 1182 (ν_s S=O), 864 (δ C_{sp2}-H) 752 (δ_o C_{sp2}-H) cm^{-1}; ^{1}H-NMR (400 MHz, CDCl$_3$) δ 3.86 (s, 3H, OCH$_3$), 5.14 (s, 2H, CH$_2$), 7.18-7.20 (m, 1H, Ar), 7.41-7.58 (m, 3H, Ar), 7.87-7.96 (m, 3H, Ar), 8.11 (s, 1H, Ar); ^{13}C-NMR (101 MHz, CDCl$_3$) δ 44.6 (CH$_2$), 55.5 (OCH$_3$), 112.4 (Ar), 120.7 (Ar), 120.9 (Ar), 121.2 (Ar), 125.5 (Ar), 127.3 (Ar), 129.9 (Ar), 134.5 (Ar), 134.9 (Ar), 135.3 (Ar), 137.9 (Ar), 159.1 (Ar), 160.0 (C=O), 188.7 (C=O). Anal. Calcd for C$_{16}$H$_{13}$NO$_5$S: C, 58.00; H, 3.95; N, 4.23. Found: C, 58.22; H, 4.11; N, 4.02.

2-(Hydroxymethyl)-*N*-(2-methylbenzyl)benzenesulfonamide (1): (2-methylbenzyl)benzo[*d*]isothiazol-3(2*H*)-one 1,1-dioxide (1.0 eq.) was suspended in 20 mL of anhydrous methanol at room temperature. An excess of NaBH$_4$ was added portionwise and the reaction monitored by TLC. After 2 h the reaction was quenched with water and the aqueous phase was extracted with dichloromethane (3 x 30 mL). The organic layers were reunited, dried over sodium sulfate, and concentrated *in vacuo* to give a crude product which was purified by column chromatography (EtOAc/*n*-hexane, 1:4). The title compound was a white solid (52% yield); mp 64-66 °C; IR ν_{max} 3459 (ν O-H), 3237 (ν N-H), 3065 (ν C_{sp2}-H), 1319 (ν_{as} S=O), 1167 (ν_s S=O), 712 (δ C_{sp2}-H) cm^{-1}; ^{1}H-NMR (400 MHz, CDCl$_3$) δ 2.25 (s, 3H, CH$_3$), 2.77 (bs, 1H, OH, D$_2$O exch.), 4.08 (s, 2H, CH$_2$), 5.01 (s, 2H, CH$_2$), 5.43 (bs, 1H, NH, D$_2$O exch.), 7.09-7.19 (m, 4H, Ar), 7.47-7.61 (m, 3H, Ar), 8.01-8.04 (m, 1H, Ar); ^{13}C-NMR (101 MHz, CDCl$_3$) δ 18.7 (CH$_3$), 45.5 (CH$_2$), 64.2 (CH$_2$), 126.2 (Ar), 128.2 (Ar), 128.5 (Ar), 128.9 (Ar), 129.6 (Ar), 129.9 (Ar), 130.5 (Ar), 131.6 (Ar), 133.2 (Ar), 134.1 (Ar), 136.6 (Ar), 138.2 (Ar).
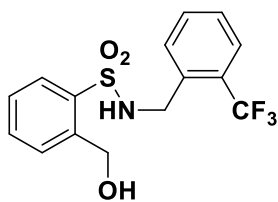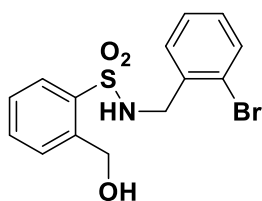
2-(Hydroxymethyl)-*N*-(2-(trifluoromethyl)benzyl)benzenesulfonamide (2): (2-trifluoromethylbenzyl)benzo[*d*]isothiazol-3(2*H*)-one 1,1-dioxide (1.0 eq.) was suspended in 20 mL of anhydrous methanol at room temperature. An excess of NaBH$_4$ was added portionwise and the reaction monitored by TLC. After 4 h the reaction was quenched with water and the aqueous phase was extracted with dichloromethane (3 x 30 mL). The organic layers were reunited, dried over sodium sulfate, and concentrated *in vacuo* to give a crude product that was purified by column chromatography (EtOAc/*n*-hexane, 1:3). The title compound was a white solid (47% yield); mp 66-68 °C; IR ν_{max} 3446 (ν O-H), 3214 (ν N-H), 1310 (ν_{as} S=O), 1157 (ν_s S=O), 714 (δ C$_{sp2}$-H) cm^{-1}; ^{1}H-NMR (400 MHz, CDCl$_3$) δ 2.81 (t, 1H, J = 5.4 Hz, OH, D$_2$O exch.), 4.17 (d, 2H, J = 6.0 Hz, CH$_2$), 4.91 (s, 2H, CH$_2$), 5.83 (m, 1H, NH, D$_2$O exch.), 7.27 (t, 1H, J = 7.6 Hz, Ar), 7.35-7.41 (m, 3H, Ar), 7.46-7.50 (m, 3H, Ar), 7.89-7.91 (m, 1H, Ar); ^{13}C-NMR (101 MHz, CDCl$_3$) δ 43.7 (CH$_2$), 63.9 (CH$_2$), 124.2 (C-F, ^{1}J$_{C-F}$ =274.8 Hz, CF$_3$), 125.9 (Ar), 126.0 (Ar), 127.9 (Ar), 128.6 (Ar), 129.7 (Ar), 130.6 (Ar), 131.6 (Ar), 132.3 (Ar), 133.3 (Ar), 135.0 (Ar), 138.0 (Ar), 138.1 (Ar); ^{19}F-NMR (564.7 MHz, CDCl$_3$) δ -56.89 (s, CF$_3$).
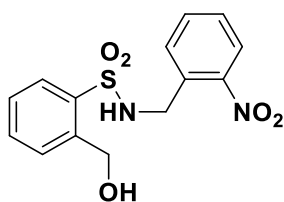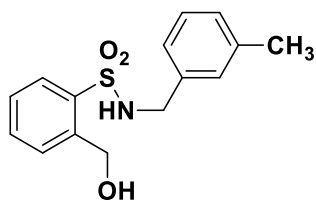

2-(Hydroxymethyl)-*N*-(2-nitrobenzyl)benzenesulfonamide (3): (2-nitrobenzyl)benzo[*d*]isothiazol-3(2*H*)-one 1,1-dioxide (1.0 eq.) was suspended in 20 mL of anhydrous methanol at room temperature. An excess of NaBH$_4$ was added portionwise and the reaction monitored by TLC. After 6 h the reaction was quenched with water and the aqueous phase was extracted with dichloromethane (3 x 30 mL). The organic layers were reunited, dried over sodium sulfate, and concentrated *in vacuo*

to give the title compound as a light brown solid (37% yield); mp 103-105 °C; IR ν_{max} 3498 (ν O-H), 3238 (ν N-H), 2973 (ν C_{sp3}-H), 1522 (ν N-O), 1327 (ν_{as} S=O), 1165 (ν_s S=O), 698 (δ C_{sp2}-H) cm^{-1}; ^{1}H-NMR (400 MHz, DMSO-d_6) δ 4.34 (d, 2H, J = 5.6 Hz, CH_2), 4.88 (s, 2H, CH_2), 5.45 (bs, 1H, OH, D_2O exch.), 7.39 (t, 1H, J = 7.2 Hz, Ar), 7.50 (t, 1H, J = 7.6 Hz, Ar), 7.60-7.68 (m, 3H, 3 x Ar), 7.74-7.79 (m, 2H, 2 x Ar), 7.96 (d, 1H, J = 8.4 Hz, Ar), 8.29 (bs, 1H, NH, D_2O exch.); ^{13}C-NMR (101 MHz, DMSO-d_6) δ 43.4 (CH_2), 60.0 (CH_2), 125.1 (Ar), 127.3 (Ar), 128.2 (Ar), 128.5 (Ar), 129.1 (Ar), 130.7 (Ar), 133.0 (Ar), 133.4 (Ar), 134.1 (Ar), 137.0 (Ar), 141.6 (Ar), 148.1 (Ar).

N-(2-Bromobenzyl)-2-(hydroxymethyl)benzenesulfonamide **(4)**: (2-bromobenzyl)benzo[d]isothiazol-3(2H)-one 1,1-dioxide (1.0 eq.) was suspended in 20 mL of anhydrous methanol at room temperature. An excess of $NaBH_4$ was added portionwise and the reaction monitored by TLC. After 6 h the reaction was quenched with water and the aqueous phase was extracted with dichloromethane (3 x 30 mL). The organic layers were reunited, dried over sodium sulfate, and concentrated *in vacuo* to give a crude product which was purified by column chromatography (EtOAc/*n*-hexane, 2:1). The title compound was a white solid (0.05 g, 11% yield); mp 162-164 °C; IR ν_{max} 3273 (ν O-H and ν N-H), 2920 (ν C_{sp3}-H), 1402 (ν_{as} S=O), 1065 (ν_s S=O), 676 (δ C_{sp2}-H) cm^{-1}; ^{1}H-NMR (400 MHz, $CDCl_3$) δ 3.45 (bs, 1H, OH, D_2O exch.), 4.14 (d, 2H, J = 6.4 Hz, CH_2), 4.93 (s, 2H, CH_2), 6.18 (m, 1H, NH, D_2O exch.), 7.03 (t, 1H, J = 7.6 Hz, Ar), 7.15 (t, 1H, J = 7.4 Hz, Ar), 7.28 (d, 1H, J = 6.8 Hz, Ar), 7.33-7.49 (m, 4H, Ar), 7.87 (d, 1H, J = 8.0 Hz, Ar); ^{13}C-NMR (101 MHz, $CDCl_3$) δ 47.4 (CH_2), 63.5 (CH_2), 123.4 (Ar), 127.6 (Ar), 128.3 (Ar), 129.4 (Ar), 129.6 (Ar), 130.3 (Ar), 131.3 (Ar), 132.7 (Ar), 133.1 (Ar), 135.6 (Ar), 137.8 (Ar), 138.4 (Ar).
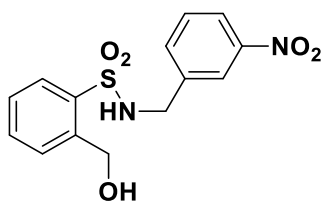
2-(Hydroxymethyl)-*N*-(3-methylbenzyl)benzenesulfonamide **(5)**: (3-methylbenzyl)benzo[*d*]isothiazol-3(2*H*)-one 1,1-dioxide (1.0 eq.) was suspended in 20 mL of anhydrous methanol at room temperature. An excess of NaBH$_4$ was added portionwise and the reaction monitored by TLC. After 7 h the reaction was quenched with water and the aqueous phase was extracted with dichloromethane (3 x 30 mL). The organic layers were reunited, dried over sodium sulfate, and concentrated *in vacuo* to give a crude product which was purified by column chromatography (EtOAc/*n*-hexane, 1:4). The title compound was a white solid (51% yield); mp 79-80 °C; IR ν_{max} 3431 (ν O-H), 3161 (ν N-H), 2936 (ν C$_{sp3}$-H), 1316 (ν_{as} S=O), 1152 (ν_s S=O), 694 (δ C$_{sp2}$-H) cm^{-1}; ^{1}H-NMR (400 MHz, CDCl$_3$) δ 2.27 (s, 3H, CH$_3$), 2.80 (bs, 1H, OH, D$_2$O exch.), 4.07 (bs, 2H, CH$_2$), 4.99 (s, 2H, CH$_2$), 5.72 (bs, 1H, NH, D$_2$O exch.), 6.96 (d, 2H, J = 7.6 Hz, Ar), 7.04 (d, 1H, J = 8.0 Hz, Ar), 7.14 (t, 1H, J = 7.4 Hz, Ar), 7.44-7.49 (m, 2H, Ar), 7.55-7.59 (m, 1H, Ar), 7.98 (d, 1H, 7.8 Hz, Ar); ^{13}C-NMR (101 MHz, CDCl$_3$) δ 21.3 (CH$_3$), 47.5 (CH$_2$), 63.8 (CH$_2$), 124.9 (Ar), 128.4 (Ar), 128.5 (Ar), 128.6 (Ar), 128.7 (Ar), 129.8 (Ar), 131.5 (Ar), 133.1 (Ar), 136.1 (Ar), 138.1 (Ar), 138.2 (Ar), 138.3 (Ar).
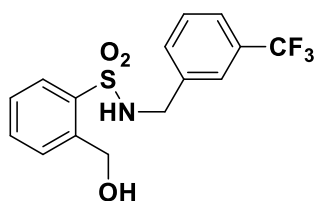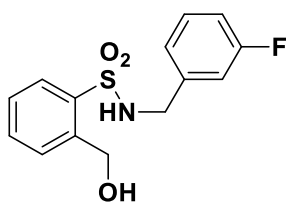

2-(Hydroxymethyl)-*N*-(3-(trifluoromethyl)benzyl)benzenesulfonamide **(6)**: (3-trifluoromethylbenzyl)benzo[*d*]isothiazol-3(2*H*)-one 1,1-dioxide (1.0 eq.) was suspended in 20 mL of anhydrous methanol at room temperature. An excess of NaBH$_4$ was added portionwise and the reaction monitored by TLC. After 8 h the reaction was quenched with water and the aqueous phase was extracted with dichloromethane (3 x 30 mL). The organic layers were reunited, dried over sodium sulfate, and concentrated
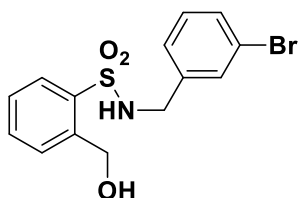
in vacuo to give a crude product which was purified by column chromatography (EtOAc/*n*-hexane, 1:3). The title compound was a white solid (71% yield); mp 76-78 °C; IR ν_{max} 3430 (ν O-H), 3278 (ν N-H), 1317 (ν_{as} S=O), 1160 (ν_s S=O), 700 (δ C$_{sp2}$-H) cm^{-1}; ^{1}H-NMR (400 MHz, CDCl$_3$) δ 2.98 (t, 1H, J = 4.8 Hz, OH, D$_2$O exch.), 4.06 (d, 2H, J = 6.4 Hz, CH$_2$), 4.91 (d, 2H, J = 4.0 Hz, CH$_2$), 6.07 (m, 1H, NH, D$_2$O exch.), 7.24-7.37 (m, 6H, Ar), 7.42-7.46 (m, 1H, Ar), 7.82 (d, 1H, J = 7.6 Hz, Ar); ^{13}C-NMR (101 MHz, CDCl$_3$) δ 46.9 (CH$_2$), 63.9 (CH$_2$), 123.9 (C-F, ^{1}J$_{C-F}$ =273.4 Hz, CF$_3$), 124.5 (Ar), 124.6 (Ar), 128.6 (Ar), 129.1 (Ar), 129.7 (Ar), 130.7 (Ar), 131.3 (Ar), 131.7 (Ar), 133.3 (Ar), 137.4 (Ar), 137.8 (Ar), 138.0 (Ar); ^{19}F-NMR (564.7 MHz, CDCl$_3$) δ -60.09 (s, CF$_3$).

2-(Hydroxymethyl)-*N*-(3-nitrobenzyl)benzenesulfonamide **(7)**: (3-nitrobenzyl)benzo[*d*]isothiazol-3(2*H*)-one 1,1-dioxide (1.0 eq.) was suspended in 20 mL of anhydrous methanol at room temperature. Excess of NaBH$_4$ was added portionwise and the reaction monitored by TLC. After 6 h the reaction was quenched with water and the aqueous phase was extracted with dichloromethane (3 x 30 mL). The organic layers were reunited, dried over sodium sulfate, and concentrated *in vacuo* to give a crude product that was purified by column chromatography (EtOAc/*n*-hexane, 2:1). The title compound was a white solid (37% yield); mp 109-111 °C; mp 109-111 °C; IR ν_{max} 3491 (ν O-H), 3164 (ν N-H), 2958 (ν C$_{sp3}$-H), 1536 (ν N-O), 1326 (ν_{as} S=O), 1162 (ν_s S=O), 695 (δ C$_{sp2}$-H) cm^{-1}; ^{1}H-NMR (400 MHz, DMSO-*d$_6$*) δ 4.16 (s, 2H, CH$_2$), 4.87 (s, 2H, CH$_2$), 5.47 (bs, 1H, OH, D$_2$O exch.), 7.33-7.37 (m, 1H, Ar), 7.51-7.60 (m, 2H, Ar), 7.64 (d, 1H, J = 7.6 Hz, Ar), 7.73-7.75 (m, 2H, Ar), 8.04 (s, 1H, Ar), 8.06 (s, 1H, Ar), 8.35 (bs, 1H, NH, D$_2$O exch.); ^{13}C-NMR (101 MHz, DMSO-*d$_6$*) δ 45.4 (CH$_2$), 59.9 (CH$_2$), 122.5 (Ar), 122.6 (Ar), 127.1 (Ar), 127.9 (Ar), 128.5 (Ar), 130.2 (Ar), 132.9 (Ar), 134.6 (Ar), 137.2 (Ar), 140.8 (Ar), 141.5 (Ar), 148.1 (Ar).
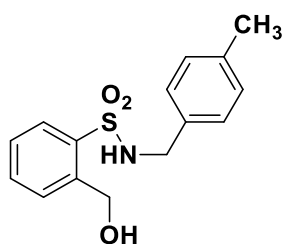
N-(3-Fluorobenzyl)-2-(hydroxymethyl)benzenesulfonamide **(8)**: (3-fluorobenzyl)benzo[*d*]isothiazol-3(2*H*)-one 1,1-dioxide (1.0 eq.) was suspended in 20 mL of anhydrous methanol at room temperature. An excess of NaBH$_4$ was added portionwise and the reaction monitored by TLC. After 5 h the reaction was quenched with water and the aqueous phase was extracted with dichloromethane (3 x 30 mL). The organic layers were reunited, dried over sodium sulfate, and concentrated *in vacuo* to give a crude product which was purified by column chromatography (EtOAc/*n*-hexane, 1:1). The title compound was a light yellow oil (67% yield); IR ν_{max} 3492 (ν O-H), 3283 (ν N-H), 2895 (ν C$_{sp3}$-H), 1318 (ν_{as} S=O), 1252 (ν C$_{sp2}$-F), 1175 (ν_s S=O), 689 (δ C$_{sp2}$-H) cm^{-1}; ^{1}H-NMR (400 MHz, CDCl$_3$) δ 2.84 (bs, 1H, OH, D$_2$O exch.), 4.05 (s, 2H, CH$_2$), 4.97 (s, 2H, CH$_2$), 6.04 (bs, 1H, NH, D$_2$O exch.), 6.85-6.94 (m, 3H, Ar), 7.17-7.20 (m, 1H, Ar), 7.39-7.55 (m, 3H, Ar), 7.92 (d, 1H, J = 7.6 Hz, Ar); ^{13}C-NMR (101 MHz, CDCl$_3$) δ 46.6 (CH$_2$), 63.6 (CH$_2$), 114.6 (Ar-F, ^{2}J$_{C-F}$ = 21.1 Hz), 114.8 (Ar-F, ^{2}J$_{C-F}$ = 22.0 Hz), 123.4 (Ar-F, $^{long-range}$J$_{C-F}$ = 2.7 Hz), 128.5 (Ar), 129.7 (Ar), 130.1 (Ar-F, ^{3}J$_{C-F}$ = 8.2 Hz), 131.6 (Ar), 133.2 (Ar), 137.9 (Ar), 138.1 (Ar), 139.0 (Ar-F, ^{3}J$_{C-F}$ = 7.3 Hz), 162.7 (Ar-F, ^{1}J$_{C-F}$ = 247.45 Hz); ^{19}F-NMR (564.7 MHz, CDCl$_3$) δ -110.03 (ddd, J$_{F-H}$ = 9.5 Hz, 8.6 Hz, 5.2 Hz, CF).
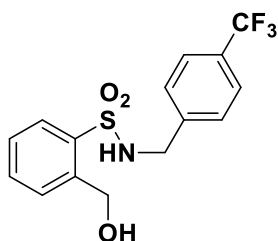

N-(3-Bromobenzyl)-2-(hydroxymethyl)-benzenesulfonamide **(9)**: (3-bromobenzyl)benzo[d]isothiazol-3(2H)-one 1,1-dioxide (1.0 eq.) was suspended in 20 mL of anhydrous methanol at room temperature. An excess of NaBH4 was added

portionwise and the reaction monitored by TLC. After 5 h the reaction was quenched with water and the aqueous phase was extracted with dichloromethane (3 x 30 mL). The organic layers were reunited, dried over sodium sulfate, and concentrated in vacuo to give a crude product which was purified by column chromatography (EtOAc/n-hexane, 1:1). The title compound was a white solid (70% yield); mp 75-76 °C; IR ν_{max} 3454 (ν O-H), 3214 (ν N-H), 2955 (ν C$_{sp3}$-H), 1319 (ν_{as} S=O), 1156 (ν_s S=O), 694 (δ C$_{sp2}$-H) cm^{-1}; ^{1}H-NMR (400 MHz, DMSO-d_6) δ 4.00 (d, 2H, J = 6 Hz, CH$_2$), 4.87 (d, 2H, J = 5.2 Hz, CH$_2$), 5.42 (bs, 1H, OH, D$_2$O exch.), 7.20 (bs, 2H, Ar), 7.38 (bs, 3H, Ar), 7.59-7.63 (m, 1H, Ar), 7.75-7.78 (m, 2H, Ar), 8.23 (bs, 1H, NH, D$_2$O exch.); ^{13}C-NMR (101 MHz, DMSO-d_6) δ 45.6 (CH$_2$), 59.9 (CH$_2$), 122.0 (Ar), 127.0 (Ar), 127.2 (Ar), 127.9 (Ar), 128.5 (Ar), 130.4 (Ar), 130.7 (Ar), 130.8 (Ar), 132.9 (Ar), 137.2 (Ar), 141.2 (Ar), 141.5 (Ar).
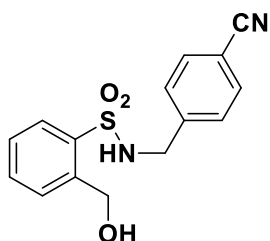

2-(Hydroxymethyl)-*N*-(4-methylbenzyl)benzenesulfonamide (10): (4-methylbenzyl)benzo[d]isothiazol-3(2H)-one 1,1-dioxide (1.0 eq.) was suspended in 20 mL of anhydrous methanol at room temperature. An excess of NaBH4 was added portionwise and the reaction monitored by TLC. After 6 h the reaction was quenched with water and the aqueous phase was extracted with dichloromethane (3 x 30 mL). The organic layers were reunited, dried over sodium sulfate, and concentrated in vacuo to give a crude product which was purified by column chromatography (EtOAc/n-hexane, 1:4). The title compound was a white solid (56% yield); mp 100-102 °C; IR ν_{max} 3437 (ν O-H), 3130 (ν N-H), 2930 (ν C$_{sp3}$-H), 1310 (ν_{as} S=O), 1151 (ν_s S=O), 701 (δ C$_{sp2}$-H) cm^{-1}; ^{1}H-NMR (400 MHz, CDCl$_3$) δ 2.31 (s, 3H, CH$_3$), 2.80 (bs, 1H, OH, D$_2$O exch.), 4.07 (d, 2H, J = 5.2 Hz, CH$_2$), 4.99 (s, 2H, CH$_2$), 5.60 (bs, 1H, NH, D$_2$O exch.), 7.06 (bs, 4H, Ar), 7.44-7.50 (m, 2H, Ar), 7.55-7.60 (m, 1H, Ar), 8.00 (d, 1H, 7.6 Hz, Ar);

^{13}C-NMR (101 MHz, CDCl$_3$) δ 21.1 (CH$_3$), 47.3 (CH$_2$), 63.8 (CH$_2$), 127.9 (Ar), 128.5 (Ar), 129.3 (Ar), 129.9 (Ar), 131.6 (Ar), 133.1 (Ar), 133.2 (Ar), 137.6 (Ar), 138.1 (Ar), 138.2 (Ar).
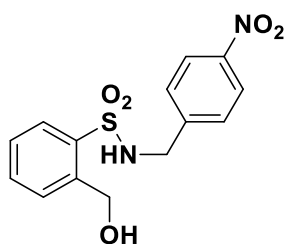

2-(Hydroxymethyl)-*N*-(4-(trifluoromethyl)benzyl)benzenesulfonamide (11): (4-trifluoromethylbenzyl)benzo[*d*]isothiazol-3(2*H*)-one 1,1-dioxide (1.0 eq.) was suspended in 20 mL of anhydrous methanol at room temperature. An excess of NaBH$_4$ was added portionwise and the reaction monitored by TLC. After 8 h the reaction was quenched with water and the aqueous phase was extracted with dichloromethane (3 x 30 mL). The organic layers were reunited, dried over sodium sulfate, and concentrated *in vacuo* to give a crude product which was purified by column chromatography (EtOAc/*n*-hexane, 1:3). The title compound was a white solid (79% yield); mp 78-80 °C; IR ν_{max} 3417 (ν O-H), 3161 (ν N-H), 3065 (ν C$_{sp2}$-H), 1321 (ν_{as} S=O), 1157 (ν_s S=O), 688 (δ C$_{sp2}$-H) cm^{-1}; ^{1}H-NMR (400 MHz, CDCl$_3$) δ 3.03 (bs, 1H, OH, D$_2$O exch.), 4.15 (d, 2H, J = 6.4 Hz, CH$_2$), 5.02 (d, 2H, J = 5.2 Hz CH$_2$), 6.14 (t, 1H, J = 6.4 Hz, NH, D$_2$O exch.), 7.32 (d, 2H, J = 8.0 Hz, Ar), 7.40-7.49 (m, 4H, Ar), 7.54-7.58 (m, 1H, Ar), 7.91 (s, 1H, Ar); ^{13}C-NMR (101 MHz, CDCl$_3$) δ 46.9 (CH$_2$), 63.9 (CH$_2$), 124.0 (C-F, ^{1}J$_{C-F}$= 273.1 Hz, CF$_3$), 125.4 (Ar), 125.5 (Ar), 128.1 (Ar), 128.6 (Ar), 129.7 (Ar), 129.8 (Ar), 130.1 (Ar), 131.7 (Ar), 133.3 (Ar), 137.8 (Ar), 138.0 (Ar), 140.4 (Ar); ^{19}F-NMR (564.7 MHz, CDCl$_3$) δ -60.08 (s, CF$_3$).
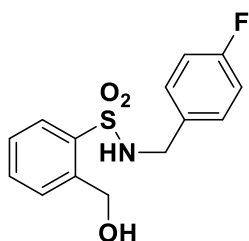

***N*-(4-Cyanobenzyl)-2-(hydroxymethyl)benzenesulfonamide (12):** (4-cyanobenzyl)benzo[*d*]isothiazol-3(2*H*)-one 1,1-dioxide (1.0 eq.) was suspended in 20

mL of anhydrous methanol at room temperature. An excess of NaBH$_4$ was added portionwise and the reaction monitored by TLC. After 8 h the reaction was quenched with water and the aqueous phase was extracted with dichloromethane (3 x 30 mL). The organic layers were reunited, dried over sodium sulfate and concentrated *in vacuo* to give a crude product, which was purified by column chromatography (EtOAc/*n*-hexane, 2:1). The title compound was a white solid (67% yield); mp 93-95 °C; IR ν_{max} 3481 (ν O-H), 3187 (ν N-H), 2949 (ν C$_{sp3}$-H), 2235 CN, 1325 (ν_{as} S=O), 1156 (ν_s S=O), 703 (δ C$_{sp2}$-H) cm^{-1}; ^{1}H-NMR (400 MHz, DMSO-d_6) δ 4.09 (s, 2H, CH$_2$), 4.88 (s, 2H, CH$_2$), 5.46 (bs, 1H, OH, D$_2$O exch.), 7.35-7.41 (m, 3H, Ar), 7.59-7.62 (m, 1H, Ar), 7.70-7.77 (m, 4H, Ar), 8.33 (bs, 1H, NH, D$_2$O exch.); ^{13}C-NMR (101 MHz, DMSO-d_6) δ 45.9 (CH$_2$), 59.9 (CH$_2$), 110.3 (Ar), 119.3 (CN), 127.2 (Ar), 127.9 (Ar), 128.5 (Ar), 128.7 (Ar), 132.6 (Ar), 132.9 (Ar), 137.1 (Ar), 141.6 (Ar), 144.3 (Ar).
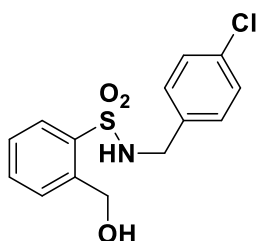

2-(Hydroxymethyl)-*N*-(4-nitrobenzyl)benzenesulfonamide **(13):** (4-nitrobenzyl)benzo[*d*]isothiazol-3(2*H*)-one 1,1-dioxide (1.0 eq.) was suspended in 20 mL of anhydrous methanol at room temperature. An excess of NaBH$_4$ was added portionwise and the reaction monitored by TLC. After 8 h the reaction was quenched with water and the aqueous phase was extracted with dichloromethane (3 x 30 mL). The organic layers were reunited, dried over sodium sulfate, and concentrated *in vacuo* to give a crude product, which was purified by column chromatography (EtOAc/*n*-hexane, 1:1). The title compound was a yellow solid (57% yield); mp 98-99 °C; IR ν_{max} 3493 (ν O-H), 3243 (ν N-H), 1515 (ν N-O), 1318 (ν_{as} S=O), 1160 (ν_s S=O), 690 (δ C$_{sp2}$-H) cm^{-1}; ^{1}H-NMR (400 MHz, CDCl$_3$) δ 2.74 (bs, 1H, OH, D$_2$O exch.), 4.21 (bs, 2H, CH$_2$), 5.08 (s, 2H, CH$_2$), 6.13 (bs, 1H, NH, D$_2$O exch.), 7.40-7.59 (m, 5H, Ar), 7.96-7.97 (m, 1H, Ar), 8.11-8.13 (m, 2H, Ar); ^{13}C-NMR (101 MHz, CDCl$_3$) δ 46.7 (CH$_2$), 64.3 (CH$_2$), 123.7 (Ar),

128.5 (Ar), 128.8 (Ar), 129.8 (Ar), 131.6 (Ar), 133.4 (Ar), 137.6 (Ar), 138.7 (Ar), 144.0 (Ar), 147.2 (Ar).
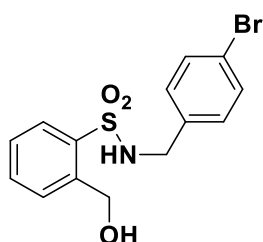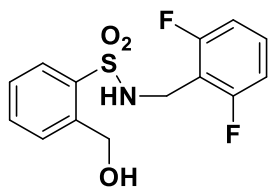

N-(4-Fluorobenzyl)-2-(hydroxymethyl)benzenesulfonamide **(14):** (4-fluorobenzyl)benzo[*d*]isothiazol-3(2*H*)-one 1,1-dioxide (1.0 eq.) was suspended in 20 mL of anhydrous methanol at room temperature. An excess of NaBH$_4$ was added portionwise and the reaction monitored by TLC. After 8 h the reaction was quenched with water and the aqueous phase was extracted with dichloromethane (3 x 30 mL). The organic layers were reunited, dried over sodium sulfate, and concentrated *in vacuo* to give a crude product which was purified by column chromatography (EtOAc/*n*-hexane, 1:3). The title compound was a light brown solid (79% yield); mp 99-100 °C; IR ν_{max} 3439 (ν O-H), 3140 (ν N-H), 1312 (ν_{as} S=O), 1151 (ν_s S=O), 696 (δ C$_{sp2}$-H) cm^{-1}; ^{1}H-NMR (400 MHz, CDCl$_3$) δ 3.18 (bs, 1H, OH, D$_2$O exch.), 4.04 (d, 2H, J = 6.4 Hz, CH$_2$), 4.98 (s, 2H, CH$_2$), 6.00 (bs, 1H, NH, D$_2$O exch.), 6.88-6.93 (m, 2H, Ar), 7.12-7.15 (m, 2H, Ar), 7.41-7.57 (m, 3H, Ar), 7.93 (d, 1H, J = 8.0 Hz, Ar); ^{13}C-NMR (101 MHz, CDCl$_3$) δ 46.7 (CH$_2$), 63.7 (CH$_2$), 115.4 (Ar-F, ^{2}J$_{C-F}$ =21.2 Hz), 128.5 (Ar), 129.6 (Ar), 129.7 (Ar), 131.6 (Ar), 132.0 (Ar), 132.1 (Ar), 133.2 (Ar), 138.0 (Ar), 138.1 (Ar), 135.4 (Ar-F, ^{1}J$_{C-F}$ =247.3 Hz); ^{19}F-NMR (564.7 MHz, CDCl$_3$) δ -111.71 (tt, J$_{F-H}$ = 8.7 Hz (ortho), 5.3 Hz (meta), CF).

N-(4-Chlorobenzyl)-2-(hydroxymethyl)benzenesulfonamide **(15):** (4-chlorobenzyl)benzo[*d*]isothiazol-3(2*H*)-one 1,1-dioxide (1.0 eq) was suspended in 20

mL of anhydrous methanol at room temperature. An excess of NaBH$_4$ was added portionwise and the reaction monitored by TLC. After 7 h the reaction was quenched with water and the aqueous phase was extracted with dichloromethane (3 x 30 mL). The organic layers were reunited, dried over sodium sulfate, and concentrated *in vacuo* to give a crude product which was purified by column chromatography (EtOAc/*n*-hexane, 1:1). The title compound was a white solid (70% yield); mp 103-105 °C; IR ν_{max} 3458 (ν O-H), 3236 (ν N-H), 2876 (ν C$_{sp3}$-H), 1314 (ν_{as} S=O), 1152 (ν_s S=O), 690 (δ C$_{sp2}$-H) cm^{-1}; ^{1}H-NMR (400 MHz, CDCl$_3$) δ 2.90 (bs, 1H, OH, D$_2$O exch.), 4.06 (d, 2H, J = 6.0 Hz, CH$_2$), 5.01 (s, 2H, CH$_2$), 5.88 (bs, 1H, NH, D$_2$O exch.), 7.11 (d, 2H, J = 8.4 Hz, Ar), 7.21 (d, 2H, J = 8.4 Hz, Ar), 7.43-7.49 (m, 2H, Ar), 7.56-7.60 (m, 1H, Ar), 7.95 (d, 1H, J = 7.6 Hz, Ar); ^{13}C-NMR (101 MHz, CDCl$_3$) δ 46.8 (CH$_2$), 63.9 (CH$_2$), 128.6 (Ar), 128.7 (Ar), 129.3 (Ar), 129.8 (Ar), 131.6 (Ar), 133.2 (Ar), 133.7 (Ar), 134.8 (Ar), 137.9 (Ar), 138.1 (Ar).
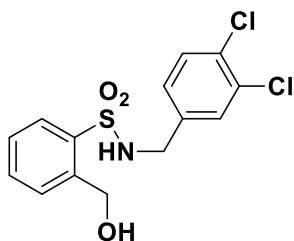

***N*-(4-bromobenzyl)-2-(hydroxymethyl)benzenesulfonamide** **(16):** (4-bromobenzyl)benzo[*d*]isothiazol-3(2*H*)-one 1,1-dioxide (1.0 eq.) was suspended in 20 mL of anhydrous methanol at room temperature. An excess of NaBH$_4$ was added portionwise and the reaction monitored by TLC. After 7 h the reaction was quenched with water and the aqueous phase was extracted with dichloromethane (3 x 30 mL). The organic layers were reunited, dried over sodium sulfate, and concentrated *in vacuo* to give a crude product which was purified by column chromatography (EtOAc/*n*-hexane, 1:2). The title compound was a white solid (53% yield); mp 124-125 °C; IR ν_{max} 3461 (ν O-H), 3234 (ν N-H), 3064 (ν C$_{sp2}$-H), 1314 (ν_{as} S=O), 1152 (ν_s S=O), 690 (δ C$_{sp2}$-H) cm^{-1}; ^{1}H-NMR (400 MHz, CDCl$_3$) δ 2.71 (bs, 1H, OH, D$_2$O exch.), 4.06 (bs, 2H, CH$_2$), 5.03 (s, 2H, CH$_2$), 5.78 (bs, 1H, NH, D$_2$O exch.), 7.06-7.08 (m, 2H, Ar), 7.37-7.59 (m, 5H,

Ar), 7.96-7.97 (m, 1H, Ar); ^{13}C-NMR (101 MHz, CDCl$_3$) δ 46.9 (CH$_2$), 64.1 (CH$_2$), 121.9 (Ar), 128.6 (Ar), 129.6 (Ar), 129.8 (Ar), 131.7 (Ar), 133.2 (Ar), 137.9 (Ar), 138.3 (Ar).
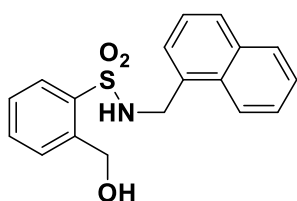

N-(2,6-Difluorobenzyl)-2-(hydroxymethyl)benzenesulfonamide **(17):** (2,6-difluorobenzyl)benzo[*d*]isothiazol-3(2*H*)-one 1,1-dioxide (1.0 eq.) was suspended in 20 mL of anhydrous methanol at room temperature. An excess of NaBH$_4$ was added portionwise and the reaction monitored by TLC. After 7 h the reaction was quenched with water and the aqueous phase was extracted with dichloromethane (3 x 30 mL). The organic layers were reunited, dried over sodium sulfate, and concentrated *in vacuo* to give a crude product which was purified by column chromatography (EtOAc/*n*-hexane, 1:1). The title compound was a white solid (67% yield); mp 128-130 °C; IR ν_{max} 3495 (ν O-H), 3159 (ν N-H), 2958 (ν C$_{sp3}$-H), 1320 (ν_{as} S=O), 1159 (ν_s S=O), 693 (δ C$_{sp2}$-H) cm^{-1}; ^{1}H-NMR (400 MHz, CDCl$_3$) δ 2.72 (bs, 1H, OH, D$_2$O exch.), 4.23 (s, 2H, CH$_2$), 4.89 (bs, 2H, CH$_2$), 6.04 (bs, 1H, NH, D$_2$O exch.), 6.79-6.73 (m, 2H, Ar), 7.10-7.14 (m, 1H, Ar), 7.26 (s, 1H, Ar), 7.33-7.48 (m, 2H, Ar), 7.92-7.94 (m, 1H, Ar); ^{13}C-NMR (101 MHz, CDCl$_3$) δ 35.1 (CH$_2$), 63.6 (CH$_2$), 111.2 (Ar-F, $^2J_{C-F}$ = 24.8 Hz), 128.3 (Ar), 129.7 (Ar), 129.9 (Ar), 130.0 (Ar), 130.1 (Ar), 131.2 (Ar), 133.1 (Ar), 137.8 (Ar), 138.2 (Ar), 161.2 (Ar-F, $^1J_{C-F}$ = 246.9 Hz); ^{19}F-NMR (564.7 MHz, CDCl$_3$) δ -112.08 (t, J$_{F-H}$ = 6.9 Hz, CF).
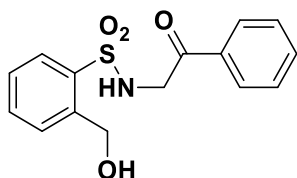

N-(3,4-Dichlorobenzyl)-2-(hydroxymethyl)benzenesulfonamide **(18):** (3,4-chlorobenzyl)benzo[*d*]isothiazol-3(2*H*)-one 1,1-dioxide (1.0 eq.) was suspended in 20

mL of anhydrous methanol at room temperature. An excess of NaBH₄ was added portionwise and the reaction monitored by TLC. After 7 h the reaction was quenched with water and the aqueous phase was extracted with dichloromethane (3 x 30 mL). The organic layers were reunited, dried over sodium sulfate, and concentrated *in vacuo* to give a crude product which was purified by column chromatography (EtOAc/*n*-hexane, 2:1). The title compound was a light brown solid (81% yield); mp 83-84 °C; IR v_{max} 3463 (v O-H), 3192 (v N-H), 2947 (v C_{sp3}-H), 1319 (v_{as} S=O), 1158 (v_s S=O), 690 (δ C_{sp2}-H) cm⁻¹; ¹H-NMR (400 MHz, CDCl₃) δ 2.88 (bs, 1H, OH, D₂O exch.), 3.96 (d, 2H, J = 6.4 Hz, CH₂), 4.93 (bs, 2H, CH₂), 6.00 (t, 1H, J = 6.0 Hz NH, D₂O exch.), 6.94-6.96 (bs, 1H, Ar), 7.17-7.22 (m, 2H, Ar), 7.33-7.39 (m, 2H, Ar), 7.46-7.48 (m, 1H, Ar), 7.83 (d, 1H, J = 7.6 Hz, Ar); ¹³C-NMR (101 MHz, CDCl₃) δ 46.3 (CH₂), 64.0 (CH₂), 127.2 (Ar), 128.6 (Ar), 129.7 (Ar), 129.8 (Ar), 130.5 (Ar), 131.7 (Ar), 131.8 (Ar), 132.6 (Ar), 133.3 (Ar), 136.7 (Ar), 137.7 (Ar), 138.1 (Ar).
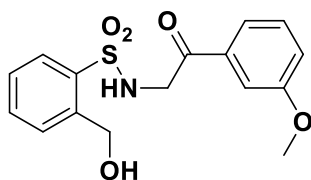

2-(Hydroxymethyl)-*N*-(naphthalen-1-ylmethyl)benzenesulfonamide **(19):** 2-(naphthalen-1-ylmethyl)benzo[*d*]isothiazol-3(2*H*)-one 1,1-dioxide (1.0 eq.) was suspended in 20 mL of anhydrous methanol at room temperature. An excess of NaBH₄ was added portionwise and the reaction monitored by TLC. After 6 h the reaction was quenched with water and the aqueous phase was extracted with dichloromethane (3 x 30 mL). The organic layers were reunited, dried over sodium sulfate, and concentrated *in vacuo* to give a crude product which was purified by column chromatography (EtOAc/*n*-hexane, 1:1). The title compound was a white solid (57% yield); mp 80-81 °C; IR v_{max} 3517 (v O-H), 3347 (v N-H), 3061 (v C_{sp2}-H), 1318 (v_{as} S=O), 1157 (v_s S=O), 690 (δ C_{sp2}-H) cm⁻¹; ¹H-NMR (400 MHz, CDCl₃) δ 2.68 (bs, 1H, OH, D₂O exch.), 4.51 (s, 2H, CH₂), 4.91 (s, 2H, CH₂), 5.69 (bs, 1H, NH, D₂O exch.), 7.29-7.55 (m, 7H, Ar), 7.74-7.86

(m, 3H, Ar), 8.05 (s, 1H, Ar); ^{13}C-NMR (101 MHz, CDCl$_3$) δ 45.6 (CH$_2$), 63.7 (CH$_2$), 123.2 (Ar), 125.2 (Ar), 126.0 (Ar), 126.6 (Ar), 127.0 (Ar), 128.4 (Ar), 128.7 (Ar), 129.0 (Ar), 130.0 (Ar), 131.1 (Ar), 131.4 (Ar), 131.5 (Ar), 133.2 (Ar), 133.7 (Ar), 137.6 (Ar), 138.3 (Ar).

N-(2-Hydroxy-2-phenylethyl)-2-(hydroxymethyl)benzenesulfonamide (20): 2-(2-oxo-2-phenylethyl)benzo[*d*]isothiazol-3(2*H*)-one 1,1-dioxide (1.0 eq.) was suspended in 20 mL of anhydrous methanol at room temperature. An excess of NaBH$_4$ was added portionwise and the reaction monitored by TLC. After 8 h the reaction was quenched with water and the aqueous phase was extracted with dichloromethane (3 x 30 mL). The organic layers were reunited, dried over sodium sulfate, and concentrated *in vacuo* to give a crude product which was purified by column chromatography (EtOAc/*n*-hexane, 2:1). The title compound was a light yellow oil (49% yield); IR ν_{max} 3291 (ν O-H and ν N-H), 2923 (ν C$_{sp3}$-H), 1316 (ν_{as} S=O), 1153 (ν_s S=O), 696 (δ C$_{sp2}$-H) cm^{-1}; ^{1}H-NMR (400 MHz, CDCl$_3$) δ 2.94 (bs, 1H, CH$_2$), 3.15 (bs, 1H, CH$_2$), 3.42 (bs, 1H, OH, D$_2$O exch.), 4.56-4.64 (m, 2H, CH$_2$), 4.91-5.03 (m, 1H, CH), 5.28 (bs, 1H, OH, D$_2$O exch.), 6.57 (bs, 1H, NH, D$_2$O exch.), 7.13-7.20 (m, 5H, Ar), 7.38-7.47 (m, 3H, Ar), 7.91 (d, 1H, J = 6.4 Hz, Ar); ^{13}C NMR (101 MHz, CDCl$_3$) δ 50.4 (CH$_2$), 62.7 (CH$_2$), 72.4 (CH), 125.8 (Ar), 127.9 (Ar), 128.2 (Ar), 128.5 (Ar), 129.5 (Ar), 131.3 (Ar), 133.3 (Ar), 137.3 (Ar), 138.6 (Ar), 140.8 (Ar).

N-(2-Hydroxy-2-(3-methoxyphenyl)ethyl)-2-(hydroxymethyl)benzenesulfonamide (21): 2-(2-hydroxy-2-(3-methoxyphenyl)ethyl)benzo[*d*]isothiazol-3(2H)-one 1,1-

dioxide (1.0 eq.) was suspended in 20 mL of anhydrous methanol at room temperature. An excess of $NaBH_4$ was added portionwise and the reaction monitored by TLC. After 8 h the reaction was quenched with water and the aqueous phase was extracted with dichloromethane (3 x 30 mL). The organic layers were reunited, dried over sodium sulfate, and concentrated *in vacuo* to give a crude product which was purified by column chromatography (EtOAc/*n*-hexane, 1:2). The title compound was a yellow oil (88% yield); IR ν_{max} 3477 (ν O-H), 3295 (ν N-H), 2935 (ν C_{sp3}-H), 1317 (ν_{as} S=O), 1160 (ν_s S=O), 697 (δ C_{sp2}-H) cm^{-1}; ^{1}H-NMR (400 MHz, CDCl$_3$) δ 2.89-2.95 (m, 1H, CH$_2$), 3.13-3.17 (m, 1H, CH$_2$), 3.64 (s, 3H, OCH$_3$), 4.41 (bs, 2H, CH$_2$), 4.58 (bs, 1H, OH), 4.87-4.91 (m, 1H, CH), 4.97 (bs, 1H, OH, D$_2$O exch.), 6.48 (bs, 1H, NH, D$_2$O exch.), 6.67-6.71 (m, 3H, Ar), 7.07-7.11 (m, 1H, Ar), 7.32-7.47 (m, 3H, Ar), 7.87 (d, 1H, J = 7.6 Hz, Ar); ^{13}C-NMR (101 MHz, CDCl$_3$) δ 50.4 (CH$_2$), 55.1 (OCH$_3$), 60.6 (CH$_2$), 72.2 (CH), 111.4, (Ar), 113.3 (Ar), 118.1 (Ar), 128.2 (Ar), 129.5 (Ar), 129.6 (Ar), 131.2 (Ar), 133.2 (Ar), 137.3 (Ar), 138.6 (Ar), 142.5 (Ar), 159.5 (ArO).

Enzyme inhibition assays

An Applied Photophysics stopped-flow instrument has been used for assaying the CA-catalyzed CO_2 hydration activity. Phenol red (0.2 mM) has been used as indicator, working at the absorbance maximum of 557 nm, with 20 mM Hepes (pH 7.5, for α-CAs) as buffer, and 20 mM NaClO$_4$ (for maintaining constant the ionic strength), following the initial rates of the CA-catalyzed CO_2 hydration reaction for a period of 10-100 s. The CO_2 concentrations ranged from 1.7 to 17 mM for the determination of the kinetic parameters and inhibition constants. For each inhibitor at least six traces of the initial 5-10% of the reaction have been used for determining the initial velocity. The uncatalyzed rates were determined in the same manner and subtracted from the total observed rates. Stock solutions of each inhibitor (1 μM) were prepared in distilled-deionized water and dilutions up to 0.1 nM were done thereafter with the assay buffer. Inhibitor and enzyme solutions were preincubated together for 15 min at room temperature prior to assay, in order to allow for the formation of the E-I complex or

for the eventual active site mediated hydrolysis of the inhibitor. The inhibition constants were obtained by non-linear least-squares methods using PRISM 3 and the Cheng-Prusoff equation, and represent the average from at least three different determinations. All recombinant CA isoforms were obtained in-house as previously reported[97].

Molecular modelling studies

Preparation of saccharin-based structures

The saccharin-based analogs **1-21** were prepared in 3D with the MOE software package (v2013.08.02, Chemical Computing Group Inc., Montreal, Canada) as previously reported[28]. All possible structural isomers of compounds were constructed. Strong acids were deprotonated and strong bases were protonated. Finally, the ligands were energy minimized using a steepest-descent protocol (MMFF94x force field).

Preparation of hCA crystal structures for docking studies

The structures of hCA I (PDB: 3LXE, 1.90 Å), hCA II (PDB: 4E3D, 1.60 Å), hCA IX (PDB: 3IAI, 2.20 Å) and hCA XII (PDB: 1JD0, 1.50 Å) were obtained from the protein databank (PDB). The protein atoms, the active site zinc ions and the zinc-bound water molecule of hCA II were retained and all other atoms were omitted. The remaining structure was protonated using the MOE software package and subsequently the obtained structure was energy-minimized (AMBER99 force field). Finally, the obtained protein models were superposed on the hCA I structure using the backbone Cα-atoms. The zinc-bound water molecule of hCA II coordinated well to the zinc ions of the other hCAs.

Docking studies

The GOLD Suite software package (v5.2, CCDC, Cambridge, UK) and the GoldScore scoring function were used to dock the derivatives into the hCA structures with and without the zinc-bound water molecule (25 dockings per ligand). The binding pocket was defined as all residues within 13 Å of a centroid (x: -17.071, y: 35.081, 43.681;

corresponding approximately to the position of the thiadiazole ring of acetazolamide in the 1JD0 structure).

Chapter 3

Design, synthesis and biological activity of saccharin/isoxazole and saccharin/isoxazoline derivatives as selective inhibitors of carbonic anhydrase IX and XII isoforms

3.1 Saccharin/isoxazoline and saccharin/isoxazoles derivatives: aim of the work

In one of our first work regarding saccharin inhibitors of hCAs, we reported a compound obtained from 1,3-dipolar cycloaddition reaction between *N*-propargyl substituted saccharin and *N*-hydroxy-4-nitrobenzimidoyl chloride (**Figure 3.1**) [109]. This compound, the first endowed with a heterocyclic "linker" between the methylene of benzyl group and phenyl ring, showed activity in the nanomolar range only towards tumor-related isoforms, being ineffective against the two off-targets.

K_I (nM) hCAI/II > 50.000
K_I (nM) hCAIX = 310
K_I (nM) hCAXII = 240
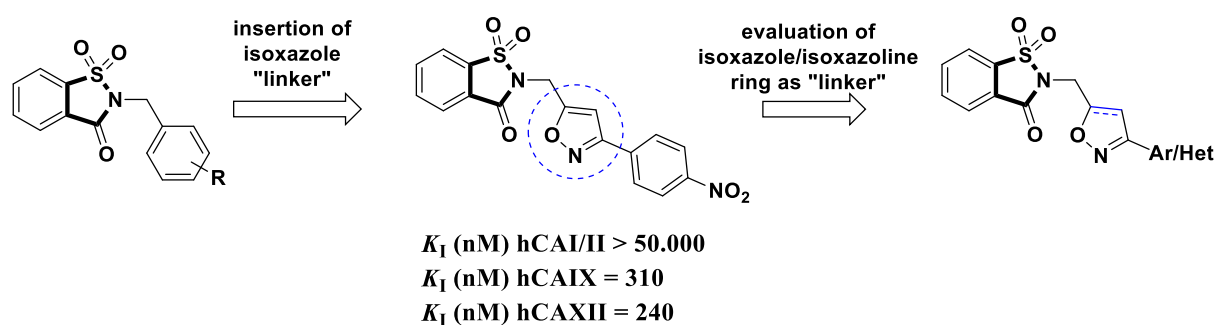
Figure 3.1. Design of new saccharin/isoxazole and saccharin/isoxazoline compounds.

In the light of the above, I designed the new inhibitors evaluating the insertion of two different systems as linker group: isoxazole and isoxazoline. The two chosen linkers possess some identical characteristic, e.g. both are five-membered rings with same heteroatoms, identical connection and position of substituents. However, there are also differences which are noteworthy. Indeed, isoxazole ring is a flat-aromatic system that could give π-stacking interaction inside the active site; on the other hands, isoxazoline, the 4,5-dihydrogenated form of isoxazole, loss aromaticity and possess two tetrahedral carbon atoms inside the ring, that alter the flat conformation (π-interaction could be established with double bond ring, yet). Furthermore, the presence of four different substituents on one of the two tetrahedral carbon (C(5) of isoxazoline), account for the existence of a stereocenter. So, all the saccharin/isoxazoline compounds exist as couple of enantiomers, that could be

resolved and tested in the future with the aim to determine the preferred configuration chosen by the enzymes and, in conclusion, the eutomer.

3.2 Chemistry

For the synthesis of new saccharin derivatives, we followed a multi-step approach [122,123], useful to obtain reagents for the final 1,3-dipolar cycloaddition reaction between olefin substituted saccharins and hydroximinoyl acid chlorides (chloro oximes), leading to final products (**Scheme 3.1, a-d**).
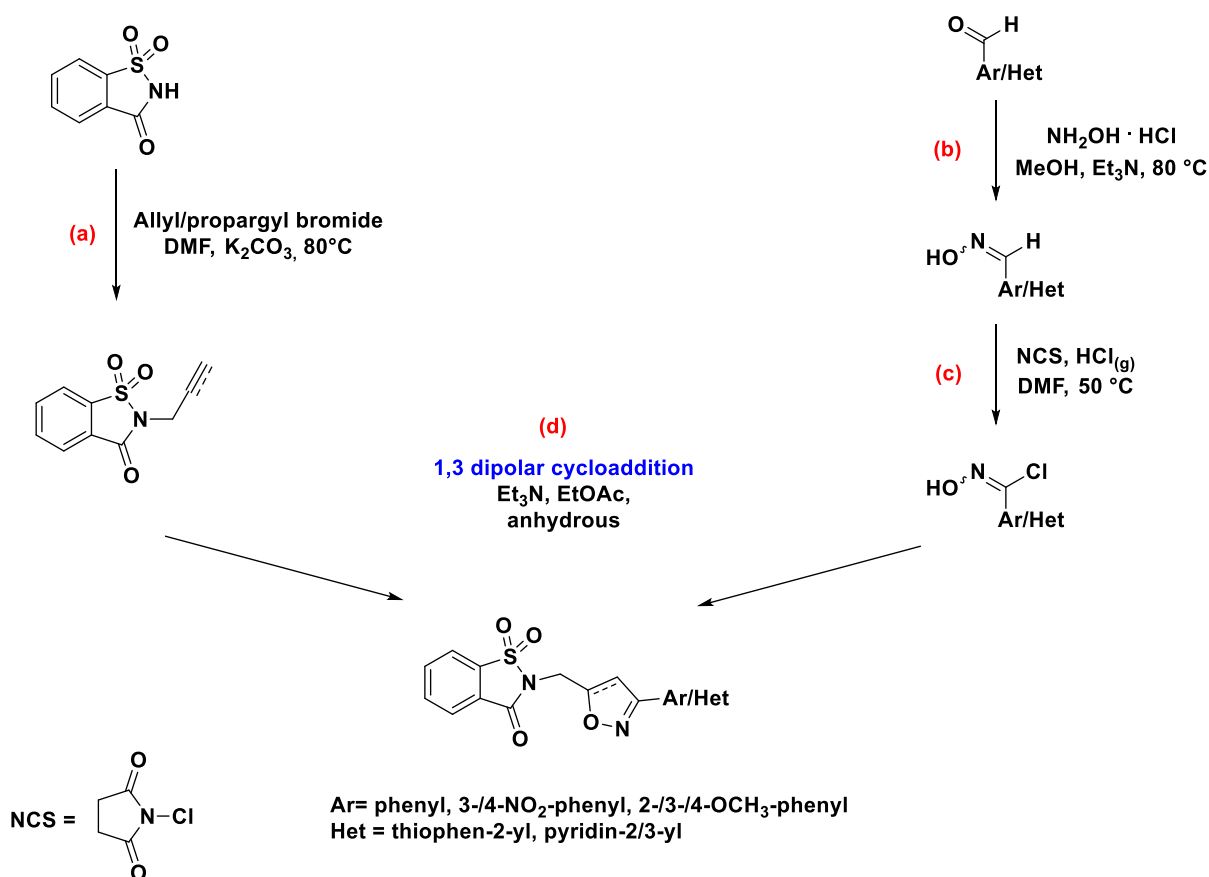
Scheme 3.1. Synthetic approach for the synthesis of new derivatives **1a**-**9a** and **1b**-**9b**.

N-alkylated saccharins were obtained following our previously reported procedure [109], through nucleophilic substitution reaction between saccharin and allyl/propargyl bromide (**Scheme 3.1, a**). The hydroximinoyl acid chlorides (chloro oximes) were synthesised in two steps from the corresponding benzaldehydes

[109,124]. The first step (**Scheme 3.1, b**) involved the reaction between the selected aldehyde and hydroxylamine hydrochloride, in the presence of triethylamine in methanol (80 °C) to obtain oximes [109]. At a later time, the freshly synthesised oxime was reacted with *N*-chlorosuccinimide (NCS) in *N,N*-dimethylformamide (DMF), adding gaseous hydrogen chloride (HCl(g)) to promote the beginning of reaction (**Scheme 3.1, c**). In fact, Howe *et al.* observed that the reaction of NCS with benzaldoximes exhibited an induction period that could be reduced through the addition of small amounts of gaseous HCl. In this way, we avoided the fairly exothermic behaviour observed when the reaction initiates in the presence of considerable portion of the NCS [124]. The resulting chloro oximes were not contaminated by side-products (i.e. ring chlorinated products) and could be used without purification in the next 1,3-dipolar cycloaddition. In this reaction the 1,3-dipole, that is the nitrile oxides generated *in situ* by dehydrohalogenation of the chloro oxime with triethylamine, reacted with the dipolarophile (*N*-allyl/propargyl saccharins) in ethyl acetate. Regioselectivities in isoxazoline ring synthesis are controlled by the energy of the atomic orbitals involved (frontiers molecular orbitals, FMO), although in some reactions electronically preferred orientations may be disfavoured by steric effects [125]. However, the reaction of nitrile oxides with monosubstituted olefins are quite exclusive, giving only or predominantly the 5-substituted isoxazoline, regardless the nature of the substituent on the dipolarophile. On the other hand, cycloaddition of nitrile oxides to acetylenic dipolarophiles leads directly to 5-substituted isoxazoles [123,125].

3.3 Two-dimensional nuclear Overhauser enhancement spectroscopy (2D-NOESY NMR)

Compound **3b** synthesised from *N*-hydroxy-pyridine-2-carbimidoyl chloride and *N*-propargyl saccharin, was subjected 2D-NMR using NOESY approach. This analysis was able to reveal spatial relationships among proximal protons, **i**n order to confirm

the regioselectivity of the 1,3-dipolar cycloaddition reaction, to give 5-substituted isoxazoles instead of 4-substituted ones (**Figure 3.2**).
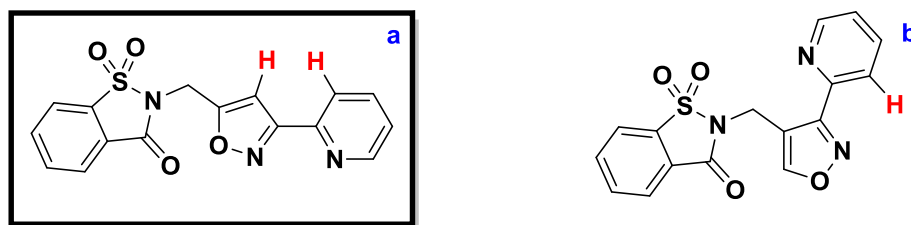

Figure 3.2. (**a**) Compound **3b** containing 5-substituted isoxazoline, proximal protons were depicted in red; (**b**) compound **3b** containing unattended 4-substituted isoxazoline and without proximal protons.

3.4 Biological evaluation

All the synthesized saccharin/isoxazoline and saccharin/isoxazole derivatives were tested to evaluate their inhibitory activity towards the ubiquitous off-target isoforms, hCA I and II, and the cancer-related ones, hCA IX and XII, by a stopped-flow, CO_2 hydrase assay method and their CA inhibition data (K_i) are summarized in **Table 3.1.**

3.5 Results and discussion

3.5.1 Inhibition of hCA I, II, IX, and XII.

Comparing the activity of compounds **1a**-**9a** and **1b**-**9b** with the *N*-alkyl/propargyl saccharins parent drugs, it is possible to asses that the insertion of isoxazoline/isoxazole ring, connected with aromatic or heteroaromatic system, improved both activity and selectivity. Data reported in **Table 3.1** show that all the synthesised compounds are selective inhibitors of tumor-related isoforms (hCA IX and hCA XII), being devoid of any activity towards the two ubiquitously expressed isoforms hCA I and hCA II, their off-target. Except for compound **9a**, all derivatives showed preferred affinity for isoform XII with K_i spanning from 7.0 nM obtained for compound **6b**, to 240 nM exhibited by **2b**. The nature of the linker (isoxazoline rather than isoxazole) or the substituents on phenyl ring, as well as heterocyclic type system,
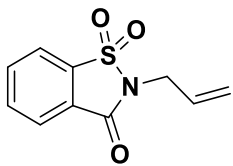
influenced the inhibitory activity against the tested isoforms. These compounds did not show a general trend; however, an important evidence was obtained. Compounds **1a** and **1b**, substituted with NO_2 on *meta* position of phenyl ring, showed a similar inhibitory activity towards isoform XII (**1a**, K_i hCA XII = 76.5 nM; **1b**, K_i hCA XII = 57.3 nM), while compound **1a** was more effective than **1b** against isoform IX (**1a**, K_I hCA IX = 102.9 nM; **1b**, K_I hCA IX = 230.2 nM). Compounds **2a** and **2b**, possessing a *p*-NO_2 substituted phenyl ring, displayed a similar trend for hCA IX inhibition, while compound **2b** containing the isoxazole linker, showed impaired activity towards isoform XII (**2a**, K_i hCA XII = 77 nM; **2b**, K_i hCA XII = 240 nM). For these four derivatives it was possible to note that starting from **1a**, containing a *m*-NO_2 substituted phenyl ring bound to the isoxazoline ring, to compound **2b** endowed with *p*-NO_2 substituted phenyl ring connected to isoxazole system, there was a decrease of activity against hCA IX (**Table 3.1**). This trend was opposite compared with derivatives ranking from **6a** to **7b**, possessing methoxy substituent (OMe). Indeed, compound **7b** endowed with isoxazole linker and *p*-OMe substituted phenyl ring, showed a good activity against isoform IX (K_I hCA IX = 22.1 nM). The other derivatives possessing a methoxy group were inactive (**5a**, **5b**, **6a**), or less effective (**6b**, **7a**) towards isoform IX, compared to **7b**. However, all the molecules containing methoxy group on phenyl ring were good inhibitors of hCA XII ($7.0 \leq K_i$ hCA XII (nM) ≤ 9.4) with the best activity exhibited by compound **6b**. From these data it seems that the nature of the linker not favoured one isoform instead of the other or influenced in a specific manner the enzyme inhibition. In fact, the isoxazoline variation of **1a** with isoxazole of **1b**, increased the activity against hCA XII while reduced that towards hCA IX. For the couple **2a**-**2b**, we observed impairment of activity towards both the tumor-related isoforms passing from isoxazoline linker to isoxazole one. The changing of the linker type for couples **6a**-**6b** and **7a**-**7b** influenced only the inhibitory activity towards hCA IX, while hCA XII was not affected, showing almost constant inhibition data. Albeit further substitution patterns have to be evaluated, these preliminary outcomes showed that
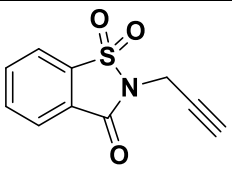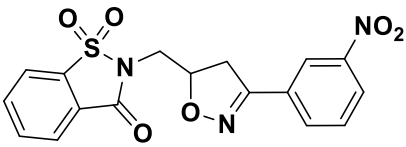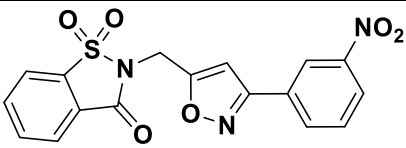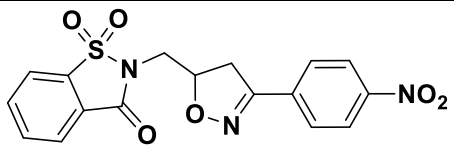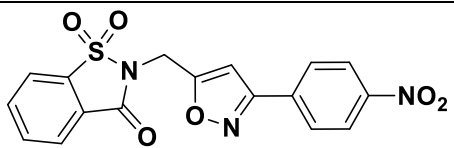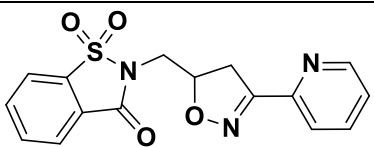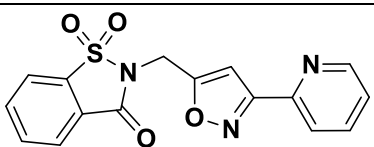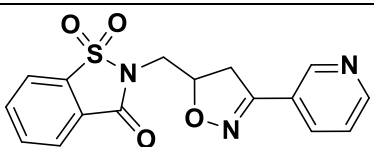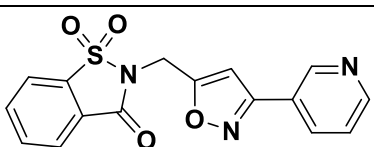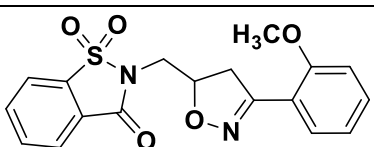
was the combination of the substituent type/position on phenyl ring along with linker combination, rather than the single feature, which affect the inhibitory activity.
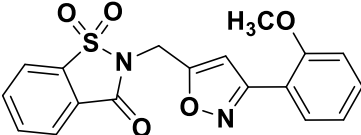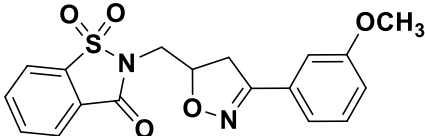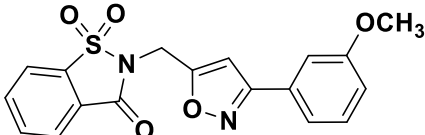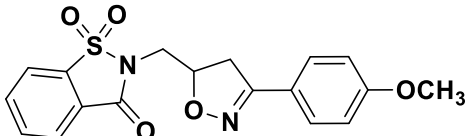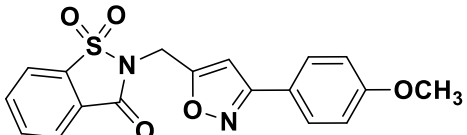
Heterocyclic systems bound to the linker moiety were also evaluated. Compounds **3a** and **3b** were endowed with pyridin-2-yl moiety bound respectively to isoxazoline and isoxazole ring. These molecules showed similar activity against hCA IX (**3a**, K_I hCA IX = 258.2 nM; **3b**, K_I hCA IX = 245.4 nM), whereas compound **3a** exhibited better activity against hCA XII (**3a**, K_i hCA XII = 9.7 nM; **3b**, K_i hCA XII = 66.5 nM). Derivatives **4a** and **4b** whit pyridin-3-yl system showed comparable activity towards isoform XII, while differed for activity on hCA IX (**4a**, K_I hCA IX = 273.5 nM; **4b**, K_I hCA IX = 86.2 nM). These data confirmed the absence of the univocal influence of li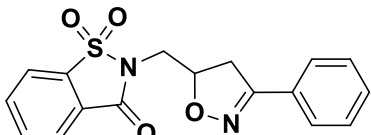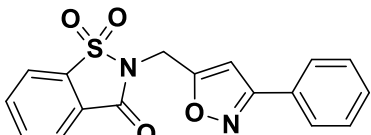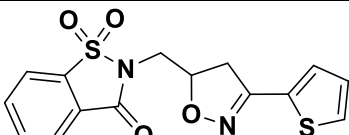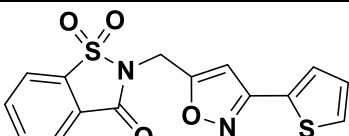nker. These data confirmed the absence of the univocal influence of linker. Compounds endowed with unsubstituted phenyl ring bound on the isooxazoline linker **8a** showed the inhibition of only hCA XII; the isoxazole counterpart **8b** was effective against both the tumor-related isoforms (**8b**, K_i hCAIX = 50.9 nM; K_i hCAXII = 7.5 nM). Finally, compounds containing thiophene **9a** and **9b** showed the best inhibitory profile with low nanomolar activity towards both hCAIX (**9a**, K_i hCA IX = 7.2 nM; **9b**, K_i hCA IX = 9.0 nM) and XII (**9a**, K_i hCA XII = 9.0 nM; **9b**, K_i hCA XII = 8.2 nM).

So, the five-membered heterocyclic system seems to be the best tolerated group bound to the linker moiety

Table 3.1. Inhibition data of selected human CA isoforms (hCA I, II, IX and XII) with compounds **1a-9a** and **1b-9b** reported here and the standard sulfonamide inhibitor acetazolamide (AAZ) by a stopped flow CO_2 hydrase assay.

Compound	Structure	K_i (nM)			
		hCA I	hCA II	hCA IX	hCA XII
S1		>10000	86	140	94

S2		>10000	58	210	570
1a		>10000	>10000	102.9	76.5
1b		>10000	>10000	230.2	57.3
2a		>10000	>10000	235.1	77.0
2b		>10000	>10000	310	240
3a		>10000	>10000	258.2	9.7
3b		>10000	>10000	245.4	66.5
4a		>10000	>10000	273.5	9.2
4b		>10000	>10000	86.2	8.0
5a		>10000	>10000	>10000	9.4

5b		>10000	>10000	>10000	9.3
6a		>10000	>10000	>10000	7.6
6b		>10000	>10000	247.1	7.0
7a		>10000	>10000	139.1	8.1
7b		>10000	>10000	22.1	8.0
8a		>10000	>10000	>10000	8.5
8b		>10000	>10000	50.9	7.5
9a		>10000	>10000	7.2	9.0
9b		>10000	>10000	7.5	8.2
AAZ		250	12	25	5.7

*Mean from 3 different assay, by a stopped flow technique (errors were in the range of $\pm$ 5-10 % of the reported values).

3.5.2 2D-NOESY NMR of compound 3b

2D-NOESY NMR spectra reported in **Figure 3.3**, displayed the presence of the interaction between the two protons previously showed in **Figure 3.2**.
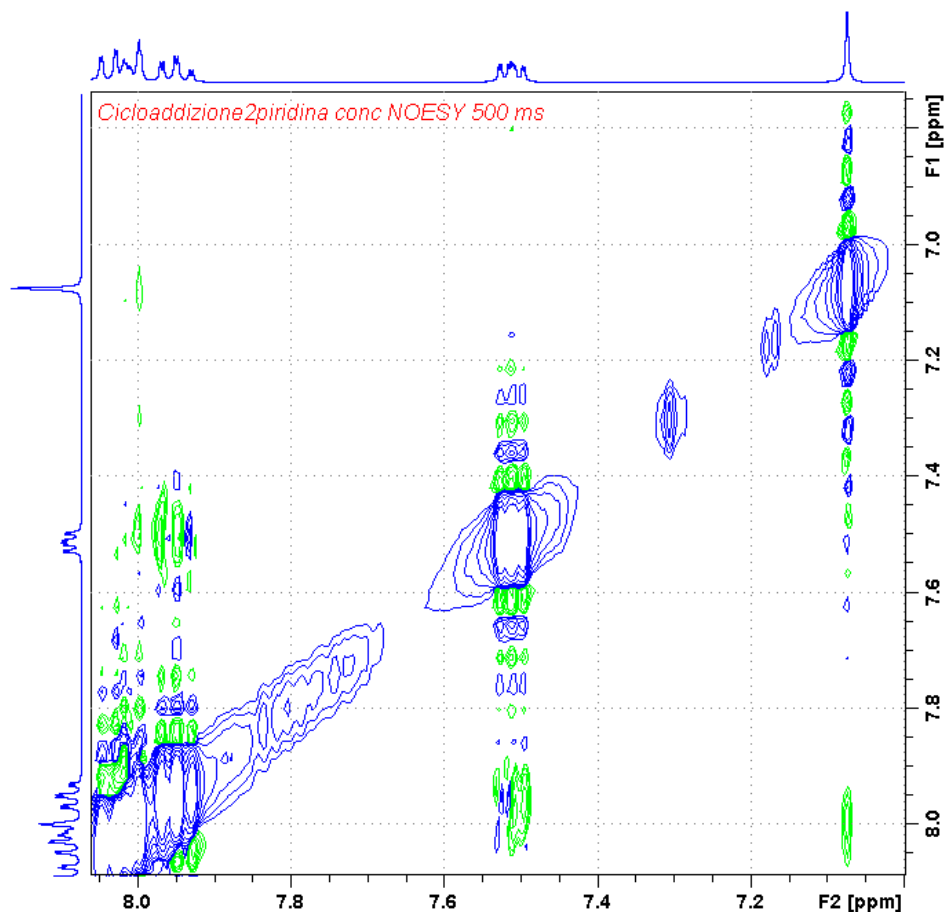
Figure 3.3. 2D-NOESY NMR of compound **3b**.

The presence of the interaction between protons with spatial proximity, was confirmed by the presence of the "green" circles present along an ideal line which connect the proton C4(H) of the isoxazole ring (singlet at ~7.06), with pyridine signals between 7.90 and 8.10 ppm containing the one of the proton at C3 position of pyridine ring. This outcome showed the interaction between the red depicted hydrogens of **Figure 3.2, a** confirming the regioselectivity of the reactions.

3.6 Conclusion

The design, synthesis, characterization and *in vitro* pharmacological evaluation of several new saccharin/isoxazoline and saccharin/isoxazole derivatives have been reported. They shown to be ineffective towards the two cytosolic off-target hCA I and II (K_is > 10 μM); conversely, most of these compounds inhibited both the tumor related isoforms hCA IX and XII in the low nanomolar range with K_is ranging between 7.0 and 310 nM. The majority of molecules **1a**-**9a** and **1b**-**9b** showed preferred activity for hCA XII, with the best result observed for compound **6b** (K_i hCA XII = 7.0 nM), although also hCA IX were inhibited in the low nanomolar range by some derivatives. The analysis of the K_i values showed the absence of an explicit correlation between the linker type and the activity/selectivity profile; rather, the activity of compounds was likely affected by the arrangement of phenyl ring substituent and linker type.

The results will be rationalized by means docking studies in order to evaluate the interactions whose affect the activity and selectivity. Furthermore, some of the saccharin/isoxazoline derivatives will be exposed to chiral resolution to obtain the enantiomers and evaluate as chiral properties affect the inhibitory activity.

3.7 Experimental section

General

Unless otherwise indicated, all reactions were carried out under a positive pressure of nitrogen (balloon pressure) in washed and oven-dried glassware. Solvents were used as supplied without further purification. Where mixtures of solvents are specified, the stated ratios are volume:volume. Reagents were used directly as supplied by Sigma-Aldrich® Italy. All melting points were measured on a Stuart® melting point apparatus SMP1, and are uncorrected. Temperatures are reported in °C. ¹H and ¹³C NMR spectra were recorded at 400 and 101 MHz, respectively, on a Bruker spectrometer using CDCl₃, DMSO-*d₆*, MeOD and CD₃CN, as the solvents at room temperature. The samples were analysed with a final concentration of ~30 mg/mL. Chemical shifts are expressed as *δ* units (parts per millions) relative to the solvent signal. ¹H spectra are reported as follows: *δ*H (*spectrometer frequency, solvent*): *chemical shift/ppm* (*multiplicity,*

J-coupling constant(s), number of protons, assignment). [13]C spectra are reported as follows: δ_C (*spectrometer frequency, solvent*): *chemical shift/ppm (assignment)*. Multiplets are abbreviated as follows: br – *broad*; s – *singlet*; d – *doublet*; t – *triplet*; q – *quartet*; m – *multiplet*. Coupling constants J are valued in Hertz (Hz). The processing and analyses of the NMR data were carried out with MestreNova. Infra-red spectra were recorded on a Bruker Tensor 27 FTIR spectrometer equipped with an attenuated total reflectance attachment with internal calibration. Absorption maxima (ν_{max}) are reported in wavenumbers (cm^{-1}). Column chromatography was carried out using Sigma-Aldrich® silica gel (high purity grade, pore size 60 Å, 230–400 mesh particle size). All the purifications and reactions were monitored by TLC performed on 0.2 mm thick silica gel-aluminium backed plates (60 F254, Merck). Visualization was carried out under ultra-violet irradiation (254 nm). Where given, systematic compound names are those generated by ChemBioDraw Ultra 12.0 following IUPAC conventions.

Synthesis and characterization data of saccharin derivatives S1-S2
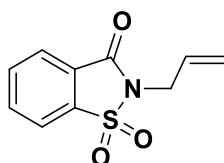
2-allylbenzo[*d*]isothiazol-3(2H)-one 1,1-dioxide (**S1**): anhydrous potassium carbonate (1.1 eq.) was added to a stirring solution of saccharin (1.0 eq.) in 10 mL of *N,N*-dimethylformamide (DMF) at room temperature. Allyl chloride (4.0 eq.) was added portionwise and the reaction mixture was stirred at 80°C for 48 h. The mixture was poured on ice and extracted with chloroform. The organics were reunited, dried over sodium sulfate and concentrated *in vacuo*. Purification by column chromatography on silica gel (ethyl acetate:petroleum ether 1:2) gave title compound as a white solid (76% yield); mp 73-75 °C; IR ν_{max} 3094 (ν C$_{sp2}$-H), 1731 (ν C=O), 1331 (ν_{as} SO$_2$), 1262 (ν C-N), 1180 (ν_s SO$_2$), 751 (δ C$_{sp2}$-H) cm^{-1}; ^{1}H-NMR (400 MHz, DMSO-*d$_6$*): δ 4.34 (s, 2H CH$_2$), 5.25 (d, J = 10.0 Hz, 1H, =CH$_2$), 5.36 (d, J = 16.8 Hz, 1H, =CH$_2$),

5.89-5.95 (m, 1H, CH=), 7.98-8.12 (m, 3H, 3 x Ar), 8.32 (d, J = 7.6 Hz, 1H, Ar); ^{13}C-NMR (101 MHz, DMSO-d_6): δ 40.99 (CH$_2$), 118.95 (CH$_2$=), 122.03 (Ar), 125.60 (Ar), 126.71 (Ar), 131.75 (CH=), 135.73 (Ar), 136.31 (Ar), 137.36 (Ar), 158.71 (C=O).
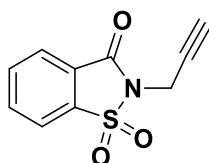
**2-(Prop-2-yn-1-yl)-1,2-benzothiazol-3(2H)-one 1,1-dioxide (S2):** anhydrous potassium carbonate (1.1 eq.) was added to a stirring solution of saccharin (1.0 eq.) in 10 mL of N,N-dimethylformamide at room temperature. Propargyl bromide (4.0 eq.) was added portionwise and the reaction mixture was stirred at room temperature for 48 h. The mixture was poured on ice and extracted with dichloromethane. The organics were reunited, dried over sodium sulfate and concentrated *in vacuo*. Purification by column chromatography on silica gel (ethyl acetate:petroleum ether 1:1) gave compound **2a** as a white solid (60% yield); mp 112-116 °C; IR ν_{max} 3273 (ν C$_{sp}$-H), 3093 (ν C$_{sp2}$-H), 2126 (ν C≡C), 1737 (ν C=O), 1332 (ν_{as} SO$_2$), 1258 (ν C-N), 1177 (ν_s SO$_2$), 751 (δ C$_{sp2}$-H) cm^{-1}; ^{1}H-NMR (400 MHz, DMSO-d_6): δ 3.39 (s, 1H, CH≡), 4.57 (s, 2H, CH$_2$), 7.97-8.´01 (m, 1H, Ar), 8.03-8.07 (m, 1H, Ar), 8.11 (d, J = 7.6 Hz, 1H, Ar), 8.32 (d, J = 7.6 Hz, 1H, Ar); ^{13}C-NMR (101 MHz, DMSO-d_6): δ 27.95 (CH$_2$), 75.68 (CH≡), 77.49 (C≡CH), 122.16 (Ar), 125.75 (Ar), 126.43 (Ar), 135.84 (Ar), 136.56 (Ar), 137.37 (Ar), 158.36 (C=O).
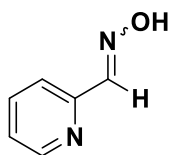
Synthesis and characterization data of oximes O1-O9
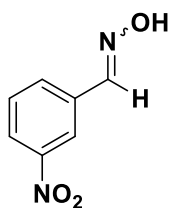
3-nitrobenzaldehyde oxime (O1): in an oven dried flask hydroxylamine hydrochloride (1.5 eq) and triethylamine (2.25 eq) were dissolved in 10 mL of

anhydrous methanol and stirred for 5 minutes at room temperature. 3-nitrobenzaldehyde (1.0 eq) was added and the reaction mixture stirred at 80 °C until complete consumption of starting material. The reaction was cooled down to room temperature and the solvent removed *in vacuo*. 20 mL of ice-cold water were added to the residue and the resulting suspension was kept at 0-4 °C overnight in order to obtain oximes precipitate, which was filtered and washed with mixture of petroleum ether/diethyl ether, obtaining the title compound as a light yellow solid (85.0 % yield); mp 108-111 °C; IR ν_{max} 3267 (ν O-H), 1618 (ν C=N), 1531 (ν_{as} N-O), 1348 (ν_s N-O), 976 (N-O, oxime), 733 (δ C$_{sp2}$-H) cm^{-1}; ^{1}H-NMR (400 MHz, DMSO-d_6): δ 7.66-7.70 (m, 1H, Ar), 8.02 (d, J = 7.6 Hz, 1H, Ar), 8.19 (d, J = 8.0 Hz, 1H, Ar), 8.30 (s, 1H, OH), 8.39 (s, 1H, Ar), 11.63 (s, 1H, HC=N-) . ^{13}C-NMR (101 MHz, DMSO-d_6): δ 121.3 (Ar), 124.1 (Ar), 130.8 (Ar), 132.8 (Ar), 135.4 (Ar), 147.1 (Ar), 148.6 (HC=N-).
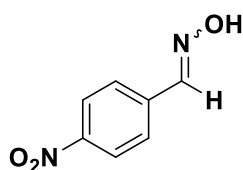
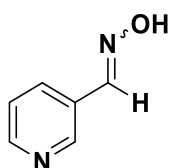**4-nitrobenzaldehyde oxime (O2):** in an oven dried flask hydroxylamine hydrochloride (1.5 eq) and triethylamine (2.25 eq) were dissolved in 10 mL of anhydrous methanol and stirred for 5 minutes at room temperature. 4-nitrobenzaldehyde (1.0 eq) was added and the reaction mixture stirred at 80 °C until complete consumption of starting material. The reaction was cooled down to room temperature and the solvent removed *in vacuo*. 20 mL of ice-cold water were added to the residue and the resulting suspension was kept at 0-4 °C overnight in order to obtain oximes precipitate, which was filtered and washed with mixture of petroleum ether/diethyl ether, obtaining the title compound as a yellow solid (95.9% yield); mp 99-102 °C; IR ν_{max} 3292 (ν O-H), 1604 (ν C=N), 1532 (ν_{as} N-O), 1346 (ν_s N-O), 942 (N-O, oxime), 747 (δ C$_{sp2}$-H) cm^{-1}; ^{1}H-NMR (400 MHz, DMSO-d_6): δ 7.83 (d, J = 7.6 Hz, 2H, Ar), 8.23 (d, J = 8 Hz, 2H, Ar), 8.28 (s, 1H, OH), 11.83 (s, 1H, HC=N-). ^{13}C-NMR (101 MHz, DMSO-d_6): δ 124.4 (2 x Ar), 127.8 (2 x Ar), 140.0 (Ar), 147.3 (Ar), 148.0 (HC=N-).

Pyridine-2-aldoxime (O3): in an oven dried flask hydroxylamine hydrochloride (1.5 eq) and triethylamine (2.25 eq) were dissolved in 10 mL of anhydrous methanol and stirred for 5 minutes at room temperature. Pyridine-2-carboxaldehyde (1.0 eq) was added and the reaction mixture stirred at 80 °C until complete consumption of starting material. The reaction was cooled down to room temperature and the solvent removed *in vacuo*. 20 mL of ice-cold water were added to the residue and the resulting suspension was kept at 0-4 °C overnight in order to obtain oximes precipitate, which was filtered and washed with mixture of petroleum ether/diethyl ether, obtaining the title compound as a white solid (70% yield); mp 64-67 °C; IR ν_{max} 2696 (ν O-H), 1519 (ν C=N), 1410 (δ O-H), 982 (N-O, oxime), 702 (δ C$_{sp2}$-H) cm^{-1}; ^{1}H-NMR (400 MHz, DMSO-d_6): δ 7.34-7.37 (m, 1H, pyr), 7.78-7.82 (m, 2H, pyr), 8.06-8.07 (m, 1H, pyr), 8.55-8.56 (m, 1H, OH), 11.67 (s, 1H, HC=N-). ^{13}C-NMR (101 MHz, DMSO-d_6): δ 120.2 (pyr), 124.4 (pyr), 137.2 (pyr), 149.4 (pyr), 149.8 (HC=N-), 152.5 (pyr).

Pyridine-3-aldoxime (O4): in an oven dried flask hydroxylamine hydrochloride (1.5 eq) and triethylamine (2.25 eq) were dissolved in 10 mL of anhydrous methanol and stirred for 5 minutes at room temperature. Pyridine-3-carboxaldehyde (1.0 eq) was added and the reaction mixture stirred at 80 °C until complete consumption of starting material, the reaction was cooled down to room temperature and the solvent removed *in vacuo*. 20 mL of ice-cold water were added to the residue and the resulting suspension was kept at 0-4 °C overnight in order to obtain oximes precipitate, which

was filtered and washed with mixture of petroleum ether/diethyl ether, obtaining the title compound as a white solid (92 % yield); mp 122-123 °C; IR ν_{max} 2773 (ν O-H), 1592 (ν C=N), 1434 (δ O-H), 975 (N-O, oxime), 735 (δ C$_{sp2}$-H) cm^{-1}; ^{1}H-NMR (400 MHz, DMSO-d_6): δ 7.40-7.42 (m, 2H, pyr), 7.96-7.98 (m, 1H, pyr), 8.18 (s, 1H, pyr), 8.53-8.54 (m, 1H, OH), 11.51 (s, 1H, HC=N-). ^{13}C-NMR (101 MHz, DMSO-d_6): δ 124.3 (pyr), 129.5 (pyr), 133.5 (pyr), 146.2 (pyr), 148.3 (HC=N-), 150.5 (pyr).
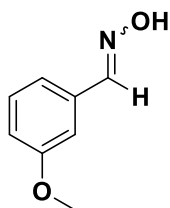

2-methoxybenzaldehyde oxime (O5): in an oven dried flask hydroxylamine hydrochloride (1.5 eq) and triethylamine (2.25 eq) were dissolved in 10 mL of anhydrous methanol and stirred for 5 minutes at room temperature. 2-methoxybenzaldehyde (1.0 eq) was added and the reaction mixture stirred at 80 °C until complete consumption of starting material. The reaction was cooled down to room temperature and the solvent removed *in vacuo*. 20 mL of ice-cold water were added to the residue and the resulting suspension was kept at 0-4 °C overnight in order to obtain oximes precipitate, which was filtered and washed with mixture of petroleum ether/diethyl ether, obtaining the title compound as a light yellow solid (89.17 % yield); mp 73-76 °C; ^{1}H-NMR (400 MHz, CDCl$_3$): δ 3.90 (s, 3H, CH$_3$), 6.94-7.01 (m, 2H, Ar), 7.36-7.40 (m, 1H, Ar), 7.66-7.68 (m, 1H, Ar), 8.50 (s, 1H, HC=N-), 9.37 (s, 1H, OH).
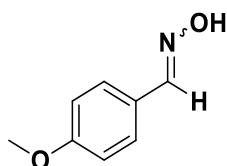

3-methoxybenzaldehyde oxime (O6): in an oven dried flask hydroxylamine hydrochloride (1.5 eq) and triethylamine (2.25 eq) were dissolved in 10 mL of

anhydrous methanol and stirred for 5 minutes at room temperature. 3-methoxybenzaldehyde (1.0 eq) was added and the reaction mixture stirred at 80 °C until complete consumption of starting material. The reaction was cooled down to room temperature and the solvent removed *in vacuo*. 20 mL of ice-cold water were added to the residue and the resulting suspension was extracted with ethyl acetate (3 x 20 mL). The organics were reunited, dried over sodium sulphate and evaporated *in vacuo* to give the title compound as thick oil (89.2% yield); ^{1}H-NMR (400 MHz, CD₃CN): δ 3.80 (s, 3H, CH₃), 6.96-6.98 (m, 2H, Ar), 7.21-7.24 (m, 2H, Ar), 7.31-7.35 (m, 1H, Ar), 8.20 (s, 1H, HC=N-), 9.45 (br, 1H, OH).
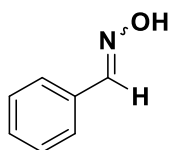

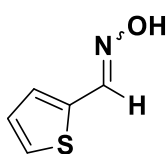**4-methoxybenzaldehyde oxime (O7):** in an oven dried flask hydroxylamine hydrochloride (1.5 eq) and triethylamine (2.25 eq) were dissolved in 10 mL of anhydrous methanol and stirred for 5 minutes at room temperature. 4-methoxybenzaldehyde (1.0 eq) was added and the reaction mixture stirred at 80 °C until complete consumption of starting material. The reaction was cooled down to room temperature and the solvent removed *in vacuo*. 20 mL of ice-cold water were added to the residue and the resulting suspension was kept at 0-4 °C overnight in order to obtain oximes precipitate, which was filtered and washed with mixture of petroleum ether/diethyl ether, obtaining the title compound as a white solid (89.2% yield); mp 31-33 °C; ^{1}H-NMR (400 MHz, CD₃CN): δ 3.81 (s, 3H, CH₃), 6.95-7.0 (m, 2H, Ar), 7.53-7.55 (m, 2H, Ar), 8.07 (s, 1H, OH), 8.95 (s, 1H, HC=N-).

Benzaldehyde oxime (O8): in an oven dried flask hydroxylamine hydrochloride (1.5 eq) and triethylamine (2.25 eq) were dissolved in 10 mL of anhydrous methanol and stirred for 5 minutes at room temperature. Benzaldehyde (1.0 eq) was added and the reaction mixture stirred at 80 °C until complete consumption of starting materials. The reaction was cooled down to room temperature and the solvent removed *in vacuo*. 20 mL of ice-cold water were added to the residue and the resulting suspension was extracted with ethyl acetate (3 x 20 mL). The organics were reunited, dried over sodium sulphate and evaporated *in vacuo* to give the title compound as colourless oil (75% yield); ^{1}H-NMR (400 MHz, CDCl$_3$): δ 7.41 (m, 3H, Ar), 7.61 (br, 2H, Ar), 8.21 (s, 1H, HC=N-), 9.38 (s, 1H, OH).

Thiophene-2-carbaldehyde oxime (O9): in an oven dried flask hydroxylamine hydrochloride (1.5 eq) and triethylamine (2.25 eq) were dissolved in 10 mL of anhydrous methanol and stirred for 5 minutes at room temperature. Thiophene-2-carbaldehyde (1.0 eq) was added and the reaction mixture stirred at 80 °C until complete consumption of starting materials. The reaction was cooled down to room temperature and the solvent removed *in vacuo*. 20 mL of ice-cold water were added to the residue and the resulting suspension was kept at 0-4 °C overnight in order to obtain oximes precipitate, which was filtered and washed with mixture of petroleum ether/diethyl ether, obtaining the title compound as a light brown solid (63% yield); ^{1}H-NMR (400 MHz, CD$_3$CN): δ 7.13-7.15 (m, 1H, thiophene), 7.44-7.66 (m, 2H, thiophene), 7.76 (s, 1H, OH), 9.70 (s, 1H, HC=N-).

Synthesis and characterization data of chloro oximes C1-C9

***N*-hydroxy-3-nitrobenzimidoyl chloride (C1):** in an oven dried flask *m*-nitrobenzaldoxime **O1** (1.0 eq) was dissolved in 10 mL of anhydrous DMF. *N*-chlorosuccinimide (0.2 eq) were added and the reaction stirred for 10 minutes at room temperature. The solution was pu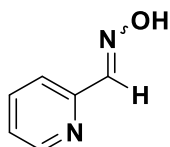rged with 20 mL of HCl(g) and the reaction stirred for 10 additional minutes and then heated up to 50 °C. *N*-chlorosuccinimide were added portion wise (0.2 eq at the time, up to 1.5 total eq.) over half an hour. The progression of the reaction was monitored using iodine starch paper. When the iodine starch paper was not turning brown anymore, the reaction was quenched with 4 volumes of ice-cold water. The aqueous phase was extracted with diethyl ether, the organics reunited were dried over sodium sulphate and evaporated *in vacuo* to give the title compound as a yellow-orange solid (49 % yield); mp 99-100 °C; IR ν_{max} 3293 (ν O-H), 1523 (ν_{as} N-O), 1349 (ν_s N-O), 979 (N-O, oxime), 728 (δ C_{sp2}-H) cm^{-1}; ^{1}H-NMR (400 MHz, DMSO-d_6): δ 7.74-7.78 (m, 1H, Ar), 8.19-8.31 (m, 2H, Ar), 8.47 (s, 1H, Ar), 12.81 (s, 1H, OH) . ^{13}C-NMR (101 MHz, DMSO-d_6): δ 121.3 (Ar), 125.3 (Ar), 131.0 (Ar), 133.0 (Ar), 134.1 (Ar), 134.5 (Ar), 148.4 (ClC=N-).
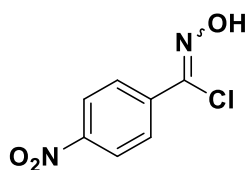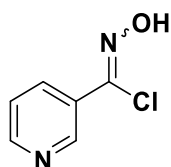
N-hydroxy-4-nitrobenzimidoyl chloride (C2): in an oven dried flask *p*-nitrobenzaldoxime **O2** (1.0 eq) was dissolved in 10 mL of anhydrous DMF. *N*-chlorosuccinimide (0.2 eq) were added and the reaction stirred for 10 minutes at room temperature. The solution was purged with 20 mL of HCl(g) and the reaction stirred for 10 additional minutes and then heated up to 50 °C. *N*-chlorosuccinimide were added portion wise (0.2 eq at the time, up to 1.5 total eq.) over half an hour. The progression of the reaction was monitored using iodine starch paper. When the iodine starch paper was not turning brown anymore, the reaction was quenched with 4 volumes of ice-cold water. The aqueous phase was extracted with diethyl ether, the organics reunited were dried over sodium sulphate and evaporated *in vacuo* to give the title compound as light yellow solid (85% yield); mp 107-110 °C; IR v_{max} 3266 (v O-H), 1598 (v C=N), 1519 (v_{as} N-O), 1349 (v_s N-O, NO$_2$), 941 (N-O, oxime), 842 (v C$_{sp2}$-Cl), (752 (δ C$_{sp2}$-H) cm^{-1}; ^{1}H-NMR (400 MHz, DMSO-d_6): δ 8.08.02 (m, 2H, Ar), 8.26-8.28 (m, 2H, Ar), 12.93 (s, 1H, OH). ^{13}C-NMR (101 MHz, DMSO-d_6): δ 124.4 (2 x Ar), 128.2 (2 x Ar), 134.5 (Ar), 138.7 (Ar), 148.7 (ClC=N-).

N-hydroxy- pyridine-2-carbimidoyl chloride (C3): in an oven dried flask pyridine-2-aldoxime **O3** (1.0 eq) was dissolved in 10 mL of anhydrous DMF. *N*-chlorosuccinimide (0.2 eq) were added and the reaction stirred for 10 minutes at room temperature. The solution was purged with 20 mL of HCl(g) and the reaction stirred for 10 additional minutes and then heated up to 50 °C. *N*-chlorosuccinimide were added portion wise (0.2 eq at the time, up to 1.5 total eq.) over half an hour. The progression of the reaction was monitored using iodine starch paper. When the iodine starch paper was not turning brown anymore, the reaction was quenched with 4 volumes of ice-cold water. The aqueous phase was extracted with diethyl ether, the organics reunited were dried over sodium sulphate and evaporated *in vacuo* to give the title compound as a light

brown solid (76.6 % yield); mp 110-110 °C; ^{1}H-NMR (400 MHz, DMSO-d_6): δ 7.46-7.49 (m, 1H, pyr), 7.86-7.88 (m, 2H, pyr), 8.64-8.65 (m, 1H, pyr), 12.64 (m, 1H, OH). ^{13}C-NMR (101 MHz, DMSO-d_6): δ 122.0 (pyr), 125.4 (pyr), 137.1 (pyr), 137.59 (pyr), 149.8 (ClC=N-), 150.2 (pyr).
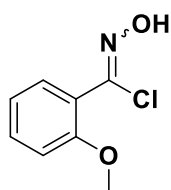

N-hydroxy-pyridine-3-carbimidoyl chloride (C4): in an oven dried flask pyridine-3-aldoxime **O4** (1.0 eq) was dissolved in 10 mL of anhydrous DMF. *N*-chlorosuccinimide (0.2 eq) were added and the reaction stirred for 10 minutes at room temperature. The solution was purged with 20 mL of HCl(g) and the reaction stirred for 10 additional minutes and then heated up to 50 °C. *N*-chlorosuccinimide were added portion wise (0.2 eq at the time, up to 1.5 total eq.) over half an hour. The progression of the reaction was monitored using iodine starch paper. When the iodine starch paper was not turning brown anymore, the reaction was quenched with 4 volumes of ice-cold water. The aqueous phase was extracted with diethyl ether, the organics reunited were dried over sodium sulphate and evaporated *in vacuo* to give the title compound as brown solid (8.85 % yield); mp 126-128 °C; IR ν_{max} 2517 (ν O-H), 1525 (ν C=N), 1417 (δ O-H), 949 (N-O, oxime), 805 (ν C $_{sp2}$-Cl), 693 (δ C$_{sp2}$-H) cm^{-1}; ^{1}H-NMR (400 MHz, DMSO-d_6): δ 7.50-7.53 (m, 1H, pyr), 8.13-8.14 (m, 1H, pyr), 8.66 (s, 1H, pyr), 8.95 (s, 1H, pyr), 12.69 (s, 1H, OH). ^{13}C-NMR (101 MHz, DMSO-d_6): δ 124.3 (pyr), 129.4 (pyr), 133.6 (pyr), 134.9 (pyr), 147.4 (ClC=N-), 151.3 (pyr).

N-hydroxy-2-methoxybenzimidoyl chloride (C5): in an oven dried flask 2-methoxybenzaldehyde oxime **O5** (1.0 eq) was dissolved in 10 mL of anhydrous DMF. N-chlorosuccinimide (0.2 eq) were added and the reaction stirred for 10 minutes at room temperature. The solution was purged with 20 mL of HCl(g) and the reaction stirred for 10 additional minutes and then heated up to 50 °C. N-chlorosuccinimide were added portion wise (0.2 eq at the time, up to 1.5 total eq.) over half an hour. The progression of the reaction was monitored using iodine starch paper. When the iodine starch paper was not turning brown anymore, the reaction was quenched with 4 volumes of ice-cold water. The aqueous phase was extracted with diethyl ether, the organics reunited were dried over sodium sulphate and evaporated *in vacuo* to give the title compound as a white solid (81 % yield); mp 105-112 °C; ^{1}H-NMR (400 MHz, CDCl$_3$): δ 3.94 (s, 3H, CH$_3$), 7.00-7.06 (m, 2H, Ar), 7.42-7.46 (m, 1H, Ar), 7.63-7.65 (m, 1H, Ar), 9.88 (br, 1H, OH).
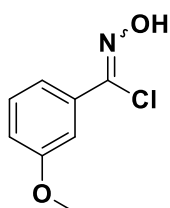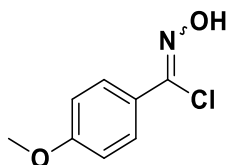

N-hydroxy-3-methoxybenzimidoyl chloride (C6): in an oven dried flask 3-methoxybenzaldehyde oxime **O6** (1.0 eq) was dissolved in 10 mL of anhydrous DMF. N-chlorosuccinimide (0.2 eq) were added and the reaction stirred for 10 minutes at room temperature. The solution was purged with 20 mL of HCl(g) and the reaction stirred for 10 additional minutes and then heated up to 50 °C. N-chlorosuccinimide were added portion wise (0.2 eq at the time, up to 1.5 total eq.) over half an hour. The progression of the reaction was monitored using iodine starch paper. When the iodine starch paper was not turning brown anymore, the reaction was quenched with 4 volumes of ice-cold water. The aqueous phase was extracted with diethyl ether, the organics reunited were dried over sodium sulphate and evaporated *in vacuo* to give the title compound as a yellow oil (81% yield); ^{1}H-NMR (400 MHz, CDCl$_3$): ^{1}H-NMR

(400 MHz, CDCl₃): δ 3.81 (s, 3H, CH₃), 6.93-6.98 (m, 1H, Ar), 7.25-7.30 (m, 2H, Ar), 7.38-7.44 (m, 1H, Ar), 10.84 (br, 1H, OH).
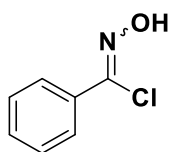

N-hydroxy-4-methoxybenzimidoyl chloride (C7): in an oven dried flask 4-methoxybenzaldehyde oxime **O7** (1.0 eq) was dissolved in 10 mL of anhydrous DMF. N-chlorosuccinimide (0.2 eq) were added and the reaction stirred for 10 minutes at room temperature. The solution was purged with 20 mL of HCl(g) and the reaction stirred for 10 additional minutes and then heated up to 50 °C. N-chlorosuccinimide were added portion wise (0.2 eq at the time, up to 1.5 total eq.) over half an hour. The progression of the reaction was monitored using iodine starch paper. When the iodine starch paper was not turning brown anymore, the reaction was quenched with 4 volumes of ice-cold water. The aqueous phase was extracted with diethyl ether, the organics reunited were dried over sodium sulphate and evaporated *in vacuo* to give the title compound as a yellow solid (58.8% yield); mp 70 °C; ¹H-NMR (400 MHz, CDCl₃): ¹H-NMR (400 MHz, CDCl₃): δ 3.97 (s, 3H, CH₃), 6.93-6.95 (m, 2H, Ar), 7.79-7.81 (m, 2H, Ar), 8.20 (br, 1H, OH).

N-hydroxybenzimidoyl chloride (C8): in an oven dried flask benzaldoxime **O8** (1.0 eq) was dissolved in 10 mL of anhydrous DMF. N-chlorosuccinimide (0.2 eq) were added and the reaction stirred for 10 minutes at room temperature. The solution was purged with 20 mL of HCl(g) and the reaction stirred for 10 additional minutes and then heated up to 50 °C. N-chlorosuccinimide were added portion wise (0.2 eq at the time, up to 1.5 total eq.) over half an hour. The progression of the reaction was

monitored using iodine starch paper. When the iodine starch paper was not turning brown anymore, the reaction was quenched with 4 volumes of ice-cold water. The aqueous phase was extracted with diethyl ether, the organics reunited were dried over sodium sulphate and evaporated *in vacuo* to give the title compound as a yellow oil (65% yield); ^{1}H-NMR (400 MHz, CDCl$_3$): δ 7.27-7.34 (m, 3H, Ar), 7.77-7.80 (m, 2H, Ar), 11.44 (br, 1H, OH).
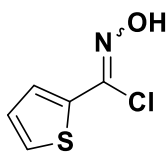

N-hydroxythiophene-2-carbimidoyl chloride (C9): in an oven dried flask thiophene-2-carbaldehyde oxime **O9** (1.0 eq) was dissolved in 10 mL of anhydrous DMF. *N*-chlorosuccinimide (0.2 eq) were added and the reaction stirred for 10 minutes at room temperature. The solution was purged with 20 mL of HCl(g) and the reaction stirred for 10 additional minutes and then heated up to 50 °C. *N*-chlorosuccinimide were added portion wise (0.2 eq at the time, up to 1.5 total eq.) over half an hour. The progression of the reaction was monitored using iodine starch paper. When the iodine starch paper was not turning brown anymore, the reaction was quenched with 4 volumes of ice-cold water. The aqueous phase was extracted with diethyl ether, the organics reunited were dried over sodium sulphate and evaporated *in vacuo* to give the title compound as a green solid (34.0% yield); mp 100-102 °C; ^{1}H-NMR (400 MHz, MeOD): δ 5.51-5.52 (m, 1H, thiophene), 5.92-5.94 (m, 1H, thiophene), 6.42 (m, 1H, thiophene), 10.44 (br, 1H, OH).

Synthesis and characterization data of saccharin/isoxazoline derivatives 1a-9a
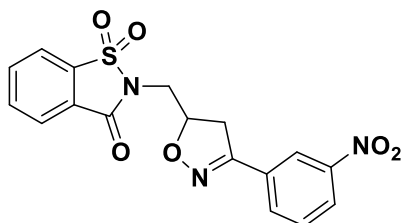
2-((3-(3-nitrophenyl)-4,5-dihydroisoxazol-5-yl)methyl)benzo[d]isothiazol-3(2H)-

one 1,1-dioxide (1a): 2-allylbenzo[*d*]isothiazol-3(2*H*)-one 1,1-dioxide **S1** (1.0 eq) and *N*-hydroxy-3-nitrobenzimidoyl chloride **C1** (1.25 eq) were dissolved in 20 mL of anhydrous ethyl acetate. 1.0 mL of a solution of 0.2 mL of triethylamine (1.25 eq) in ethyl acetate were added dropwise over 30 mins. A white suspension was formed, and the reaction stirred overnight at room temperature. The reaction was quenched with 40 mL of water and the resulting suspension was extracted with dichloromethane (3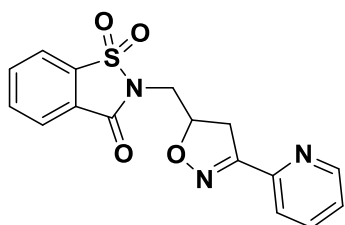x20mL). The organics reunited were dried over sodium sulphate and evaporated *in vacuo* to give the title compound as a light yellow solid (7% yield); mp 175–177 °C; IR ν_{max} 3088 (ν C$_{sp2}$-H), 1744 (ν C=O), 1593 (ν C=N), 1525 (ν_{as} N-O, NO$_2$), 1343 (ν_s N-O, NO$_2$), 1323 (ν_{as} S=O), 1302 (ν N-O), 1263 (ν C-N), 1177 (ν_s S=O), 719 (δ C$_{sp2}$-H), 674 (δ C$_{sp2}$-H) cm^{-1}. ^{1}H-NMR (400 MHz, DMSO-d_6): δ 3.44 (dd, ^2J = 17.2 Hz, ^3J = 6.6 Hz, 1H C(4)H$_2$-isoxazoline), 3.68 (dd, ^2J = 17.0 Hz, ^3J = 11.0 Hz, 1H, C(4)H$_2$-isoxazoline), 3.90 (dd, ^2J = 15.2 Hz, ^3J = 4.4 Hz, 1H, CH$_2$), 4.03 (dd, ^2J = 15.2 Hz, ^3J = 7.2 Hz, 1H, CH$_2$), 5.14-5.21 (m, 1H, C(5)H-isoxazoline), 7.73-7.77 (m, 1H, Ar), 7.98-8.13 (m, 4H, Ar), 8.29- 8.33 (m, 2H, Ar), 8.37 (s, 1H, Ar). ^{13}C (101 MHz, CDCl$_3$): δ 38.3 (C(4)H$_2$-isoxazoline), 41.5 (CH$_2$), 78.3 (C(5)H-isoxazoline), 121.2 (Ar), 121.7 (Ar), 124.8 (Ar), 125.5 (Ar), 126.9 (Ar), 129.9 (Ar), 130.9 (Ar), 132.4 (Ar), 134.6 (Ar), 135.2 (Ar), 137.5 (Ar), 148.5 (Ar), 154.9 (C=N, isoxazoline), 159.4 (C=O).
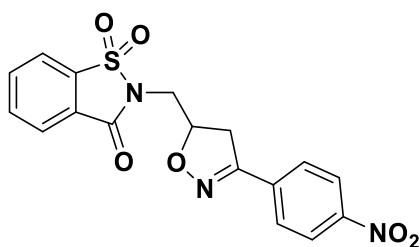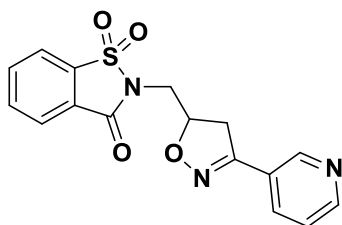
2-((3-(4-nitrophenyl)-4,5-dihydroisoxazol-5-yl)methyl)benzo[d]isothiazol-3(2*H*)-one 1,1-dioxide (2a): 2-allylbenzo[*d*]isothiazol-3(2*H*)-one 1,1-dioxide **S1** (1.0 eq) and *N*-hydroxy-4-nitrobenzimidoyl chloride **C2** (1.25 eq) were dissolved in 20 mL of anhydrous ethyl acetate. 1.0 mL of a solution of 0.2 mL of triethylamine (1.25 eq) in ethyl acetate were added dropwise over 30 mins. A white suspension was formed, and the reaction stirred overnight at room temperature. The reaction was quenched with 40 mL of water and the resulting suspension was filtered to give title compound as a light yellow solid (64% yield); mp 210-213 °C; IR v_{max} 3076 (v C_{sp2}-H), 1735 (v C=O), 1580 (v C=N), 1509 (v_{as} N-O), 1326 (v_{as} S=O), 1308 (v_s N-O), 1247 (v C-N), 1181 (v_s S=O), 849 (δ C_{sp2}-H), 749 (δ C_{sp2}-H) cm^{-1}. ^{1}H-NMR (400 MHz, DMSO-d_6): δ 3.41 (dd, ^{2}J = 16.2 Hz, ^{3}J = 7.2 Hz, 1H C(4)H$_2$-isoxazoline), 3.66 (dd, ^{2}J =17.6 Hz, ^{3}J = 10.8 Hz, 1H, C(4)H$_2$-isoxazoline), 3.91 (dd, ^{2}J = 15.4 Hz, ^{3}J = 4.6 Hz, 1H, CH$_2$), 4.04 (dd, ^{2}J = 15.2 Hz, ^{3}J = 7.2 Hz, 1H, CH$_2$), 5.17-5.19 (m, 1H, C(5)H-isoxazoline), 7.90 (d, ^{3}J = 8.4 Hz, 2H, Ar), 8.00-8.12 (m, 3H, Ar), 8.27-8.32 (m, 3H, Ar). ^{13}C (101 MHz, DMSO-d_6): δ 38.0 (C(4)H$_2$, isoxazoline), 42.1 (CH$_2$), 79.0 (C(5)H-isoxazoline), 122.1 (Ar), 124.5 (2xAr), 125.7 (Ar), 126.6 (Ar), 128.3 (2xAr), 135.7 (Ar), 135.8 (Ar), 136.4 (Ar), 137.2 (Ar), 148.5 (Ar), 156.4 (C=N, isoxazoline), 159.4 (C=O).

2-((3-(pyridin-2-yl)-4,5-dihydroisoxazol-5-yl)methyl)benzo[d]isothiazol-3(2*H*)-one 1,1-dioxide (3a): 2-allylbenzo[*d*]isothiazol-3(2*H*)-one 1,1-dioxide **S1** (1.0 eq) and *N*-hydroxy- pyridine-2-carbimidoyl chloride **C3** (1.25 eq) were dissolved in 20 mL of

anhydrous ethyl acetate. 1.0 mL of a solution of 0.2 mL of triethylamine (1.25 eq) in ethyl acetate were added dropwise over 30 mins. A white suspension was formed, and the reaction stirred overnight at room temperature. The reaction was quenched with 40 mL of water and the resulting suspension was extracted with dichloromethane (3x20mL). The organics reunited were dried over sodium sulphate and evaporated *in vacuo* to give the title compound as a light orange solid (99% yield); mp 133-135 °C; IR ν_{max} 2928 (ν C_{sp2}-H), (1739 (ν C=O), 1578 (ν C=N), 1320 (ν_{as} S=O), 1300 (ν N-O), 1288 (ν C-N), 1173 (ν_s S=O), 778 (δ C_{sp2}-H), 745 (δ C_{sp2}-H) cm^{-1}. ^{1}H-NMR (400 MHz, DMSO-d_6): δ 3.39-3.45 (m, 1H C(4)H$_2$-isoxazoline), 3.59-3.66 (m, 1H, C(4)H$_2$-isoxazoline), 3.89-3.94 (m, 1H, CH$_2$), 3.99-4.04 (m, 1H, CH$_2$), 5.11-5.12 (m, 1H, C(5)H-isoxazoline), 7.42-7.45 (m, 1H, pyr), 7.84-7.92 (m, 1H Ar + 1H pyr), 7.97-8.11 (m, 2H Ar + 1H pyr), 8.30-8.32 (m, 1H, Ar), 8.61 (s, 1H, pyr). ^{13}C (101 MHz, DMSO-d_6): δ 38.4 (C(4)H$_2$-isoxazoline), 42.2 (CH$_2$), 78.5 (C(5)H-isoxazoline), 121.8 (pyr), 122.1 (Ar), 125.2 (pyr), 125.7 (Ar), 126.6 (pyr), 135.8 (Ar), 136.4 (Ar), 137.1 (Ar), 137.4 (pyr), 148.9 (Ar), 149.9 (pyr), 158.9 (C=N, isoxazoline), 159.4 (C=O).
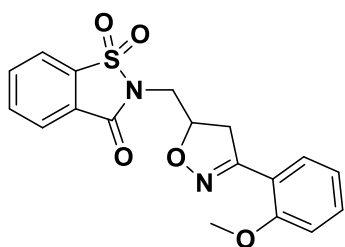

2-((3-(pyridin-3-yl)-4,5-dihydroisoxazol-5-yl)methyl)benzo[d]isothiazol-3(2H)-one 1,1-dioxide (4a): 2-allylbenzo[*d*]isothiazol-3(*2H*)-one 1,1-dioxide **S1** (1.0 eq) and *N*-hydroxy- pyridine-3-carbimidoyl chloride **C4** (1.25 eq) were dissolved in 20 mL of anhydrous ethyl acetate. 1.0 mL of a solution of 0.2 mL of triethylamine (1.25 eq) in ethyl acetate were added dropwise over 30 mins. A white suspension was formed, and the reaction stirred overnight at room temperature. The reaction was quenched with 40 mL of water and the resulting suspension was extracted with dichloromethane (3x20mL). The organics reunited were dried over sodium sulphate and evaporated *in vacuo.* Purification by column chromatography on silica gel (ethyl acetate:*n*-hexane 1:1)

gave the title compound as a light orange solid (32% yield); mp 98-100 °C; IR ν_{max} 3041 (ν C_{sp2}-H), 1733 (ν C=O), 1596 (ν C=N), 1335 (ν_{as} S=O), 1301 (ν N-O), 1260 (ν C-N), 1180 (ν_s S=O), 748 (δ C_{sp2}-H), 673 (δ C_{sp2}-H) cm^{-1}. ^{1}H-NMR (400 MHz, CDCl$_3$): δ 3.31 (dd, ^{2}J = 17.0 Hz, ^{3}J = 6.6 Hz, 1H, C(4)H$_2$-isoxazoline), 3.45 (dd, ^{2}J =17.0 Hz, ^{3}J = 10.6 Hz, 1H, C(4)H$_2$-isoxazoline), 3.86 (dd, ^{2}J = 14.8 Hz, ^{3}J = 6.8 Hz, 1H, CH$_2$), 3.99 (dd, ^{2}J = 15.0 Hz, ^{3}J = 5.8 Hz, 1H, CH$_2$), 5.16-5.23 (m, 1H, C(5)H-isoxazoline), 7.24-7.27 (m, 1H, pyr), 7.76-7.88 (m, 2H Ar + 1 H pyr), 7.86-7.98 (m, 1H Ar + 1H pyr), 8.53-8.54 (m, 1H, Ar), 8.74-8.75 (m, 1H, pyr). ^{13}C (101 MHz, CDCl$_3$): δ 38.4 (C(4)H$_2$-isoxazoline), 41.6 (CH$_2$), 79.2 (C(5)H-isoxazoline), 121.1 (Ar), 123.6 (pyr), 125.3 (pyr), 125.4 (Ar), 126.8 (Ar), 133.9 (pyr), 134.6 (Ar), 135.2 (pyr), 137.3 (Ar), 147.8 (Ar), 151.1 (pyr), 154.3 (C=N, isoxazoline), 159.3 (C=O).

2-((3-(2-methoxyphenyl)-4,5-dihydroisoxazol-5-yl)methyl)benzo[*d*]isothiazol-3(2*H*)-one 1,1-dioxide (5a): 2-allylbenzo[*d*]isothiazol-3(2*H*)-one 1,1-dioxide **S1** (1.0 eq) and *N*-hydroxy-2-methoxybenzimidoyl chloride **C5** (1.25 eq) were dissolved in 20 mL of anhydrous ethyl acetate. 1.0 mL of a solution of 0.2 mL of triethylamine (1.25 eq) in ethyl acetate were added dropwise over 30 mins. A white suspension was formed, and the reaction stirred overnight at room temperature. The reaction was quenched with 40 mL of water and the resulting suspension was extracted with dichloromethane (3x20mL). The organics reunited were dried over sodium sulphate and evaporated *in vacuo.* Purification by column chromatography on silica gel (ethyl acetate:*n*-hexane 1:1) gave the title compound as a white solid (36% yield); mp 138-140 °C; IR ν_{max} 2940 (ν C_{sp2}-H), 1735 (ν C=O), 1333 (ν_{as} S=O), 1599 (ν C=N), 1302 (ν N-O), 1256 (ν C-N), 1174 (ν_s S=O), 770 (δ C_{sp2}-H), 753 (δ C_{sp2}-H) cm^{-1}. ^{1}H-NMR (400 MHz, CDCl$_3$): δ 3.51 (dd, ^{2}J =

17.8 Hz, ^3J = 6.2 Hz, 1H C(4)H$_2$-isoxazoline), 3.60 (dd, ^2J =17.8 Hz, ^3J = 10.2 Hz, 1H, C(4)H$_2$-isoxazoline), 3.86-3.93 (m, 3H OCH$_3$ + 1H CH$_2$), 4.05 (dd, ^2J = 14.8 Hz, ^3J = 6.0 Hz, 1H, CH$_2$), 5.16-5.23 (m, 1H, C(5)H-isoxazoline), 6.93-7.00 (m, 2H, Ar), 7.37-7.41 (m, 1H, Ar), 7.73- 7.75 (m, 1H, Ar), 7.84-7.96 (m, 3H, Ar), 8.08 (d, ^3J = 7.6 Hz, 1H, Ar). ^{13}C (101 MHz, CDCl$_3$): δ 41.4 (C(4)H$_2$-isoxazoline), 41.9 (CH$_2$), 55.5 (OCH$_3$), 77.2 (C(5)H-isoxazoline), 111.4 (Ar), 118.3 (Ar), 120.8 (Ar), 121.1 (Ar), 125.4 (Ar), 127.1 (Ar), 129.6 (Ar), 131.5 (Ar), 134.5 (Ar), 135.1 (Ar), 137.5 (Ar), 156.1 (C=N, isoxazoline), 157.6 (Ar), 159.3 (C=O).
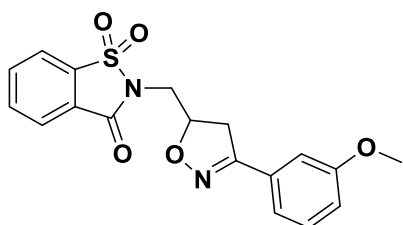
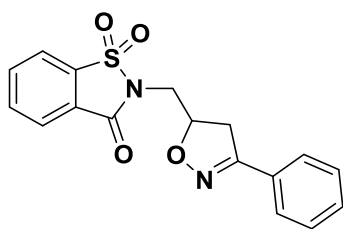**2-((3-(3-methoxyphenyl)-4,5-dihydroisoxazol-5-yl)methyl)benzo[d]isothiazol-3(2H)-one 1,1-dioxide (6a):** 2-allylbenzo[d]isothiazol-3(2H)-one 1,1-dioxide **S1** (1.0 eq) and N-hydroxy-3-methoxybenzimidoyl chloride **C6** (1.25 eq) were dissolved in 20 mL of anhydrous ethyl acetate. 1.0 mL of a solution of 0.2 mL of triethylamine (1.25 eq) in ethyl acetate were added dropwise over 30 mins. A white suspension was formed, and the reaction stirred overnight at room temperature. The reaction was quenched with 40 mL of water and the resulting suspension was extracted with dichloromethane (3x20mL). The organics reunited were dried over sodium sulphate and evaporated *in vacuo.* Purification by column chromatography on silica gel (ethyl acetate:petroleum ether 1:3) gave the title compound as a highly thick oil (31% yield); IR ν_{max} 2938 (ν C$_{sp2}$-H), 1727 (ν C=O), 1595 (ν C=N), 1330 (ν_{as} S=O), 1301 (ν N-O), 1254 (ν C-N), 1183(ν_s S=O), 765 (δ C$_{sp2}$-H), 673 (δ C$_{sp2}$-H) cm^{-1}. ^{1}H-NMR (400 MHz, CDCl$_3$): δ 3.32-3.36 (m, 1H C(4)H$_2$-isoxazoline), 3.43-3.50 (m, 1H C(4)H$_2$-isoxazoline), 3.78-3.80 (m, 3H, OCH$_3$), 3.87-3.92 (m, 1H CH$_2$), 4.02-4.06 (m, 1H, CH$_2$), 5.20 (br, 1H, C(5)H-isoxazoline), 6.93-6.95 (m, 1H, Ar), 7.18-7.28 (m, 3H, Ar), 7.83- 7.91 (m, 3H, Ar), 8.02-8.04 (m, 1H, Ar). ^{13}C (101 MHz, CDCl$_3$): δ 38.8 (C(4)H$_2$-isoxazoline), 41.8 (CH$_2$), 55.4 (OCH$_3$), 77.2 (C(5)H-

isoxazoline), 111.5 (Ar), 116.6 (Ar), 119.5 (Ar), 121.1 (Ar), 125.4 (Ar), 126.9 (Ar), 129.8 (Ar), 130.3 (Ar), 134.6 (Ar), 135.2 (Ar), 137.4 (Ar), 156.5 (C=N, isoxazoline), 159.3 (Ar), 159.7 (C=O).
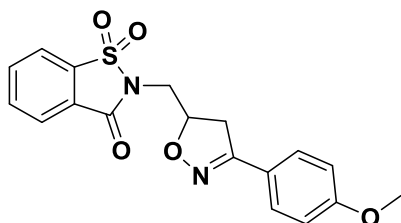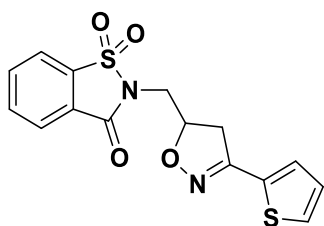

2-((3-(4-methoxyphenyl)-4,5-dihydroisoxazol-5-yl)methyl)benzo[*d*]isothiazol-3(2*H*)-one 1,1-dioxide (7a): 2-allylbenzo[*d*]isothiazol-3(2*H*)-one 1,1-dioxide **S1** (1.0 eq) and *N*-hydroxy-4-methoxybenzimidoyl chloride **C7** (1.25 eq) were dissolved in 20 mL of anhydrous ethyl acetate. 1.0 mL of a solution of 0.2 mL of triethylamine (1.25 eq) in ethyl acetate were added dropwise over 30 mins. A white suspension was formed, and the reaction stirred overnight at room temperature. The reaction was quenched with 40 mL of water and the resulting suspension was filtered to give title compound as a white solid (62% yield); mp 148-153 °C; IR ν_{max} 3069 (ν C_{sp2}-H), 1740 (ν C=O), 1607 (ν C=N), 1321 (ν_{as} S=O), 1301 (ν N-O), 1248 (ν C-N), 1178 (ν_{s} S=O), 752 (δ C_{sp2}-H), 672 (δ C_{sp2}-H) cm^{-1}. ^{1}H-NMR (400 MHz, DMSO-d_6): δ 3.32 (dd, ^2J = 17.2 Hz, ^3J = 6.8 Hz, 1H C(4)H$_2$-isoxazoline), 3.56 (dd, ^2J = 17.2 Hz, ^3J = 10.4 Hz, 1H, C(4)H$_2$-isoxazoline), 3.79 (s, 3H, OCH$_3$), 3.85 (dd, ^2J = 15.2 Hz, ^3J = 4.8 Hz, 1H, CH$_2$), 3.97 (dd, ^2J = 15.2 Hz, ^3J = 7.6 Hz, 1H, CH$_2$), 5.02-5.10 (m, 1H, C(5)H-isoxazoline), 7.00 (d, ^3J = 8.8 Hz, 2H, Ar), 7.60 (d, ^3J = 8.8 Hz, 2H, Ar), 7.99-8.13 (m, 3H, Ar), 8.30 (d, ^3J = 7.6 Hz, 2H, Ar). ^{13}C (101 MHz, DMSO-d_6): δ 38.9 (C(4)H$_2$-isoxazoline), 42.5 (CH$_2$), 55.8 (OCH$_3$), 77.5 (C(5)H-isoxazoline), 114.7 (2 x Ar), 115.7 (Ar), 121.9 (Ar), 122.0 (Ar), 126.6 (Ar), 128.7 (2 x Ar), 135.8 (Ar), 136.2 (Ar), 137.1 (Ar), 157.0 (C=N, isoxazoline), 159.6 (Ar), 161.8 (C=O).
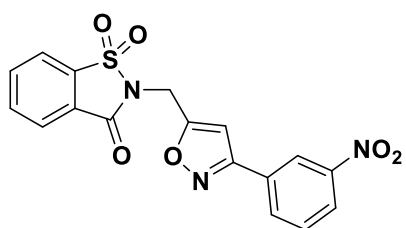
2-((3-phenyl-4,5-dihydroisoxazol-5-yl)methyl)benzo[d]isothiazol-3(2*H*)-one 1,1-dioxide (8a): 2-allylbenzo[*d*]isothiazol-3(2*H*)-one 1,1-dioxide **S1** (1.0 eq) and *N*-hydroxybenzimidoyl chloride **C8** (1.25 eq) were dissolved in 20 mL of anhydrous ethyl acetate. 1.0 mL of a solution of 0.2 mL of triethylamine (1.25 eq) in ethyl acetate were added dropwise over 30 mins. A white suspension was formed, and the reaction stirred overnight at room temperature. The reaction was quenched with 40 mL of water and the resulting suspension was extracted with dichloromethane (3x20mL). The organics reunited were dried over sodium sulphate and evaporated *in vacuo.* Purification by column chromatography on silica gel (ethyl acetate:petroleum ether 1:3) gave the title compound as a thick oil (60% yield); IR v_{max} 2935 (v C_{sp2}-H), 1729 (v C=O), 1594 (v C=N), 1331 (v_{as} S=O), 1302 (v N-O), 1256 (v C-N), 1175 (v_s S=O), 748 (δ C_{sp2}-H), 675 (δ C_{sp2}-H) cm^{-1}. ^{1}H-NMR (400 MHz, CDCl$_3$): δ 3.32-3.36 (m, 1H, C(4)H$_2$-isoxazoline), 3.42-3.49 (m, 1H, C(4)H$_2$-isoxazoline), 3.85-3.90 (m, 1H, CH$_2$), 4.01-4.05 (m, 1H, CH$_2$), 5.19 (br, 1H, C(5)H-isoxazoline), 7.35 (br, 3H, Ar), 7.64 (br, 2H, Ar), 7.77-7.86 (m, 3H, Ar), 7.96-7.98 (m, 1H, Ar). ^{13}C (101 MHz, CDCl$_3$): δ 38.7 (C(4)H$_2$-isoxazoline), 41.8 (CH$_2$), 77.7 (C(5)H-isoxazoline), 121.1 (Ar), 125.3 (Ar), 126.9 (2 x Ar), 128.8 (2 x Ar), 129.1 (Ar), 130.3 (Ar), 134.6 (Ar), 135.3 (Ar), 137.3 (Ar), 156.6 (C=N, isoxazoline), 159.3 (C=O).

2-((3-(thiophen-2-yl)-4,5-dihydroisoxazol-5-yl)methyl)benzo[d]isothiazol-3(2*H*)-one 1,1-dioxide (9a): 2-allylbenzo[*d*]isothiazol-3(2*H*)-one 1,1-dioxide **S1** (1.0 eq) and *N*-
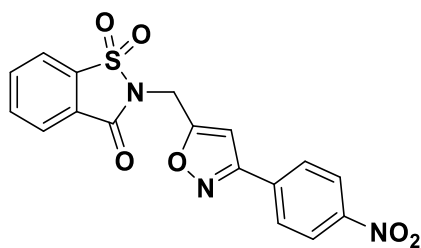
hydroxythiophene-2-carbimidoyl chloride **C9** (1.25 eq) were dissolved in 20 mL of anhydrous ethyl acetate. 1.0 mL of a solution of 0.2 mL of triethylamine (1.25 eq) in ethyl acetate were added dropwise over 30 mins. A white suspension was formed, and the reaction stirred overnight at room temperature. The reaction was quenched with 40 mL of water and the resulting suspension was extracted with dichloromethane (3x20mL). The organics reunited were dried over sodium sulphate and evaporated *in vacuo.* Purification by column chromatography on silica gel (ethyl acetate:*n*-hexane 1:3) gave the title compound as a brown highly thick oil (16% yield); IR ν_{max} 3091 (ν C_{sp2}-H), 1730 (ν C=O), 1636 (ν C=N), 1332 (ν_{as} S=O), 1311 (ν N-O), 1260 (ν C-N), 1178 (ν_s S=O), 752 (δ C_{sp2}-H), 698 (δ C_{sp2}-H) cm^{-1}. ^{1}H-NMR (400 MHz, CDCl$_3$): δ 3.38 (dd, ^2J = 16.4 Hz, ^3J = 6.4 Hz, 1H, C(4)H$_2$-isoxazoline), 3.51 (dd, ^2J = 16.8 Hz, ^3J = 10.4 Hz, 1H, C(4)H$_2$-isoxazoline), 3.90 (dd, ^2J = 14.8 Hz, ^3J = 7.2 Hz, 1H, CH$_2$), 4.05 (dd, ^2J = 14.8 Hz, ^3J = 5.6 Hz, 1H, CH$_2$), 5.18-5.22 (m, 1H, C(5)H-isoxazoline), 7.04-7.06 (m, 1H, thiophene), 7.04-7.06 (m, 1H, thiophene), 7.22-7.23 (m, 1H, thiophene), 7.39-7.40 (m, 1H, thiophene), 7.84-7.95 (m, 3H, Ar), 8.06 (d, ^3J = 7.2 Hz, 1H, Ar). ^{13}C (101 MHz, CDCl$_3$): δ 39.6 (C(4)H$_2$-isoxazoline), 41.6 (CH$_2$), 77.8 (C(5)H-isoxazoline), 121.2 (Ar), 125.4 (thiophene), 126.9 (thiophene), 127.4 (Ar), 128.7 (thiophene), 129.0 (thiophene), 131.3 (Ar), 134.7 (Ar), 135.2 (Ar), 137.4 (Ar), 152.3 (C=N, isoxazoline), 159.3 (C=O).

Synthesis and characterization data of saccharin/isoxazole derivatives 1b-9b

2-((3-(3-nitrophenyl)isoxazol-5-yl)methyl)benzo[*d*]isothiazol-3(2*H*)-one 1,1-dioxide (1b): 2-(prop-2-yn-1-yl)benzo[d]isothiazol-3(2H)-one 1,1-dioxide **S2** (1.0 eq) and *N*-hydroxy-3-nitrobenzimidoyl chloride **C1** (1.25 eq) were dissolved in 20 mL of anhydrous ethyl acetate. 1.0 mL of a solution of 0.2 mL of triethylamine (1.25 eq) in ethyl acetate were added dropwise over 30 mins. A white suspension was formed, and the reaction stirred overnight at room temperature. The reaction was quenched with 40 mL of water and the resulting suspension was extracted with dichloromethane (3x20mL). The organics reunited were dried over sodium sulphate and evaporated *in vacuo.* Purification by column chromatography on silica gel (ethyl acetate:*n*-hexane 1:1) gave the title compound as a white solid (26% yield); mp 191-193 °C; IR ν_{max} 1731 (ν C=O), 1605 (ν C=N), 1539 (ν_{as} N-O, NO_2), 1334 (ν_{as} S=O), 1303 (ν_s N-O, NO_2), 1262 (ν C-N), 1185 (ν_s S=O), 755 (δ C_{sp2}-H), 670 (δ C_{sp2}-H) cm^{-1}. ^{1}H-NMR (400 MHz, DMSO-d_6): δ 5.23 (s, 2H, CH_2), 7.37 (s, 1H, C(4)H, isoxazole), 7.79-7.81 (m, 1H, Ar), 8.02-8.10 (m, 2H, Ar), 8.15-8.17 (m, 1H, Ar), 8.31-8.33 (m, 2H, Ar), 8.35-8.37 (m, 1H, Ar), 8.61 (br, 1H, Ar). ^{13}C (101 MHz, DMSO-d_6): δ 33.9 (CH_2), 102.7 (C(4)H-isoxazole), 121.6 (Ar), 122.3 (Ar), 125.4 (Ar), 125.9 (Ar), 126.6 (Ar), 130.2 (Ar), 131.4 (Ar), 133.4 (Ar), 135.9 (Ar), 136.6 (Ar), 137.3 (Ar), 148.8 (Ar), 158.7 (C(5)-isoxazole), 161.1 (C=N, isoxazole), 168.2 (C=O).

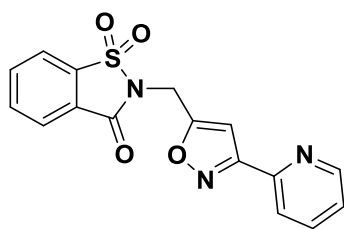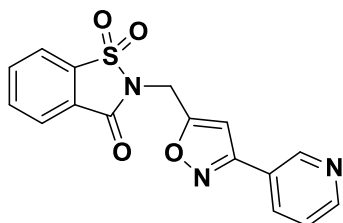**2-((3-(4-nitrophenyl)isoxazol-5-yl)methyl)benzo[*d*]isothiazol-3(2*H*)-one 1,1-dioxide (2b):** 2-(prop-2-yn-1-yl)benzo[d]isothiazol-3(2H)-one 1,1-dioxide **S2** (1.0 eq) and *N*-

hydroxy-4-nitrobenzimidoyl chloride **C2** (1.25 eq) were dissolved in 20 mL of anhydrous ethyl acetate. 1.0 mL of a solution of 0.2 mL of triethylamine (1.25 eq) in ethyl acetate were added dropwise over 30 mins. A white suspension was formed, and the reaction stirred overnight at room temperature. The reaction was quenched with 40 mL of water and the resulting suspension was filtered to give title compound as a white solid (40% yield); mp 260-262 °C; IR ν_{max} 3145 (ν C_{sp2}-H), 1597 (ν C=N), 1720 (ν C=O), 1511 (ν_{as} N-O, NO_2), 1334 (ν_{as} S=O), 1303 (ν_s N-O), 1268 (ν C-N), 1184 (ν_s S=O), 755 (δ C_{sp2}-H), 677 (δ C_{sp2}-H) cm^{-1}. ^{1}H-NMR (400 MHz, DMSO-d_6): δ 5.23 (s, 2H, CH_2), 7.31 (s, 1H, C(4)H-isoxazole), 8.02-8.10 (m, 2H, Ar), 8.13-8.17 (m, 3H, Ar), 8.31-8.37 (m, 3H, Ar). ^{13}C (101 MHz, DMSO-d_6): δ 33.8 (CH_2), 102.9 (C(4)H-isoxazole), 122.3 (Ar), 124.8 (2 x Ar), 125.9 (Ar), 126.6 (Ar), 128.4 (2 x Ar), 134.6 (Ar), 135.9 (Ar), 136.6 (Ar), 137.3 (Ar), 148.9 (Ar), 155.2 (C=N, isoxazole), 158.7 (C(5)-isoxazole), 168.3 (C=O).
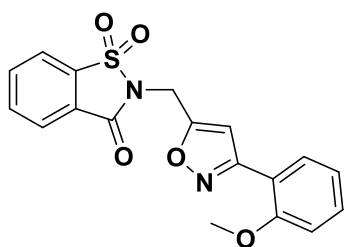

2-((3-(pyridin-2-yl)isoxazol-5-yl)methyl)benzo[d]isothiazol-3(2H)-one   1,1-dioxide (3b): 2-(prop-2-yn-1-yl)benzo[d]isothiazol-3(2H)-one 1,1-dioxide **S2** (1.0 eq) and *N*-hydroxy- pyridine-2-carbimidoyl chloride **C3** (1.25 eq) were dissolved in 20 mL of anhydrous ethyl acetate. 1.0 mL of a solution of 0.2 mL of triethylamine (1.25 eq) in ethyl acetate were added dropwise over 30 mins. A white suspension was formed, and the reaction stirred overnight at room temperature. The reaction was quenched with 40 mL of water and the resulting suspension was filtered to give title compound as a light brown solid (22% yield); mp 161-164 °C; IR ν_{max} 3101 (ν C_{sp2}-H), 1735 (ν C=O), 1593 (ν C=N), 1326 (ν_{as} S=O), 1303 (ν N-O) 1269 (ν C-N), 1180 (ν_s S=O), 785 (δ C_{sp2}-H), 749 (δ C_{sp2}-H) cm^{-1}. ^{1}H-NMR (400 MHz, DMSO-d_6): 5.25 (s, 2H, CH_2), 7.06 (s, 1H, C(4)H-isoxazole), 7.48-7.50 (m, 1H, pyr), 7.92-8.08 (m, 2H Ar + 2H pyr), 8.14-8.16 (m, 1H, Ar), 8.35-8.37 (m, 1H, Ar), 8.68 (s, 1H, pyr). ^{13}C (101 MHz, DMSO-d_6): δ 33.8 (CH_2), 103.0

(C(4)H-isoxazole), 121.8 (pyr), 122.2 (Ar), 125.7 (Ar), 125.9 (pyr), 135.9 (Ar), 136.6 (Ar), 137.3 (Ar), 138.0 (Ar), 147.5 (pyr), 147.7 (pyr), 150.5 (pyr), 158.7 (C(5)-isoxazole), 163.5 (C=N, isoxazole), 167.7 (C=O).
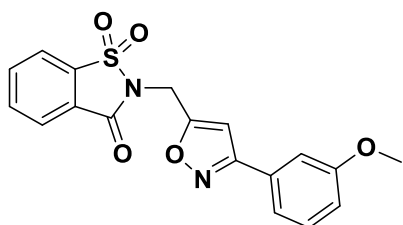

2-((3-(pyridin-3-yl)isoxazol-5-yl)methyl)benzo[d]isothiazol-3(2*H*)-one 1,1-dioxide (4b): 2-(prop-2-yn-1-yl)benzo[d]isothiazol-3(2H)-one 1,1-dioxide **S2** (1.0 eq) and *N*-hydroxy- pyridine-3-carbimidoyl chloride **C4** (1.25 eq) were dissolved in 20 mL of anhydrous ethyl acetate. 1.0 mL of a solution of 0.2 mL of triethylamine (1.25 eq) in ethyl acetate were added dropwise over 30 mins. A white suspension was formed, and the reaction stirred overnight at room temperature. The reaction was quenched with 40 mL of water and the resulting suspension was extracted with dichloromethane (3x20mL). The organics reunited were dried over sodium sulphate and evaporated *in vacuo.* Purification by column chromatography on silica gel (ethyl acetate:*n*-hexane 1:1) gave the title compound as a light brown solid (34% yield); mp 140-143 °C; IR ν_{max} 3084 (ν C$_{sp2}$-H), 1736 (ν C=O), 1610 (ν C=N), 1327(ν_{as} S=O), 1292 (ν N-O), 1260 (ν C-N), 1173 (ν_s S=O), 747 (δ C$_{sp2}$-H), 671 (δ C$_{sp2}$-H) cm^{-1}. ^{1}H-NMR (400 MHz, CDCl$_3$): 5.11 (s, 2H, CH$_2$), 6.74 (s, 1H, C(4)H-isoxazole), 7.37-7.40 (m, 1H, pyr), 7.87-7.99 (m, 2H Ar + 1H pyr), 8.11-8.13 (d, J = 7.6, 2H, Ar), 8.67-8.68 (m, 1H, pyr), 8.98 (s, 1H, pyr). ^{13}C (101 MHz, CDCl$_3$): δ 33.6 (CH$_2$), 101.9 (C(4)H-isoxazole), 121.3 (Ar), 123.8 (pyr), 125.6 (Ar), 126.1 (pyr), 126.8 (Ar), 134.2 (pyr), 134.7 (Ar), 135.4 (Ar), 137.7 (Ar), 146.9 (pyr), 147.9 (pyr), 151.1 (C=N, isoxazole), 158.4 (C(5)-isoxazole), 166.6 (C=O).
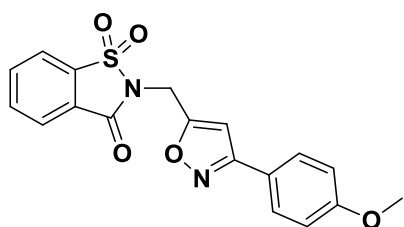
2-((3-(2-methoxyphenyl)isoxazol-5-yl)methyl)benzo[d]isothiazol-3(2*H*)-one 1,1-dioxide (5b): 2-(prop-2-yn-1-yl)benzo[d]isothiazol-3(2H)-one 1,1-dioxide **S2** (1.0 eq) and *N*-hydroxy-2-methoxybenzimidoyl chloride **C5** (1.25 eq) were dissolved in 20 mL of anhydrous ethyl acetate. 1.0 mL of a solution of 0.2 mL of triethylamine (1.25 eq) in ethyl acetate were added dropwise over 30 mins. A white suspension was formed, and the reaction stirred overnight at room temperature. The reaction was quenched with 40 mL of water and the resulting suspension was extracted with dichloromethane (3x20mL). The organics reunited were dried over sodium sulphate and evaporated *in vacuo.* Purification by column chromatography on silica gel (ethyl acetate:*n*-hexane 1:1) gave the title compound as a white solid (27% yield); mp 126-131 °C; IR ν_{max} 1733 (ν C=O), 1603 (ν C=N), 1337 (ν_{as} S=O), 1300 (ν N-O), 1250 (ν C-N), 1185 (ν_s S=O), 760 (δ C_{sp2}-H), 671 (δ C_{sp2}-H) cm^{-1}. ^{1}H-NMR (400 MHz, CDCl$_3$): δ 3.88 (s, 3H, OCH$_3$), 5.10 (s, 2H, CH$_2$), 6.93 (s, 1H, C(4)H-isoxazole), 6.97-7.04 (m, 2H, Ar), 7.39-7.42 (m, 1H, Ar), 7.86-7.91 (m, 3H, Ar), 7.94-7.96 (m, 1H, Ar), 8.08-8.10 (m, 1H, Ar). ^{13}C (101 MHz, CDCl$_3$): δ 33.6 (CH$_2$), 55.6 (OCH$_3$), 105.8 (C(4)H-isoxazole), 111.4 (Ar), 117.6 (Ar), 120.9 (Ar), 121.2 (Ar), 125.5 (Ar), 126.9 (Ar), 129.5 (Ar), 131.4 (Ar), 134.6 (Ar), 135.2 (Ar), 137.6 (Ar), 157.2 (Ar), 158.5 (C(5)-isoxazole), 160.4 (C=N, isoxazole), 164.3 (C=O).

2-((3-(3-methoxyphenyl)isoxazol-5-yl)methyl)benzo[*d*]isothiazol-3(2*H*)-one 1,1-dioxide (6b): 2-(prop-2-yn-1-yl)benzo[d]isothiazol-3(2H)-one 1,1-dioxide **S2** (1.0 eq) and *N*-hydroxy-3-methoxybenzimidoyl chloride **C6** (1.25 eq) were dissolved in 20 mL

of anhydrous ethyl acetate. 1.0 mL of a solution of 0.2 mL of triethylamine (1.25 eq) in ethyl acetate were added dropwise over 30 mins. A white suspension was formed, and the reaction stirred overnight at room temperature. The reaction was quenched with 40 mL of water and the resulting suspension was extracted with dichloromethane (3x20mL). The organics reunited were dried over sodium sulphate and evaporated *in vacuo.* Purification by column chromatography on silica gel (ethyl acetate:petroleum ether 1:3) gave the title compound as a pale yellow solid (21% yield); mp 144-149 °C; IR ν_{max} 2937 (ν C_{sp2}-H), 1740 (ν C=O), 1603 (ν C=N), 1328 (ν_{as} S=O), 1300 (ν N-O), 1255 (ν C-N), 1163 (ν_s S=O), 755 (δ C_{sp2}-H), 675 (δ C_{sp2}-H) cm^{-1}.^{1}H-NMR (400 MHz, DMSO-d_6): δ 3.80 (s, 3H, OCH$_3$), 5.22 (s, 2H, CH$_2$), 7.05-7.07 (m, 1H, Ar), 7.18 (s, 1H, C(4)H-isoxazole), 7.39-7.45 (m, 3H, Ar), 8.02 (t, ^{3}J = 7.6 Hz, 1H, Ar), 8.07-8.11 (m, 1H, Ar), 8.16 (d, ^{3}J = 7.6 Hz, 1H, Ar), 8.37 (d, ^{3}J = 7.6 Hz, 1H, Ar). ^{13}C (101 MHz, DMSO-d_6): δ 33.8 (CH$_2$), 55.7 (OCH$_3$), 102.6 (C(4)H-isoxazole), 112.2 (Ar), 116.6 (Ar), 119.4 (Ar), 122.4 (Ar), 125.8 (Ar), 126.6 (Ar), 129.9 (Ar), 130.7 (Ar), 135.8 (Ar), 136.5 (Ar), 137.3 (Ar), 158.7 (C(5)-isoxazole), 160.1 (Ar), 162.5 (C=N, isoxazole), 167.3 (C=O).
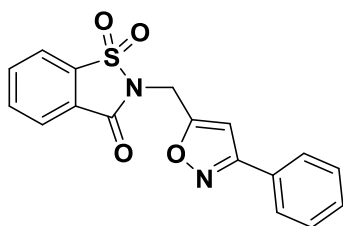

2-((3-(4-methoxyphenyl)isoxazol-5-yl)methyl)benzo[d]isothiazol-3(2*H*)-one 1,1-dioxide (7b): 2-(prop-2-yn-1-yl)benzo[d]isothiazol-3(2H)-one 1,1-dioxide **S2** (1.0 eq) and *N*-hydroxy-4-methoxybenzimidoyl chloride **C7** (1.25 eq) were dissolved in 20 mL of anhydrous ethyl acetate. 1.0 mL of a solution of 0.2 mL of triethylamine (1.25 eq) in ethyl acetate were added dropwise over 30 mins. A white suspension was formed, and the reaction stirred overnight at room temperature. The reaction was quenched with 40 mL of water and the resulting suspension was filtered to give the title compound as a white solid (69% yield); mp 179-185 °C; IR ν_{max} 3127 (ν C_{sp2}-H), 1739 (ν C=O), 1614 (ν C=N), 1333 (ν_{as} S=O), 1294 (ν N-O), 1248 (ν C-N), 1169 (ν_s S=O), 834 (δ C_{sp2}-H), 752

(δ C$_{sp2}$-H) cm^{-1}; ^{1}H-NMR (400 MHz, DMSO-d_6): δ 3.80 (s, 3H, OCH$_3$), 5.18 (s, 2H, CH$_2$), 7.03-7.06 (m, 2H Ar + 1H C(4)H-isoxazole), 7.78-7.80 (m, 2H, Ar), 8.03-8.09 (m, 2H, Ar), 8.16-8.17 (m, 1H, Ar), 8.35-8.36 (m, 1H, Ar). ^{13}C (101 MHz, DMSO-d_6): δ 33.8 (CH$_2$), 55.7 (OCH$_3$), 102.1 (C(4)H-isoxazole), 115.0 (2 x Ar), 121.0 (Ar), 122.2 (Ar), 124.8 (Ar), 125.9 (Ar), 128.6 (2 x Ar), 135.9 (Ar), 136.6 (Ar), 137.2 (Ar), 156.0 (Ar), 158.7 (C(5)-isoxazole), 161.5 (C=N, isoxazole), 166.9 (C=O).
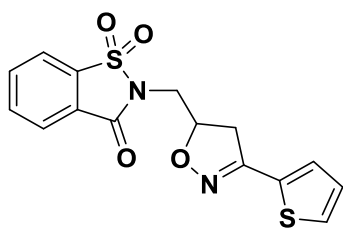

2-((3-phenylisoxazol-5-yl)methyl)benzo[d]isothiazol-3(2H)-one 1,1-dioxide (8b): 2-(prop-2-yn-1-yl)benzo[d]isothiazol-3(2H)-one 1,1-dioxide **S2** (1.0 eq) and *N*-hydroxybenzimidoyl chloride **C8** (1.25 eq) were dissolved in 20 mL of anhydrous ethyl acetate. 1.0 mL of a solution of 0.2 mL of triethylamine (1.25 eq) in ethyl acetate were added dropwise over 30 mins. A white suspension was formed, and the reaction stirred overnight at room temperature. The reaction was quenched with 40 mL of water and the resulting suspension was extracted with dichloromethane (3x20mL). The organics reunited were dried over sodium sulphate and evaporated *in vacuo.* Purification by column chromatography on silica gel (ethyl acetate:petroleum ether 1:3) gave the title compound as a pale yellow solid (23% yield); mp 126-130 °C; IR ν_{max} 3129 (ν C$_{sp2}$-H), 1741 (ν C=O), 1608 (ν C=N), 1333 (ν_{as} S=O), 1292 (ν N-O), 1256 (ν C-N), 1181 (ν_s S=O), 754 (δ C$_{sp2}$-H), 694 (δ C$_{sp2}$-H) cm^{-1}. ^{1}H-NMR (400 MHz, CDCl$_3$): δ 5.10 (s, 2H, CH$_2$), 6.71 (s, 1H, CH-isoxazole), 7.42-7.44 (m, 3H, Ar), 7.77-7.79 (m, 2H, Ar), 7.83-7.92 (m, 2H, Ar), 7.96 (d, ^{3}J = 7.2 Hz, 1H, Ar), 8.09 (d, ^{3}J = 7.6 Hz, 1H, Ar). ^{13}C (101 MHz, CDCl$_3$): δ 33.7 (CH$_2$), 102.2 (C(4)H-isoxazole), 121.3 (Ar), 125.6 (Ar), 126.8 (Ar), 126.9 (2 x Ar), 128.6 (Ar), 128.9 (2 x Ar), 130.2 (Ar), 134.7 (Ar), 135.3 (Ar), 137.6, 158.5 (C(5)-isoxazole), 162.7 (C=N, isoxazole), 165.9 (C=O).

2-((3-(thiophen-2-yl)isoxazol-5-yl)methyl)benzo[d]isothiazol-3(2*H*)-one 1,1-dioxide

(9b): 2-(prop-2-yn-1-yl)benzo[d]isothiazol-3(2H)-one 1,1-dioxide **S2** (1.0 eq) and *N*-hydroxythiophene-2-carbimidoyl chloride **C9** (1.25 eq) were dissolved in 20 mL of anhydrous ethyl acetate. 1.0 mL of a solution of 0.2 mL of triethylamine (1.25 eq) in ethyl acetate were added dropwise over 30 mins. A white suspension was formed, and the reaction stirred overnight at room temperature. The reaction was quenched with 40 mL of water and the resulting suspension was extracted with dichloromethane (3x20mL). The organics reunited were dried over sodium sulphate and evaporated *in vacuo.* Purification by column chromatography on silica gel (ethyl acetate:*n*-hexane 1:3) gave the title compound as a white solid, mp 140-146 °C, 27% yield; IR ν_{max} 3136 (ν C_{sp2}-H), 1724 (ν C=O), 1612 (ν C=N), 1332 (ν_{as} S=O), 1300 (ν N-O), 1268 (ν C-N), 1175 (ν_s S=O), 752 (δ C_{sp2}-H), 706 (δ C_{sp2}-H) cm^{-1}. ^{1}H-NMR (400 MHz, CDCl$_3$): δ 5.09 (s, 2H, CH$_2$), 6.63 (s, 1H, C(4)H-isoxazole), 7.09-7.12 (m, 1H, thiophene), 7.42-7.46 (m, 2H, thiophene), 7.90-7.99 (m, 3H, Ar), 8.01-8.15 (m, 1H, Ar). ^{13}C (101 MHz, CDCl$_3$): δ 33.6 (CH$_2$), 102.2 (C(4)H, isoxazole), 121.3 (Ar), 125.6 (Ar), 126.8 (Ar), 127.6 (Ar, thiophene), 127.8 (Ar, thiophene), 127.9 (Ar, thiophene), 130.2 (Ar, thiophene), 134.7 (Ar), 135.3 (Ar), 137.6 (Ar), 157.9 (C=N, isoxazole), 158.5 (C(5)-isoxazole), 165.9 (C=O).

CA Inhibition Screening Assay

An Applied Photophysics stopped-flow instrument has been used for assaying the CA-catalyzed CO$_2$ hydration activity. Phenol red (at a concentration of 0.2 mM) has been used as an indicator, working at the maximum absorbance of 557 nm, with 20 mM Hepes (pH 7.5 for α-CAs) as buffer, and 20 mM Na$_2$SO$_4$ (for maintaining constant the ionic strength). The initial rates of the CA-catalysed CO$_2$ hydration reaction were followed for a period of 10−100 s. The CO$_2$ concentrations ranged from 1.7 to 17 mM

for the determination of the kinetic parameters and inhibition constants. For each inhibitor, at least six traces of the initial 5−10% of the reaction have been used for determining the initial velocity. The uncatalyzed rates were determined in the same manner and subtracted from the total observed rates. Stock solutions of inhibitor (0.1 mM) were prepared in distilled−deionized water, and dilutions up to 0.01 nM were done thereafter with distilled−deionized water. Inhibitor and enzyme solutions were preincubated together for 15 min at room temperature prior to assay to allow for the formation of the E−I complex. The inhibition constants were obtained by nonlinear least-squares methods using the Cheng−Prusoff equation and represent the mean from at least three different determinations. Errors were in the range of ± 5−10% of the reported K_I values. CA isoforms were recombinant enzymes obtained in house as reported earlier [97]. The enzyme concentrations in the assay system were: hCA I, 13.2 nM; hCA II, 8.4 nM; hCA IX, 7.9 nM; hCA XII, 15.2 nM.

I have spent the last part of my PhD in the discovery and synthesis of new inhibitors based on benzo[b]thiophen-3-ole scaffold effective against human monoamine oxidases.

Chapter 4

Human monoamine oxidases (hMAOs)

4.1 Introduction

Monoamine oxidases (MAOs; EC 1.4.3.4) are mitochondrial bound flavoenzymes which catalyse the oxidative degradation of amines. In human have been observed two different isoforms called respectively A and B (hMAO-A / hMAO-B). The initial discovery of mammalian MAOs was done in 1928 by Hare, who observed a tyramine oxidase activity in rabbit liver, not explainable with tyrosinase function [126]. The presence of these enzymes in the main organ addicted to the chemical inactivation of xenobiotics, prompted Hare to postulate that they were mainly involved in the metabolism of potentially toxic exogenous amines. Follow-up studies showed that these enzymes are effective to catalyse the oxidative deamination of some neurologically important amine substrates, including dopamine, norepinephrine, epinephrine, serotonin and phenethylamine [127]. This reaction occurs due to the presence of flavin adenine dinucleotide cofactor (FAD, depicted in yellow in **Figure 4.1**) that works as electron acceptor for the oxidation of amines, forming iminium ion and $FADH_2$. The regeneration of FAD active form is then accomplished through the electron transfer to an oxygen molecule producing hydrogen peroxide (**Figure 4.1**).
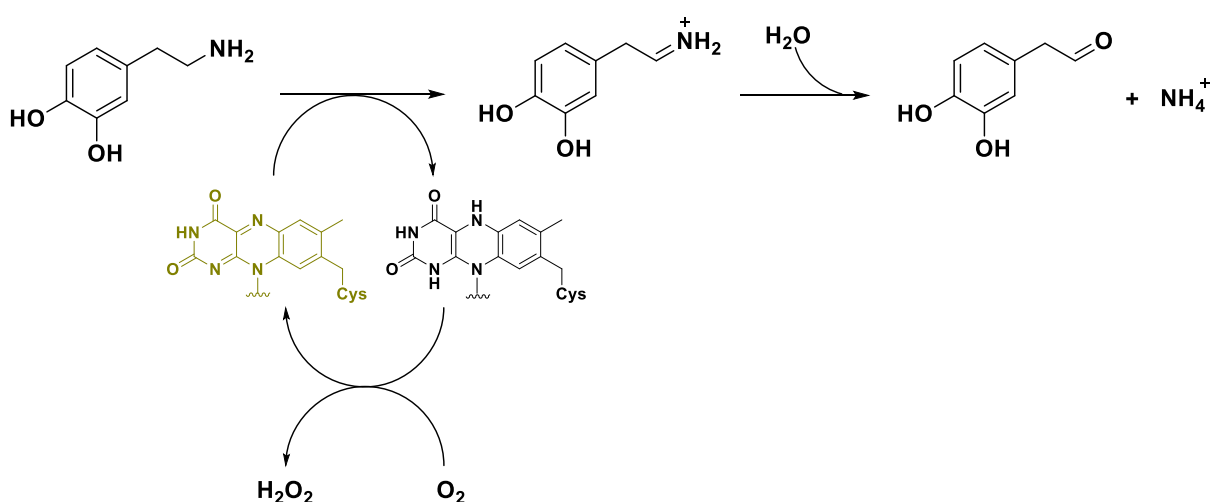

Figure 4.1. Chemical reaction catalysed by hMAOs using dopamine as an example of neurotransmitter substrate. The flavin cofactor is reported in yellow and undergoes a two-

electron reduction substrate oxidation. Regeneration to its functional form is accomplished by molecular oxygen, leading to hydrogen peroxide production [128].

The fate of iminium ion is determined by the aqueous medium which provokes its hydrolysis to ammonium ion and aldehyde.The latter is then oxidized to carboxylic acids by aldehyde dehydrogenase (ALDH) or reduced to alcohol by aldehyde reductase (ALR) [129]. The preferred substrates for hMAOs enzymes are primary amines, albeit they also can catalyse the oxidation of secondary amines. On the other hand, they have little or no activity in the oxidation of tertiary amines, with few exceptions as the bioactivation of 1-methyl-4-phenyl-1,2,3,6-tetrahydropyridine (MPTP). MPTP was an impurity of synthetic heroin, which once converted in 1-methyl-4-phenylpyridinium ion (MPP$^+$), led to the development of symptoms resembling those of Parkinson's patients (**Figure 4.2**) [130].
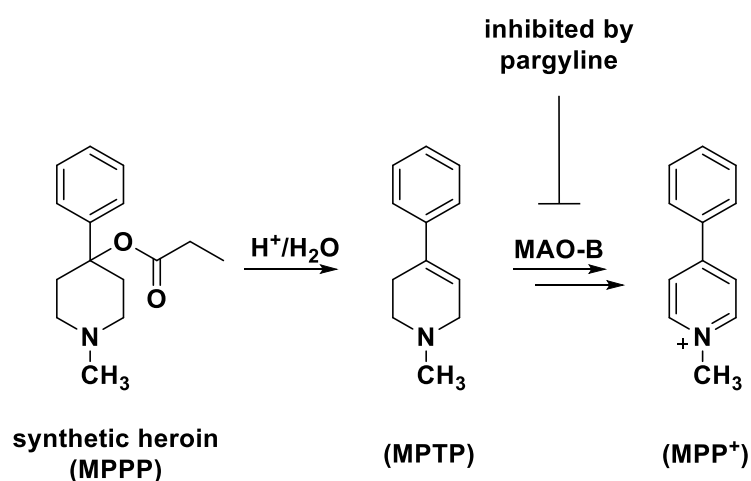

Figure 4.2. Bioactivation of MPTP to MPP$^+$, favoured by MAO B.

The discovery that these symptoms could be stopped by the administration of the acetylenic MAO-B inhibitor pargyline, confirmed the implication of this enzyme in MPTP bioactivation [131], and set in motion the quest for new MAO-B inhibitors as potential anti-Parkinson drugs.

4.2. Structural properties and catalytic mechanism of hMAOs

The two isoforms of human monoamine oxidase are quite similar sharing ~70% sequence identity [132,133]. Both the enzymes possess a dimeric organization structure. Each monomeric unit comprises a membrane binding domain anchoring the enzyme to the outer mitochondrial membrane, and a "globular" part which extends out of the membrane. The "globular" part contains the flavin-binding domain and a substrate-binding domain [128] (**Figure 4.3**).
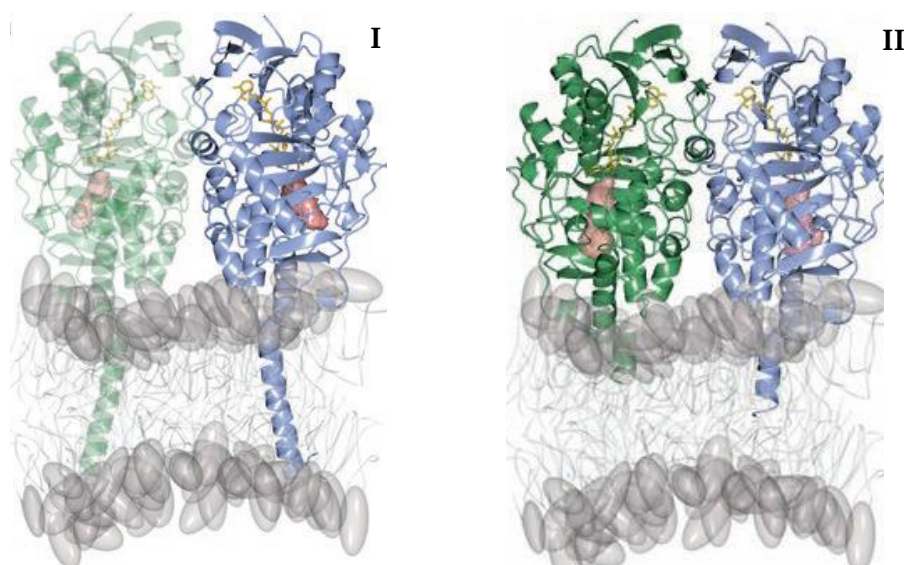

Figure 4.3. Overall crystal structure of human MAO A (**I**) and MAO B (**II**) represented as models of the protein dimer inserted in the phospholipid bilayer. FAD cofactor is reported in yellow and the active site cavity surface in pink [128,134,135].

Among the two isoforms, only hMAO-B has been purified as a dimer, while hMAO-A was separated only as monomer because of the lower biochemical stability of the two monomers that dissociate upon detergent-mediated extraction from the membrane. Nevertheless, there are some evidences which confirmed the dimeric organization of hMAO-A on the membrane [136].

The membrane binding domains of hMAOs are located in the C-terminal region of the proteins. These sites have an α-helix organization containing residues able to create an

apolar surface that facilitate their insertion into the membrane, and aminoacidic side chains positively-charged (e.g. arginine, lysine) which bind the phospholipidic heads [134,135]. The globular cores comprise two domains, one that contain the covalently-bound FAD cofactor and the other involved in substrate binding (**Figure 4.4**, [128]).
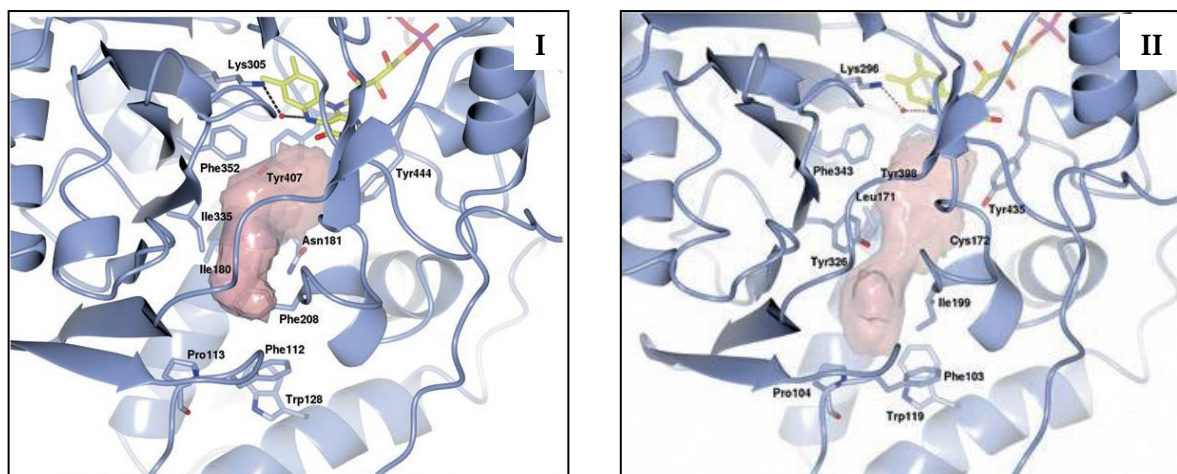

Figure 4.4. Detailed representation of substrate-binding site of hMAO-A (**I**) and hMAO-B (**II**).

The two substrate-binding domains of hMAOs share some conserved aminoacidic residues which line the cavity, like Phe 352 of hMAO-A corresponding to the Phe 343 of hMAO-B. The two aminoacids Tyr 407 / Tyr 444 are disposed in a face to face manner in order to create an "aromatic caged environment" that is responsible for the correct alignment of the substrate toward the catalytic FAD (similar to the couple of Tyr398 / Tyr 435 of hMAO-B). Furthermore, the three residues Pro 113, Phe 112 and Trp 128 of hMAO-A (corresponding to Pro 104, Phe 103 and Trp 119 of hMAO-B), located at the bottom of the protein near the membrane surface, constitute the "cap" of a loop that seals the active site from the exterior and may serve as "gating switch", because the movement of this loop permits the access to the entrance cavity.

Both the isoforms share a substrate binding cavity of ~ 400 Å³. However, hMAO-B is endowed with a further small hydrophobic cavity of 290 Å³. This additional chamber, named "entrance cavity", can be coupled (producing a single cavity with a total

volume of ~ 700 Å³) or not with the substrate cavity depending on Ile 199 side chain conformation, which works as a "gate" existing in either a "closed" or "open" conformations. The Ile 199 controlled connection of the two pockets in a single cavity, can be exploited to design selective inhibitors for hMAO-B [137].

FAD cofactor is covalently-bound *via* a thioether linkage by means a Cys residue of the enzyme (Cys 406 for hMAO-A; Cys 397 for hMAO-B) to the 8a-methylene of isoalloxazine ring and is involved in the oxidative deamination.

In the last years two proposals have been suggested to explain the mechanism of electron transfer from the amine to the flavin ring. The first is the single electron transfer (SET) mechanism proposed by Silverman [138–140] (**Scheme 4.1**).
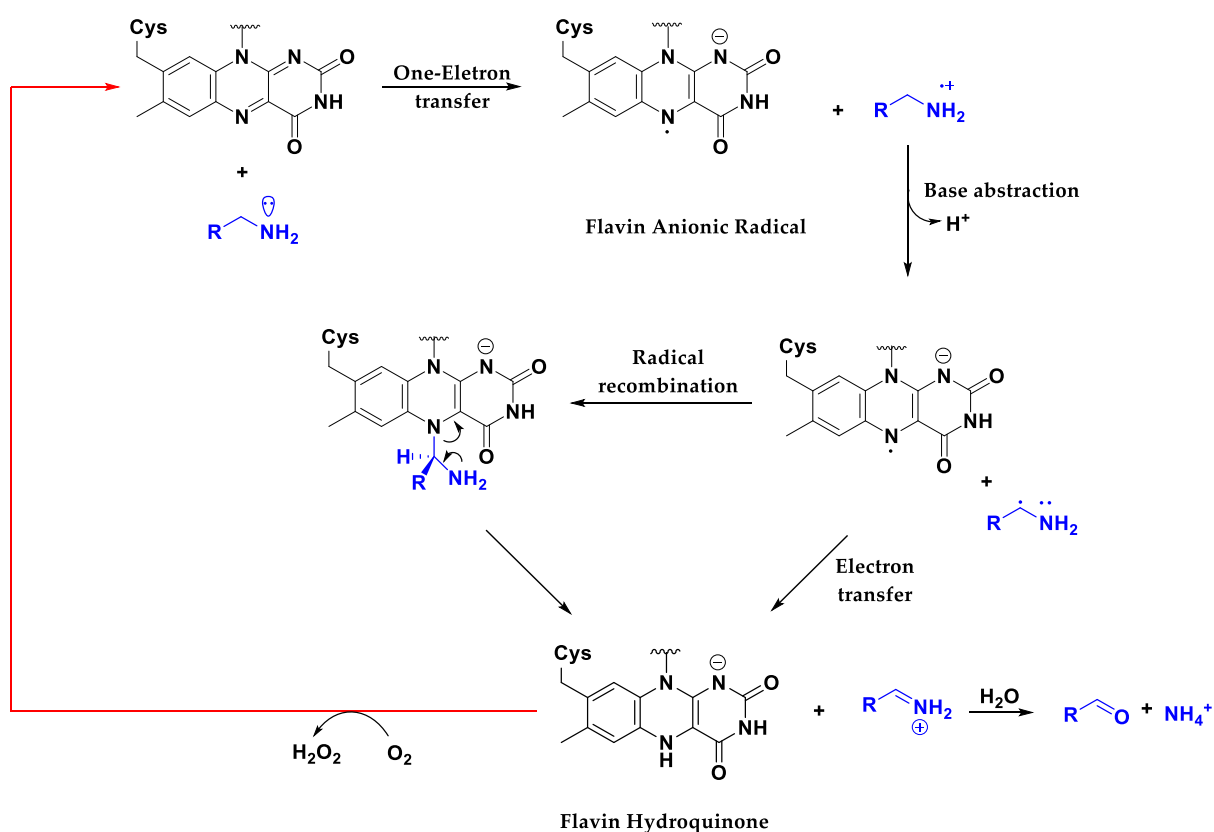
Scheme 4.1. Single electron transfer (SET) mechanism of action of monoamine oxidases [141].

Attempts to provide any experimental support for SET mechanism failed, enforcing the conclusion that this "route" is both kinetically and thermodynamically

improbable. In 1999 Edmonson proposed the polar nucleophilic mechanism (**Scheme 4.2**) which is more in accordance with experimental evidences [142].
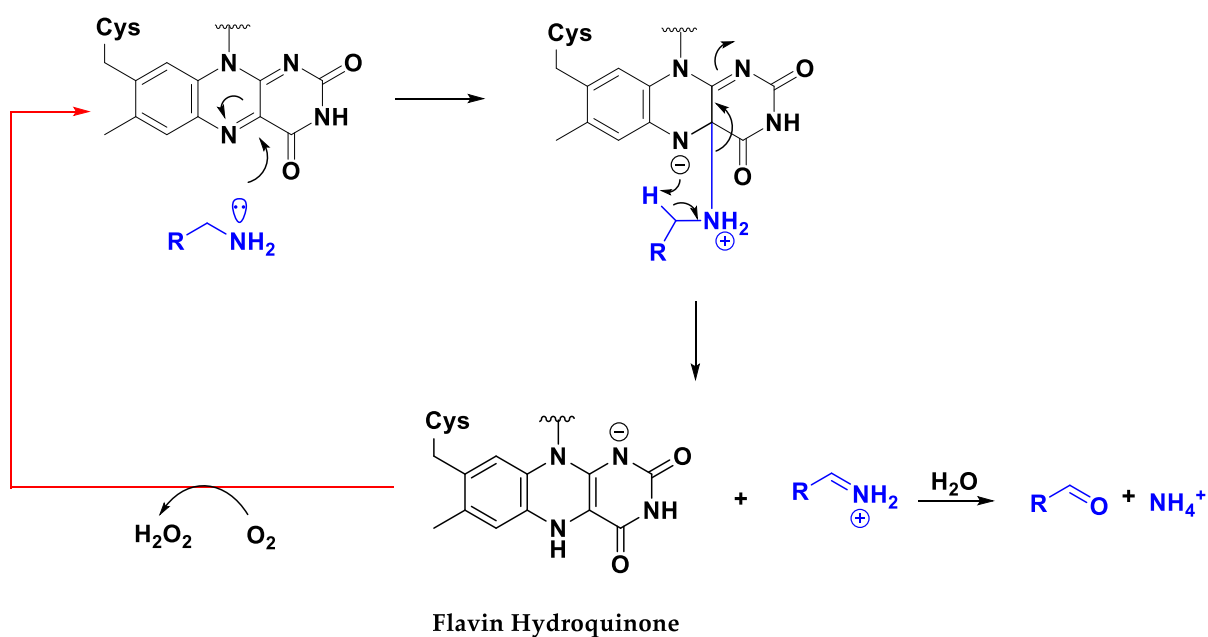
Scheme 4.2. Polar nucleophilic mechanism of action of monoamine oxidases [142].

This hypothesis did not lie on radical mechanism. The nucleophilic attack of amine nitrogen on C(4a) position of isoalloxazine ring, produces an adduct with a positively-charged nitrogen deriving from the amine substrate, and a negatively-charged nitrogen N(5) of the FAD. This condition increases the pKa of the α-carbon protons that can be easily abstracted due to the proximal distance to the isoalloxazine negatively-charged N(5), producing the iminium ion (**Scheme 4.2**).

The main by-product of this metabolic pathway is hydrogen peroxide which is normally deactivated by glutathione peroxidase (GDO). However, if the levels of glutathione (GSH) in the brain are low, hydrogen peroxide can be converted by Fe^{2+} ions (the Fenton reaction) into highly reactive oxygen species (ROS), which have been proposed to be involved in the neurotoxicity observed in some neurodegenerative disorders [143–146].

4.3 Pathological roles and inhibitors of hMAOs

Physiological and pathological roles of hMAO-A and hMAO-B have been extensively studied [127,131,139,147–152]. The two enzymes share similar affinity for some substrate as dopamine, epinephrine, norepinephrine, and tyramine. Serotonin is the preferred substrate for hMAO-A while benzylamine for hMAO-B [153].

hMAOs are coexpressed in almost all human tissues except for placenta, which predominantly expresses hMAO-A and platelets and lymphocytes, which predominantly express hMAO-B. Furthermore, hMAO-A is prevalent in the intestinal tract, while hMAO-B is found mostly in the brain and liver. The localization of these proteins reflects their functions. In fact, hMAO in peripheral tissues seems to protect the body by oxidizing amines from the blood or by preventing their entry into the circulation. hMAO-B in the microvessels of the blood brain barrier (BBB) presumably has a similar protective function, acting as a metabolic barrier [154]. In the central nervous system (CNS) they affect monoamines concentration controlling in this way the physiological and functional concentration of some neurotransmitters as dopamine, norepinephrine and serotonin. So, the use of hMAOs inhibitors able to act in the CNS, reduce the degradation of neurotransmitters. This has beneficial effects for the treatment of pathologies spanning from mental illness like depression to Parkinson's disease and other neurodegenerative disorders. While hMAO-A inhibitors positively affect depression due to the increasing of serotonin and norepinephrine levels [151], hMAO-B inhibitors ameliorate neurodegenerative disorders conditions raising dopaminergic tone.

Furthermore, hMAOs inhibition reduces the products (aldehyde and ammonium ion) and by-product (hydrogen peroxide, H_2O_2) amounts. Albeit aldehydes do not appear to accumulate in the healthy brain, some studies have shown that elevate concentration of this product exert cytotoxic effects [155].

Concerning H_2O_2 the cells usually possess some machinery systems able to act as defenders against this oxidant molecule. Abnormal expression or increased activity of hMAOs lead to excessive production of H_2O_2 which can corrode all the protective

109

agents of the cells, exposing these to the oxidative damages. The presence of some cations as Fe^{2+} and/or Cu^+ affect and increase the rate of production of reactive species of oxygen (ROS). ROS are less stable than H_2O_2 and react suddenly with the surrounding protein systems, with structural/functional damage leading to cells death. This cellular stress has been associated with different pathologies as neurodegenerative disorders and cardiomyopathies [156–158], so hMAOs inhibition reduces the amount of produced hydrogen peroxide and so, the exposure to oxidative stress.

The first indication for hMAO inhibitors was for the treatment of depression after the serendipitous discovery that the mood elevating properties of antitubercular agent isoniazid were related to the inhibition of hMAOs [159]. Iproniazid possessing similar structure of isoniazid but with minor toxicity, was the first hMAO inhibitor approved for the treatment of major depression [160]. The neurotransmitters involved in depressive illness are serotonin and norepinephrine. They undergo the activity of hMAO-A in the brain, so one approach for development of antidepressant was the design of specific and irreversible inhibitors of the hMAO-A isoform [161,162]. Nowadays some irreversibly acting compounds such as tranylcypromine (**Figure 4.5**) are still used for the treatment of major depression, although appropriate dietary restrictions must be observed to avoid the "cheese reaction" resulting in hypertensive crisis and brain haemorrhages [163–165].

To avoid the drawbacks of these compounds, reversible inhibitors such as moclobemide and toloxatone have been developed and used in the therapy of depression. They are safer and better-tolerated, not showing the effect of tyramine on blood-pression, likely because the increase of amount of physiological substrate displaces the inhibitors that reversibly bound the enzyme [166,167].

As mentioned before hMAO-A specific inhibitors may find future also as protectants against cardiac cellular degeneration [168], while ongoing studies are evaluating the involvement of hMAO-A overexpression in cancer [169,170].
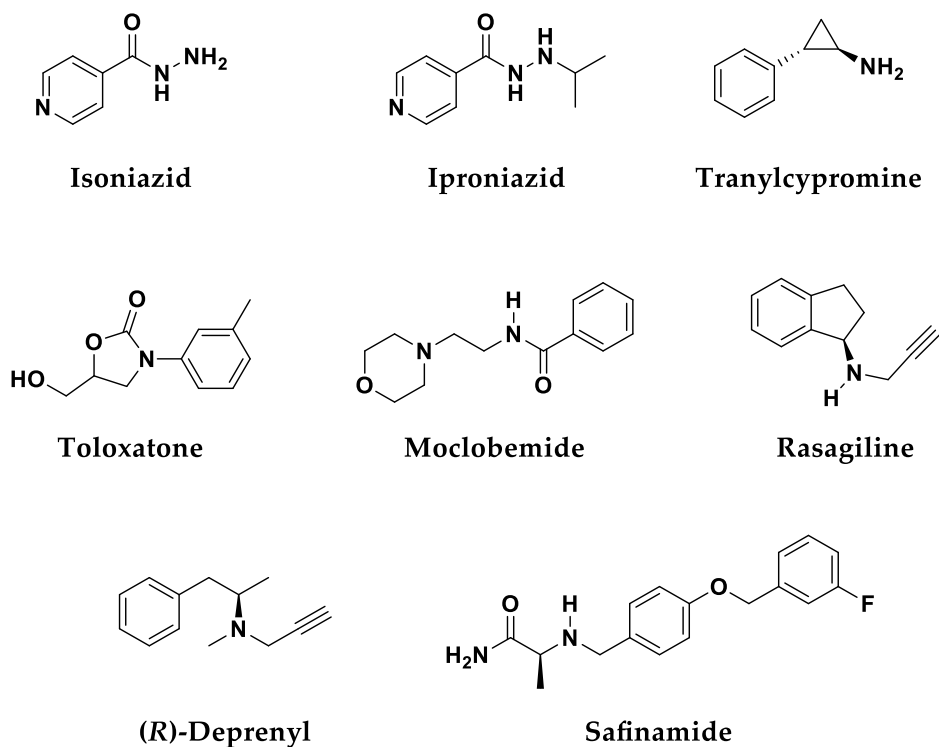
Figure 4.5. Irreversible and reverible inhibitors of hMAOs.

hMAO-B inhibitors are useful in the treatment of Parkinson's disease reducing the degradation of central dopamine. They were used both as monotherapy in the early phase of disease delaying the need for L-dopa [171], or co-administered with L-dopa enhancing the levels of dopamine "artificially" derived from L-dopa [172,173].

Increased hMAO-B expression as well as iron levels in other neurodegenerative disorders like Alzheimer's disease have been observed [30]. So, these compounds potentially act also as neuroprotective molecules reducing the amount of by-product deriving from hMAOs activity, whose expression increase with the age.

Up to day, two hMAO-B inhibitors are used for the treatment of Parkinson's disease: (R)-deprenyl (also known as selegiline) and rasagiline (**Figure 4.5**). These compounds exhibited irreversible mechanism based on the propargylamine functional group. The reversible hMAO-B inhibitor, safinamide, has recently been approved for the management of Parkinson's disease [174,175].

Chapter 5

Benzo[b]tiophen-3-ol derivatives as effective inhibitors of hMAOs:

design, synthesis and biological activity

5.1 Development of new inhibitors of hMAOs: aim of the work

An extensive number of natural and synthetic compounds have shown effective inhibition of human MAOs [152,157]. Keeping in mind the structure and properties of endogenous substrates and reversible inhibitors that bind to hMAOs, Wouters et al. [176] proposed that ideal MAO inhibitors should be flat molecules (**Figure 5.1**) with specific dimensions depending on the isoform (11.5 x 5.5 x 1.8 Å for hMAO-A and 8.5 x 5.1 x 1.8 Å for hMAO-B).
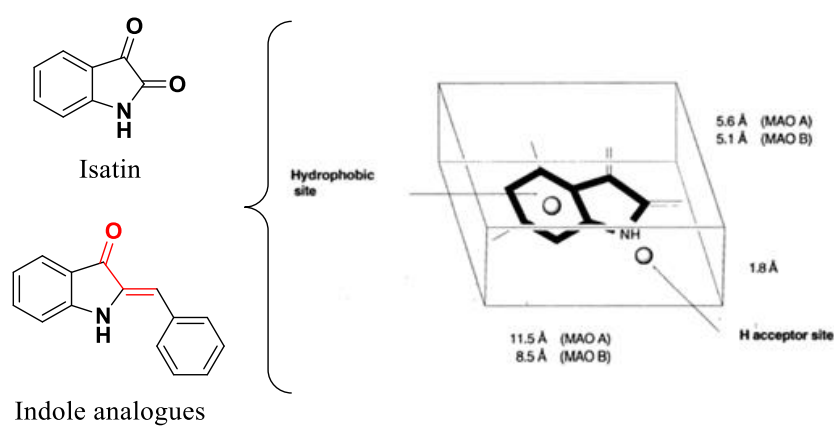

Figure 5.1. Molecular properties of the pharmacophore for the inhibition of the hMAOs. The part of the structure shown in red corresponds to the chalcone moiety.

The pharmacophore reported in **Figure 5.1** was inspired by isatin and indole analogues which possess different enzyme specificities, inhibiting respectively hMAO-B and hMAO-A [137,177]. Although the dimensions of compounds may explain the different affinities for the MAO isoforms (hMAO-A can accommodate larger molecule than hMAO-B), the changes of the electron density in the molecules play an important role in enzyme selectivity. As a matter of the fact, follow-up studies focused on the isosteric substitution of the nitrogen of the indole system with an oxygen atom or methylene group, to obtain respectively aurone [178] and indanone derivatives [179,180] (**Figure 5.2**).
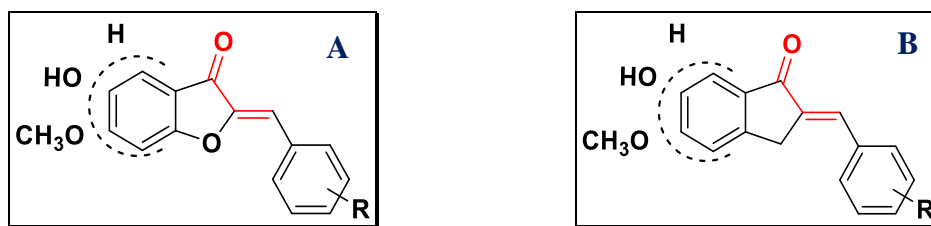
Figure 2. Structure of aurone (**A**) and indanone (**B**) derivatives. Chalcone moiety has been depicted in red.

Aurone derivatives (**Figure 5.2**, **A**) showed selective inhibition towards rat MAO-B (rMAO-B) with IC_{50} values ranging from 11.6 μM to 26.3 μM, without activity against the A isoform of rMAO ($IC_{50} > 100$ μM). On the other hand, indanone derivatives showed good inhibitory profile in the low micromolar range especially for hMAO-B ($0.0052 < IC_{50}$ hMAO-B (μM) < 2.74). All these structures (indole analogues, aurone and indanone derivatives) show a common structural feature, similar to the chalcone moiety (highlighted in red), whose ability to bind to hMAO enzymes have been reported in the past by our group [181]. With the aim to explore new structures for the inhibition of hMAO, I proposed a new scaffold based on benzo[b]thiophen-3-ol structure (**Figure 5.3**). This scaffold retained some similarity with the compounds discussed above, for example the presence of bicyclic system connected with a "bridge" to aromatic/heteroaromatic ring. The bridge, for indole, aurone and indanone derivatives is the β-carbon of the α,β-unsaturated ketone. Conversely, for the structure of benzo[b]thiophen-3-ol, the carbonyl moiety of the α,β-unsaturated ketone is the "bridge".
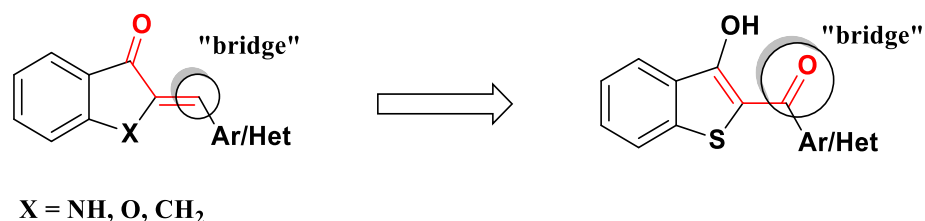

Figure 5.3. Benzo[b]thiophen-3-ole scaffold. Similarities and differences with previously reported scaffolds.

Other important differences among these scaffolds are the isosteric replacement of the oxygen atom of aurones with sulphur and the presence of 1,3-diketonic system that, via keto-enol tautomerism, generates the corresponding chalcone while also possessing the potential for metal chelation [182]. This is a very interesting aspect and provides the possibility to obtain multi-target drug in the light of the evidence that some cations (e.g. Fe^{2+} and Cu^+) may contribute to neurodegeneration in central nervous system tissues. In fact, these ions are implicated in the Fenton reaction [183] which catalyse the production of hydroxyl radicals from hydrogen peroxide, a well-known by-product of MAO enzymatic activity [145,146]. Since hydroxyl radicals possess a very short half-life, estimated at 1 ns, they can be highly toxic to biomolecules and the use of chelating agents should repair this metal dyshomeostasis leading to reduced damage derived from oxidative stress.

5.2 Chemistry

The structure of benzo[*b*]thiophen-3-ol has been previously studied from a chemical point of view, and several research groups have proposed synthetic strategies to obtain this class of compounds [184–186]. Here I propose a new one-step, very simple synthetic procedure which allowed us to obtain the desired compounds **PM1**-**PM20** (**Scheme 5.1**). Methyl 2-mercaptobenzoate and α-bromo acetophenone in equimolar amount, were reacted in methanol in the presence of potassium hydroxide. The reaction was performed in a nitrogen atmosphere (to avoid sulphur oxidation) and at room temperature for 1-2 h. After this time, an excess of potassium hydroxide was added, and the temperature was raised to 60 °C. The completion of reactions was usually reached in 4-5 hours producing all the compounds **PM1**-**PM20** in moderate to high yields.
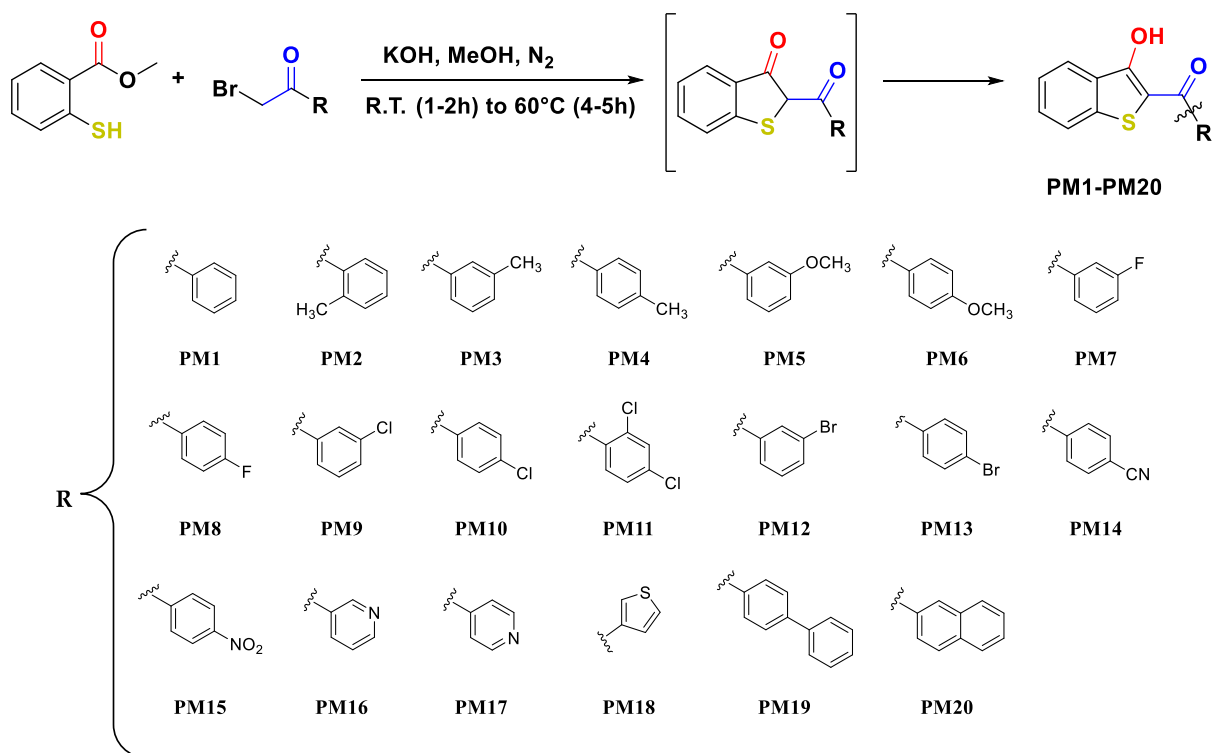
Scheme 5.1. Synthesis of compounds **PM1**-**PM20**.

We proposed a reaction mechanism for the synthesis of the benzo[*b*]thiophen-3-ol derivatives as reported in **Scheme 5.2**. The reaction starts with the nucleophilic attack of deprotonated thiol group on alfa brominated position of the ketone to obtain the intermediate **W** (**Scheme 5.2**, **I**). Then, an intramolecular crossed aldolic reaction take place (**Scheme 5.2**, **II**). The methylene **y** attacks methyl ester functional group with consequent methanol elimination, producing the benzo[*b*]thiophen-3-ol [187].
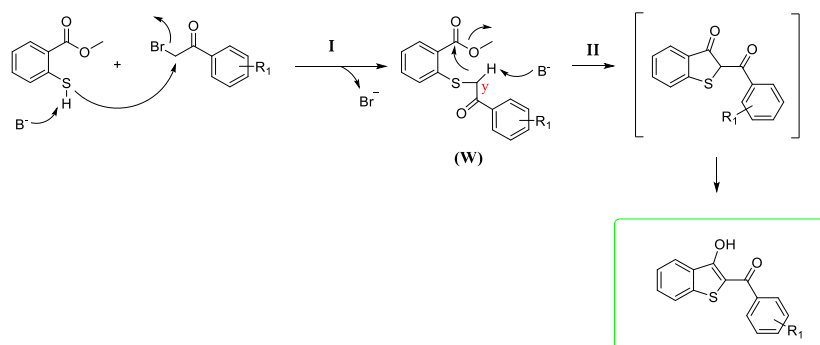
Scheme 2. Proposed mechanism of reaction.

5.3 Biological assays

5.3.1 hMAO-A and hMAO-B inhibition studies

The synthesised compounds **PM1**-**PM20** were evaluated as hMAO inhibitors using the recombinant hMAOs as enzyme sources. For these assays, kynuramine was used as substrate for both hMAO isoforms. The oxidation of kynuramine by the hMAOs yields 4-hydroxyquinoline which was measured by fluorescence spectrophotometry. By measuring the hMAO-Activities in the presence of a range of different inhibitor concentrations (0.003-100 µM), the IC_{50} values were measured. The inhibitory activities of compounds **PM1**-**PM20** are summarized in **Table 5.1** along with selectivity index (SI) values given as the ratio (IC_{50} hMAO-A)/(IC_{50} hMAO-B).

5.3.2 Evaluation of DOPAC/DA ratio and LDH activity

Compounds that showed the best inhibitory activity towards hMAO (**PM4**, **PM5**, **PM6**, **PM9**, **PM10**, **PM12**, **PM13**) were also been tested with cortex synaptosomes in both basal and LPS-induced inflammatory conditions, to estimate the capability of reducing DOPAC/DA ratio and LDH activity. DOPAC/DA ratio describes the extent of dopamine turnover and could be considered an indirect index of MAO-B activity [188]. On the other hand, LDH has long been considered a valuable marker of tissue damage [189,190], and thus the neuroprotective effects of the new compounds were also evaluated.

5.4 Result and discussion
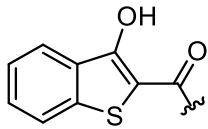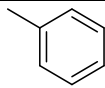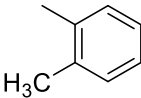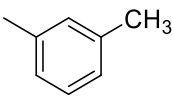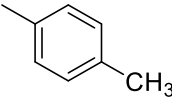
5.4.1 In vitro MAO inhibition study
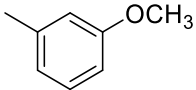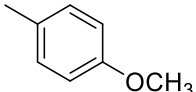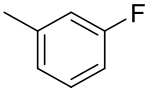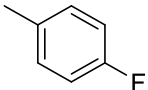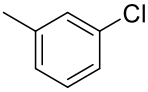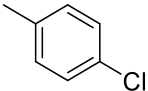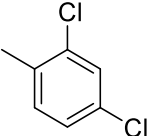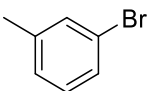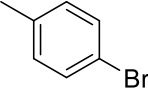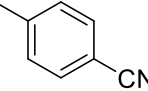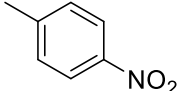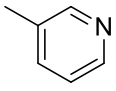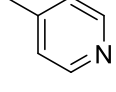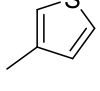
All the synthesised compounds **PM1**-**PM20** have been evaluated as potential inhibitors of hMAO-A and hMAO-B and the activities are given as the IC_{50} values in **Table 5.1**. Among these derivatives only compounds **PM2**, **PM17** and **PM18** were superior inhibitors of hMAO-A compared to hMAO-B, although only to a small extent. All the other compounds were selective hMAO-B inhibitors with IC_{50} values in the
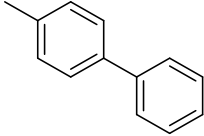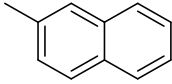
micromolar/low micromolar range. The simplest compound of this series, **PM1**, containing an unsubstituted phenyl ring bound to the carbonyl "bridge", showed similar inhibition against both the isoforms with poor selectivity (IC_{50} hMAO-A = 13.27 µM; IC_{50} hMAO-B = 7.39 µM; SI_{PM1} = 1.8). When phenyl ring was substituted, we observed different effects depending on the position and chemical nature of the substituent. In fact, the presence of a weak electron donor such as the methyl group on phenyl ring, improved inhibition activity towards hMAO-B when it was placed on *meta-* (**PM3**, IC_{50} hMAO-B = 1.81 µM) or *para-* (**PM4**, IC_{50} hMAO-B = 0.47 µM) positions. **PM4** also displayed improved inhibition activity towards hMAO-A (**PM4**, IC_{50} hMAO-A = 2.71 µM), accounting for the slightly reduced SI compared with **PM3** (**PM3**, IC_{50} hMAO-A = 12.59 µM). On the other hand, when this substituent was located at the *ortho*-position, we observed reduced inhibitory activity against both the isoforms, with a slight preference for hMAO-A (**PM2**, IC_{50} hMAO-A = 18.66 µM; IC_{50} hMAO-B = 23.38 µM; SI = 0.8). A similar trend was observed for compounds substituted with the methoxy group, which is considered to be a stronger electron donor than the methyl (**PM5-PM6**). For these two derivatives we also recorded different inhibition activities towards hMAO-B, with the best outcome observed when methoxy group was placed on the *para*-position of the phenyl ring (**PM6**, IC_{50} hMAO-B = 0.28 µM). Similar to the methyl substituted derivatives, the placement of the methoxy substituent on *meta*-position negatively affected inhibition activity against hMAO-A (**PM5**, IC_{50} hMAO-A = 32.97 µM), thus improving the selectivity index (SI = 42.3). In the light of the above, it may be concluded that electron donor groups improve inhibitory activity towards hMAO-B when they were on *meta-* and *para*-positions. Furthermore, when these groups are on *meta*-position, they also led to an increase in selectivity due to the reduction of hMAO-A inhibition. A different trend was observed for halogen-substituted derivatives (**PM7**-**PM13**). The data show that when substitution is changed from the fluorine, to chlorine and finally to bromine, there is an incremental increase of inhibitory activity and selectivity towards hMAO-B, according with the increased size and reduced electronegativity of the halogen, with the best inhibition shown by

compound **PM12** (IC$_{50}$ hMAO-B = 0.35 μM; SI = 180.4). In the light of the above, we conclude that halogens, which represent electron-withdrawing groups, positively affect both inhibition activity and selectivity when they are placed in *meta*-position (e.g. **PM12**, IC$_{50}$ hMAO-B = 0.35 μM *vs.* **PM13**, IC$_{50}$ hMAO-B = 0.88 μM). This trend differs from that observed with the electron donor groups (e.g. methyl or methoxy). Other compounds such as **PM14** and **PM15** which are substituted on *para*-position with CN and NO$_2$, exhibited hMAO-B inhibition in the low micromolar range (**PM14**, IC$_{50}$ hMAO-B = 4.51 μM; **PM15**, IC$_{50}$ hMAO-B = 2.75 μM) with little selectivity between the two isoforms (**PM14** SI = 4.7; **PM15** SI = 6.8). The presence of a heterocyclic ring for compounds **PM16**-**PM19** negatively affected the inhibition of hMAO-B. Finally, substitution of the phenyl ring with the bulky naphthyl, but not biphenyl, improved both activity and selectivity towards hMAO-B (**PM20**, IC$_{50}$ hMAO-B = 1.08 μM; SI = 39.4).

Table 5.1. Inhibitory activity (IC$_{50}$) and selectivity index (SI) towards hMAO-A and hMAO-B of compounds **PM1**-**PM20**.

Compound	Substituent	IC$_{50}$ ± SD (μM)[a]		SI[b]
		hMAO-A	hMAO-B	
PM1		13.27 ± 0.29	7.39 ± 0.15	1.8
PM2		18.66 ± 2.99	23.38 ± 3.03	0.8
PM3		12.59 ± 1.58	1.81 ± 0.13	6.9
PM4		2.71 ± 0.14	0.47 ± 0.02	5.8

PM5	3-OCH₃	32.97 ± 0.88	0.78 ± 0.07	42.3
PM5	(structure: 3-OCH₃ toluene)	32.97 ± 0.88	0.78 ± 0.07	42.3
PM6	(structure: 4-OCH₃ toluene)	4.18 ± 0.77	0.28 ± 0.03	14.9
PM7	(structure: 3-F toluene)	25.05 ± 2.17	1.44 ± 0.40	17.4
PM8	(structure: 4-F toluene)	13.40 ± 0.92	2.28 ± 0.18	5.8
PM9	(structure: 3-Cl toluene)	51.04 ± 1.72	0.55 ± 0.09	92.8
PM10	(structure: 4-Cl toluene)	13.75 ± 0.51	0.89 ± 0.07	15.4
PM11	(structure: 2,4-diCl toluene)	43.36 ± 2.81	37.31 ± 1.01	1.2
PM12	(structure: 3-Br toluene)	63.16 ± 3.48	0.35 ± 0.08	180.4
PM13	(structure: 4-Br toluene)	21.05 ± 1.98	0.88 ± 0.08	23.9
PM14	(structure: 4-CN toluene)	21.21 ± 3.27	4.51 ± 0.13	4.7
PM15	(structure: 4-NO₂ toluene)	18.80 ± 1.53	2.75 ± 0.02	6.8
PM16	(structure: 3-methylpyridine)	50.05 ± 2.56	49.73 ± 1.90	1.0
PM17	(structure: 4-methylpyridine)	53.75 ± 2.90	56.93 ± 5.62	0.9
PM18	(structure: methylthiophene)	6.44 ± 0.68	7.56 ± 0.70	0.8

PM19		36.45 ± 1.07	5.59 ± 0.74	6.5
PM20		42.54 ± 1.88	1.08 ± 0.097	39.4

[a]Values are the mean ± SD of triplicate determinations. [b]Selectivity index for the MAO-B isoform, given as the ratio: (IC_{50} hMAO-A)/(IC_{50} hMAO-B).

5.4.2 Evaluation of DOPAC/DA ratio and LDH activity

Figures 5.4-5.7 show that deprenyl, an irreversible and selective MAO-B inhibitor, and the new MAO inhibitors **PM4**, **PM5**, **PM6**, **PM9**, **PM10**, **PM12** and **PM13** were able to exert modulatory effects on cortex synaptosomes DA/DOPAC ratio and LDH activity, in both basal and LPS-induced inflammatory conditions.

Particularly, in **Figure 4** it is possible to observe that deprenyl and **PM9** stimulated DOPAC/DA ratio, while **PM10**, **PM12** and **PM13** inhibited basal DOPAC/DA ratio. On the other hand, no significant effect was exerted by **PM4**, **PM5** and **PM6**. When synaptosomes were challenged with inflammatory LPS stimulus (**Figure 5.5**), we observed that deprenyl and all **PM** inhibitors were able to reduce DOPAC/DA ratio. Additionally, the present molecules were more effective than deprenyl, with the highest inhibitory effects displayed by **PM10**, **PM12** and **PM13**.

DOPAC/DA ratio has long been proposed as an index of MAO-B activity [188], while microdialysis studies demonstrated the ability of LPS to increase monoamine degradation and extracellular DOPAC levels, in mouse prefrontal cortex [191]. Additionally, we have recently reported that the pro-oxidant stimulus induced by amyloid β-peptide could reduce monoamine levels, in rat cortex synaptosomes [192]. Despite there being agreement between the data reported in **Figure 5.5** and the MAO-B inhibitory activity described in **Table 5.1**, whereas the contrasting results obtained in basal condition (**Figure 5.4**), following **PMs** treatment, suggest the possible onset of pro-inflammatory/pro-oxidant effects, which could have overcome the intrinsic MAO inhibitory activity of these molecules, thus leading to increased DA turnover in rat

cortex synaptosomes. In order to test this hypothesis, we performed a second set of experiments to evaluate the effect of deprenyl and the **PM** inhibitors on cortex synaptosome LDH activity, in both basal and LPS-induced inflammatory condition (**Figures 5.6**-5.**7**).

LDH has long been considered a valuable marker of tissue damage [189,190]. Additionally, antioxidants resulted able to downregulate its activity, ex vivo [193]. In the present study we observed that, except for compound **PM13,** most of the **PM** inhibitors upregulated basal LDH activity (**Figure 5.6**). Conversely, when synaptosomes were perfused with Krebs-Ringer buffer added with LPS, deprenyl inhibited LDH activity at the lowest concentration (20 nM), which is very close to its MAO-B IC_{50} value (17 nM) [194], despite exerting a stimulatory effect at the highest tested concentration (1 μM). We cannot exclude that the highest tested deprenyl concentration (1 μM) could be toxic for cortex synaptosomes. Similarly, the **PM** inhibitors displayed a significant LDH inhibitory activity, which is more evident around their respective IC_{50} values, which are included in the range 0.1-1 μM (**Table 5.1**). Unlike deprenyl, all the **PM** molecules inhibited LDH activity in the concentration range (0.1-1 μM). Our findings of reduced LPS-induced LDH activity by both deprenyl (20 nM) and **PMs** (0.1-1 μM), in rat cortex synaptosomes, are consistent with the reported antioxidant activity of MAO inhibitors, in vivo [195,196]. On the other hand, we should consider that the contrasting finding of stimulation of LDH activity (**Figure 5.6**), induced by deprenyl and **PM** inhibitors in basal condition, could be related to the employed *ex vivo* experimental model. Specifically, it is well known that antioxidants in the cell medium could exert pro-oxidative effects, by generating hydrogen peroxide and thus activating adaptive responses of cells to mild oxidative stress [197]. In this context, it is rational to hypothesize that our results of blunted LPS-induced DOPAC/DA ratio and LDH activity, in cortex synaptosomes treated with both deprenyl and **PMs**, could be related to both MAO-B inhibition activity and improved neuron antioxidant defence system. Taken together, these findings support further deepening of **PM** inhibitor efficacy in *in vivo* experimental models of

122

neuroinflammation and oxidative stress. Particularly, future studies should involve inhibitors **PM10**, **PM12** and **PM13** which exerted the highest inhibitory efficacy on both LPS-induced DOPAC/DA ratio and LDH activity (**Figures 5.5** and **5.7**).
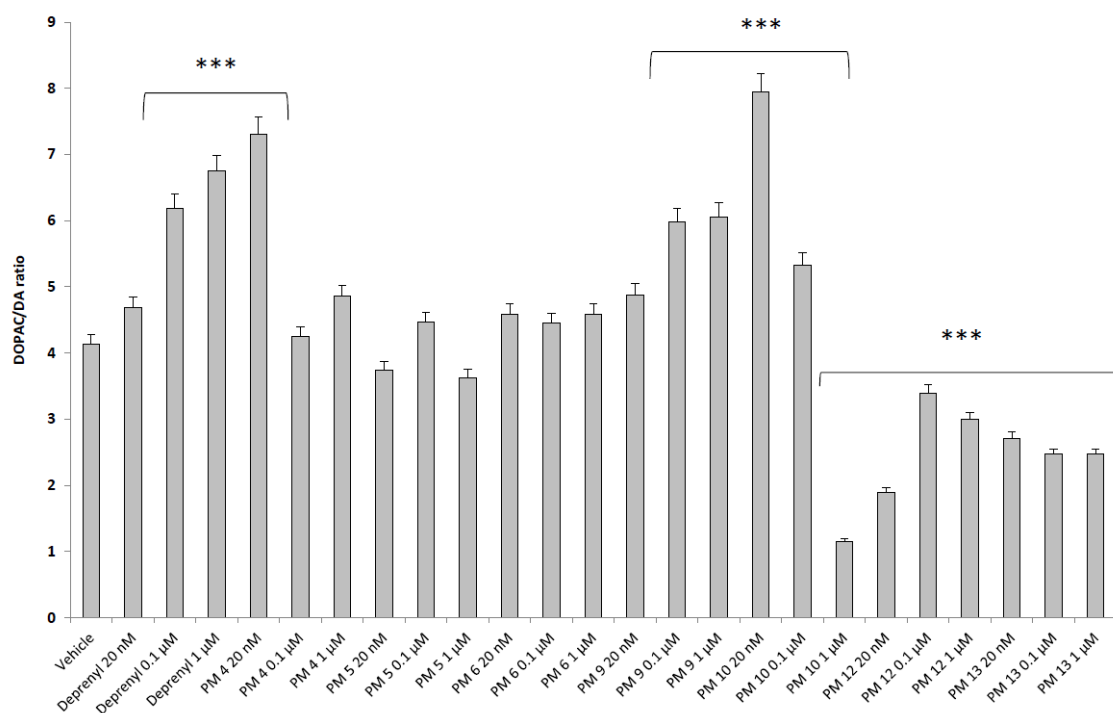
Figure 5.4. Effect of PMs on DOPAC/DA ratio in rat cortex synaptosomes. ANOVA: P<0.0001; post-hoc: ***P<0.001 *vs.* Vehicle group.
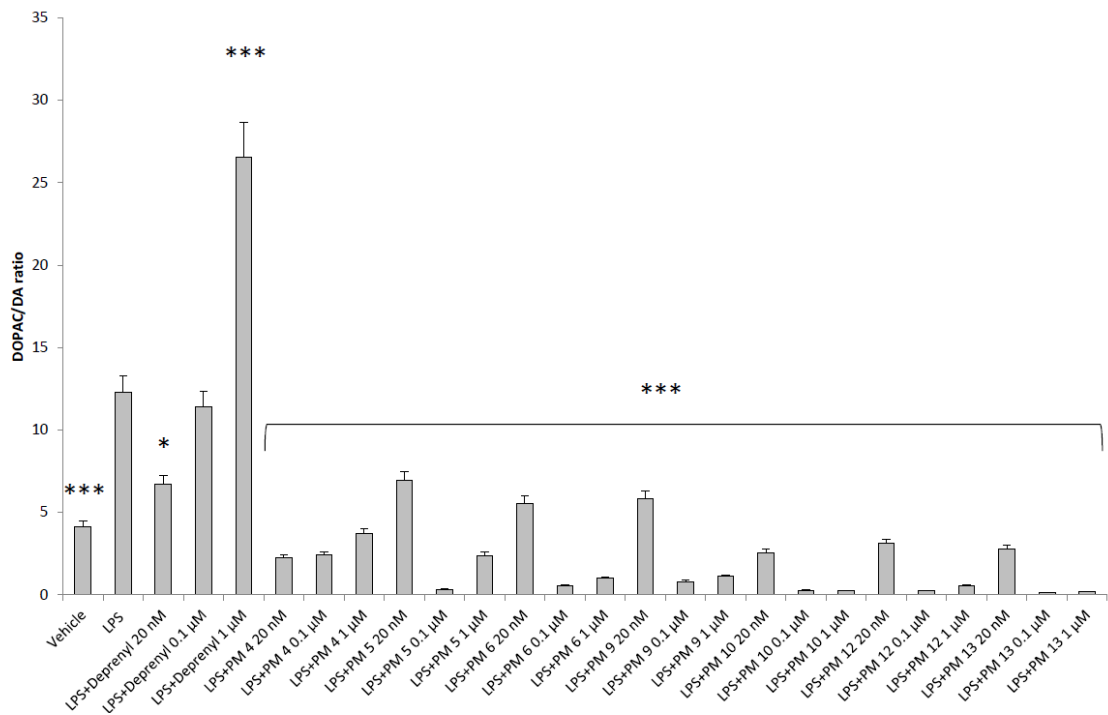
Figure 5.5. Effect of PMs on DOPAC/DA ratio in rat cortex synaptosomes challenged with LPS. ANOVA: P<0.0001; post-hoc: *P<0.05, ***P<0.001 *vs.* LPS group.
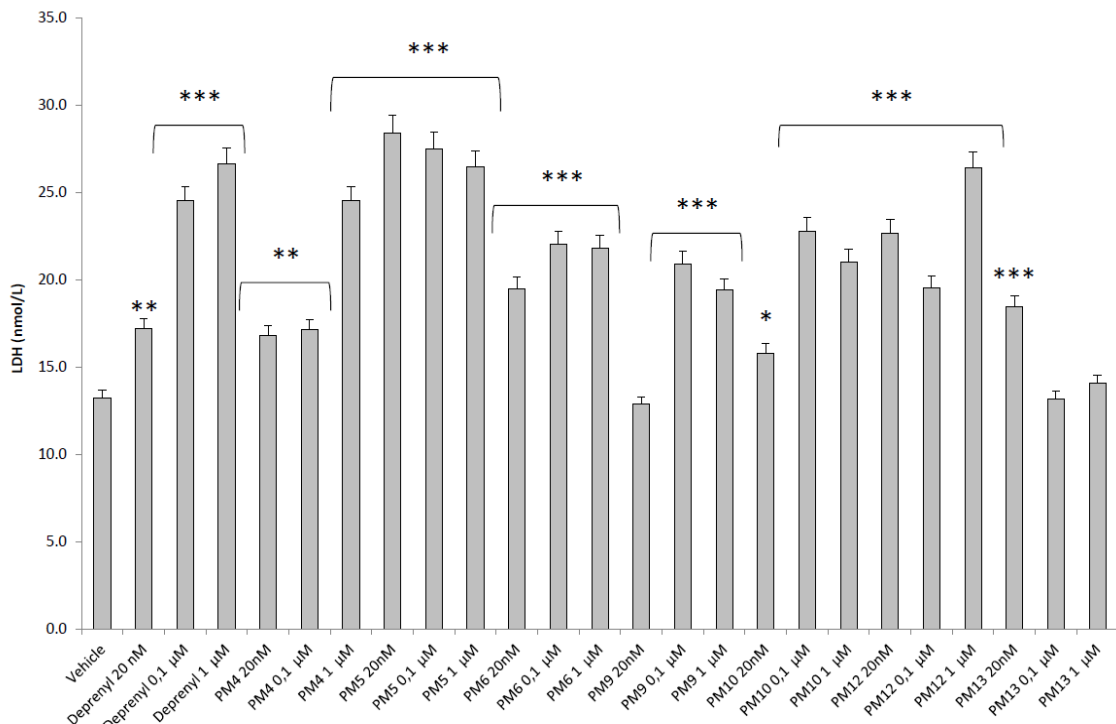
Figure 5.6. Effect of PMs on LDH activity in rat cortex synaptosomes. ANOVA: P<0.0001; post-hoc: *P<0.05, **P<0.01, ***P<0.001 *vs.* Vehicle group.
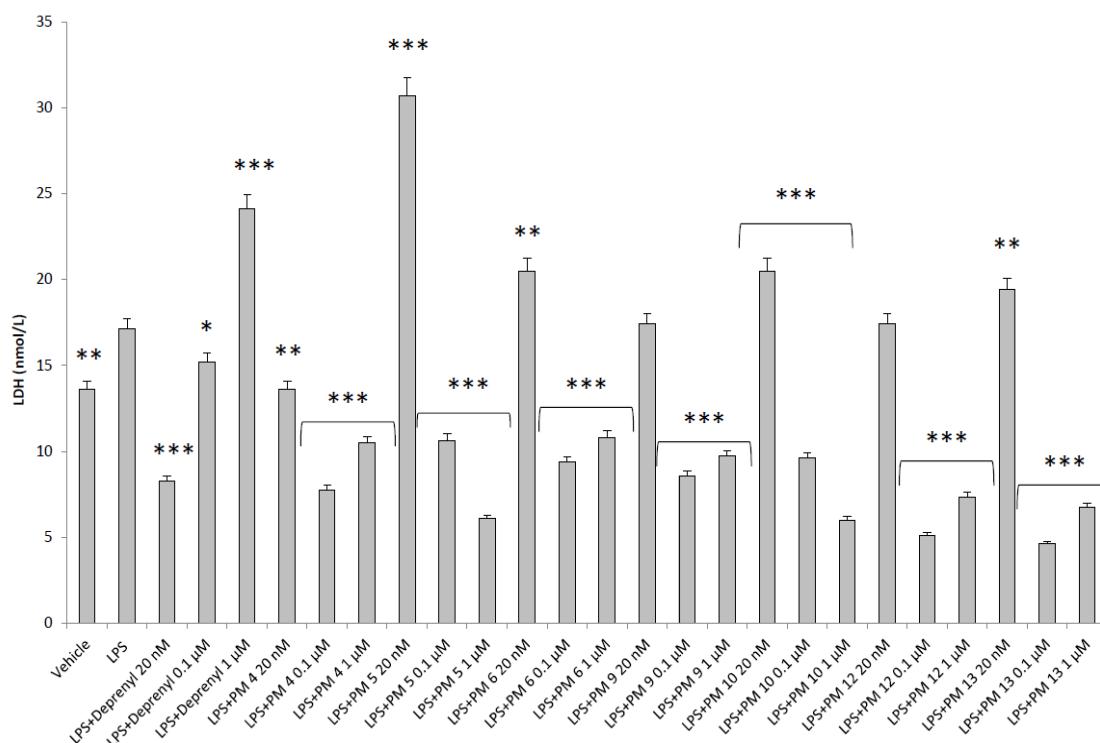
Figure 5.7. Effect of PMs on LDH activity in rat cortex synaptosomes challenged with LPS. ANOVA: P<0.0001; post-hoc: *P<0.05, **P<0.01, ***P<0.001 *vs.* LPS group.

5.5 Conclusions

The design, synthesis, characterization and *in vitro* biological activity evaluation of some novel benzo[*b*]thiophen-3-ol derivatives as inhibitors of hMAO-B have been reported. These compounds have been synthesised through a new simple synthetic approach consisting in a one-step reaction, with moderate to high yields. The compounds **PM1**-**PM20** showed activity in the micromolar/low micromolar range against hMAO-B, with the best activity exhibited by **PM6** with K_i = 0.28 μM, however possessing only a little selectivity index (SI = 14.9). On the other hand, the halogen-substituted compounds, showed a better inhibition profile, with increased activity, with the best performance obtained for compound **PM12**, containing *meta*-bromo substituted phenyl ring (K_i hMAO-B = 0.35 μM; SI = 180).

Compounds **PM1**-**PM20** have also been tested with cortex synaptosomes in both basal and LPS-induced inflammatory conditions to evaluate their ability to affect the DOPAC/DA ratio as well as LDH activity. DOPAC/DA ratio is an indirect index of MAO-B activity, and all the tested compounds are effective in reducing this value in cortex synaptosomes challenged with LPS, showing outcomes better than the reference drug deprenyl. Furthermore, all the **PM** molecules inhibited LDH activity in the concentration range 0.1-1 µM, showing potential activity as neuroprotective agents.

5.6 Experimental section

General

Unless otherwise indicated, all reactions were carried out under a positive nitrogen pressure (balloon pressure) in washed and oven-dried glassware. Solvents were used as supplied without further purification. Where mixtures of solvents are specified, the stated ratios are volume:volume. Reagents were used directly as supplied by Sigma-Aldrich® (Italy). All melting points were measured on a Stuart® melting point apparatus SMP1, and are uncorrected. Temperatures are reported in °C. Fluorescence spectrophotometry was carried out with a Varian Cary Eclipse fluorescence spectrophotometer. ^{1}H and ^{13}C NMR spectra were recorded at 400 and 101 MHz, respectively, on a Bruker spectrometer using CDCl$_3$ and DMSO-d_6 as the solvents at room temperature. The samples were analysed with a final concentration of ~30 mg/mL. Chemical shifts are expressed as δ units (parts per millions) relative to the solvent signal. ^{1}H spectra are reported as follows: δ_H (*spectrometer frequency, solvent*): *chemical shift/ppm (multiplicity, J-coupling constant(s), number of protons, assignment)*. ^{13}C spectra are reported as follows: δ_C (*spectrometer frequency, solvent*): *chemical shift/ppm (assignment)*. Multiplets are abbreviated as follows: br – *broad*; s – *singlet*; d – *doublet*; t – *triplet*; q – *quartet*; m – *multiplet.* Coupling constants *J* are valued in Hertz (Hz). The processing and analyses of the NMR data were carried out with MestreNova. Column chromatography was carried out using Sigma-Aldrich® silica gel (high purity grade, pore size 60 Å, 230–400 mesh particle size). All the purifications and reactions were monitored by TLC performed on 0.2 mm thick silica gel-aluminium backed plates (60 F254, Merck). Visualization was carried out under ultra-violet irradiation (254 nm). Where given, systematic compound names are those generated by ChemBioDraw Ultra 12.0 following IUPAC conventions. Microsomes from insect cells containing recombinant hMAO-A and hMAO-B (5 mg protein/mL) and kynuramine dihydrobromide were obtained from Sigma–Aldrich.

Chemistry

General procedure for the synthesis of derivatives **PM1**-**PM20**: *in* an oven dried flask containing a stirring solution of methyl 2-mercaptobenzoate (1.0 eq.) in methanol (10 mL), were added freshly ground potassium hydroxide (1.5 eq.) and the appropriate α-bromoacetophenone (1.0 eq). The reaction was performed at room temperature for 1-2 hours. After this time, an excess of potassium hydroxide was added (1.5 eq.) and the temperature was raised to 60 °C. The progression of reaction was monitored by TLC and completion was usually reached in 4-5 hours. The reaction was poured on ice-cold water (30 mL) and the pH was adjusted to the value of ~7 to induce the complete precipitation of compound. The resulting benzo[*b*]thiophen-3-ol was collected by filtration and washed with hot methanol (20 mL). This procedure was used in order to obtain all the compounds **PM1**-**PM20** in moderate to high yields and a good level of purity.

Chemical characterization of compounds PM1-PM20
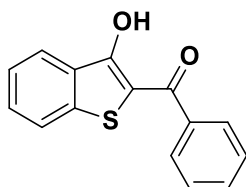
(3-hydroxybenzo[b]thiophen-2-yl)(phenyl)methanone (PM1)

Yellow powder, mp 117-120 °C, 80% yield; ^{1}H NMR (400 MHz, DMSO-d$_6$): δ 7.48-7.52 (m, 1H, benzothiophene), 7.58-7.72 (m, 3H Ar + 1H benzothiophene), 7.92-7.95 (m, 2H, Ar), 7.98 (d, J = 8.2 Hz, 1H, benzothiophene), 8.05 (d, J = 8.0 Hz, 1H, benzothiophene), 12.02 (br, 1H, OH, D$_2$O exch.). ^{13}C NMR (101 MHz, DMSO-d$_6$): δ 112.2 (benzothiophene), 123.9 (benzothiophene), 124.0 (benzothiophene), 125.5 (benzothiophene), 128.8 (2 x Ar), 129.1 (2 x Ar), 130.4 (benzothiophene), 131.1 (Ar), 133.1 (Ar), 138.6 (benzothiophene), 140.0 (benzothiophene), 160.3 (C$_{benzothiophene}$-OH), 190.9 (C=O).
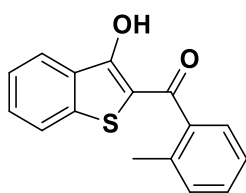
(3-hydroxybenzo[b]thiophen-2-yl)(o-tolyl)methanone (PM2)

Yellow powder, mp 131-133 °C, 86% yield; ^{1}H NMR (400 MHz, CDCl3): δ 2.50 (s, 3H, CH3), 7.32-7.36 (m, 2H, Ar), 7.43-7.48 (m, 1H Ar + 1H benzothiophene), 7.54-7.58 (m, 1H, benzothiophene), 7.63-7.65 (m, 1H, Ar), 7.71 (d, J = 8.2 Hz, 1H, benzothiophene), 8.09 (d, J = 8.0 Hz, 1H, benzothiophene), 12.84 (br, 1H, OH, D2O exch.). ^{13}C NMR (101 MHz, CDCl3): δ 19.7 (CH3), 112.0 (benzothiophene), 123.1 (benzothiophene), 124.0 (benzothiophene), 124.7 (benzothiophene), 125.5 (Ar), 127.4 (Ar), 130.0 (benzothiophene), 130.5 (benzothiophene), 130.9 (Ar), 131.3 (Ar), 136.3 (Ar), 138.3 (Ar), 141.0 (benzothiophene), 160.3 (Cbenzothiophene -OH), 190.9 (C=O).
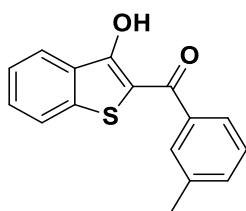
(3-hydroxybenzo[b]thiophen-2-yl)(m-tolyl)methanone (PM3)

Yellow powder, mp 122-124 °C, 76% yield; ^{1}H NMR (400 MHz, CDCl3): δ 2.49 (s, 3H, CH3), 7.44-7.48 (m, 2H Ar + 1H benzothiophene), 7.56-7.60 (m, 1H, benzothiophene), 7.76 (d, J = 8.2 Hz, 1H, benzothiophene), 7.87-7.89 (m, 2H, Ar), 8.09 (d, J = 8.0 Hz, 1H, benzothiophene), 13.49 (br, 1H, OH, D2O exch.). ^{13}C NMR (101 MHz, CDCl3): δ 21.5 (CH3), 109.7 (benzothiophene), 123.0 (benzothiophene), 124.0 (benzothiophene), 124.7 (benzothiophene), 125.6 (Ar), 128.6 (Ar), 128.9 (Ar), 130.1 (benzothiophene), 130.3 (benzothiophene), 133.4 (Ar), 138.3 (Ar), 138.7 (Ar), 140.8 (benzothiophene), 165.3 (Cbenzothiophene-OH), 192.1 (C=O).
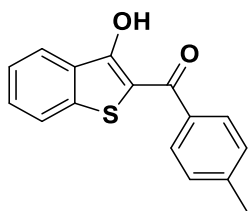
(3-hydroxybenzo[b]thiophen-2-yl)(p-tolyl)methanone (PM4)

Yellow powder, mp 99-101 °C, 77% yield; ^{1}H NMR (400 MHz, CDCl$_3$): δ 2.49 (s, 3H, CH$_3$), 7.35-7.37 (m, 2H, Ar), 7.43-7.47(m, 1H, benzothiophene), 7.55-7.59 (m, 1H, benzothiophene), 7.75 (d, J = 8.2 Hz, 1H, benzothiophene), 7.87-7.89 (m, 2H, Ar), 7.99-8.01 (m, 2H, Ar), 8.09 (d, J = 8.0 Hz, 1H, benzothiophene), 13.6 (br, 1H, OH, D$_2$O exch.). ^{13}C NMR (101 MHz, CDCl$_3$): δ 21.7 (CH$_3$), 109.5 (benzothiophene), 122.9 (benzothiophene), 123.9 (benzothiophene), 124.7 (benzothiophene), 128.6 (2 x Ar), 129.4 (2 x Ar), 130.0 (benzothiophene), 130.3 (benzothiophene), 135.5 (Ar), 140.7 (benzothiophene), 143.5 (Ar), 165.3 (C$_{benzothiophene}$-OH), 191.4 (C=O).
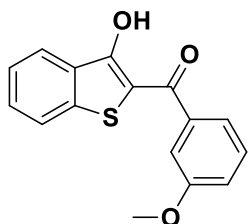
(3-hydroxybenzo[b]thiophen-2-yl)(3-methoxyphenyl)methanone (PM5)

Yellow powder, mp 100-104 °C, 63% yield; ^{1}H NMR (400 MHz, CDCl$_3$): δ 3.93 (s, 3H, OCH$_3$), 7.16-7.19 (m, 1H, Ar), 7.44-7.49 (m, 1H Ar + 1H benzothiophene), 7.56-7.60 (m, 1H Ar + 1H benzothiophene), 7.66-7.69 (m, 1H, Ar), 7.76 (d, J = 8.2 Hz, 1H, benzothiophene), 7.87-7.89 (m, 2H, Ar), 8.09 (d, J = 8.1 Hz, 1H, benzothiophene), 13.45 (br, 1H, OH, D$_2$O exch.). ^{13}C NMR (101 MHz, CDCl$_3$): δ 55.5 (OCH$_3$), 109.7 (benzothiophene), 119.2 (Ar), 120.8 (Ar), 123.0 (benzothiophene), 124.0 (benzothiophene), 124.8 (benzothiophene), 129.8 (Ar), 130.2 (benzothiophene), 130.3 (benzothiophene), 139.5 (Ar), 140.8 (benzothiophene), 159.8 (Ar), 165.4 (C$_{benzothiophene}$-OH), 191.6 (C=O).

(3-hydroxybenzo[b]thiophen-2-yl)(4-methoxyphenyl)methanone (PM6)

Yellow powder, mp 181-183 °C, 73% yield; ^{1}H NMR (400 MHz, DMSO-d_6): δ 3.88 (s, 3H, OCH$_3$), 7.13-7.15 (m, 2H, Ar), 7.49-7.53 (m, 1H, benzothiophene), 7.62-7.66 (m, 1H, benzothiophene), 7.98-8.01 (m, 2H Ar + 1H benzothiophene), 8.03 (d, J = 8.0 Hz, 1H, benzothiophene), 12.76 (br, 1H, OH, D$_2$O exch.). ^{13}C NMR (101 MHz, DMSO-d_6): δ 56.1 (OCH$_3$), 111.4 (benzothiophene), 114.6 (2 x Ar), 123.7 (benzothiophene), 123.9 (benzothiophene), 125.5 (benzothiophene), 130.3 (benzothiophene), 130.7 (benzothiophene), 130.9 (Ar), 131.3 (2 x Ar), 139.7 (benzothiophene), 160.9 (Ar), 163.5 (C$_{benzothiophene}$-OH), 189.5 (C=O).
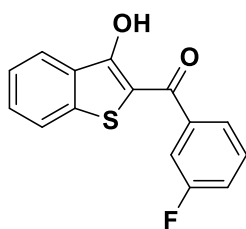
(3-fluorophenyl)(3-hydroxybenzo[b]thiophen-2-yl)methanone (PM7)

Yellow powder, mp 114-118 °C, 82% yield; ^{1}H NMR (400 MHz, CDCl$_3$): δ 7.31-7.36 (m, 1H, Ar), 7.45-7.49 (m, 1H, benzothiophene), 7.52-7.62 (m, 1H Ar + 1H benzothiophene), 7.74-7.77 (m, 1H Ar + 1H benzothiophene), 7.88 (d, J = 7.7 Hz, 1H, Ar), 8.09 (d, J = 8.1 Hz, 1H, benzothiophene), 13.49 (br, 1H, OH, D$_2$O exch.). ^{13}C NMR (101 MHz, CDCl$_3$): δ 109.4 (benzothiophene), 115.4 (d, J$_{C-F}$ = 23.1 Hz, Ar), 119.5 (d, J$_{C-F}$ = 21.3 Hz, Ar), 123.0 (benzothiophene), 124.1 (benzothiophene), 124.2 (d, J$_{C-F}$ = 3.2 Hz, Ar), 124.9 (benzothiophene), 130.2 (benzothiophene), 130.4 (benzothiophene), 130.4 (d, J$_{C-F}$ = 7.8 Hz, Ar), 140.2 (d, J$_{C-F}$ = 6.8 Hz, Ar), 140.8 (benzothiophene), 162.7 (d, J$_{C-F}$ = 248.5 Hz, Ar), 165.8 (C$_{benzothiophene}$-OH), 190.2 (C=O).

(4-fluorophenyl)(3-hydroxybenzo[b]thiophen-2-yl)methanone (PM8)

Yellow powder, mp 96-100 °C, 87% yield; ^{1}H NMR (400 MHz, CDCl$_3$): δ 7.12 (t, J = 8.6 Hz, 2H, Ar), 7.34 (t, J = 7.6 Hz, 1H, benzothiophene), 7.46 (t, J = 7.6 Hz, 1H, benzothiophene), 7.63 (d, J = 8.2 Hz, 1H, benzothiophene), 7.95-8.01 (m, 2H Ar + 1H benzothiophene), 13.32 (br, 1H, OH, D$_2$O exch.). ^{13}C NMR (101 MHz, CDCl$_3$): δ 109.2 (benzothiophene), 115.9 (d, J$_{C-F}$ = 21.9 Hz, 2 x Ar), 123.0 (benzothiophene), 124.0 (benzothiophene), 124.8 (benzothiophene), 130.2 (benzothiophene), 130.3 (benzothiophene), 131.0 (d, J$_{C-F}$ = 9.2 Hz, 2 x Ar), 134.4 (d, J$_{C-F}$ = 3.0 Hz, Ar), 140.6 (benzothiophene), 165.4 (d, J$_{C-F}$ = 254.7 Hz, Ar), 165.6 (C$_{benzothiophene}$-OH), 190.2 (C=O).

(3-chlorophenyl)(3-hydroxybenzo[b]thiophen-2-yl)methanone (PM9)

Yellow powder, mp 148-158 °C, 89% yield; ^{1}H NMR (400 MHz, CDCl$_3$): δ 7.45-7.52 (m, 1H Ar + 1H benzothiophene), 7.58-7.62 (m, 1H Ar + 1H benzothiophene), 7.76 (d, J = 8.2 Hz, 1H, benzothiophene), 7.94-7.96 (m, 1H, Ar), 8.03-8.04 (m, 1H, Ar), 8.09 (d, J = 8.0 Hz, 1H, benzothiophene), 13.29 (br, 1H, OH, D$_2$O exch.). ^{13}C NMR (101 MHz, CDCl$_3$): δ 109.4 (benzothiophene), 123.0 (benzothiophene), 124.1 (benzothiophene), 124.9 (benzothiophene), 126.5 (Ar), 128.5 (Ar), 130.0 (Ar), 130.2 (benzothiophene), 130.5 (benzothiophene), 132.6 (Ar), 135.0 (Ar), 139.8 (Ar), 140.8 (benzothiophene), 165.7 (C$_{benzothiophene}$-OH), 190.2 (C=O).
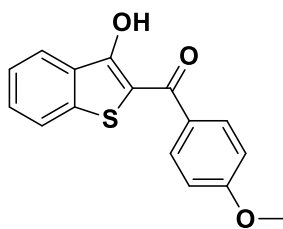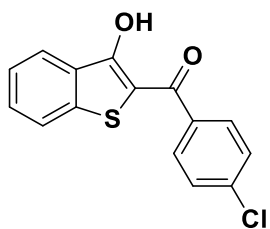
(4-chlorophenyl)(3-hydroxybenzo[b]thiophen-2-yl)methanone (PM10)

Yellow powder, mp 136-138 °C, 88% yield; ^{1}H NMR (400 MHz, CDCl$_3$): δ 7.44-7.48 (m, 1H, benzothiophene), 7.52-7.55 (m, 2H, Ar), 7.57-7.61 (m, 1H, benzothiophene), 7.75 (d, J = 8.2 Hz, 1H, benzothiophene), 8.00-8.04 (m, 2H, Ar), 8.08 (d, J = 8.1 Hz, 1H, benzothiophene), 13.40 (br, 1H, OH, D$_2$O exch.). ^{13}C NMR (101 MHz, CDCl$_3$): δ 109.3 (benzothiophene), 123.0 (benzothiophene), 124.1 (benzothiophene), 124.9 (benzothiophene), 129.1 (2 x Ar), 129.9 (2 x Ar), 130.2 (benzothiophene), 130.4 (benzothiophene), 136.5 (Ar), 139.1 (Ar), 140.7 (benzothiophene), 165.7 (C$_{benzothiophene}$-OH), 190.3 (C=O).
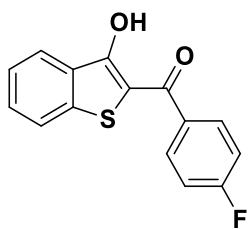

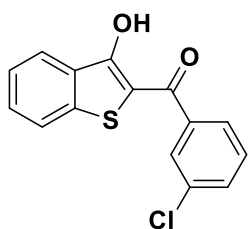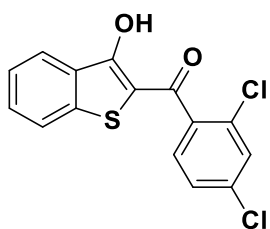**(2,4-dichlorophenyl)(3-hydroxybenzo[b]thiophen-2-yl)methanone (PM11)**

White powder, mp 138-140 °C, 88% yield; ^{1}H NMR (400 MHz, DMSO-d_6): δ 7.44 (t, J = 7.6 Hz, 1H, benzothiophene), 7.58-7.60 (m, 2H Ar + 1H benzothiophene), 7.78 (s, 1H, Ar), 7.94 (d, J = 8.1 Hz, 1H, benzothiophene), 8.06 (d, J = 8.1 Hz, 1H, benzothiophene), 11.74 (br, 1H, OH, D$_2$O exch.). ^{13}C NMR (101 MHz, DMSO-d_6): δ 116.5 (benzothiophene), 124.2 (Ar + benzothiophene), 125.2 (benzothiophene), 128.0 (Ar), 129.4 (Ar), 130.0 (Ar), 130.1 (benzothiophene), 131.2 (Ar), 132.2 (benzothiophene), 135.1 (Ar), 139.5 (benzothiophene), 140.0 (benzothiophene), 157.3 (C$_{benzothiophene}$-OH), 186.7 (C=O).

(3-bromophenyl)(3-hydroxybenzo[b]thiophen-2-yl)methanone (PM12)

Yellow powder, mp 152-158 °C, 90% yield; ^{1}H NMR (400 MHz, CDCl$_3$): δ 7.42-7.49 (m, 1H Ar + 1H benzothiophene), 7.58-7.62 (m, 1H, benzothiophene), 7.74-7.77 (m, 1H Ar + 1H benzothiophene), 7.99 (d, J = 7.8 Hz, 1H, Ar), 8.09 (d, J = 8.0 Hz, 1H, benzothiophene), 8.18-8.19 (m, 1H, Ar), 13.27 (br, 1H, OH, D$_2$O exch.). ^{13}C NMR (101 MHz, CDCl$_3$): δ 109.4 (benzothiophene), 123.0 (Ar), 123.1 (benzothiophene), 124.1 (benzothiophene), 124.9 (benzothiophene), 126.9 (Ar), 130.1 (benzothiophene), 130.3 (Ar), 130.5 (benzothiophene), 131.4 (Ar), 135.5 (Ar), 140.0 (Ar), 140.8 (benzothiophene), 165.7 (C$_{benzothiophene}$-OH), 190.1 (C=O).
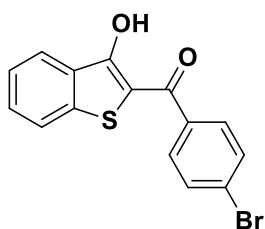
(4-bromophenyl)(3-hydroxybenzo[b]thiophen-2-yl)methanone (PM13)

Yellow powder, mp 142-147 °C, 74% yield; ^{1}H NMR (400 MHz, CDCl$_3$): δ 7.46 (t, J = 7.6 Hz, 1H, benzothiophene), 7.59 (t, J = 7.6 Hz, 1H, benzothiophene), 7.70 (d, J = 8.5 Hz, 2H, Ar), 7.75 (d, J = 8.2 Hz, 1H, benzothiophene), 7.94 (d, J = 8.5 Hz, 2H, Ar), 8.08 (d, J = 8.0 Hz, 1H, benzothiophene), 13.39 (br, 1H, OH, D$_2$O exch.). ^{13}C NMR (101 MHz, CDCl$_3$): δ 109.3 (benzothiophene), 123.0 (benzothiophene), 124.1 (benzothiophene), 124.9 (benzothiophene), 127.7 (Ar), 130.0 (2 x Ar), 130.2 (benzothiophene), 130.4 (benzothiophene), 132.0 (2 x Ar), 136.9 (Ar), 140.7 (benzothiophene), 165.7 (C$_{benzothiophene}$-OH), 190.4 (C=O).
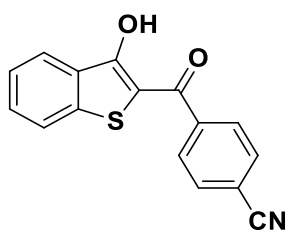
4-(3-hydroxybenzo[b]thiophene-2-carbonyl)benzonitrile (PM14)

Orange powder, mp 192-200 °C, 61% yield; ^{1}H NMR (400 MHz, DMSO-d_6): δ 7.48 (t, J = 7.6 Hz, 1H, benzothiophene), 7.62 (t, J = 7.6 Hz, 1H, benzothiophene), 7.96-8.04 (m, 4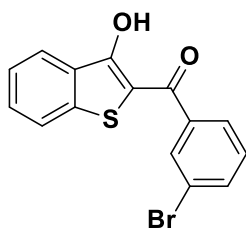H Ar + 1H benzothiophene), 8.08 (d, J = 8.1 Hz, 1H, benzothiophene), 11.95 (br, 1H, OH, D_2O exch.). ^{13}C NMR (101 MHz, DMSO-d_6): δ 114.2 (Ar), 114.5 (benzothiophene), 118.8 (CN), 124.1 (benzothiophene), 124.2 (benzothiophene), 125.4 (benzothiophene), 129.4 (2 x Ar), 130.2 (benzothiophene), 131.8 (benzothiophene), 132.8 (2 x Ar), 140.0 (benzothiophene), 143.1 (Ar), 158.3 (C_benzothiophene-OH), 188.9 (C=O).
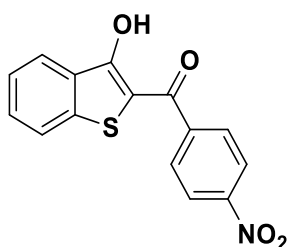
(3-hydroxybenzo[b]thiophen-2-yl)(4-nitrophenyl)methanone (PM15)

Orange powder, mp 205-207 °C, 79% yield; ^{1}H NMR (400 MHz, DMSO-d_6): δ 7.49 (t, J = 7.6 Hz, 1H, benzothiophene), 7.58-7.71 (m, 1H, benzothiophene), 7.99 (d, J = 8.1 Hz, 1H, benzothiophene), 8.06-8.11 (m, 2H Ar + 1H benzothiophene), 8.38 (d, J = 8.1 Hz, 2H, Ar), 11.94 (br, 1H, OH, D_2O exch.). ^{13}C NMR (101 MHz, DMSO-d_6): δ 114.5 (benzothiophene), 123.9 (2 x Ar), 124.1(benzothiophene), 124.2 (benzothiophene), 125.4 (benzothiophene), 130.1 (2 x Ar), 130.2 (benzothiophene), 131.9 (benzothiophene), 140.0 (benzothiophene), 144.8 (Ar), 149.6 (Ar-NO_2), 158.1 (C_benzothiophene-OH), 188.5 (C=O).
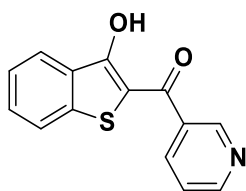
(3-hydroxybenzo[b]thiophen-2-yl)(pyridin-3-yl)methanone (PM16)

Orange powder, mp 132-134 °C, 79% yield; ^{1}H NMR (400 MHz, DMSO-d_6): δ 7.47-7.51 (m, 1H, benzothiophene), 7.58-7.64 (m, 1H Pyr + 1H benzothiophene), 7.99 (d, J = 8.1 Hz, 1H, benzothiophene), 8.10 (d, J = 8.1 Hz, 1H, benzothiophene), 8.21-8.24 (m, 1H, Pyr), 8.79-8.80 (m, 1H, Pyr), 9.00-9.01 (m, 1H, Pyr), 11.92 (br, 1H, OH, D_2O exch.). ^{13}C NMR (101 MHz, DMSO-d_6): δ 109.5 (benzothiophene), 123.1 (benzothiophene), 123.8 (Pyr), 124.2 (benzothiophene), 125.1 (benzothiophene), 130.0 (benzothiophene), 130.7 (benzothiophene), 136.3 (Pyr), 136.4 (Pyr), 140.8 (benzothiophene), 148.8 (Pyr), 152.4 (Pyr), 165.9 ($C_{benzothiophene}$-OH), 189.3 (C=O).
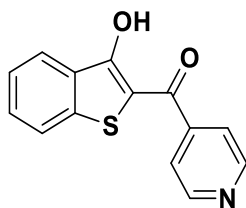
(3-hydroxybenzo[b]thiophen-2-yl)(pyridin-4-yl)methanone (PM17)

Orange powder, mp 203-205 °C, 65% yield; ^{1}H NMR (400 MHz, CDCl$_3$): δ 7.46-7.50 (m, 1H, benzothiophene), 7.60-7.64 (m, 1H, benzothiophene), 7.76 (d, J = 8.2 Hz, 1H, benzothiophene), 7.85-7.86 (m, 2H, Pyr), 8.10 (d, J = 8.1 Hz, 1H, benzothiophene), 8.87-8.89 (m, 1H, Pyr), 13.12 (br, 1H, OH, D_2O exch.). ^{13}C NMR (101 MHz, CDCl$_3$): δ 109.4 (benzothiophene), 121.6 (2 x Pyr), 123.1 (benzothiophene), 124.3 (benzothiophene), 125.1 (benzothiophene), 130.0 (benzothiophene), 130.9 (benzothiophene), 141.0 (benzothiophene), 144.7 (Pyr), 150.6 (2 x Pyr), 165.4 ($C_{benzothiophene}$-OH), 189.7 (C=O).
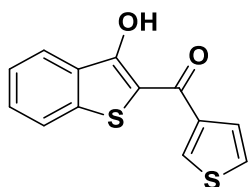
(3-hydroxybenzo[b]thiophen-2-yl)(thiophen-3-yl)methanone (PM18)

Yellow powder, mp 114-116 °C, 63% yield; ^{1}H NMR (400 MHz, CDCl$_3$): δ 7.44-7.48 (m, 1H thiophene + 1H benzothiophene), 7.57-7.61 (m, 1H, benzothiophene), 7.78 (d, J = 8.2 Hz, 1H, benzothiophene), 7.80-7.81 (m, 1H, thiophene), 8.07 (d, J = 8.0 Hz, 1H, benzothiophene), 8.39-8.40 (m, 1H, thiophene), 13.55 (br, 1H, OH, D$_2$O exch.). ^{13}C NMR (101 MHz, CDCl$_3$): δ 109.4 (benzothiophene), 123.0 (benzothiophene), 123.9 (benzothiophene), 124.8 (benzothiophene), 126.6 (thiophene), 127.6 (thiophene), 130.2 (benzothiophene), 130.4 (benzothiophene), 132.2 (thiophene), 140.2 (thiophene), 141.0 (benzothiophene), 165.7 (C$_{benzothiophene}$-OH), 184.6 (C=O).
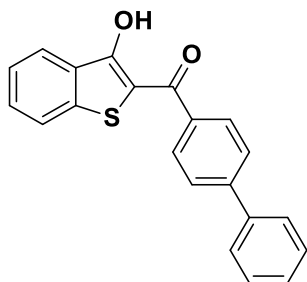
[1,1'-biphenyl]-4-yl(3-hydroxybenzo[b]thiophen-2-yl)methanone (PM19)

Yellow powder, mp 150-154 °C, 89% yield; ^{1}H NMR (400 MHz, CDCl$_3$): δ 7.44-7.54 (m, 3H Ar + 1H benzothiophene), 7.57-7.61 (m, 1H, benzothiophene), 7.69-7.71 (m, 2H, Ar), 7.77-7.80 (m, 2H Ar + 1H benzothiophene), 8.11 (d, J = 8.1 Hz, 1H, benzothiophene), 8.17-8.19 (m, 2H, Ar), 13.61 (br, 1H, OH, D$_2$O exch.). ^{13}C NMR (101 MHz, CDCl$_3$): δ 109.6 (benzothiophene), 123.0 (benzothiophene), 124.0 (benzothiophene), 124.8 (benzothiophene), 127.3 (2 x Ar), 127.4 (2 x Ar), 128.3 (Ar), 129.0 (2 x Ar), 129.1 (2 x Ar), 130.2 (benzothiophene), 130.3 (benzothiophene), 136.9 (Ar), 139.8 (benzothiophene), 140.8 (Ar), 145.5 (Ar), 165.6 (C$_{benzothiophene}$-OH), 191.14 (C=O).
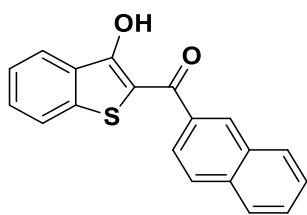
(3-hydroxybenzo[b]thiophen-2-yl)(naphthalen-2-yl)methanone (PM20)

Yellow powder, mp 126-128 °C, 60% yield; ^{1}H NMR (400 MHz, CDCl3): δ 7.44-7.49 (m, 1H, benzothiophene), 7.57-7.68 (m, 2H Ar + 1H benzothiophene), 7.78 (d, 2H, J = 8.2 Hz, 1H, benzothiophene), 7.93-7.95 (m, 1H, Ar), 7.99-8.05 (m, 2H, Ar), 8.09-8.12 (m, 1H Ar + 1H benzothiophene), 8.65 (s, 1H, Ar), 13.58 (br, 1H, OH, D2O exch.). ^{13}C NMR (101 MHz, CDCl3): δ 109.8 (benzothiophene), 123.0 (benzothiophene), 124.0 (benzothiophene), 124.4 (Ar), 124.8 (benzothiophene), 127.0 (Ar), 127.9 (Ar), 128.5 (Ar), 128.7 (Ar), 129.5 (Ar), 129.9 (Ar), 130.2 (benzothiophene), 130.4 (benzothiophene), 132.4 (Ar), 135.3 (Ar), 135.3 (Ar), 139.8, 140.8 (benzothiophene), 145.5 (Ar), 165.6 (Cbenzothiophene-OH), 191.14 (C=O).

Biological assays

hMAO-A and hMAO-B inhibition studies

IC50 values for the inhibition of hMAO-A and hMAO-B were measured according to the literature protocol [198,199] with the commercially available recombinant enzymes (Sigma-Aldrich) serving as enzyme sources. The enzyme reactions (200 μL) were carried out in white 96-well microtiter plates (Eppendorf) in potassium phosphate buffer (pH 7.4, 100 mM) and contained kynuramine (50 μM), the test inhibitors spanning at least three order of magnitude (0.003-100 μM) and hMAO-A (0.0075 mg protein/mL) or hMAO-B (0.015 mg protein/mL). The reactions were initiated with the addition of enzyme, incubated for 20 min at 37 °C, and at endpoint were treated with 2 N NaOH (80 μL) to terminate the enzyme reactions. The fluorescence intensity of 4-hydroxyquinoline, the product formed by the MAO-catalyzed oxidation of kynuramine, was measured (λ_{ex} = 310 nm; λ_{em} = 400 nm). Sigmoidal plots of catalytic rate versus logarithm of inhibitor concentration were constructed and the IC50 values

were estimated and reported as the mean ± standard deviation (SD) of triplicate measurements.

Rat cortex synaptosomes

Male adult Sprague-Dawley rats (200-250 g) were housed in Plexiglass cages (40 cm × 25 cm × 15 cm), two rats per cage, in climatized colony rooms (22 ± 1 °C; 60% humidity), on a 12 h/12 h light/dark cycle (light phase: 07:00–19:00 h), with free access to tap water and food, 24 h/day throughout the study, with no fasting periods. Rats were fed a standard laboratory diet (3.5% fat, 63% carbohydrate, 14% protein, 19.5% other components without caloric value; 3.20 kcal/g). Housing conditions and experimentation procedures were strictly in accordance with the European Union ethical regulations on the care of animals for scientific research. According to the recognized ethical principles of "Replacement, Refinement and Reduction of Animals in Research", specimens were obtained as residual material from vehicle-treated rats randomized in our previous experiments approved by Local Ethical Committee (University "G. d'Annunzio" of Chieti-Pescara) and Italian Health Ministry (Project N. 880 definitely approved by Italian Health Ministry on 24th August 2015).

Synaptosomes were prepared from a pool of frontal and parietal cortex, which are more sensitive to oxidative stress, compared to other areas such as occipital and dorsal cortex [200]. Briefly, the frontal and parietal cortex was quickly dissected, homogenized in 0.32 M saccharose solution and centrifuged, first at 4000×g for 10 min, and then at 12000×g for 20 min, to isolate neuronal endings from cell nuclei and glia. The purified synaptosomes were suspended at 37 °C, under O_2/CO_2 95%/5%, pH 7.35–7.45, in Krebs-Ringer buffer (mM: NaCl 125, KCl 3, $MgSO_4$ 1.2, $CaCl_2$ 1.2, Tris–HCl 10, glucose 10). Then, the synaptosome suspension was divided into fractions (each containing 100 mg of tissue in 3 mL medium) that were incubated at 37 °C, under agitation for 30 min (incubation period), and treated with a pharmacological stimulus as follows: i) Krebs-Ringer buffer (vehicle); ii) vehicle plus oxidant stimulus [LPS

10 µg/mL]; iii) vehicle plus oxidant stimulus and I-MAO inhibitors (20 nM-1µM). After the incubation period, synaptosome suspension was centrifuged (12000×g for 20 min) and the supernatant assayed for LDH, DA and DOPAC determination.

LDH activity determination

LDH activity was measured by evaluating the consumption of NADH in 20 mM HEPES-K$^+$ (pH 7.2), 0.05% bovine serum albumin, 20 µM NADH and 2 mM pyruvate using a microplate reader (excitation 340 nm, emission 460 nm) according to manufacturer's protocol (Sigma-Aldrich). Extracts were tested at 25 µg/mL. Data were obtained from triplicate test and expressed as relative variations compared to vehicle-treated cells [201].

Neurotransmitter extraction and high performance liquid chromatography (HPLC) determination

Extracellular DA, 5-HT and NE levels were analysed through HPLC apparatus consisting of a Jasco (Tokyo, Japan) PU-2080 chromatographic pump and an ESA (Chelmsford, MA, USA) Coulochem III coulometric detector, equipped with microdialysis cell (ESA-5014b) porous graphite working electrode and solid state palladium reference electrode. The analytical conditions for biogenic amine identification and quantification were selected as previously reported [202]. Briefly, the analytical cell was set at −0.150 V, for detector 1 and at +0.300 V, for detector 2, with a range of 100 nA. The chromatograms were monitored at the analytical detector 2. Integration was performed by Jasco Borwin Chromatography software, version 1.5. The chromatographic separation was performed by isocratic elution on Phenomenex Kinetex reversed-phase column (C18, 150 mm×4.6 mm i.d., 2.6 µm). The mobile phase was (10:90, v/v) acetonitrile and 75 mM, pH 3.00 phosphate buffer containing octanesulfonic acid 1.8 mM, EDTA 30 µM and triethylamine 0.015% *v:v*. Flow rate was 0.6 mL/min and the samples were manually injected through a 20 µL loop. Neurotransmitter peaks were identified by comparison with the retention time of pure standard. Neurotransmitter concentrations in the samples were calculated by linear

regression curve (y = bx + m) obtained with standard. Neither internal nor external standard were necessary for neurotransmitter quantification and all tests performed for method validation yielded results in accordance to limits indicated in official guidelines for applicability in laboratory trials. The standard stock solutions of DA, and DOPAC at 2 mg/mL were prepared in bi-distilled water containing 0.004% EDTA and 0.010% sodium bisulfite. The stock solutions were stored at 4 °C. Work solutions (1.25-20.00 ng/mL) were obtained daily progressively diluting stock solutions in mobile phase.

Statistical analysis

GraphPad Prism version 5.01 for Windows (GraphPad Software, San Diego, CA) was used as statistical analysis software. Experiments were performed at least in triplicate and results are presented as mean ± standard deviation (SD). One-way analysis of variance (ANOVA) followed by Newman-Keuls post-hoc test was employed to assess significant differences (p<0.05). As regards the animals randomized for each experimental group, the number was calculated on the basis of the "Resource Equation" N=(E+T)/T [203].

References

1.   Capasso, C.; Supuran, C. T. An overview of the alpha-, beta- and gamma-carbonic anhydrases from Bacteria: Can bacterial carbonic anhydrases shed new light on evolution of bacteria? *J. Enzyme Inhib. Med. Chem.* **2015**, *30*, 325–332, doi:10.3109/14756366.2014.910202.

2.   Dedeoglu, N.; DeLuca, V.; Isik, S.; Yildirim, H.; Kockar, F.; Capasso, C.; Supuran, C. T. Sulfonamide inhibition study of the β-class carbonic anhydrase from the caries producing pathogen Streptococcus mutans. *Bioorg. Med. Chem. Lett.* **2015**, *25*, 2291–2297, doi:10.1016/j.bmcl.2015.04.037.

3.   Ferry, J. G. The γ class of carbonic anhydrases. *Biochim. Biophys. Acta - Proteins Proteomics* 2010, *1804*, 374–381.

4.   Macauley, S. R.; Zimmerman, S. A.; Apolinario, E. E.; Evilia, C.; Hou, Y.; Ferry, J. G.; Sowers, K. R. The Archetype γ -Class Carbonic Anhydrase (Cam) Contains Iron When Synthesized in Vivo †. *Biochemistry* **2009**, *48*, 817–819.

5.   Coleman, J. E. Zinc enzymes. *Curr. Opin. Chem. Biol.* **1998**, *2*, 222–234, doi:10.1016/S1367-5931(98)80064-1.

6.   Maren, T. H. Carbonic anhydrase: chemistry, physiology, and inhibition. *Physiol. Rev.* **1967**, *47*, 595–781, doi:10.1152/physrev.1967.47.4.595.

7.   Coleman, J. E. Mechanism of Action of Carbonic Anhydrase. *J. Biochem.* **1967**, *242*, 5212–5219.

8.   Alterio, V.; Fiore, A. Di; Ambrosio, K. D.; Supuran, C. T.; Simone, G. De Multiple Binding Modes of Inhibitors to Carbonic Anhydrases : How to Design Speci fi c Drugs Targeting 15 Di ff erent Isoforms ? *Am. Chem. Soc. Publ.* **2012**, *112*, 4421–4468.

9.   Kikutani, S.; Nakajima, K.; Nagasato, C.; Tsuji, Y.; Miyatake, A.; Matsuda, Y.

Thylakoid luminal θ-carbonic anhydrase critical for growth and photosynthesis in the marine diatom *Phaeodactylum tricornutum*. *Proc. Natl. Acad. Sci.* **2016**, *113*, 9828–9833, doi:10.1073/pnas.1603112113.

10.   Xu, Y.; Feng, L.; Jeffrey, P. D.; Shi, Y.; Morel, F. M. M. Structure and metal exchange in the cadmium carbonic anhydrase of marine diatoms. *Nature* **2008**, *452*, 56–61, doi:10.1038/nature06636.

11.   Supuran, C. T. Structure and function of carbonic anhydrases. *Biochem. J.* **2016**, *473*, 2023–2032, doi:10.1042/BCJ20160115.

12.   Supuran, C. T. Carbonic anhydrases: novel therapeutic applications for inhibitors and activators. *Nat. Rev. Drug Discov.* **2008**, *7*, 168–181, doi:10.1038/nrd2467.

13.   Smith, K. S.; Jakubzick, C.; Whittam, T. S.; Ferry, J. G. Carbonic anhydrase is an ancient enzyme widespread in prokaryotes. *Proc. Natl. Acad. Sci.* **1999**, *96*, 15184–15189, doi:10.1073/pnas.96.26.15184.

14.   Scozzafava, A.; Carta, F.; Supuran, C. T. Secondary and tertiary sulfonamides: a patent review (2008 – 2012). *Expert Opin. Ther. Pat.* **2013**, *23*, 203–213, doi:10.1517/13543776.2013.742065.

15.   Hunt, J. B.; Rhee, M. J.; Storm, C. B. A rapid and convenient preparation of apocarbonic anhydrase. *Anal. Biochem.* **1977**, *79*, 614–617, doi:10.1016/0003-2697(77)90444-4.

16.   Xu, H. J.; Zhao, X. Y.; Deng, J.; Fu, Y.; Feng, Y. S. Efficient C-S cross coupling catalyzed by Cu2O. *Tetrahedron Lett.* **2009**, *50*, 434–437, doi:10.1016/j.tetlet.2008.11.029.

17.   Tripp, B. C.; Bell, C. B.; Cruz, F.; Krebs, C.; Ferry, J. G. A Role for Iron in an Ancient Carbonic Anhydrase. *J. Biol. Chem.* **2004**, *279*, 6683–6687,

doi:10.1074/jbc.M311648200.

18.   Aggarwal, M.; Boone, C. D.; Kondeti, B.; McKenna, R. Structural annotation of human carbonic anhydrases. *J. Enzyme Inhib. Med. Chem.* **2012**, *28*, 267–277, doi:10.3109/14756366.2012.737323.

19.   Alterio, V.; Di Fiore, A.; D'Ambrosio, K.; Supuran, C. T.; De Simone, G. Multiple binding modes of inhibitors to carbonic anhydrases: How to design specific drugs targeting 15 different isoforms? *Chem. Rev.* **2012**, *112*, 4421–4468, doi:10.1021/cr200176r.

20.   Supuran, C. T. Structure-based drug discovery of carbonic anhydrase inhibitors. *J. Enzyme Inhib. Med. Chem.* **2012**, *27*, 759–772, doi:10.3109/14756366.2012.672983.

21.   Wang, X.; Conway, W.; Burns, R.; McCann, N.; Maeder, M. Comprehensive study of the hydration and dehydration reactions of carbon dioxide in aqueous solution. *J. Phys. Chem. A* **2010**, *114*, 1734–1740, doi:10.1021/jp909019u.

22.   Supuran, C. T. Carbonic anhydrases: From biomedical applications of the inhibitors and activators to biotechnological use for CO2capture. *J. Enzyme Inhib. Med. Chem.* **2013**, *28*, 229–230, doi:10.3109/14756366.2013.761876.

23.   Neri, D.; Supuran, C. T. Interfering with pH regulation in tumours as a therapeutic strategy. *Nat. Rev. Drug Discov.* **2011**, *10*, 767–777, doi:10.1038/nrd3554.

24.   Akiba, Y.; Ghayouri, S.; Takeuchi, T.; Mizumori, M.; Guth, P. H.; Engel, E.; Swenson, E. R.; Kaunitz, J. D. Carbonic Anhydrases and Mucosal Vanilloid Receptors Help Mediate the Hyperemic Response to Luminal CO2 in Rat Duodenum. *Gastroenterology* **2006**, *131*, 142–152, doi:10.1053/j.gastro.2006.04.018.

25. Luca, V. De; Vullo, D.; Scozzafava, A.; Carginale, V.; Rossi, M.; Supuran, C. T.; Capasso, C. An α-carbonic anhydrase from the thermophilic bacterium Sulphurihydrogenibium azorense is the fastest enzyme known for the CO2hydration reaction. *Bioorganic Med. Chem.* **2013**, *21*, 1465–1469, doi:10.1016/j.bmc.2012.09.047.

26. Floryszak-Wieczorek, J.; Arasimowicz-Jelonek, M. The multifunctional face of plant carbonic anhydrase. *Plant Physiol. Biochem.* **2017**, *112*, 362–368, doi:10.1016/j.plaphy.2017.01.007.

27. Aspatwar, A.; Haapanen, S.; Parkkila, S. An update on the metabolic roles of carbonic anhydrases in the model alga chlamydomonas reinhardtii. *Metabolites* 2018, *8*, 22.

28. Supuran, C. T. Advances in structure-based drug discovery of carbonic anhydrase inhibitors. *Expert Opin. Drug Discov.* 2017, *12*, 61–88.

29. Silverman, D. N.; Tu, C.; Chen, X.; Tanhauser, S. M.; Kresge, A. J.; Laipis, P. J. Rate-Equilibria Relationships in Intramolecular Proton Transfer in Human Carbonic Anhydrase III. *Biochemistry* **1993**, *32*, 10757–10762, doi:10.1021/bi00091a029.

30. Elleuche, S.; Pöggeler, S. Carbonic anhydrases in fungi. *Microbiology* 2010, *156*, 23–29.

31. Tresguerres, M.; Buck, J.; Levin, L. R. Physiological carbon dioxide, bicarbonate, and pH sensing. *Pflügers Arch. - Eur. J. Physiol.* **2010**, *460*, 953–964, doi:10.1007/s00424-010-0865-6.

32. Lindskog, S. Structure and mechanism of carbonic anhydrase. *Pharmacol. Ther.* **1997**, *74*, 1–20, doi:10.1016/S0163-7258(96)00198-2.

33. Henry, R. P. Multiple roles of carbonic anhydrase in cellular transport and

metabolism. *Annu. Rev. Physiol.* **1996**, *58*, 523–538, doi:10.1146/annurev.physiol.58.1.523.

34.   Esbaugh, A. J.; Tufts, B. L. The structure and function of carbonic anhydrase isozymes in the respiratory system of vertebrates. *Respir. Physiol. Neurobiol.* **2006**, *154*, 185–198, doi:10.1016/j.resp.2006.03.007.

35.   Supuran, C. T.; Scozzafava, A. Carbonic anhydrase inhibitors and their therapeutic potential. *Expert Opin. Ther. Pat.* **2000**, *10*, 575–600, doi:10.1517/13543776.10.5.575.

36.   Sjoblom, B.; Polentarutti, M.; Djinovic-Carugo, K. Structural study of X-ray induced activation of carbonic anhydrase. *Proc. Natl. Acad. Sci.* **2009**, *106*, 10609–10613, doi:10.1073/pnas.0904184106.

37.   Tu, C.; Silverman, D. N.; Forsman, C.; Jonsson, B. H.; Lindskog, S. Role of Histidine 64 in the Catalytic Mechanism of Human Carbonic Anhydrase II Studied with a Site-Specific Mutant. *Biochemistry* **1989**, *28*, 7913–7918, doi:10.1021/bi00445a054.

38.   An, H.; Tu, C.; Ren, K.; Laipis, P. J.; Silverman, D. N. Proton transfer within the active-site cavity of carbonic anhydrase III. *Biochim. Biophys. Acta - Proteins Proteomics* **2002**, *1599*, 21–27, doi:10.1016/S0167-4838(02)00374-6.

39.   Ren, X.; Tu, C.; Laipis, P. J.; Silverman, D. N. Proton Transfer by Histidine 67 in Site-Directed Mutants of Human Carbonic Anhydrase III. *Biochemistry* **1995**, *34*, 8492–8498, doi:10.1021/bi00026a033.

40.   Tu, C.; Qian, M.; Earnhardt, J. N.; Laipis, P. J.; Silverman, D. N. Properties of intramolecular proton transfer in carbonic anhydrase III. *Biophys. J.* **1998**, *74*, 3182–3189, doi:10.1016/S0006-3495(98)78024-5.

41.   Supuran, C. T.; Scozzafava, A.; Casini, A. Carbonic anhydrase inhibitors. *Med.*

Res. Rev. **2003**, *23*, 146–189, doi:10.1002/med.10025.

42. Nishimori, I.; Vullo, D.; Minakuchi, T.; Scozzafava, A.; Capasso, C.; Supuran, C. T. Restoring catalytic activity to the human carbonic anhydrase (CA) related proteins VIII, X and XI affords isoforms with high catalytic efficiency and susceptibility to anion inhibition. *Bioorganic Med. Chem. Lett.* **2013**, *23*, 256–260, doi:10.1016/j.bmcl.2012.10.103.

43. Frost, S. C. *Carbonic Anhydrase: Mechanism, Regulation, Links to Disease, and Industrial Applications*; 2014; Vol. 75; ISBN 978-94-007-7358-5.

44. Gao, B. B.; Clermont, A.; Rook, S.; Fonda, S. J.; Srinivasan, V. J.; Wojtkowski, M.; Fujimoto, J. G.; Avery, R. L.; Arrigg, P. G.; Bursell, S. E.; Aiello, L. P.; Feener, E. P. Extracellular carbonic anhydrase mediates hemorrhagic retinal and cerebral vascular permeability through prekallikrein activation. *Nat. Med.* **2007**, *13*, 181–188, doi:10.1038/nm1534.

45. De Simone, G.; Angeli, A.; Bozdag, M.; Supuran, C. T.; Winum, J.-Y.; Monti, S. M.; Alterio, V. Inhibition of carbonic anhydrases by a substrate analog: benzyl carbamate directly coordinates the catalytic zinc ion mimicking bicarbonate binding. *Chem. Commun.* **2018**, *54*, 10312–10315, doi:10.1039/C8CC05755A.

46. Gilmour, K. M. Perspectives on carbonic anhydrase. *Comp. Biochem. Physiol. - A Mol. Integr. Physiol.* **2010**, *157*, 193–197, doi:10.1016/j.cbpa.2010.06.161.

47. Sly, W. S.; Hewett-Emmett, D.; Whyte, M. P.; Yu, Y. S.; Tashian, R. E. Carbonic anhydrase II deficiency identified as the primary defect in the autosomal recessive syndrome of osteopetrosis with renal tubular acidosis and cerebral calcification. *Proc. Natl. Acad. Sci. U. S. A.* **1983**, *80*, 2752–2756, doi:10.1073/pnas.80.9.2752.

48. Räisänen SR1, Lehenkari P, Tasanen M, Rahkila P, Härkönen PL, V. H. " Middle Molecules " Plasma Level Under. *Faseb J.* **1999**, *13*, 513–22.

49. Lii, C. K.; Chai, Y. C.; Zhao, W.; Thomas, J. A.; Hendrich, S. S-Thiolation and Irreversible Oxidation of Sulfhydryls on Carbonic Anhydrase III during Oxidative Stress: A Method for Studying Protein Modification in Intact Cells and Tissues. *Arch. Biochem. Biophys.* 1994, *308*, 231–239.

50. Chai, Y. C.; Jung, C. H.; Lii, C. K.; Ashraf, S. S.; Hendrich, S.; Wolf, B.; Sies, H.; Thomas, J. A. Identification of an abundant S-thiolated rat liver protein as carbonic anhydrase III; characterization of S-thiolation and dethiolation reactions. *Arch. Biochem. Biophys.* **1991**, *284*, 270–278, doi:10.1016/0003-9861(91)90295-T.

51. Sender, S.; Decker, B.; Fenske, C. D.; Sly, W. S.; Carter, N. D.; Gros, G. Localization of carbonic anhydrase IV in rat and human heart muscle. *J. Histochem. Cytochem.* **1998**, *46*, 855–861.

52. Brion, L. P.; Suarez, C.; Zhang, H.; Cammer, W. Up-Regulation of Carbonic Anhydrase Isozyme IV in CNS Myelin of Mice Genetically Deficient in Carbonic Anhydrase II. *J. Neurochem.* **1994**, *63*, 360–366, doi:10.1046/j.1471-4159.1994.63010360.x.

53. Hageman, G. S.; Zhu, X. L.; Waheed, A.; Sly, W. S. Localization of carbonic anhydrase IV in a specific capillary bed of the human eye. *Proc. Natl. Acad. Sci.* **1991**, *88*, 2716–2720, doi:10.1073/pnas.88.7.2716.

54. Wistrand, P. J.; Carter, N. D.; Conroy, C. W.; Mahieu, I. Carbonic anhydrase IV activity is localized on the exterior surface of human erythrocytes. *Acta Physiol. Scand.* **1999**, *165*, 211–218, doi:10.1046/j.1365-201x.1999.00478.x.

55. Datta, R.; Waheed, A.; Bonapace, G.; Shah, G. N.; Sly, W. S. Pathogenesis of retinitis pigmentosa associated with apoptosis-inducing mutations in carbonic anhydrase IV. *Proc. Natl. Acad. Sci. U. S. A.* **2009**, *106*, 3437–3442, doi:10.1073/pnas.0813178106.

56. Tang, Y.; Xu, H.; Du, X.; Lit, L.; Walker, W.; Lu, A.; Ran, R.; Gregg, J. P.; Reilly, M.; Pancioli, A.; Khoury, J. C.; Sauerbeck, L. R.; Carrozzella, J. A.; Spilker, J.; Clark, J.; Wagner, K. R.; Jauch, E. C.; Chang, D. J.; Verro, P.; Broderick, J. P.; Sharp, F. R. Gene expression in blood changes rapidly in neutrophils and monocytes after ischemic stroke in humans: A microarray study. *J. Cereb. Blood Flow Metab.* **2006**, *26*, 1089–1102, doi:10.1038/sj.jcbfm.9600264.

57. Supuran, C. Carbonic Anhydrases An Overview. *Curr. Pharm. Des.* **2008**, *14*, 603–614, doi:10.2174/138161208783877884.

58. Imtaiyaz Hassan, M.; Shajee, B.; Waheed, A.; Ahmad, F.; Sly, W. S. Structure, function and applications of carbonic anhydrase isozymes. *Bioorganic Med. Chem.* **2013**, *21*, 1570–1582, doi:10.1016/j.bmc.2012.04.044.

59. Supuran, C. T. Carbonic anhydrase inhibitors as emerging drugs for the treatment of obesity. *Expert Opin. Emerg. Drugs* **2012**, *17*, 11–15, doi:10.1517/14728214.2012.664132.

60. Picco, D. D. C. R.; Lopes, L. M.; Rocha Marques, M.; Line, S. R. P.; Parisotto, T. M.; Nobre dos Santos, M. Children with a higher activity of carbonic anhydrase VI in saliva are more likely to develop dental caries. *Caries Res.* **2017**, *51*, 394–401, doi:10.1159/000470849.

61. Frasseto, F.; Parisotto, T. M.; Peres, R. C. R.; Marques, M. R.; Line, S. R. P.; Nobre Dos Santos, M. Relationship among salivary carbonic anhydrase vi activity and flow rate, biofilm ph and caries in primary dentition. *Caries Res.* **2012**, *46*, 194–200, doi:10.1159/000337275.

62. Thiry, A.; Dogne, J.-M.; Masereel, C. T. S. and B. Carbonic Anhydrase Inhibitors as Anticonvulsant Agents. *Curr. Top. Med. Chem.* 2007, *7*, 855–864.

63. Aspatwar, A.; Tolvanen, M. E. E.; Ortutay, C.; Parkkila, S. Carbonic anhydrase related protein VIII and its role in neurodegeneration and cancer. *Curr. Pharm.*

Des. **2010**, *16*, 3264–3276, doi:10.2174/138161210793429823.

64. Di Fiore, A.; Monti, S. M.; Hilvo, M.; Parkkila, S.; Romano, V.; Scaloni, A.; Pedone, C.; Scozzafava, A.; Supuran, C. T.; De Simone, G. Crystal structure of human carbonic anhydrase XIII and its complex with the inhibitor acetazolamide. *Proteins Struct. Funct. Bioinforma.* **2009**, *74*, 164–175, doi:10.1002/prot.22144.

65. Pastorekova, S.; Zatovicova, M.; Pastorek, J. Cancer-Associated Carbonic Anhydrases and Their Inhibition. *Curr. Pharm. Des.* **2008**, *14*, 685–698, doi:10.2174/138161208783877893.

66. Sedlakova, O.; Svastova, E.; Takacova, M.; Kopacek, J.; Pastorek, J.; Pastorekova, S. Carbonic anhydrase IX, a hypoxia-induced catalytic component of the pH regulating machinery in tumors. *Front. Physiol.* **2014**, *4 JAN*, 1–14, doi:10.3389/fphys.2013.00400.

67. Nocentini, A.; Supuran, C. T. Carbonic anhydrase inhibitors as antitumor/antimetastatic agents: a patent review (2008–2018). *Expert Opin. Ther. Pat.* **2018**, *28*, 1–12, doi:10.1080/13543776.2018.1508453.

68. Hilvo, M.; Baranauskiene, L.; Salzano, A. M.; Scaloni, A.; Matulis, D.; Innocenti, A.; Scozzafava, A.; Monti, S. M.; Di Fiore, A.; De Simone, G.; Lindfors, M.; Jänis, J.; Valjakka, J.; Pastoreková, S.; Pastorek, J.; Kulomaa, M. S.; Nordlund, H. R.; Supuran, C. T.; Parkkila, S. Biochemical characterization of CA IX, one of the most active carbonic anhydrase isozymes. *J. Biol. Chem.* **2008**, *283*, 27799–27809, doi:10.1074/jbc.M800938200.

69. Svastova, E.; Pastorekova, S. Carbonic anhydrase IX: A hypoxia-controlled "catalyst" of cell migration. *Cell Adhes. Migr.* 2013, *7*, 226–231.

70. Alterio, V.; Hilvo, M.; Di Fiore, A.; Supuran, C. .; Pan, P.; Parkkila, S.; Scaloni, A.; Pastorek, J.; Pastorekova, S.; Pedone, C.; Scozzafava, A.; Monti, S. .; De

Simone, G. Crystal structure of the catalytic domain of the tumor-associated human carbonic anhydrase IX. *Proc.Natl.Acad.Sci.USA* **2009**, *106*, 16233–16238, doi:19805286.

71. Dubois, L.; Peeters, S.; Lieuwes, N. G.; Geusens, N.; Thiry, A.; Wigfield, S.; Carta, F.; McIntyre, A.; Scozzafava, A.; Dogné, J. M.; Supuran, C. T.; Harris, A. L.; Masereel, B.; Lambin, P. Specific inhibition of carbonic anhydrase IX activity enhances the in vivo therapeutic effect of tumor irradiation. *Radiother. Oncol.* **2011**, *99*, 424–431, doi:10.1016/j.radonc.2011.05.045.

72. Türeci, O.; Sahin, U.; Vollmar, E.; Siemer, S.; Göttert, E.; Seitz, G.; Parkkila, a K.; Shah, G. N.; Grubb, J. H.; Pfreundschuh, M.; Sly, W. S. Human carbonic anhydrase XII: cDNA cloning, expression, and chromosomal localization of a carbonic anhydrase gene that is overexpressed in some renal cell cancers. *Proc. Natl. Acad. Sci. U. S. A.* **1998**, *95,* 7608–13, doi:10.1073/pnas.95.13.7608.

73. Barnett, D. H.; Sheng, S.; Charn, T. H.; Waheed, A.; Sly, W. S.; Lin, C. Y.; Liu, E. T.; Katzenellenbogen, B. S. Estrogen receptor regulation of carbonic anhydrase XII through a distal enhancer in breast cancer. *Cancer Res.* **2008**, *68*, 3505–3515, doi:10.1158/0008-5472.CAN-07-6151.

74. Watson, P. H.; Chia, S. K.; Wykoff, C. C.; Han, C.; Leek, R. D.; Sly, W. S.; Gatter, K. C.; Ratcliffe, P.; Harris, A. L. Carbonic anhydrase XII is a marker of good prognosis in invasive breast carcinoma. *Br. J. Cancer* **2003**, *88*, 1065–1070, doi:10.1038/sj.bjc.6600796.

75. Ulmasov, B.; Waheed, A.; Shah, G. N.; Grubb, J. H.; Sly, W. S.; Tu, C.; Silverman, D. N. Purification and kinetic analysis of recombinant CA XII, a membrane carbonic anhydrase overexpressed in certain cancers. *Proc. Natl. Acad. Sci. U. S. A.* **2000**, *97*, 14212–14217, doi:10.1073/pnas.97.26.14212.

76. Ilie, M. I.; Hofman, V.; Ortholan, C.; Ammadi, R. El; Bonnetaud, C.; Havet, K.;

Venissac, N.; Mouroux, J.; Mazure, N. M.; Pouysségur, J.; Hofman, P. Overexpression of carbonic anhydrase XII in tissues from resectable non-small cell lung cancers is a biomarker of good prognosis. *Int. J. Cancer* **2011**, *128*, 1614–1623, doi:10.1002/ijc.25491.

77.   Hsieh, M. J.; Chen, K. S.; Chiou, H. L.; Hsieh, Y. S. Carbonic anhydrase XII promotes invasion and migration ability of MDA-MB-231 breast cancer cells through the p38 MAPK signaling pathway. *Eur. J. Cell Biol.* **2010**, *89*, 598–606, doi:10.1016/j.ejcb.2010.03.004.

78.   Semenza, G. L. Hypoxia-inducible factor 1: Master regulator of O2 homeostasis. *Curr. Opin. Genet. Dev.* **1998**, *8*, 588–594, doi:10.1016/S0959-437X(98)80016-6.

79.   Semenza, G. L. HIF-1: mediator of physiological and pathophysiological responses to hypoxia. *J. Appl. Physiol.* **2000**, *88*, 1474–1480, doi:10.1152/japplphysiol.00373.2011.

80.   David, R.; Michael, I. Targeting of HIF (alpha) to the von Hippel-Lindau ubiquitylation ... *Science (80-.).* **2001**, *292*, 468–472.

81.   Kondo, K.; Klco, J.; Nakamura, E.; Lechpammer, M.; Kaelin, W. G. Inhibition of HIF is necessary for tumor suppression by the von Hippel-Lindau protein. *Cancer Cell* **2002**, *1*, 237–246, doi:10.1016/S1535-6108(02)00043-0.

82.   Semenza, G. L. HIF-1 and tumor progression: Pathophysiology and therapeutics. *Trends Mol. Med.* **2002**, *8*, 62–67, doi:10.1016/S1471-4914(02)02317-1.

83.   Pugh, C. W.; Ratcliffe, P. J. Regulation of angiogenesis by hypoxia: role of the HIF system. *Nat. Med.* **2003**, *9*, 677–684, doi:10.1038/nm0603-677.

84.   Semenza, G. L. Targeting HIF-1 for cancer therapy. *Nat. Rev. Cancer* **2003**, *3*,

721–732, doi:10.1038/nrc1187.

85. Semenza, G. L. Evaluation of HIF-1 inhibitors as anticancer agents. *Drug Discov. Today* **2007**, *12*, 853–859, doi:10.1016/j.drudis.2007.08.006.

86. Xia, Y.; Choi, H. K.; Lee, K. Recent advances in hypoxia-inducible factor (HIF)-1 inhibitors. *Eur. J. Med. Chem.* **2012**, *49*, 24–40, doi:10.1016/j.ejmech.2012.01.033.

87. Pastorek, J.; Pastorekova, S. Hypoxia-induced carbonic anhydrase IX as a target for cancer therapy: From biology to clinical use. *Semin. Cancer Biol.* **2014**, *31*, 52–64, doi:10.1016/j.semcancer.2014.08.002.

88. De Simone, G.; Supuran, C. T. Carbonic anhydrase IX: Biochemical and crystallographic characterization of a novel antitumor target. *Biochim. Biophys. Acta* **2010**, *1804*, 404–409, doi:10.1016/j.bbapap.2009.07.027.

89. Parks, S. K.; Chiche, J.; Pouyssegur, J. Disrupting proton dynamics and energy metabolism for cancer therapy. *Nat. Rev. Cancer* **2013**, *13*, 611–623, doi:10.1038/nrc3579.

90. Mboge, M. Y.; Mahon, B. P.; McKenna, R.; Frost, S. C. Carbonic anhydrases: Role in pH control and cancer. *Metabolites* 2018, *8*.

91. Supuran, C. T. How many carbonic anhydrase inhibition mechanisms exist? *J. Enzyme Inhib. Med. Chem.* **2016**, *31*, 345–360, doi:10.3109/14756366.2015.1122001.

92. Krasavin, M.; Shetnev, A.; Sharonova, T.; Baykov, S.; Tuccinardi, T.; Kalinin, S.; Angeli, A.; Supuran, C. T. Heterocyclic periphery in the design of carbonic anhydrase inhibitors: 1,2,4-Oxadiazol-5-yl benzenesulfonamides as potent and selective inhibitors of cytosolic hCA II and membrane-bound hCA IX isoforms. *Bioorg. Chem.* **2018**, *76*, 88–97, doi:10.1016/j.bioorg.2017.10.005.

93. Sapegin, A.; Kalinin, S.; Angeli, A.; Supuran, C. T.; Krasavin, M. Unprotected primary sulfonamide group facilitates ring-forming cascade en route to

polycyclic [1,4]oxazepine-based carbonic anhydrase inhibitors. *Bioorg. Chem.* **2018**, *76*, 140–146, doi:10.1016/j.bioorg.2017.11.014.

94.   Aday, B.; Ulus, R.; Tanç, M.; Kaya, M.; Supuran, C. T. Synthesis of novel 5-amino-1,3,4-thiadiazole-2-sulfonamide containing acridine sulfonamide/carboxamide compounds and investigation of their inhibition effects on human carbonic anhydrase I, II, IV and VII. *Bioorg. Chem.* **2018**, *77*, 101–105, doi:10.1016/j.bioorg.2017.12.035.

95.   Lolak, N.; Akocak, S.; Bua, S.; Koca, M.; Supuran, C. T. Design and synthesis of novel 1,3-diaryltriazene-substituted sulfonamides as potent and selective carbonic anhydrase II inhibitors. *Bioorg. Chem.* **2018**, *77*, 542–547, doi:10.1016/j.bioorg.2018.02.015.

96.   Nocentini, A.; Moi, D.; Balboni, G.; Salvadori, S.; Onnis, V.; Supuran, C. T. Synthesis and biological evaluation of novel pyrazoline-based aromatic sulfamates with potent carbonic anhydrase isoforms II, IV and IX inhibitory efficacy. *Bioorg. Chem.* **2018**, *77*, 633–639, doi:10.1016/j.bioorg.2018.02.021.

97.   Bozdag, M.; Ferraroni, M.; Nuti, E.; Vullo, D.; Rossello, A.; Carta, F.; Scozzafava, A.; Supuran, C. T. Combining the tail and the ring approaches for obtaining potent and isoform-selective carbonic anhydrase inhibitors: Solution and X-ray crystallographic studies. *Bioorganic Med. Chem.* **2014**, *22*, 334–340, doi:10.1016/j.bmc.2013.11.016.

98.   Tibell, L.; Forsman, C.; Simonsson, I.; Lindskog, S. The inhibition of human carbonic anhydrase II by some organic compounds. *Biochim. Biophys. Acta - Protein Struct. Mol. Enzymol.* **1985**, *829*, 202–208, doi:10.1016/0167-4838(85)90189-X.

99.   Carta, F.; Temperini, C.; Innocenti, A.; Scozzafava, A.; Kaila, K.; Supuran, C. T. Polyamines inhibit carbonic anhydrases by anchoring to the zinc-coordinated

water molecule. *J. Med. Chem.* **2010**, *53*, 5511–5522, doi:10.1021/jm1003667.

100. Innocenti, A.; Vullo, D.; Scozzafava, A.; Casey, J. R.; Supuran, C. Carbonic anhydrase inhibitors. Interaction of isozymes I, II, IV, V, and IX with carboxylates. *Bioorganic Med. Chem. Lett.* **2005**, *15*, 573–578, doi:10.1016/j.bmcl.2004.11.057.

101. Maresca, A.; Temperini, C.; Vu, H.; Pham, N. B.; Poulsen, S. A.; Scozzafava, A.; Quinn, R. J.; Supuran, C. T. Non-zinc mediated inhibition of carbonic anhydrases: Coumarins are a new class of suicide inhibitors. *J. Am. Chem. Soc.* **2009**, *131*, 3057–3062, doi:10.1021/ja809683v.

102. Temperini, C.; Innocenti, A.; Scozzafava, A.; Parkkila, S.; Supuran, C. T. The coumarin-binding site in carbonic anhydrase accommodates structurally diverse inhibitors: The antiepileptic lacosamide as an example and lead molecule for novel classes of carbonic anhydrase inhibitors. *J. Med. Chem.* **2010**, *53*, 850–854, doi:10.1021/jm901524f.

103. D'Ambrosio, K.; Carradori, S.; Monti, S. M.; Buonanno, M.; Secci, D.; Vullo, D.; Supuran, C. T.; De Simone, G. Out of the active site binding pocket for carbonic anhydrase inhibitors. *Chem. Commun. (Camb).* **2015**, *51*, 302–5, doi:10.1039/c4cc07320g.

104. Ivanova, J.; Carta, F.; Vullo, D.; Leitans, J.; Kazaks, A.; Tars, K.; Žalubovskis, R.; Supuran, C. T. N -Substituted and ring opened saccharin derivatives selectively inhibit transmembrane, tumor-associated carbonic anhydrases IX and XII. *Bioorg. Med. Chem.* **2017**, 1–7, doi:10.1016/j.bmc.2017.04.007.

105. D'Ascenzio, M.; Guglielmi, P.; Carradori, S.; Secci, D.; Florio, R.; Mollica, A.; Ceruso, M.; Akdemir, A.; Sobolev, A. P.; Supuran, C. T. Open saccharin-based secondary sulfonamides as potent and selective inhibitors of cancer-related carbonic anhydrase IX and XII isoforms. *J. Enzyme Inhib. Med. Chem.* **2017**, *32*,

51–59, doi:10.1080/14756366.2016.1235040.

106. Carradori, S.; Secci, D.; De Monte, C.; Mollica, A.; Ceruso, M.; Akdemir, A.; Sobolev, A. P.; Codispoti, R.; De Cosmi, F.; Guglielmi, P.; Supuran, C. T. A novel library of saccharin and acesulfame derivatives as potent and selective inhibitors of carbonic anhydrase IX and XII isoforms. *Bioorg. Med. Chem.* **2016**, *24*, 22–25, doi:10.1016/j.bmc.2016.01.038.

107. Coviello, V.; Marchi, B.; Sartini, S.; Quattrini, L.; Marini, A. M.; Simorini, F.; Taliani, S.; Salerno, S.; Orlandi, P.; Fioravanti, A.; Desidero, T. Di; Vullo, D.; Da Settimo, F.; Supuran, C. T.; Bocci, G.; La Motta, C. 1,2-Benzisothiazole Derivatives Bearing 4-, 5-, or 6-Alkyl/arylcarboxamide Moieties Inhibit Carbonic Anhydrase Isoform IX (CAIX) and Cell Proliferation under Hypoxic Conditions. *J. Med. Chem.* **2016**, *59*, 6547–6552, doi:10.1021/acs.jmedchem.6b00616.

108. Alterio, V.; Tanc, M.; Ivanova, J.; Zalubovskis, R.; Vozny, I.; Monti, S. M.; Di Fiore, A.; De Simone, G.; Supuran, C. T. X-ray crystallographic and kinetic investigations of 6-sulfamoyl-saccharin as a carbonic anhydrase inhibitor. *Org. Biomol. Chem.* **2015**, *13*, 4064–4069, doi:10.1039/c4ob02648a.

109. D'Ascenzio, M.; Carradori, S.; De Monte, C.; Secci, D.; Ceruso, M.; Supuran, C. T. Design, synthesis and evaluation of N-substituted saccharin derivatives as selective inhibitors of tumor-associated carbonic anhydrase XII. *Bioorg. Med. Chem.* **2014**, *22*, 1821–31, doi:10.1016/j.bmc.2014.01.056.

110. Alp, C.; Maresca, A.; Alp, N. A.; Gültekin, M. S.; Ekinci, D.; Scozzafava, A.; Supuran, C. T. Secondary / tertiary benzenesulfonamides with inhibitory action against the cytosolic human carbonic anhydrase isoforms I and II. **2013**, *28*, 294–298, doi:10.3109/14756366.2012.658788.

111. Carta, F.; Di Cesare Mannelli, L.; Pinard, M.; Ghelardini, C.; Scozzafava, A.;

McKenna, R.; Supuran, C. T. A class of sulfonamide carbonic anhydrase inhibitors with neuropathic pain modulating effects. *Bioorganic Med. Chem.* **2015**, *23*, 1828–1840, doi:10.1016/j.bmc.2015.02.027.

112. Thibaudeau, S.; Carreyre, H.; Mingot, A.; Supuran, C. T. Next-generation secondary/tertiary sulfonamide carbonic anhydrase inhibitor. In *Targeting Carbonic Anhydrases*; Future Science Ltd: Unitec House, 2 Albert Place, London N3 1QB, UK, 2014; pp. 52–67 ISBN 9781909453913.

113. Moeker, J.; Peat, T. S.; Bornaghi, L. F.; Vullo, D.; Supuran, C. T.; Poulsen, S. A. Cyclic secondary sulfonamides: Unusually good inhibitors of cancer-related carbonic anhydrase enzymes. *J. Med. Chem.* **2014**, *57*, 3522–3531, doi:10.1021/jm500255y.

114. Mollica, A.; Costante, R.; Akdemir, A.; Carradori, S.; Stefanucci, A.; Macedonio, G.; Ceruso, M.; Supuran, C. T. Exploring new Probenecid-based carbonic anhydrase inhibitors: Synthesis, biological evaluation and docking studies. *Bioorg. Med. Chem.* **2015**, *23*, 5311–5318, doi:10.1016/j.bmc.2015.07.066.

115. D'Ascenzio, M.; Carradori, S.; Secci, D.; Vullo, D.; Ceruso, M.; Akdemir, A.; Supuran, C. T. Selective inhibition of human carbonic anhydrases by novel amide derivatives of probenecid: Synthesis, biological evaluation and molecular modelling studies. *Bioorg. Med. Chem.* **2014**, *22*, 3982–3988, doi:10.1016/j.bmc.2014.06.003.

116. Métayer, B.; Martin-Mingot, A.; Vullo, D.; Supuran, C. T.; Thibaudeau, S. Superacid synthesized tertiary benzenesulfonamides and benzofuzed sultams act as selective hCA IX inhibitors: toward understanding a new mode of inhibition by tertiary sulfonamides. *Org. Biomol. Chem.* **2013**, *11*, 7540–9, doi:10.1039/c3ob41538d.

117. Metayer, B.; Mingot, A.; Vullo, D.; Supuran, C. T.; Thibaudeau, S. New

superacid synthesized (fluorinated) tertiary benzenesulfonamides acting as selective hCA IX inhibitors: toward a new mode of carbonic anhydrase inhibition by sulfonamides. *Chem. Commun.* **2013**, *49*, 6015–6017, doi:10.1039/C3CC40858B.

118. Ivanova, J.; Leitans, J.; Tanc, M.; Kazaks, A.; Zalubovskis, R.; Supuran, C. T.; Tars, K. X-ray crystallography-promoted drug design of carbonic anhydrase inhibitors. *Chem. Commun.* **2015**, *51*, 7108–7111, doi:10.1039/C5CC01854D.

119. Ivanova, J.; Carta, F.; Vullo, D.; Leitans, J.; Kazaks, A.; Tars, K.; Žalubovskis, R.; Supuran, C. T. N-Substituted and ring opened saccharin derivatives selectively inhibit transmembrane, tumor-associated carbonic anhydrases IX and XII. *Bioorganic Med. Chem.* **2017**, *25*, 3583–3589, doi:10.1016/j.bmc.2017.04.007.

120. Rice, L. M.; Grogan, C. H.; Reid, E. E. N-Alkyl Saccharins and their Reduction Products. *J. Am. Chem. Soc.* **1953**, *75*, 4304–4305, doi:10.1021/ja01113a047.

121. Hettler, H. Chapman-mumm rearrangement of pseudosaccharinethers. *Tetrahedron Lett.* **1968**, *9*, 1793–1796, doi:10.1016/S0040-4039(00)76365-9.

122. Gothelf, K. V; Jørgensen, K. A. Asymmetric 1 , 3-Dipolar Cycloaddition Reactions. *Chem. Rev.* **1998**, *98*, 863–909.

123. Mabrour, M.; Bougrin, K.; Benhida, R.; Loupy, A.; Soufiaoui, M. An efficient one-step regiospecific synthesis of novel isoxazolines and isoxazoles of N-substituted saccharin derivatives through solvent-free microwave-assisted [3+2] cycloaddition. *Tetrahedron Lett.* **2007**, *48*, 443–447, doi:10.1016/j.tetlet.2006.11.067.

124. Shelton, B. R.; Howe, R.; Liu, K. C. A Particularly Convenient Preparation of Benzohydroximinoyl Chlorides (Nitrile Oxide Precursors). *J. Org. Chem.* **1980**, *45*, 3916–3918, doi:10.1021/jo01307a039.

125. 1,3-Dipolar Cycloaddition Reactions. In *Tetrahedron Organic Chemistry Series*; 1990; Vol. 8, pp. 269–331.

126. Youdim, M. B. H. Monoamine oxidase inhibitors, and iron chelators in depressive illness and neurodegenerative diseases. *J. Neural Transm.* **2018**, *0*, 0, doi:10.1007/s00702-018-1942-9.

127. Blaschko, H.; Richter, D.; Schlossmann, H. The inactivation of adrenaline. *J. Physiol.* **1937**, *90*, 1–17, doi:10.1113/jphysiol.1937.sp003497.

128. Edmondson, D. E.; Binda, C. *Membrane Protein Complexes: Structure and Function*; Harris, J. R., Boekema, E. J., Eds.; Subcellular Biochemistry; Springer Singapore: Singapore, 2018; Vol. 87; ISBN 978-981-10-7756-2.

129. Gesi, M.; Santinami, A.; Ruffoli, R.; Conti, G.; Fornai, F. Novel aspects of dopamine oxidative metabolism. *Pharmacol Toxicol.* **2001**, *89*, 217–224.

130. Langston, J. W.; Irwin, I.; Langston, E. B.; Forno, L. S. 1-Methyl-4-phenylpyridinium ion (MPP+): Identification of a metabolite of MPTP, a toxin selective to the substantia nigra. *Neurosci. Lett.* **1984**, *48*, 87–92, doi:10.1016/0304-3940(84)90293-3.

131. Langston, J. W.; Irwin, I. A. N.; Langston, E. B.; Forno, L. S. Pargyline prevents MPTP-induced parkinsonism in primates. *Science (80-.).* **1984**, *225*, 1480–1482, doi:10.1126/science.6332378.

132. Grimsby, J.; Chen, K.; Wang, L.-J.; Lan, N. C.; Shih, J. C. Human monoamine oxidase A and B genes exhibit identical exon-intron organization (human MAOA aud MAOB genes/genomic organization). *Neurobiology* **1991**, *88*, 3637–3641, doi:10.1073/pnas.88.9.3637.

133. Chen, K.; Shih, J. C. Monoamine Oxidase A and B: Structure, Function, and Behavior. *Adv. Pharmacol.* **1997**, *42*, 292–296, doi:10.1016/S1054-3589(08)60747-4.

134. Binda, C.; Wang, J.; Pisani, L.; Caccia, C.; Carotti, A.; Salvati, P.; Edmondson, D. E.; Mattevi, A. Structures of human monoamine oxidase B complexes with selective noncovalent inhibitors: Safinamide and coumarin analogs. *J. Med. Chem.* **2007**, *50*, 5848–5852, doi:10.1021/jm070677y.

135. Son, S.-Y.; Ma, J.; Kondou, Y.; Yoshimura, M.; Yamashita, E.; Tsukihara, T. Structure of human monoamine oxidase A at 2.2-A resolution: the control of opening the entry for substrates/inhibitors. *Proc. Natl. Acad. Sci. U. S. A.* **2008**, *105*, 5739–5744, doi:10.1073/pnas.0710626105.

136. Upadhyay, A. K.; Edmondson, D. E. Development of Spin-Labeled Pargyline Analogues as Specific Inhibitors of Human Monoamine Oxidases A and B. *Biochemistry* **2009**, *48*, 3928–3935, doi:10.1021/bi9002106.

137. Binda, C.; Li, M.; Hubalek, F.; Restelli, N.; Edmondson, D. E.; Mattevi, A. Insights into the mode of inhibition of human mitochondrial monoamine oxidase B from high-resolution crystal structures. *Proc. Natl. Acad. Sci. U. S. A.* **2003**, *100*, 9750–9755, doi:10.1073/pnas.1633804100.

138. Jonsson, T.; Edmondson, D. E.; Klinman, J. P. Hydrogen tunneling in the flavoenzyme monoamine oxidase B. *Biochemistry* **1994**, *33*, 14871–14878, doi:10.1021/bi00253a026.

139. Silverman, R. B. Radical Ideas about Monoamine Oxidase. *Acc. Chem. Res.* **1995**, *28*, 335–342, doi:10.1021/ar00056a003.

140. Silverman, R. B.; Hoffman, S. J.; Catus, W. B. A Mechanism for Mitochondrial Monoamine Oxidase Catalyzed Amine Oxidation. *J. Am. Chem. Soc.* **1980**, *102*, 7126–7128, doi:10.1021/ja00543a052.

141. Edmondson, D. E.; Mattevi, A.; Binda, C.; Li, M.; Hubálek, F.; Hubalek, F. Structure and Mechanism of Monoamine Oxidase. *Burger's Med. Chem. Drug Discov.* **2004**, *11*, 1983–1993, doi:10.1002/0471266949.bmc111.

142. Miller, J. R.; Edmondson, D. E. Structure-activity relationships in the oxidation of para-substituted benzylamine analogues by recombinant human liver monoamine oxidase A. *Biochemistry* **1999**, *38*, 13670–13683, doi:10.1021/bi990920y.

143. Carradori, S.; Secci, D.; Petzer, J. P. MAO inhibitors and their wider applications: a patent review. *Expert Opin. Ther. Pat.* **2018**, *28*, 211–226, doi:10.1080/13543776.2018.1427735.

144. Perez, C.; Tong, Y.; Guo, M. Iron Chelators as Potential Therapeutic Agents for Parkinson's Disease. *Curr. Bioact. Compd.* **2008**, *4*, 150–158, doi:10.2174/157340708786305952.Iron.

145. Budimir, A. Metal ions, Alzheimer's disease and chelation therapy. *Acta Pharm.* **2011**, *61*, 1–14, doi:10.2478/v10007-011-0006-6.

146. Ward, R. J.; Dexter, D. T.; Crichton, R. R. Chelating agents for neurodegenerative diseases. *Curr. Med. Chem.* **2012**, *19*, 2760–72, doi:10.2174/092986712800609689.

147. Hare, M. Tyramine Oxidase: A New Enzyme System in Liver. *Biochem. J.* **1928**, *22*, 968–972.

148. Bradley, P. B. Synaptic Transmission in the Central Nervous System and Its Relevance for Drug Action. *Int. Rev. Neurobiol.* **1967**, *11*, 1–56, doi:10.1016/S0074-7742(08)60383-9.

149. Efange, S. M. N.; Boudreau, R. J. Molecular determinants in the bioactivation of the dopaminergic neurotoxin N-methyl-4-phenyl-1,2,3,6-tetrahydropyridine (MPTP). *J. Comput. Aided. Mol. Des.* **1991**, *5*, 405–417, doi:10.1007/BF00125661.

150. Laux, G.; Volz, H. P.; Möller, H. J. Newer and Older Monoamine Oxidase Inhibitors: A Comparative Profile. *CNS Drugs* **1995**, *3*, 145–158,

doi:10.2165/00023210-199503020-00006.

151. Finberg, J. P. M.; Rabey, J. M. Inhibitors of MAO-A and MAO-B in psychiatry and neurology. *Front. Pharmacol.* **2016**, *7*, 1–15, doi:10.3389/fphar.2016.00340.

152. Carradori, S.; Gidaro, M. C.; Petzer, A.; Costa, G.; Guglielmi, P.; Chimenti, P.; Alcaro, S.; Petzer, J. P. Inhibition of Human Monoamine Oxidase: Biological and Molecular Modeling Studies on Selected Natural Flavonoids. *J. Agric. Food Chem.* **2016**, *64*, 9004–9011, doi:10.1021/acs.jafc.6b03529.

153. Wimbiscus, M.; Kostenko, O.; Malone, D. MAO inhibitors: Risks, benefits, and lore. *Cleve. Clin. J. Med.* **2010**, *77*, 859–882, doi:10.3949/ccjm.77a.09103.

154. Youdim, M. B. H.; Edmondson, D.; Tipton, K. F. The therapeutic potential of monoamine oxidase inhibitors. *Nat. Rev. Neurosci.* **2006**, *7*, 295–309, doi:10.1038/nrn1883.

155. Lamensdorf, I.; Eisenhofer, G.; Harvey-White, J.; Nechustan, A.; Kirk, K.; Kopin, irwan J. 3,4-Dihydroxyphenylacetaldehyde potentiates the toxic effects of metabolic stress in PC12 cells. *Brain Res.* **2000**, *868*, 191–201, doi:10.1016/S0006-8993(00)02309-X.

156. Tipton, K. F. *90 Years of Monoamine Oxidase: Some Progress and Some Confusion*; Springer Vienna, 2018; ISBN 0123456789.

157. Carradori, S.; Ortuso, F.; Petzer, A.; Bagetta, D.; De Monte, C.; Secci, D.; De Vita, D.; Guglielmi, P.; Zengin, G.; Aktumsek, A.; Alcaro, S.; Petzer, J. P. Design, synthesis and biochemical evaluation of novel multi-target inhibitors as potential anti-Parkinson agents. *Eur. J. Med. Chem.* **2018**, *143*, 1543–1552, doi:10.1016/j.ejmech.2017.10.050.

158. Xuan, M.; Guan, X.; Gu, Q.; Shen, Z.; Yu, X.; Qiu, T.; Luo, X.; Song, R.; Jiaerken, Y.; Xu, X.; Huang, P.; Luo, W.; Zhang, M. Different iron deposition patterns in

early- and middle-late-onset Parkinson's disease. *Park. Relat. Disord.* **2017**, *44*, 23–27, doi:10.1016/j.parkreldis.2017.08.013.

159. López-Muñoz, F.; Álamo, C.; Juckel, G.; Assion, H.-J. Half a Century of Antidepressant Drugs. *J. Clin. Psychopharmacol.* **2007**, *27*, 555–559, doi:10.1016/j.jfluchem.2015.08.017.

160. Zeller, E.; Barsky, J. In vivo Inhibition of Liver and Brain Monoamine Oxidase by 1-Isonicotinyl-2-Isopropyl Hydrazine. *Exp. Biol. Med.* **1952**, *81*, 459–461, doi:10.3181/00379727-81-19910.

161. Article, C. M. E. R. CNS SPECTRUMS CME Review Article. **2016**.

162. Dickinson, H. G.; Bell, P. R. Nucleocytoplasmic interaction at the nuclear envelope in post meiotic microspores of Pinus banksiana. *J. Ultrasructure Res.* **1970**, *33*, 356–359, doi:10.1017/S1092852912000594.

163. Anderson, M. C.; Hasan, F.; McCrodden, J. M.; Tipton, K. F. Monoamine oxidase inhibitors and the cheese effect. *Neurochem. Res.* **1993**, *18*, 1145–1149, doi:10.1007/BF00978365.

164. Ulrich, S.; Ricken, R.; Adli, M. Tranylcypromine in mind (Part I): Review of pharmacology. *Eur. Neuropsychopharmacol.* **2017**, *27*, 697–713, doi:10.1016/j.euroneuro.2017.05.007.

165. Finberg, J. P. M. Update on the pharmacology of selective inhibitors of MAO-A and MAO-B: Focus on modulation of CNS monoamine neurotransmitter release. *Pharmacol. Ther.* **2014**, *143*, 133–152, doi:10.1016/j.pharmthera.2014.02.010.

166. Bonnet, U. Moclobemide: Therapeutic Use and Clinical Studies. *CNS Drug Rev.* **2006**, *9*, 97–140, doi:10.1111/j.1527-3458.2003.tb00245.x.

167. Provost, J. C.; Funck-Brentano, C.; Rovei, V.; D'Estanque, J.; Ego, D.; Jaillon, P.

Pharmacokinetic and pharmacodynamic interaction between toloxatone, a new reversible monoamine oxidase-A inhibitor, and oral tyramine in healthy subjects. *Clin. Pharmacol. Ther.* **1992**, *52*, 384–393, doi:10.1038/clpt.1992.159.

168. Maurel, A.; Hernandez, C.; Kunduzova, O.; Bompart, G.; Cambon, C.; Parini, A.; Francés, B. Age-dependent increase in hydrogen peroxide production by cardiac monoamine oxidase A in rats. *Am. J. Physiol. Heart Circ. Physiol.* **2003**, *284*, H1460–H1467, doi:10.1152/ajpheart.00700.2002.

169. Peehl, D. M.; Coram, M.; Khine, H.; Reese, S.; Nolley, R.; Zhao, H. The Significance of Monoamine Oxidase-A Expression in High Grade Prostate Cancer. *J. Urol.* **2008**, *180*, 2206–2211, doi:10.1016/j.juro.2008.07.019.

170. Flamand, V.; Zhao, H.; Peehl, D. M. Targeting monoamine oxidase A in advanced prostate cancer. *J. Cancer Res. Clin. Oncol.* **2010**, *136*, 1761–1771, doi:10.1007/s00432-010-0835-6.

171. Pålhagen, S.; Heinonen, E. H.; Hägglund, J.; Kaugesaar, T.; Kontants, H.; Mäki-Ikola, O.; Palm, R.; Turunen, J. Selegiline delays the onset of disability in de novo parkinsonian patients. *Neurology* **1998**, *51*, 520–525, doi:10.1212/WNL.51.2.520.

172. Fernandez, H. H.; Chen, J. J. Monoamine Oxidase-B Inhibition in the Treatment of Parkinson's Disease. *Pharmacotherapy* **2007**, *27*, 174S–185S, doi:10.1592/phco.27.12part2.174S.

173. Finberg, J. P. M.; Wang, J.; Bankiewicz, K.; Harvey-White, J.; Kopin, I. J.; Goldstein, D. S. Increased striatal dopamine production from L-DOPA following selective inhibition of monoamine oxidase B by R(+)-N-propargyl-1-aminoindan (rasagiline) in the monkey BT - MAO — The Mother of all Amine Oxidases. In; Finberg, J. P. M., Youdim, M. B. H., Riederer, P., Tipton, K. F., Eds.; Springer Vienna: Vienna, 1998; pp. 279–285.

174. deSouza, R. M.; Schapira, A. Safinamide for the treatment of Parkinson's disease. *Expert Opin. Pharmacother.* **2017**, *18*, 937–943, doi:10.1080/14656566.2017.1329819.

175. Borgohain, R.; Szasz, J.; Stanzione, P.; Meshram, C.; Bhatt, M. H.; Chirilineau, D.; Stocchi, F.; Lucini, V.; Giuliani, R.; Forrest, E.; Rice, P.; Anand, R.; Illiyas Sahadulla, M.; Kardan, U.; Keshava, B. S.; Kishore, A.; Kothari, S. S.; Krishna Murthy, J. M.; Kumar, S.; Kumar Pal, P.; Mehta, N.; Prabhakar, S.; Prabhakar, S. K.; Pradhan, S.; Roy, A. K.; Sankhla, C.; Sethi, P. K.; Shah, A. B.; Shankar, N.; Shukla, R.; Sowani, A.; Srinivasa, R.; Varma, M.; Vasudevan, D.; Vavilikolanu Sreenivas, P.; Velmurugendran, C. U.; Vijayan, K.; Bajenaru, O.; Bulboaca, A.; Campeanu, A.; Chirileanu, D.; Muresanu, D.; Panea, C.; Popescu, C.; Simu, M.; Szasz, J.; Ticmeanu, M.; Avarello, T.; Bonuccelli, U.; Eleopra, R.; Onofrj, M.; Quatrale, R.; Stanzione, P.; Stocchi, F. Two-Year, randomized, controlled study of safinamide as add-on to levodopa in mid to late Parkinson's disease. *Mov. Disord.* **2014**, *29*, 1273–1280, doi:10.1002/mds.25961.

176. Wouters, J. Structural aspects of monoamine oxidase and its reversible inhibition. *Curr. Med. Chem.* **1998**, *5*, 137–162.

177. Medvedev, A. E.; Ivanov, A. S.; Kamyshanskaya, N. S.; Kirkel, A. Z.; Moskvitina, T. A.; Gorkin, V. Z.; Li, N. Y.; Marshakov, Vy. Interaction of indole derivatives with monoamine oxidase A and B. Studies on the structure-inhibitory activity relationship. *Biochem Mol Biol Int* **1995**, *36*, 113–122.

178. Morales-Camilo, N.; Salas, C. O.; Sanhueza, C.; Espinosa-Bustos, C.; Sepúlveda-Boza, S.; Reyes-Parada, M.; Gonzalez-Nilo, F.; Caroli-Rezende, M.; Fierro, A. Synthesis, biological evaluation, and molecular simulation of chalcones and aurones as selective MAO-B inhibitors. *Chem. Biol. Drug Des.* **2015**, *85*, 685–695, doi:10.1111/cbdd.12458.

179. Nel, M. S.; Petzer, A.; Petzer, J. P.; Legoabe, L. J. 2-Heteroarylidene-1-indanone

derivatives as inhibitors of monoamine oxidase. *Bioorg. Chem.* **2016**, *69*, 20–28, doi:10.1016/j.bioorg.2016.09.004.

180. Nel, M. S.; Petzer, A.; Petzer, J. P.; Legoabe, L. J. 2-Benzylidene-1-indanone derivatives as inhibitors of monoamine oxidase. *Bioorganic Med. Chem. Lett.* **2016**, *26*, 4599–4605, doi:10.1016/j.bmcl.2016.08.067.

181. Chimenti, F.; Fioravanti, R.; Bolasco, A.; Chimenti, P.; Secci, D.; Rossi, F.; Yáñez, M.; Orallo, F.; Ortuso, F.; Alcaro, S. Chalcones: A valid scaffold for monoamine oxidases inhibitors. *J. Med. Chem.* **2009**, *52*, 2818–2824, doi:10.1021/jm801590u.

182. Uzoukwu, B. A. Some metal complexes of 1,3-diketone: syntheses, UV-Vis, IR, 1H, 13C and 19F NMR spectral studies of the complexes of U(VI), Fe(III), V(V) and Ca(II) with 2-thenoyltrifluoroacetone (HTTA). *Inorganica Chim. Acta* **1990**, *176*, 143–148, doi:10.1016/S0020-1693(00)85105-1.

183. Winterbourn, C. C. Toxicity of iron and hydrogen peroxide: the Fenton reaction. *Toxicol. Lett.* **1995**, *82–83*, 969–974, doi:10.1016/0378-4274(95)03532-X.

184. Trapani, P.; Kvapil, L.; Hradil, P.; Soural, M. Use of Phenacyl Thiosalicylates for the Preparation of 3-Hydroxybenzo[b]thiophene Derivatives. *Synlett* **2018**, *29*, 810–814, doi:10.1055/s-0036-1591875.

185. Pan, B.; Ren, P.; Song, H.; Wang, Z. Facile synthesis of 2-substituted benzo[b]thiophen-3-ols in water. *Synth. Commun.* **2013**, *43*, 1337–1344, doi:10.1080/00397911.2011.633203.

186. Chan, S. L. F.; Low, K. H.; Yang, C.; Cheung, S. H. F.; Che, C. M. Iron-ligand coordination in tandem radical cyclizations: Synthesis of benzo[b]thiophenes by a one-pot reaction of iron 1,3-diketone complexes with 2-thiosalicylic acids. *Chem. - A Eur. J.* **2011**, *17*, 4709–4714, doi:10.1002/chem.201100377.

187. Zhou, Z. Z.; Deng, Y. H.; Jiang, Z. H.; Chen, W. H. Microwave-assisted Dieckmann reaction: Efficient one-step synthesis of 2-aroylbenzofuran-3-ols. *Adv. Synth. Catal.* **2010**, *352*, 1909–1913, doi:10.1002/adsc.201000256.

188. Lee, J. J.; Chang, C. K.; Liu, I. M.; Chi, T. C.; Yu, H. J.; Cheng, J. T. Changes in endogenous monoamines in aged rats. *Clin. Exp. Pharmacol. Physiol.* **2001**, *28*, 285–289, doi:10.1046/j.1440-1681.2001.03439.x.

189. Kannan, N.; Guruvayoorappan, C. Protective effect of Bauhinia tomentosa on acetic acid induced ulcerative colitis by regulating antioxidant and inflammatory mediators. *Int. Immunopharmacol.* **2013**, *16*, 57–66, doi:10.1016/j.intimp.2013.03.008.

190. Nagarjun, S.; Dhadde, S. B.; Veerapur, V. P.; Thippeswamy, B. S.; Chandakavathe, B. N. Ameliorative effect of chromium-D-phenylalanine complex on indomethacin-induced inflammatory bowel disease in rats. *Biomed. Pharmacother.* **2017**, *89*, 1061–1066, doi:10.1016/j.biopha.2017.02.042.

191. Van Heesch, F.; Prins, J.; Konsman, J. P.; Korte-Bouws, G. A. H.; Westphal, K. G. C.; Rybka, J.; Olivier, B.; Kraneveld, A. D.; Korte, S. M. Lipopolysaccharide increases degradation of central monoamines: An in vivo microdialysis study in the nucleus accumbens and medial prefrontal cortex of mice. *Eur. J. Pharmacol.* **2014**, *725*, 55–63, doi:10.1016/j.ejphar.2014.01.014.

192. Ferrante, C.; Recinella, L.; Locatelli, M.; Guglielmi, P.; Secci, D.; Leporini, L.; Chiavaroli, A.; Leone, S.; Martinotti, S.; Brunetti, L.; Vacca, M.; Menghini, L.; Orlando, G. Protective Effects Induced by Microwave-Assisted Aqueous Harpagophytum Extract on Rat Cortex Synaptosomes Challenged with Amyloid β-Peptide. *Phyther. Res.* **2017**, *31*, 1257–1264, doi:10.1002/ptr.5850.

193. Mollica, A.; Stefanucci, A.; Zengin, G.; Locatelli, M.; Macedonio, G.; Orlando, G.; Ferrante, C.; Menghini, L.; Recinella, L.; Leone, S.; Chiavaroli, A.; Leporini,

L.; Di Nisio, C.; Brunetti, L.; Tayrab, E.; Ali, I.; Musa, T. H.; Musa, H. H.; Ahmed, A. A. Polyphenolic composition, enzyme inhibitory effects ex-vivo and in-vivo studies on two Brassicaceae of north-central Italy. *Biomed. Pharmacother.* **2018**, *107*, 129–138, doi:10.1016/j.biopha.2018.07.169.

194. Wagmann, L.; Brandt, S. D.; Kavanagh, P. V.; Maurer, H. H.; Meyer, M. R. In vitro monoamine oxidase inhibition potential of alpha-methyltryptamine analog new psychoactive substances for assessing possible toxic risks. *Toxicol. Lett.* **2017**, *272*, 84–93, doi:10.1016/j.toxlet.2017.03.007.

195. Liu, Y.-H.; Wu, W.-C.; Lu, Y.-L.; Lai, Y.-J.; Hou, W.-C. Antioxidant and amine oxidase inhibitory activities of hydroxyurea. *Biosci. Biotechnol. Biochem.* **2010**, *74*, 1256–1260, doi:10.1271/bbb.100096.

196. Takao, K.; Toda, K.; Saito, T.; Sugita, Y. Synthesis of Amide and Ester Derivatives of Cinnamic Acid and Its Analogs: Evaluation of Their Free Radical Scavenging and Monoamine Oxidase and Cholinesterase Inhibitory Activities. *Chem. Pharm. Bull. (Tokyo).* **2017**, *65*, 1020–1027, doi:10.1248/cpb.c17-00416.

197. Halliwell, B.; Clement, M. V.; Ramalingam, J.; Long, L. H. Hydrogen Peroxide. Ubiquitous in Cell Culture and In vivo? *IUBMB Life* **2001**, *50*, 251–257, doi:10.1080/713803727.

198. Mostert, S.; Petzer, A.; Petzer, J. P. Indanones as high-potency reversible inhibitors of monoamine oxidase. *ChemMedChem* **2015**, *10*, 862–873, doi:10.1002/cmdc.201500059.

199. Mostert, S.; Petzer, A.; Petzer, J. P. Inhibition of monoamine oxidase by benzoxathiolone analogues. *Bioorganic Med. Chem. Lett.* **2016**, *26*, 1200–1204, doi:10.1016/j.bmcl.2016.01.034.

200. Brunetti, L.; Michelotto, B.; Orlando, G.; Recinella, L.; Di Nisio, C.; Ciabattoni, G.; Vacca, M. Aging increases amyloid β-peptide-induced 8-iso-prostaglandin

F2αrelease from rat brain. *Neurobiol. Aging* **2004**, *25*, 125–129, doi:10.1016/S0197-4580(03)00038-1.

201. Menghini, L.; Leporini, L.; Vecchiotti, G.; Locatelli, M.; Carradori, S.; Ferrante, C.; Zengin, G.; Recinella, L.; Chiavaroli, A.; Leone, S.; Brunetti, L.; Orlando, G. Crocus sativus L. stigmas and byproducts: Qualitative fingerprint, antioxidant potentials and enzyme inhibitory activities. *Food Res. Int.* **2018**, *109*, 91–98, doi:10.1016/j.foodres.2018.04.028.

202. Ferrante, C.; Orlando, G.; Recinella, L.; Leone, S.; Chiavaroli, A.; Di Nisio, C.; Shohreh, R.; Manippa, F.; Ricciuti, A.; Vacca, M.; Brunetti, L. Central inhibitory effects on feeding induced by the adipo-myokine irisin. *Eur. J. Pharmacol.* **2016**, *791*, 389–394, doi:10.1016/j.ejphar.2016.09.011.

203. Charan, J.; Kantharia, N. How to calculate sample size in animal studies? *J. Pharmacol. Pharmacother.* **2013**, *4*, 303, doi:10.4103/0976-500X.119726.

Publications

1. Talapatra, S. K.; Tham, C. L.**; Guglielmi, P.;** Cirilli, R.; Chandrasekaran, B.; Karpoormath, R.; Carradori, S.; Kozielski, F. Crystal structure of the Eg5 - K858 complex and implications for structure-based design of thiadiazole-containing inhibitors. *Eur. J. Med. Chem.* **2018**, *156*, 641–651.

2. Bellusci, M.; **Guglielmi, P.;** Masi, A.; Padella, F.; Singh, G.; Yaacoub, N.; Peddis, D.; Secci, D. Magnetic Metal–Organic Framework Composite by Fast and Facile Mechanochemical Process. *Inorg. Chem.* **2018**, *57*, 1806–1814

3. Carradori, S.; Ortuso, F.; Petzer, A.; Bagetta, D.; De Monte, C.; Secci, D.; De Vita, D.; **Guglielmi, P.;** Zengin, G.; Aktumsek, A.; Alcaro, S.; Petzer, J. P. Design, synthesis and biochemical evaluation of novel multi-target inhibitors as potential anti-Parkinson agents. *Eur. J. Med. Chem.* **2018**, *143*, 1543-1552.

4. Ferrante, C.; Recinella, L.; Locatelli, M.; **Guglielmi, P.;** Secci, D.; Leporini, L.; Chiavaroli, A.; Leone, S.; Martinotti, S.; Brunetti, L.; Vacca, M.; Menghini, L.; Orlando, G. Protective Effects Induced by Microwave-Assisted Aqueous Harpagophytum Extract on Rat Cortex Synaptosomes Challenged with Amyloid β-Peptide. *Phyther. Res.* **2017**, *31*, 1257–1264.

5. Carradori, S.; Secci, D.; Bizzarri, B.; Chimenti, P.; De Monte, C.; **Guglielmi, P.;** Campestre, C.; Rivanera, D.; Bordón, C.; Jones-Brando, L. Synthesis and biological evaluation of anti-Toxoplasma gondii activity of a novel scaffold of thiazolidinone derivatives. *J. Enzyme Inhib. Med. Chem.* **2017**, *32*, 746–758.

6. Ferretti, R.; Carradori, S.; **Guglielmi, P.;** Pierini, M.; Casulli, A.; Cirilli, R. Enantiomers of triclabendazole sulfoxide: Analytical and semipreparative HPLC separation, absolute configuration assignment, and transformation into sodium salt. *J. Pharm. Biomed. Anal.* **2017**, *140*, 38–44.

7. Campestre, C.; Locatelli, M.; **Guglielmi, P.;** De Luca, E.; Bellagamba, G.; Menta, S.; Zengin, G.; Celia, C.; Di Marzio, L.; Carradori, S. Analysis of imidazoles and triazoles in biological samples after MicroExtraction by packed sorbent. *J.*

Enzyme Inhib. Med. Chem. **2017**, *32*, 1–11.

8. D'Ascenzio, M.; **Guglielmi, P.**; Carradori, S.; Secci, D.; Florio, R.; Mollica, A.; Ceruso, M.; Akdemir, A.; Sobolev, A. P.; Supuran, C. T. Open saccharin-based secondary sulfonamides as potent and selective inhibitors of cancer-related carbonic anhydrase IX and XII isoforms. *J. Enzyme Inhib. Med. Chem.* **2017**, *32*, 51–59.

9. Cirilli, R.; **Guglielmi, P.**; Formica, F. R.; Casulli, A.; Carradori, S. The sodium salt of the enantiomers of ricobendazole: Preparation, solubility and chiroptical properties. *J. Pharm. Biomed. Anal.* **2017**, *139*, 1–7.

10. Carradori, S.; Gidaro, M. C.; Petzer, A.; Costa, G.; **Guglielmi, P.**; Chimenti, P.; Alcaro, S.; Petzer, J. P. Inhibition of Human Monoamine Oxidase: Biological and Molecular Modeling Studies on Selected Natural Flavonoids. *J. Agric. Food Chem.* **2016**, *64*, 9004–9011.

11. Sabia, R.; Carradori, S.; **Guglielmi, P.**; Nescatelli, R.; Gigante, G.; Menta, S. Novel synthetic approaches for the synthesis of Alanine-Proline chimeras. *Curr. Bioact. Compd.* **2016**, *12*, 207–220.

12. Carradori, S.; Secci, D.; De Monte, C.; Mollica, A.; Ceruso, M.; Akdemir, A.; Sobolev, A. P.; Codispoti, R.; De Cosmi, F.; **Guglielmi, P.**; Supuran, C. T. A novel library of saccharin and acesulfame derivatives as potent and selective inhibitors of carbonic anhydrase IX and XII isoforms. *Bioorg. Med. Chem.* **2016**, *24*, 22–25.

13. De Monte, C.; D'Ascenzio, M.; **Guglielmi, P.**; Mancini, V.; Carradori, S. Opening New Scenarios for Human MAO Inhibitors. *Cent. Nerv. Syst. Agents Med. Chem.* **2016**, *16*, 98-104.

14. De Monte, C.; Carradori, S.; Secci, D.; D'Ascenzio, M.; **Guglielmi, P.**; Mollica, A.; Morrone, S.; Scarpa, S.; Aglianò, A. M.; Giantulli, S.; Silvestri, I. Synthesis and pharmacological screening of a large library of 1,3,4-thiadiazolines as innovative therapeutic tools for the treatment of prostate cancer and melanoma. *Eur. J. Med. Chem.* **2015**, *105*, 245–262.